CHARACTERISATION OF Y-BOX PROTEIN 3 (MSY3) IN THE DEVELOPING MURINE CENTRAL NERVOUS SYSTEM

Dissertation

zur Erlangung des akademischen Grades

Doctor rerum naturalium
(Dr. rer. nat.)

Anna Natalia Grzyb

Technische Universität Dresden
2006

CHARACTERISATION OF Y-BOX PROTEIN 3 (MSY3) IN THE DEVELOPING MURINE CENTRAL NERVOUS SYSTEM

Dissertation

zur Erlangung des akademischen Grades

Doctor rerum naturalium
(Dr. rer. nat.)

vorgelget der
Fakultät Mathematik und Naturwissenschaften
der Technischen Universität Dresden

von

Anna Natalia Grzyb
Diplom-Molekularbiologin

geboren am 01. April 1977 in Warschau, Polen

Gutachter: Prof. Dr. Wieland B. Huttner, MPI-CBG, Dresden
Prof. Dr. Michele Solimena, Technische Universität Dresden
Dr. Gerd Kempermann, Max-Delbrück-Centrum für Molekulare Medizin, Berlin

Eingereicht am:

Verteidigt am:

DECLARATION

I herewith declare that I have produced this paper without the prohibited assistance of third parties and without making use of aids other than those specified; notions taken over directly or indirectly from other sources have been identified as such. This paper has not previously been presented in identical or similar form to any other German or foreign examination board.

The thesis work was conducted from the 15th of June 2002 to the 30th of September 2006 under the supervision of Prof. Dr. Wieland B. Huttner at The Max Planck Institute of Molecular Cell Biology and Genetics, Dresden.

October 30, 2006

Mojej Mamie

SUMMARY

Neurons, astrocytes and oligodendrocytes of the central nervous system (CNS) arise from a common pool of multipotent neuroepithelial progenitor cells, lining the walls of the neural tube. Within the thickness of the neural tube, progenitor cells extend between the ventricular surface and the basal lamina. They are coupled by adherence and tight junctions and exhibit the apical-basal polarity with the distinct apical and basolateral plasma membrane domains.

Initially, neuroepithelial cells undergo symmetric proliferative divisions, thereby expanding the progenitor pool and determining the size of brain compartments. At the onset of neurogenesis, a subset of progenitors divides asymmetrically, which is accompanied by transformation of neuroepithelial cells into radial glia. Radial glia cells display certain astrocytic characteristics, such as expression of the brain lipid binding protein (BLBP) and astrocyte-specific glutamate transporter (GLAST). Neuroepithelial/radial progenitors in the telencephalon give rise to the third progenitor type, the basal progenitor, which as an intermediate precursor undergoes terminal neurogenic divisions at the basal aspect of the neuroepithelium. As the diversity of cell types in the mammalian CNS arises in the stereotyped temporal sequence, it is necessary to maintain progenitor cells via asymmetric and/or symmetric proliferative divisions throughout development.

Prior to the neural tube closure, neuroepithelial cells initiate expression of *Hes* genes from the bHLH family of translational repressors, which inhibit neuronal differentiation. Upon the switch from proliferation to neurogenesis, expression of *Hes* genes, and thus maintenance of progenitor cells, becomes dependent on Notch signalling, which is then downregulated when cells are selected, through the process called lateral inhibition, to undergo symmetric terminal divisions and enter the differentiation program.

The mechanisms responsible for the maintenance of progenitor cells proliferation are far from being fully understood. The family of Y-box proteins is involved in control of proliferation and transformation in various normal and pathological cellular systems, and therefore was considered as a candidate to exert such a function. Y-box proteins have a capacity to bind DNA and RNA, thereby controlling gene expression from transcription to translation. Particularly, the canine and human Y-box protein 3 (ZONAB/dbpA) were shown to increase proliferation and cell density in mature monolayers of MDCK and MCF-10A epithelial cell lines, respectively. This function is linked with the subcellular localisation: in cells at a low density, ZONAB/dbpA is localised in the nucleus and acts as a transcription factor for genes encoding growth related proteins. With increasing cell density and formation of functional tight junctions, ZONAB/dbpA translocates form the nucleus to the cytoplasm, where it binds to the peripheral junctional protein zonula occludens-1 (ZO-1). Importantly, the pro-proliferative effects of ZONAB/dbpA are counteracted by ZO-1, which is believed to sequester the protein from the nucleus at junctions. Because ZO-1 expression increases upon closure of the neural tube and prior to the onset of neurogenesis, the mouse Y-box protein 3 (MSY3) in the neuroepithelium could be involved in the control of progenitor maintenance in a manner opposite to ZO-1. This study aimed to examine the expression of MSY3 in the developing murine nervous system and elucidate its putative role in regulation of proliferation of progenitor cells.

As presented in this thesis, the MSY3 protein in the developing CNS is expressed solely in progenitor cells and not neurons. Moreover, as shown by two independent approaches: morphologically, i.e. using immunofluorescence and confocal microscopy, and

biochemically, MSY3 expression is downregulated concomitantly with the spatiotemporal progression of neurogenesis,: i) from caudal to rostral along the anteroposterior axis of the brain; ii) from ventral do dorsal; iii) in the telencephalon from rostrolateral to caudomedial; iv) in the cortical hem prior to other regions. In addition, MSY3 was absent from specialised regions of the neural tube, which are largely composed from post-mitotic cells: the floor plate, the roof plate, and the choroid plexus epithelium. The time of downregulation of MSY3 coincides with the lengthening of the cell cycle of progenitor cells.

Furthermore, it was shown here that the downregulation of MSY3 parallels the developmental progression of GLAST induction, and also the onset of active Notch signalling as visualised using the *Hes5*-GFP transgenic mouse, in which expression of GFP from the *Hes5* promoter is entirely dependent on the active Notch. Since the expression of GLAST and activation of Notch characterise the transition from neuroepithelial cells to radial glia, MSY3 appears to be downregulated in radial glia, which undergo mostly asymmetric divisions.

After the onset of neurogenesis, MSY3 expression declines but is still expressed by progenitor cells at variable levels. Nonetheless, the presence of the MSY3 protein did not seem to correlate with a particular division mode of neuroepithelial cells. First, in the *Tis21*-GFP heterozygous knock-in embryos, in which expression of GFP marks all neurogenic, but not proliferating cells, expression of MSY3 was not selectively downregulated in many GFP-positive cells. Second, in the *Hes5*-GFP embryos MSY3 was present randomly in GFP positive and GFP negative cells, the latter presumably being progenitors selected for differentiation.

Given that MSY3 correlates with initial proliferation of neuroepithelial cells and is reduced with the appearance of restricted neurogenic progenitors, it was tempting to speculate that MSY3 positively regulates proliferation, or/and its downregulation is necessary for differentiation. To test this hypothesis, the levels of the MSY3 protein in the progenitors were acutely downregulated or elevated by electroporation of RNAi or MSY3 expression plasmids, respectively. Neither premature reduction of MSY3 in the neuroepithelium (E9.5-E11.5) nor prolonged expression at the developmental time when this protein is endogenously downregulated (E10.5-14.5) did affect proliferation versus the cell cycle exit of progenitors. Knockdown of MSY3 also did not induce prematurely radial glial markers or increase of the abundance of basal progenitors. Moreover, in *Notch1*-deficient progenitors in the cerebellar anlage, which exhibit precocious differentiation, MSY3 was not prematurely downregulated, suggesting that MSY3 also is not an early marker of differentiation.

Interestingly, in preliminary results it was shown that MSY3 is expressed in Dcx-positive transient amplifying precursors in germinal zones of the adult brain, and in EGF-dependent neurospheres.

In attempt to understand the function of MSY3 in neuroepithelial cells, its subcellular localisation was investigated by light and electron microscopy, as well as by differential centrifugation. In the neuroepithelium, the MSY3 protein was distributed throughout the cytoplasm and, unlike ZONAB/dbpA in epithelial cell lines, was not found in the nucleus or at junctions, suggesting that it acts through a distinct mechanism than regulation of transcription. Indeed, differential centrifugation, immunoprecipitation and polysomal analysis performed in this study revealed that the MSY3 protein in the developing embryo, as well as in Neuro-2A cells, is associated with RNA. On a sucrose density gradient MSY3 co-fractionates with ribosomes and actively translating polysomes, suggesting that it might have a role in regulation of translation. However, downregulation or overexpression of

MSY3 in the Neuro-2A cell line did not affect global translation rates. Other researchers suggested that the MSY3 protein has the redundant function with Y-box protein 1 (YB-1). Accordingly, in our system the MSY3 protein could be co-immunoprecipitated with YB-1.

Importantly, developmentally regulated expression of MSY3 is not a hallmark of general translation apparatus, as several other proteins involved in translation, namely eukaryotic initiation factor 4E (eIF4E), fragile X mental retardation protein (FMRP) and YB-1, did not show similar downregulation.

To conclude, this work showed that the MSY3 protein is a marker of proliferation of progenitor cells in the embryonic and adult brain, being absent from neurons, but also from slowly dividing stem and progenitor cells. Discovery of the molecular mechanism by which MSY3 exerts its role in the cell could provide the link between the translational machinery and proliferation.

TABLE OF CONTENTS

ACKNOWLEDGEMENTS

I am thankful to **Wieland Huttner** for giving me the opportunity to work in his laboratory, for his support, and freedom in research.

I would like to thank **Anne-Marie Marzesco**, who had initiated the study on the MSY3 protein, and supported me during my work.

Michele Solimena and **Wolfgang Zachariae** were members of my *Thesis Advisory Committee*, and contribute to this project with constructive suggestions.

Karl Matter has provided an antibody against the MSY3 protein.

I am grateful to **Verdon Taylor** and members of his laboratory for teaching me neurosphere cultures and for invaluable discussions. From **Onur Basak** I have received the *Hes5*-GFP and cerebellar *Notch1* knockout embryos.

I would like to acknowledge **Karla Neugebauer** and **Christian Eckmann** for great help with interpreting the data and designing experiments.

Michaela Wilsch-Bräuninger did the EM analysis of MSY3.

Special thanks to **Klaus Fabel**, who encouraged me to explore adult neurogenesis, performed the staining for MSY3 in postnatal brains and did the confocal analysis.

I would like to express my gratitude to **Lilla Farkas**, who introduced me in the world of neurogenesis and was a supportive friend during my stay in Dresden.

Big thanks to the Animal Facility and Light Microscopy Facility, especially to **Jan Peychel**, **Jeremy Sanderson**, **Jussi Helppi**, **Anke Münch-Wuttke** and **Kerstin Menzer**.

Thanks to **Jeremy Pulvers**, who read through my thesis and help me with understanding the mysteries of articles in English.

Last, but not least, I would like to thank colleagues in the laboratory and the Institute for good atmosphere, helpful discussions and technical help.

1 INTRODUCTION

The mammalian telencephalon, which gives rise to the cerebral cortex and basal ganglia, is a venue of motor coordination, emotions, memory, higher cognition and consciousness. The final shape, size and organisation of the brain is tightly linked with the birth and assembly of different cell types in high-order systems during embryonic development and the early postnatal period. Initially, to generate the cellular diversity and pattern, proliferation and differentiation of progenitors must be strictly controlled, which is achieved by integrating environmental and intrinsic cues. Here, I focused on the intrinsic mechanisms regulating proliferation and the cell cycle exit of progenitor cells. In the second part of the *Introduction*, I reviewed current background on the Y-box family of nucleic acid binding proteins, which are implicated in the control of proliferation in various cellular systems.

1.1 Neurogenesis in the central nervous system

1.1.1 Origin and organisation of the neural tube

Neurons, astrocytes and oligodendrocytes of the central nervous system arise from a common pool of multipotent progenitor cells, which originally derive from an unspecified cellular sheet of the ectoderm. Subsequent tissue movements result in bending of the neural plate and closure of the neural groove, thereby forming the neural tube (Colas and Schoenwolf, 2001). The neural tissue is patterned along the anteroposterior axis into distinct compartments (Figure I) (reviewed in: Rallu et al., 2002; Wilson and Houart, 2004). The anterior neural tube expands into prominent vesicles, which represent anlage of the forebrain (prosencephalon), the midbrain (mesencephalon) and the hindbrain (rhombencephalon). The neural tube caudally to the hindbrain gives rise to the spinal cord. The forebrain subdivides further into the dorsally positioned telencephalon and eyes, the ventrally positioned hypothalamus and the more caudally located diencephalon. Specification, maintenance and pattering of the CNS divisions rely on the interplay between various signalling pathways and differential cellular response to the same signal over time (Ciani and Salinas, 2005; Liu and Niswander, 2005; Rallu et al., 2002; Rao and Jacobson, 2005; Wilson and Houart, 2004). In the brain, each structure undergoes additional pattering and morphogenesis, which in the dorsal telencephalon leads to emergence of the cortex, and ventrally three distinct eminences: the medial and lateral ganglionic eminences (MGE and LGE) anteriorly, and the caudal ganglionic eminence (CGE) posteriorly (Fuccillo et al., 2006; Rallu et al., 2002).

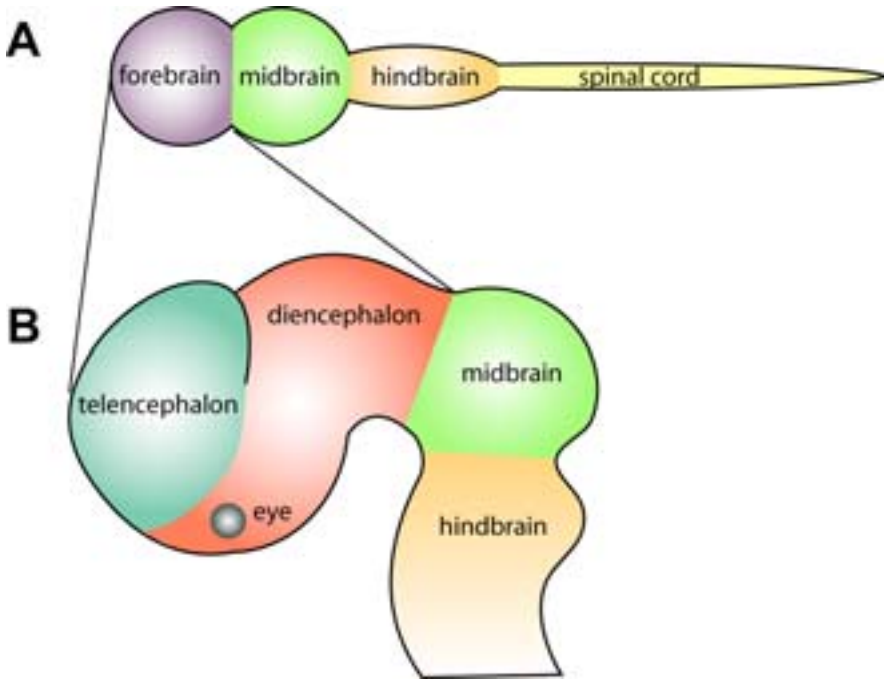

Figure I. Regionalisation of the neural tube. (**A**) Schematic representation of the neural plate of the mouse embryo at around embryonic day 8 (E8). The neural plate subdivides anteriorly into forebrain and midbrain, and caudally into hindbrain and spinal cord. (**B**) Side view of the brain of mouse embryo at E10. Forebrain undergoes further specification into the rostral telencephalon and caudally positioned diencephalon. Modified from Rallu et al., 2002.

1.1.2 Division modes of progenitor cells: how to generate cellular diversity

Stem cells can undergo three types of divisions in terms of the fate of daughter cells: i) a symmetric proliferative division, which generates two daughter stem cells; ii) a symmetric terminal division, which generates two postmitotic cells; and iii) an asymmetric, self-renewing division, which produces one postmitotic cell, whereas the other daughter continues to proliferate (Morrison and Kimble, 2006). Prior to the onset of neurogenesis, neuroepithelial cells undergo proliferative symmetric divisions, thereby establishing the original pool of progenitors available to generate neurons at the onset of neurogenesis (Bayer and Altman, 1991). This type of divisions is believed to determine the size of brain compartments, particularly of the cortex (Caviness et al., 1995; Rakic, 1995). Subsequently, a subset of neuroepithelial cells switch to asymmetric and terminal neurogenic divisions. All three types of divisions coexist in the neural tube throughout the entire period of neurogenesis, with increase of neurogenic terminal divisions as neurogenesis proceeds (Cai et al., 2002; Kornack and Rakic, 1998; Mione et al., 1997; Reznikov et al., 1997; Takahashi et al., 1996). Notably, most of neurons in the rodent telencephalon is produced by symmetric terminal divisions (Haubensak et al., 2004).

In addition to spatial specification of progenitors, the variety of cell types in the mammalian brain arises in the stereotyped temporal sequence. Therefore, the maintenance of progenitors throughout development, through symmetric proliferative or asymmetric divisions, is essential for generation of full diversity of neuronal and glial cells. Neurons emerge primarily during the embryonic period, while most glia are produced after birth (Bayer and Altman, 1991). Among glial lineages, generation of astrocytes precedes oligodendrogenesis (Parnavelas, 1999). Particularly in the cortex, the time of birth of projection (pyramidal) neurons is linked with specification of laminar fate. The earliest born neurons are designed for the subplate and deep layer VI, whereas the later born neurons

intercalate between these two layers and occupy progressively more superficial layers V-II (Berry and Rogers, 1965). Moreover, spatial, but also temporal, origin of interneurons predicts their physiological profile, subtype, and layer positioning in the mature cortex (Butt et al., 2005; Wonders and Anderson, 2006).

The pattern of generation of distinct neuronal and glial cells can be recapitulated in cultures of isolated cortical cells (Qian et al., 2000; Shen et al., 2006). Importantly, these studies provided an insight into the division modes and potential of individual progenitors. The multipotent stem cells, which produce large clones containing neuronal and glial progeny, constitute around 10% of progenitor cells isolated from cortices at the onset of neurogenesis (Davis and Temple, 1994; Qian et al., 1998; Qian et al., 2000). These stem cells give rise to more restricted progenitors, which undergo stereotyped modes of divisions to generate neurons or glia. Glioblasts are generated after the majority of neuroblasts and undergo a series of proliferative divisions before differentiation (Qian et al., 2000).

1.1.3 Progenitor cell types during the neurogenic period

Neuroepithelial cells

Initially, the neuroepithelial tissue is a one-cell-thick layer of collumnar cells. As the neural tube closes, elongation and proliferation of the neuroepithelial cells result in thickening of the walls of the neural tube and pseudostratified organisation of the neuroepithelium. The neuroepithelial cells inherit the apical-basal polarity of the ectoderm, extending from the ventricular, apical surface of the neural tube towards the basal lamina. Within the thickness of the neural tube, the nuclei of neuroepithelial cells undergo a to-and-fro movement, which is synchronised with the cell cycle, accordingly called interkinetic nuclear migration (Sauer, 1935) (Figure II). Neuroepithelial cells during mitosis round up at the apical side of the neural tube, and during G_1 phase the nuclei of daughter cells migrate basally to undergo S phase. During G_2 the nuclei migrate back to the apical surface.

Radial glia

During the neurogenic interval, three distinct, yet related, types of progenitors can be distinguished (reviewed in: Campbell, 2005; Gotz and Huttner, 2005; Guillemot, 2005; Huttner and Kosodo, 2005) (Figure II). The early neuroepithelial cells give rise to the earliest-born neurons. As neurons migrate basally and accumulate forming neuronal layers, the progenitor cell bodies become separated from the pia. This process is accompanied by transformation of neuroepithelial cells into radial glia, which differ from neuroepithelial cells ultrastructurally as containing glycogen granules, and express a set of markers characteristic to differentiated astrocytes, such as the astrocyte-specific glutamate transporter (GLAST), brain lipid binding protein (BLBP), and Tenascin C (Anthony et al., 2004; Campbell and Gotz, 2002; Gotz and Barde, 2005; Hartfuss et al., 2001; Malatesta et al., 2003). Primate radial glia express also the glia-fibrillary acidic protein (GFAP). Radial glia maintain the connection to the pial surface (Misson et al., 1988; Wilson, 1983). In the dorsal telencephalon, radial glia, directly and indirectly, are the major source of projection neurons, whilst in the basal telencephalon, the extent to which they contribute to neuronal production remains controversial (Anthony et al., 2004; Gotz and Barde, 2005; Gotz and Huttner, 2005; Malatesta et al., 2003; Noctor et al., 2002). Time-lapse studies revealed that the majority of radial glia cells divide asymmetrically at the apical surface of the neuroepithelium (Chenn and McConnell, 1995; Miyata et al., 2001; Miyata et al., 2004;

Noctor et al., 2001; Noctor et al., 2004; Tamamaki et al., 2001). Several studies indicated that all cells in the ventricular zone, except basal progenitors (see below), are radial glia, i.e. after the onset of neurogenesis all neuroepithelial cells acquire radial glia fate (Anthony et al., 2004; Hartfuss et al., 2001; Noctor et al., 2002). However, other studies showed that during the neurogenic interval, two populations of radial progenitors coexist in the ventricular zone: i) radial glia cells that span the entire neocortical wall and maintain contacts with the ventricular and pial surfaces; and ii) short neural precursors, equivalent to neuroepithelial cells, which possess a basal process of variable length that do not contact the pia (Gadisseaux et al., 1992; Gal et al., 2006; Koch, 2000). These two cell populations show differential activity of reporter promoters, indicating distinct molecular characteristics (Gal et al., 2006). Radial glia, except being neuronal progenitors, have also a scaffolding function and guide neuronal migration (Bentivoglio and Mazzarello, 1999; Gadisseux et al., 1990; Haubst et al., 2006; Noctor et al., 2001; Rakic, 1972). After the period of neurogenesis they transform into astrocytes (Misson et al., 1988; Voigt, 1989).

Basal progenitors

Neuroepithelial/radial glial cells give rise to the third progenitor type, the basal progenitor, which as an intermediate precursor undergoes symmetric neurogenic divisions distantly from the ventricular surface, i.e. at the basal side of the ventricular zone (Haubensak et al., 2004; Miyata et al., 2004; Noctor et al., 2004). In rare cases (10%) these cells expand for one additional division (Noctor et al., 2004). Basal progenitors are present already at the onset of neurogenesis (Haubensak et al., 2004), and in the mid-neurogenesis form the subventricular zone (SVZ) (Bayer and Altman, 1991), contributing to a large fraction of cortical neurons (Haubensak et al., 2004; Miyata et al., 2004). Whereas radial glia and neuroepithelial cells are ubiquitous progenitors throughout the developing CNS, the SVZ is confined to the telencephalon, conceivably to answer a demand for large neuronal production (Haubensak et al., 2004; Smart et al., 2002). Moreover, basal progenitors lose the ventricular process (Miyata et al., 2004), and exhibit different molecular markers, such as downregulation of nestin and Pax6 and expression of transcription factors Tbr2 (Englund et al., 2005), Cux1 and Cux2 (Nieto et al., 2004; Zimmer et al., 2004) and non-coding RNA Svet1 (Tarabykin et al., 2001).

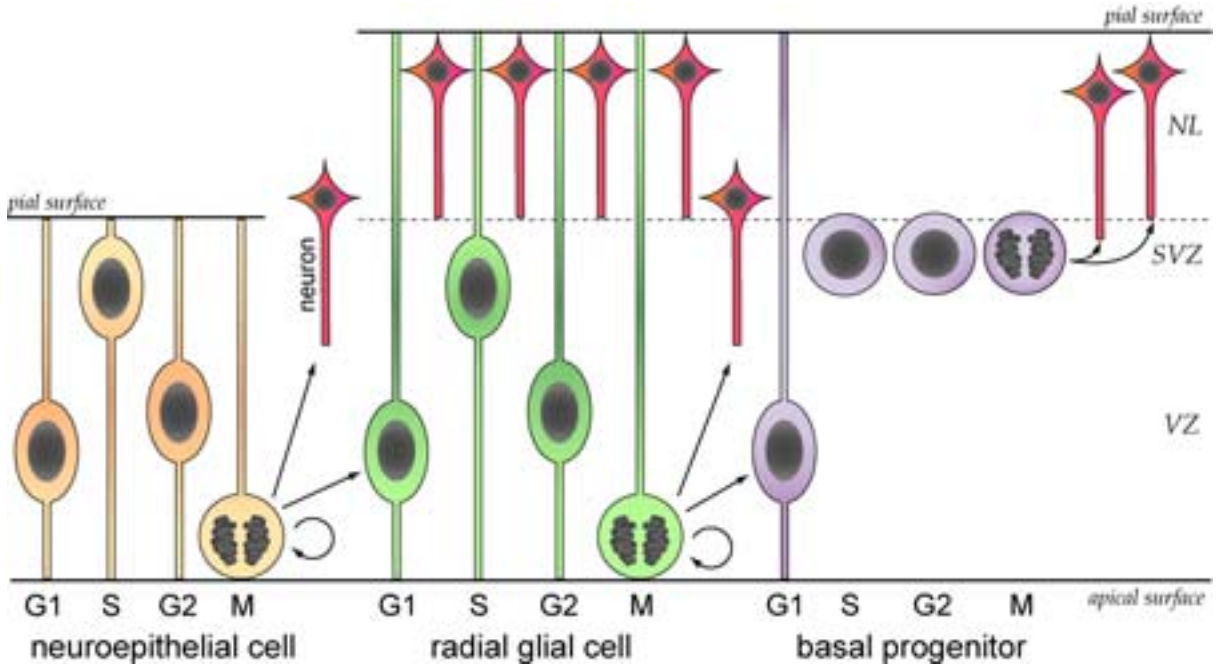

Figure II. Several types of progenitors generate neurons in the mammalian CNS. Before and at the beginning of neurogenesis, neuroepithelial cells (yellow, left), which extend from the ventricular, apical, surface (towards bottom) and basal lamina (up), form the ventricular zone (*VZ*). With accumulation of neurons in the neuronal layer (*NL*), a subset of neuroepithelial cells transforms into radial glia (green, middle) exhibiting characteristics of neuroepithelial and glial cells. Neuroepithelial and radial glial progenitors undergo interkinetic nuclear migration, and divide at the apical surface either symmetrically in a proliferative manner, or asymmetrically to generate a progenitor cell which remains in the ventricular zone, and a cell destined to the neuronal lineage: a neuron (red), which migrates basally to the neuronal layer, or a basal progenitor (light blue, right), which moves to the subventricular zone (*SVZ*) and divides symmetrically giving rise to two neurons. Modified from Gotz and Huttner, 2005; Guillemot, 2005.

1.1.4 Cell cycle dynamics: proliferation versus differentiation

Histogenesis of the developing CNS is tightly linked with the division mode and cell cycle parameters (reviewed in: Caviness et al., 2003; Caviness et al., 1995; Cremisi et al., 2003; Ohnuma and Harris, 2003). The fraction of progenitors that exit the cell cycle increases as neurogenesis proceeds (Takahashi et al., 1996). Moreover, in temporal and spatial correlation with neurogenesis, the average cell cycle length of progenitor cells constantly increases from approximately 8 h at the onset of neurogenesis to about 18 h at the end of the neurogenic period (Takahashi et al., 1995). This difference is primarily accounted for by the lengthening of G_1 phase, which in the course of neurogenesis increases fourfold (Takahashi et al., 1995). Although early reports suggested that the cell cycle length is homogenous in the ventricular zone at the time when neurogenesis is peaking and neurogenic and proliferative divisions coexist (Cai et al., 1997a), other studies indicated a variability of cell cycle parameters among progenitors (Calegari et al., 2005b; Hartfuss et al., 2001; Reznikov et al., 1997). Notably, progenitors which undergo neurogenic divisions exhibit a significantly longer cell cycle than the proliferative population (Calegari et al., 2005b).

At the molecular level, progenitors which generate neurons, in asymmetric or symmetric divisions, express the anti-proliferative gene *Tis21/BTG2/PC3* (Haubensak et al., 2004; Iacopetti et al., 1994; Iacopetti et al., 1999), here for convenience referred to as *Tis21*. The Tis21 mRNA is expressed only during G_1 phase, prior to the cell division, and the protein is inherited by daughter cells. *In vitro*, Tis21 induces cell cycle arrest in G_1 by inhibiting the transcription of cyclin D1 and delaying the expression of cyclin E and cyclin dependent

kinase 4 (Cdk4) (Guardavaccaro et al., 2000; Lim et al., 1998). Tis21 also inhibits degradation of cyclin A and B1, and binds to Cdc2/Cdk1 (cell division cycle 2), which may lead to the failure of mitotic exit (Lim, 2006; Ryu et al., 2004). Overexpression of Tis21/PC3 in a transgenic mouse model leads to prematurely increased neurogenesis at the expense of progenitor proliferation (Canzoniere et al., 2004).

The cyclin dependent kinase inhibitor $p27^{Kip1}$ is a critical part of the internal regulatory mechanism controlling proliferation and differentiation of progenitor cells. Its expression in the ventricular zone is regulated coordinately with the progression of neurogenesis (Delalle et al., 1999). Similarly, $p27^{Kip1}$ gradually accumulates in cultured proliferating oligodendrocyte progenitors (Durand et al., 1997). It has been proposed that when the concentration of $p27^{Kip1}$ reaches an appropriate level it causes cell cycle exit of progenitors and differentiation (Durand and Raff, 2000). Mice lacking $p27^{Kip1}$ show an increased body size and enlarged brains (Fero et al., 1996; Nakayama et al., 1996). Specifically, less progenitors exit the cell cycle during mid-neurogenesis, resulting in an increase in late born cortical neurons and glial cells (Goto et al., 2004). Overexpression of $p27^{Kip1}$ leads to an increase in cell cycle exit of progenitors during mid-neurogenesis in the cortex, hence augmenting neuronal production designed to deeper layers (Tarui et al., 2005), and in the retina drives progenitors out of the cell cycle, hence promotes early cell fates at the expense of later generated bipolar neurons and Müller glia (Dyer and Cepko, 2001). In *Xenopus*, $p27^{Kip1}$ is sufficient to increase neurogenesis when overexpressed, and is indispensable for neuronal differentiation (Vernon et al., 2003). Other antiproliferative proteins such as $p57^{Kip2}$ and $p19^{Ink4d}$, as well as p53 and p73, might play complementary roles in governing differentiation of neural and glial progenitors (Billon et al., 2004; Coskun and Luskin, 2001; Cunningham et al., 2002; Dyer and Cepko, 2001).

It has to be mentioned, however, that cell cycle regulators, such as $p27^{Kip1}$ or Tis21, have multiple roles and modes of action. Therefore, not all effects observed upon manipulation of levels of cell cycle regulators act solely on cell cycle progression (Canzoniere et al., 2004; Lim, 2006; Nguyen et al., 2006; Vernon et al., 2003). It has been suggested, nevertheless, that lengthening of G_1 phase *per se* might lay upstream of cell differentiation, rather than being its consequence. Indeed, application of a Cdk inhibitor, which increased the G_1 length without blocking of the cell cycle, was shown to induce premature neurogenesis (Calegari and Huttner, 2003).

1.1.5 Notch and bHLH transcription factors: the master and commanders

Multiple basic helix-loop-helix (bHLH) transcription factors are the major intrinsic regulators of neurogenesis (Bertrand et al., 2002; Kageyama et al., 2005; Ross et al., 2003). There are two classes of bHLH genes: the repressor and activator types.

Proneural bHLH genes

The activator bHLH genes are known as a family of proneural genes, and include *Mash, Math* and *Neurogenin*, which are homologues of the *Drosophila achete-scute* complex and *atonal*. The proneural genes are expressed at low levels by progenitors, and transient increase in their expression mediates commitment of multipotent cells to the neuronal lineage; consistently, upon misexpression they induce ectopic neurons (Blader et al., 1997; Kim et al., 1997; Ma et al., 1996; Mizuguchi et al., 2001; Turner and Weintraub, 1994). The proneural factors not only induce expression of pan-neuronal genes, but simultaneously inhibit glial fates (Nieto et al., 2001; Tomita et al., 2000). Moreover, activator bHLH genes are involved in the specification of progenitors to a particular subtype identity and are

required for neuronal differentiation (Ben-Arie et al., 1997; Cau et al., 2000; Gowan et al., 2001; Kay et al., 2001; Parras et al., 2002; Scardigli et al., 2001). The proneural genes bind to their target promoters as heterodimers formed with ubiquitous bHLH E proteins, thereby activate a cascade of neuronal differentiation genes, such as other bHLH factors of the *NeuroD* family, which are expressed in immature neurons (Farah et al., 2000; Lee et al., 1995). Expression of proneural genes causes cell cycle exit, presumably via induction of cell cycle inhibitors, such as $p27^{Kip1}$ (Farah et al., 2000).

Repressor-type bHLH genes: *Hes* and *Id* families

In the neural progenitor cells, the activity and transcription of proneural genes is repressed by *Hes/Her* bHLH factors, homologues of *Drosophila hairy* and *Enhancer of split* [*E*(*spl*)]. In the nervous system three *Hes* genes are expressed: *Hes1*, *Hes3* and *Hes5*; and two *Hes*-related genes *Hesr1/Hey1* and *Hesr2/Hey2* (Kageyama et al., 2005). The loss of *Hes* genes leads to precocious exit of progenitors from the cell cycle and their differentiation into neurons *in vivo* (Cau et al., 2000; Hatakeyama et al., 2004; Ishibashi et al., 1995; Ohtsuka et al., 1999) and *in vitro* (Ohtsuka et al., 1999; Ohtsuka et al., 2001). Moreover, in double *Hes1/Hes5* and triple *Hes1/Hes5/Hes3* knockout mice occurs massive differentiation of progenitors (Hatakeyama et al., 2004). It has to be emphasised that in these mutant mice the neuroepithelium initially forms properly, thus the neural stem cells change their characteristics over time from *Hes*-independent to *Hes*-dependent, just prior to the closure of the neural tube. Embryos lacking single *Hes* genes exhibit milder phenotypes (Ishibashi et al., 1995; Ohtsuka et al., 1999), indicating that functions of Hes proteins are redundant. Not only are the *Hes* genes essential for maintenance of progenitors, but upon misexpression of *Hes* and *Hesr* genes, neuronal differentiation is inhibited and progenitors remain as radial glial cells (Hirata et al., 2000; Ishibashi et al., 1994; Ohtsuka et al., 2001; Sakamoto et al., 2003).

The second group of repressors are Id (Inhibitor of DNA binding) helix-loop-helix factors (Ross et al., 2003). They miss the basic region, therefore are not capable of DNA binding. Id proteins form heterodimers with E proteins, thus sequestering them from bHLH factors and repressing differentiation into neurons and oligodendrocytes. In addition, Ids stimulate cell cycle progression by relieving the transcription factor E2F from retinoblastoma (Rb) mediated repression.

Notch signalling and its role in the maintenance of progenitors

An essential ability of the proneural proteins is to restrict their own activity to single cells within the neuroepithelium in the process termed *lateral inhibition*, which is mediated by the Notch signalling pathway (Artavanis-Tsakonas et al., 1995; Louvi and Artavanis-Tsakonas, 2006; Yoon and Gaiano, 2005). In mammals, there are four *Notch* genes, which are involved in maintenance of the progenitor pool. Notch receptors are activated by the interaction with ligands Delta and Jagged/Serrate on the surface of adjacent cells. Notably, Delta and Jagged are among the targets of proneural genes (Casarosa et al., 1999; Chitnis and Kintner, 1996; Horton et al., 1999).

Notch and Delta are large single-pass transmembrane proteins rich in EGF and Ankyrin repeats. Binding of the ligand initiates a series of proteolytic cleavages of Notch that leads to the release of the inrtacellular domain of the receptor and its nuclear translocation (Schroeter et al., 1998). Once in the nucleus, the Notch intracellular domain converts the ubiquitous transcription repressor RBP-Jκ/CBP1 complex (a homologue of *Drosophila suppressor of hairless*) into an activator, leading to transcription of target genes (Fortini and Artavanis-Tsakonas, 1994; Honjo, 1996; Kato et al., 1997). In neural progenitors, Notch

controls expression of the *Hes1* and *Hes5* genes, which in turn confer the ability of Notch to inhibit neuronal differentiation (Ohtsuka et al., 1999). It is important to note, however, that *Hes1* is likely to be regulated also by other signalling cascades and *Hes3* expression is largely Notch-independent (Hatakeyama et al., 2004; Hitoshi et al., 2002; Hitoshi et al., 2004; Ohtsuka et al., 1999).

The activities of proneural genes and Notch are combined into a negative feedback loop. The expression of a ligand in a cell committed for differentiation activates the Notch signalling cascade in neighbouring cells, resulting in expression of *Hes/Her* inhibitory genes and a block of differentiation. Thus, single progenitors can be selected for differentiation, whereas others keep proliferating. In keeping with its role in activation of inhibitory bHLH genes, sustained induction of Notch pathway by overexpressing Delta blocks differentiation, while upon removal of Notch signalling with dominant negative Delta all progenitors exit the cell cycle and differentiate into neurons (Henrique et al., 1997). Similarly, removal of *Notch-1* or *RBP-J* genes drives progenitors into premature differentiation (de la Pompa et al., 1997; Lütolf et al., 2002), whilst overexpression of activated Notch results in an expanded pool of progenitors and decrease in neuronal production (Lardelli et al., 1996). Consistently, the function of Notch is indispensable for stem cell renewal *in vitro* (Alexson et al., 2006; Hitoshi et al., 2002), however, as in *Hes* mutant embryos, formation and maintenance of early neuroepithelial cells is not hampered by removal of Notch signalling *in vivo* (de la Pompa et al., 1997; Hatakeyama et al., 2004) and *in vitro* (Hitoshi et al., 2002).

Onset of *Notch1* expression proceeds in a pattern spatiotemporally correlated with neurogenesis, when progenitor cells undergo asymmetric divisions (Hatakeyama and Kageyama, 2006). Notch signalling is thought to keep a pool of cycling progenitors available for the generation of later cell types. In agreement with this hypothesis, upon transient expression of activated Notch, progenitors resume generating neurons destined to the appropriate later fate once Notch signalling is relieved (Mizutani and Saito, 2005). Moreover, constitutive activation of the Notch pathway in progenitors transforms them into radial glia, which postnatally differentiate into astrocytes (Dang et al., 2006; Gaiano et al., 2000). It has been speculated that Notch signalling supports the generation of distinct progenitor subtypes (Yoon and Gaiano, 2005), and promotes asymmetric divisions of progenitor cells (Hatakeyama and Kageyama, 2006).

1.1.6 Polarity of progenitor cells and asymmetric division

Neuroepithelial and radial glia cells are coupled via adherens junctions (Aaku-Saraste et al., 1996; Chenn et al., 1998) and contribute to the formation and maintenance of the basal lamina, which separates the neuroepithelium from the surface mesoderm (Hatakeyama et al., 2004; Haubst et al., 2006; Thomas and Dziadek, 1993). These features provide the foundation for histogenesis: loss of progenitors leads to the disruption of inner and outer barriers of the neural tube and spilling of neurons into the lumen and surrounding tissues (Hatakeyama et al., 2004; Junghans et al., 2005).

As their predecessors epithelial cells, neuroepithelial cells are polarised, showing distinct basolateral and apical domains, whose integrity is maintained by tight junctions (Aaku-Saraste et al., 1996; Aaku-Saraste et al., 1997; Chenn et al., 1998). With the neural tube closure and the onset of neurogenesis, the neuroepithelium downregulates some of the epithelial features. The tight junctions undergo remodelling, such as the loss of a structural component occludin and of the paracellular barrier (Aaku-Saraste et al., 1996), which is accompanied by downregulation of polarised transport of selected apical membrane proteins (Aaku-Saraste et al., 1997). Moreover, at adherens junctions E-cadherin is replaced

by N-cadherin (Nose and Takeichi, 1986). Nevertheless, progenitor cells express a panel of tight junctional proteins, namely claudin-10, 15 and 18, as well as show ultrastructural features of tight junctions (Hatakeyama et al., 2004). Interestingly, zonula occludens 1 (ZO-1), a peripheral tight junction protein, appears to be upregulated at the onset of neurogenesis (Aaku-Saraste et al., 1996).

It has been proposed that proliferative or asymmetric divisions of progenitor cells rely on the cleavage plane orientation with respect to the apical plasma membrane and junctions (Chenn and McConnell, 1995; Huttner and Brand, 1997; Kosodo et al., 2004; Wodarz and Huttner, 2003). Asymmetric cell division resulting from unequal distribution of cell fate determinants upon mitosis has been extensively studied in *C. elegans* and *Drosophila* (Betschinger and Knoblich, 2004; Wodarz, 2005; Yu et al., 2006). In *Drosophila* neuroblasts, the conserved complex PAR3/PAR6/aPKC (Partitioning defective/Atypical Protein Kinase C) is localised to the apical cell cortex and governs polarised distribution of differentiation determinants Numb and homeobox domain transcription factor Prospero to the basal pole, as well as the positioning of the mitotic spindle, such that division occurs in the apical-basal axis. Notably, Numb is a negative regulator of Notch signalling (Schweisguth, 2004).

In vertebrates, the apical domain of neuroepithelial cells also harbours homologues of the PAR3/PAR6/aPKC complex (Manabe et al., 2002). Moreover, mammalian Numb has been shown to form an apical crescent in neural progenitors (Cayouette and Raff, 2003; Cayouette et al., 2001). Despite that the majority of mitotic divisions occurs perpendicular to the ventricular, i.e. apical, surface of the neuroepithelium (Kosodo et al., 2004; Lyons et al., 2003; Reznikov et al., 1997), in radial progenitors the apical plasma membrane constitutes a minute fraction of the total plasma membrane and can be distributed to one daughter cell even upon vertical cleavage (Kosodo et al., 2004). Notably, in neurogenic progenitors the cleavage plane bypasses the apical plasma membrane, whereas in proliferative progenitors the cleavage plane divides the apical plasma membrane between daughter cells (Kosodo et al., 2004).

Together, by analogy to *Drosophila*, it has been suggested that the loss of the apical plasma membrane, and possibly junctional complexes, is associated with cell differentiation (Gotz and Huttner, 2005; Huttner and Brand, 1997; Kosodo et al., 2004). In support, basal progenitors before the final division lose the apical attachment (Miyata et al., 2004). Junctional complexes also cluster proteins involved in the control of proliferation and tissue morphogenesis, such as ZO-1, AF-6, PTEN, Cdc42, or β-catenin (Matter and Balda, 2003), most of which are expressed in neural progenitor cells (Aaku-Saraste et al., 1996; Cappello et al., 2006; Chenn et al., 1998; Zhadanov et al., 1999). Loss-of-function or gain-of-function experiments with these molecules showed complex roles of the apical domain in regulation of progenitor maintenance and identity.

The loss of the apical-basal polarity and junctions observed in mice deficient in the *Lgl1* gene, a mammalian homologue of *Drosophila lethal giant larvae*, is coupled with mislocalisation of Numb and hyperproliferation of progenitors (Klezovitch et al., 2004). It has to be mentioned, however, that the role of Numb in Notch signalling and neurogenesis in mammals is tangled (Yoon and Gaiano, 2005). In turn, removal of Cdc42 specifically in the cortex results in disorganisation of the apical components of ventricular zone progenitors, namely the loss of PAR3/aPKC complex, β-catenin, actin and a stem cell marker prominin-1 (Cappello et al., 2006), which in the wild-type neuroepithelium localises to the apical plasma membrane (Fargeas et al., 2006; Weigmann et al., 1997). These events are paralleled by ventricular detachment of progenitors, and, as a consequence, their gradual conversion to basal progenitors (Cappello et al., 2006). The most remarkable phenotype is

associated with manipulation of β-catenin, which has a dual role: as a structural component of adherens junctions and as a transducer of the Wnt signalling pathway. Constitutive activation of β-catenin in the neuroepithelium leads to dramatic expansion of neural progenitors (Chenn and Walsh, 2002; Chenn and Walsh, 2003; Zechner et al., 2003), whereas loss of β-catenin results in precocious neurogenesis (Zechner et al., 2003).

With regard to the basal domain of radial progenitors, it was proposed that asymmetric inheritance of a basal process upon mitosis and, accordingly, an attachment to the basal lamina, underlies an asymmetric fate of daughter cells (Fishell and Kriegstein, 2003; Miyata et al., 2001). However, loss of the contact to the basal lamina by progenitor cells in the laminin γ1III4 knockout mice hampers neuronal migration and differentiation, but does not influence progenitor proliferation or net neuronal production (Haubst et al., 2006), thus suggesting that signals from the basal lamina are not controlling progenitor divisions directly.

1.1.7 Neurogenesis in the adult brain

Although most of the neurons are born during the embryonic period, neurogenesis persists in restricted regions of the adult brain: the striatal subventricular zone (SVZ) of the lateral ventricle and the subgranular zone (SGZ) of the hippocampal dentate gyrus (reviewed in: Alvarez-Buylla and Lim, 2004; Alvarez-Buylla et al., 2002; Emsley et al., 2005; Kempermann et al., 2004) (Figure III).

Subventricular zone

In rodents, neurogenesis in the SVZ is linked with olfaction. Cells born in the SVZ migrate in chains ensheathed by glial cells to the olfactory bulb where they differentiate into interneurons (Lois and Alvarez-Buylla, 1994; Lois et al., 1996). Migratory neuroblasts form the so-called rostral migratory stream (RMS). During the first two postnatal weeks, mouse ventricular zone radial glia transform into multiciliated ependymal cells lining the ventricle and SVZ astrocytes (Tramontin et al., 2003). It is a subpopulation of SVZ astrocytes, as descendants of embryonic radial glia, that functions as stem cells in the adult brain (Doetsch et al., 1999a; Doetsch et al., 1999b; Garcia et al., 2004; Tramontin et al., 2003). Slowly dividing stem cells give rise to rapidly proliferating transient amplifying cells, which form clusters scattered along neuroblasts of the RMS (Doetsch et al., 1999a; Doetsch et al., 1997) (Figure III A, bottom panel). Intriguingly, some of SVZ astrocytes contact the ventricle and extend a short primary cilium into the lumen, hence it was speculated that ventricular contact may underly self-renewal of adult SVZ stem cells (Doetsch et al., 1999b; Tramontin et al., 2003).

It should be noted that although chain migration of neuroblasts born in the SVZ has been described in the macaque adult brain (Kornack and Rakic, 1999), the human germinal zone is distinct. It contains a subependymal ribbon of dividing astrocytes, which have properties of stem cells *in vitro*, yet the RMS is absent (Sanai et al., 2004).

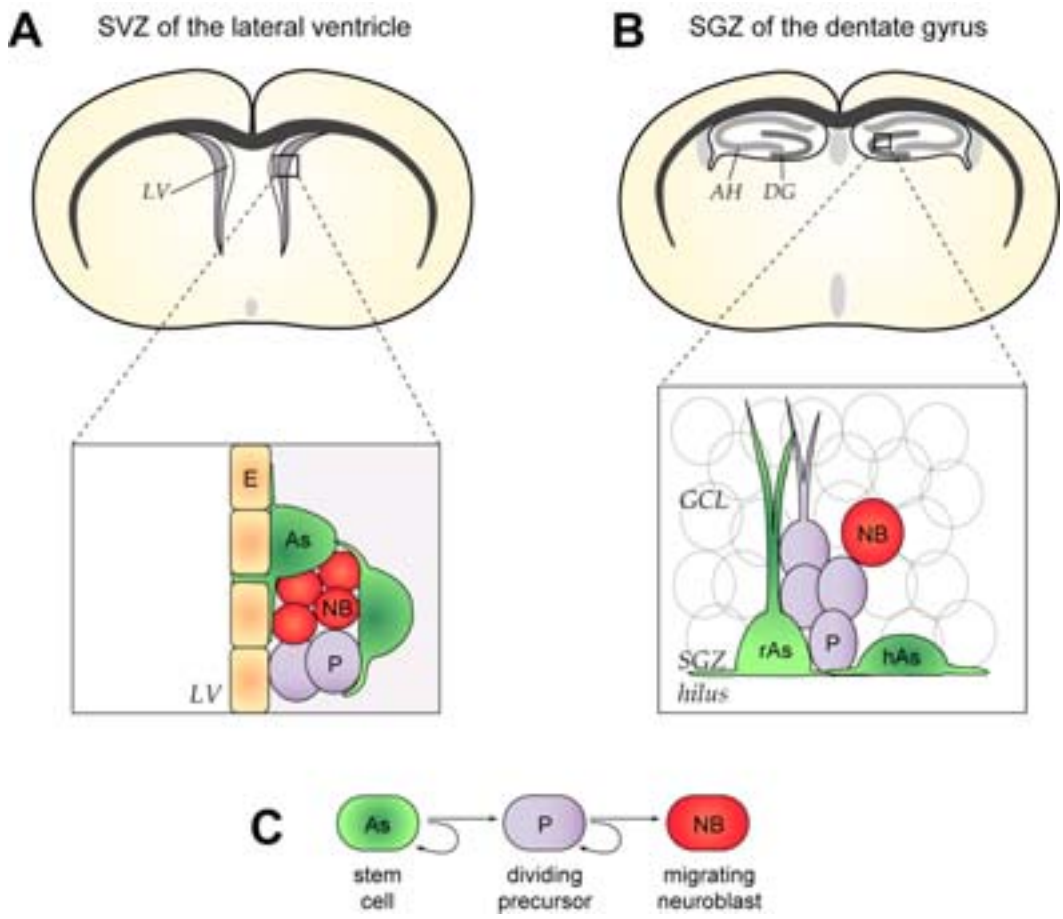

Figure III. Organisation of neurogenic niches in the adult brain. (**A**) Cross-section of the adult mouse brain rostrally indicates the position of the lateral ventricle (*LV*); the expanded panel illustrate schematically the composition and architecture of the subventricular zone (*SVZ*) (bottom panel). Above the ependymal layer (*E*), slowly dividing astrocytes (*As*, green) form tunnels, in which chains of neuroblasts (*NB*, red) migrate to the olfactory bulb. Scattered clusters of rapidly dividing precursors are found along the network of chains (*P*, light blue). Occasionally, astrocytes extend a process between ependymal cells to contact the ventricle. (**B**) Caudal cross-section through the mouse brain indicates the position of the hippocampus and its subdivisions: the Ammon's horn (*AH*) and the dentate gyrus (*DG*). The subgranular zone (*SGZ*) located at the base of granular cell layer (*GCL*) nests radial astrocytes (*rAs*, green), which extend long processes that penetrate the GCL, and short tangential astrocytes lying parallel to the GCL (*hAs*). Astrocytes in the SGZ enwrap and isolate from the hilus neuronal precursor cells (*P*, light blue), and maturating neuroblasts (*NB*, red). Granule neurons are shown as open grey circles. (**C**) The lineage of both adult germinal zones comprises slowly dividing stem cells with characteristics of astrocytes, which generate transient amplifying precursors that divide and mature into new neurons. Modified from Alvarez-Buylla et al., 2002; Seri et al., 2004.

Dentate gyrus of the hippocampus

The hippocampus is derived from the medial part of the developing cortex, i.e. the archicortex, which folds inwards acquiring a sea horse shape (Figure III B). Projection pyramidal neurons of the hippocampus localise in the Ammon's horn (*Cornu Ammonis*) and arise from the embryonic VZ and SVZ, similarly as in other parts of the cortex (Altman and Bayer, 1990b; Altman and Bayer, 1990c). At the end of cortical neurogenesis, a subpopulation of SVZ progenitors build the outer shell of the granular cell layer (GCL) of the U-shaped (or V-shaped) dentate gyrus opposing the Ammon's horn pyramidal layer (Altman and Bayer, 1990a). Postnatally, the interiorly located polymorph layer of the dentate gyrus, also referred to as the *hilus*, nests proliferating derivatives of the SVZ progenitors which eventually, in the juvenile period, settle at the base of the granule cell layer to form the subgranular zone (SGZ) (Figure III B, bottom panel). These cells in the adult brain contribute to continuous production of new granule neurons in an outside-in sequence

(Altman and Bayer, 1990a; van Praag et al., 2002). Consequently, in the granule cell layer the first born cells are found on the outside of the dentate gyrus, whereas newborn cells localise interiorly. Although the function of hippocampal neurogenesis is obscure, it is increased upon various stimuli, such as an enriched environment or voluntary physical activity (Kronenberg et al., 2003). Notably, generation of new neurons in the dentate gyrus was reported also in human patients (Eriksson et al., 1998), and is a subject to alteration in various pathological conditions (reviewed in: Emsley et al., 2005).

Similarly as in the SVZ, the hippocampal putative stem cells have characteristics of radial astrocytes with soma in the SGZ and processes reaching into the granule cell layer to arborise in the molecular layer (Garcia et al., 2004; Seri et al., 2004; Seri et al., 2001). Astrocytes in the SGZ divide slowly to give rise to proliferating transient amplifying precursors, which eventually differentiate into new granule cells (Seri et al., 2001) (Figure III C).

1.2 The Y-box family of nucleic acid binding proteins

The Y-box factors have the capacity to bind DNA and RNA, thereby regulating gene expression from transcription to translation (Kohno et al., 2003; Matsumoto and Wolffe, 1998; Sommerville, 1999; Wolffe, 1994). They were identified due to, and named after, the ability to bind the CCAAT sequence present in the Y-box regulatory element found in the promoters and enhancers of the mammalian major histocompatibility complex class II (MHC II) genes (Didier et al., 1988). Notably, the Y-box sequence is present in promoters of various genes encoding growth and stress related proteins, such as cyclin D1, epidermal growth factor receptor, proliferating cell nuclear antigen (PCNA), DNA polymerase, thymidine kinase, topoisomerase IIα, and Y-box proteins were implicated in regulation of proliferation and transformation (Ladomery and Sommerville, 1995; Swamynathan et al., 1998).

In vertebrates, three distinct Y-box paralogues have been identified, which are highly conserved between species. Identification of the same protein in a different functional context by independent researchers led to a non-unified nomenclature and numbers associated with Y-box factors reflect the chronology of discovery rather than indicating orthologues. The nomenclature is summarised in Table I.

Species	Y-box 1	Y-box 2	Y-box 3
mouse	MSY1	MSY2	MSY3, YB3, MSY4, CSDA
human	YB-1, p50, CSDB, dbpB (98%)	dbpC, contrin (98%)	CSDA, dbpA (86%)
rat	EFI_A, YB-1, rBYB1 (98%)	* XM_220618 (98%)	YB2/RYB-a, MY1 (99%)
rabbit	YB-1, p50 (95%)	-	-
dog	* XM_851016 (96%)	* XM_546585 (98%)	ZONAB (87%)
chicken	YB-1 (89%)	-	chk-YB-2 (67%)
frog	FRGY1 (80%)	FRGY2, mRNP4 (69%)	-

Table I. Nomenclature of Y-box proteins. Othologous proteins are listed in columns and independent names of the same protein are separated by commas; rows indicate paralogues in the same species. Asterisks mark predicted proteins and their NCBI accession number is given. The percent of identity to mouse proteins is shown in brackets. Abbreviations: dpb, DNA binding protein; CSD, cold shock domain; mRNP, messenger ribonucleoprotein particle; ZONAB, ZO-1 associated nucleic acid binding protein.

1.2.1 Structure of vertebrate Y-box proteins

Y-box proteins are characterised by a central, highly conserved, cold shock domain (CSD) that consist of 80 amino acids and exhibits more than 40% identity to bacterial cold shock proteins (Wolffe et al., 1992; Yamanaka et al., 1998). CSD-containing proteins are found in all eukaryotes examined, with an exception of *Saccharomyces cerevisiae* (Matsumoto and Wolffe, 1998). The CSD has a high content of aromatic and charged residues and forms a five-stranded β-barrel comprised of two β-sheets that include two RNA binding motifs, RNP1 and RNP2 (Kloks et al., 2002; Schindelin et al., 1994; Yamanaka et al., 1998). This is the major nucleic acid binding domain of Y-box proteins and confers sequence specifity (Bouvet et al., 1995; Matsumoto et al., 1996; Tafuri and Wolffe, 1991; Yu et al., 2003). In vertebrates, the CSD is flanked by a variable alanine- and proline-rich N-terminal domain (A/P) and a C-terminal domain (CTD), which has preserved structural organisation with four clusters of alternating basic/aromatic and acidic residues, though is not strictly conserved in the primary amino acid sequence. The A/P domain has been implicated in the interaction with actin filaments (Ruzanov et al., 1999), and the CTD also participates in RNA binding (Matsumoto et al., 1996; Skabkin et al., 2004), but primarily mediates multimerisation of Y-box proteins (Ladomery and Sommerville, 1994; Tafuri and Wolffe, 1991). The domain structure of Y-box proteins is depicted in Figure IV.

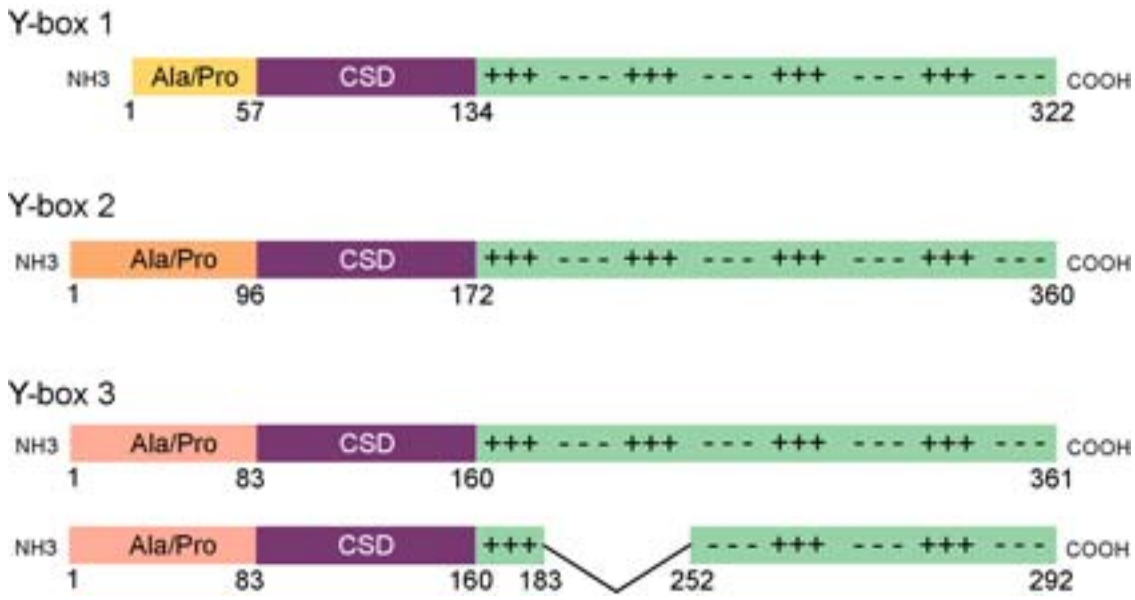

Figure IV. General domain organisation of vertebrate Y-box family members. The N-terminal alanine- and proline-rich domain (*Ala/Pro*) of Y-box proteins has the most variable sequence between different members of the family. The highly conserved nucleic acid binding cold shock domain (*CSD*) is followed by the C-terminal domain containing interchanging clusters of basic/aromatic and acidic amino acids (+++/- - -), which supports nucleic acid binding and multimerisation. Additionally, Y-box 3 mRNA is a subject of alternative splicing, resulting in two isoforms different in the C-terminal domain.

1.2.2 Y-box protein 1

YB-1 is the most ubiquitous and also best studied among Y-box factors. In bacteria, cold shock proteins act as DNA/RNA chaperons being responsible for promoting the correct folding of nucleic acids during adaptation to cold shock or other cellular stresses, when improper secondary structures could be stabilised. Similarly, YB-1 has been implicated

in a broad range of processes, such as DNA recombination, transcription, splicing, oligonucleotide annealing and strand exchange, translation regulation and RNA stabilisation, suggesting a general role in nucleic acid structural arrangements and packaging (Evdokimova et al., 2006a; Evdokimova and Ovchinnikov, 1999; Skabkin et al., 2001).

YB-1 controls translation in a dose-dependent manner

All mRNAs in eukaryotic cells are associated with proteins to form messenger ribonucleoprotein particles (mRNPs). YB-1, along with the poly(A)-binding protein (PABP), is one of the two major and universal proteins tightly bound to cytoplasmic mRNAs (Evdokimova et al., 1995). YB-1 represents approximately 0.1% of total protein in COS-1 and HeLa cells, which is nearly equimolar to that of ribosomes and translation initiation factors, being 5-10 fold higher than the mRNA level (Davydova et al., 1997). The protein exhibits little sequence specifity and binds RNA with exceptionally high affinity (2.5×10^8 M^{-1}) (Minich et al., 1993).

Interestingly, translational status of mRNAs, i.e. whether they are a component of inactive non-translated mRNPs or associated with actively translating polyribosomes, correlates with a high and low molar ratio of YB-1 to the message, respectively. At the YB-1/mRNA weight ratio of 2 or less, which is characteristic for polysomes, YB-1 binds to mRNA as a monomer using the CSD and CTD; as this ratio is increased above 3, YB-1 molecules oligomerise via their CTD, which is concomitantly displaced from mRNA, into globular particles of approximately 700 kDa (Skabkin et al., 2004). mRNA is exposed on the surface of the globule and binding of YB-1 to mRNA involves only the sugar-phosphate backbone of mRNA, leaving nucleotide bases free for interaction with other proteins (Pisarev et al., 2002). Importantly, depletion of YB-1 from the reticulocyte lysate results in a dramatic inhibition of translation initiation (Evdokimova et al., 1998), thus low amounts of YB-1 are indispensable for protein synthesis, possibly because YB-1 promotes binding of the 40 S ribosomal subunit to RNA and formation of the 48 S pre-initiation complex (Pisarev et al., 2002). On the contrary, high molar ratios of YB-1 to mRNA result in inhibition of translation *in vitro* (Evdokimova et al., 1998) and *in vivo* (Bader et al., 2003; Bader and Vogt, 2005; Davydova et al., 1997; Evdokimova et al., 2001). YB-1 binds in close proximity to the mRNA cap structure and displaces initiation factors eIF4G and eIF4E, thereby blocking formation of the pre-initiation complex, which leads to mRNA silencing (Evdokimova et al., 2001; Nekrasov et al., 2003). However, binding of YB-1 to the cap does not simply result in translation repression but also mediates significant mRNA stabilisation, presumably by protecting mRNA from decapping and exonucleolytic degradation (Evdokimova et al., 2001). Notably, the association of YB-1 with RNA within the storage particles is dynamic and YB-1 easily migrates from one mRNA molecule to another (Skabkin et al., 2004), suggesting that mRNAs can easily be recruited into translation upon modification of YB-1 affinity to RNA or alterations in its local concentration.

In addition to the universal function as an mRNA packaging protein in somatic cells, MSY1 was found to be bound to stored messages in maturating sperm cells (Mastrangelo and Kleene, 2000; Tafuri and Wolffe, 1993).

YB-1 associates with mRNAs involved in growth and signalling

The messages associated with YB-1 mRNPs were identified in K-Ras transformed NIH3T3 cells by immunoprecipitation and microarrays (Evdokimova et al., 2006a). Among 1457 transcripts bound to YB-1, 302 were not detected in the total RNA pool, suggesting that a specific mRNA subset may be selectively enriched within YB-1 complexes. Interestingly, low abundance messages encoding cell growth and maintenance molecules

constituted one-third of the unique YB-1 bound transcripts. Additionally, a higher proportion of YB-1 messages compared to the total RNA encodes transcription and growth factors, receptors and signal transduction proteins, suggesting that many growth-related mRNAs are kept silent in the complex with YB-1. This hypothesis is supported by the fact that some of the abundant messages, e.g. ribosomal protein L32 mRNA, are not associated with YB-1. The fraction of mRNAs bound by YB-1 appears to be regulated in response to transformation by oncogenes K-Ras or ETV6-NTRK3 (gene fusion in congenital fibrosarcoma with the helix-loop-helix dimerisation domain of the transcription factor ETV6 fused to the protein tyrosine kinase domain of NTRK3). In transformed cells, a different set of mRNAs was found to be associated with YB-1 compared to non-transformed NIH3T3 cells, despite the constant level of these transcripts in the total cellular RNA pool (Evdokimova et al., 2006b). It has been suggested that phosphorylation of YB-1 on Ser-102 located within the CSD by Akt kinase is responsible to relieve the translational repression (Evdokimova et al., 2006a; Sutherland et al., 2005). Notably, overexpression of YB-1 overcomes PI3K- and Akt-induced oncogenesis by inhibiting protein synthesis (Bader et al., 2003; Bader and Vogt, 2005). Another mechanism to relieve translational repression is mediated by displacing YB-1 from mRNPs by association with other proteins, such as the YB-1-associated acidic protein (YBAP1)/p32 (Matsumoto et al., 2005).

In addition to global effects on translation, YB-1 exhibits a preference for binding to the Y-box recognition consensus sequence (YRS) 5'-U/C/A-C/A-C-A-U/C-C-A/C/U first revealed in the 3' untranslated region (UTR) of the protamine 1 mRNA (Coles et al., 2004; Davies et al., 2000; Giorgini et al., 2001), and exerts specific functions on various mRNAs. YB-1 was implicated in YRS-dependent stabilisation of mRNAs encoding vascular endothelial growth factor (VEGF) and interleukin 2 (IL-2) in concert with polypyrimidine tract binding protein (PTB) and nucleolin, respectively (Chen et al., 2000; Coles et al., 2004). YB-1 also stabilises granulocyte-marocphage colony stimulating factor (GM-CSF) mRNA via binding to AU-rich instability elements (ARE) present in its 3'UTR (Capowski et al., 2001). Binding of YB-1 to the YRS of its own message represses translation at concentrations, which are stimulatory for general protein synthesis (Skabkina et al., 2005). Interestingly, YB-1 binds to a similar sequence present in the CD44 pre-mRNA and increases alternative exon inclusion (Stickeler et al., 2001). Binding of YB-1 to a splicing factor SRp30c has been reported (Raffetseder et al., 2003). Thus, specific recognition of sequences and binding to various proteins modulates the function of YB-1 in mRNA metabolism.

YB-1 in transcription, DNA repair and cancer

YB-1 contains in its CTD a non-canonical nuclear localisation signal (NLS) and a cytoplasmic retention signal (CRS), which prevails over the NLS (Bader and Vogt, 2005; Sorokin et al., 2005), therefore the YB-1 protein localises predominantly in the cytoplasm (Bader and Vogt, 2005; Davydova et al., 1997; Funakoshi et al., 2003; Raffetseder et al., 2003; Sorokin et al., 2005; Stenina et al., 2001). However, YB-1 translocates to the nucleus at G_1/S transition in HeLa cells (Jurchott et al., 2003). Translocation to the nucleus has also been reported upon various cellular stresses and stimuli, such as UV irradiation (Koike et al., 1997), hypothermia (Stein et al., 2001), treatment with genotoxic agents (Okamoto et al., 2000; Zhang et al., 2003) and after an infection with adenovirus type 5 (Holm et al., 2002). In accordance, several drug resistant cancer cell lines exhibit nuclear YB-1 (Ohga et al., 1996). Upon treatment with DNA damaging agents, but not after other cellular stresses, the CRS of YB-1 is specifically cleaved by the proteasome and YB-1 translocates to the nucleus

(Sorokin et al., 2005). Similar cleavage was observed after induction of endothelial cells with thrombin (Stenina et al., 2001). Interestingly, the cleaved form of YB-1 is unable to bind RNA. Moreover, various YB-1 deletion mutants in which RNA binding is impaired exhibit the nuclear localisation (Bader et al., 2003; Bader and Vogt, 2005), suggesting that RNA binding is one of the mechanisms sequestering YB-1 in the cytoplasm. It is plausible that nuclear YB-1 becomes associated with mRNA concomitantly with transcription, as it was shown for the dipteran YB-1-like protein (Soop et al., 2003), and exported from the nucleus together with the message. The Y-box-protein associated acidic protein (YBAP1), which binds to and releases YB-1 from mRNA, might facilitate nuclear translocation of YB-1 (Matsumoto et al., 2005). Release of YB-1 from mRNA and its nuclear translocation in the MCF-7 cell line depends on the presence of Ser 102, which can be phosphorylated by Akt (Sutherland et al., 2005).

YB-1 was thought to be implicated in the control of cell proliferation (Ladomery and Sommerville, 1995). The *YB-1* knockout mice show growth retardation leading to severe hypoplasia in multiple organs, improper neural tube closure and exencephaly, and, eventually, late embryonic or perinatal death (Lu et al., 2005). YB-1 deficient cells exhibit slower proliferation, accelerated senescence and growth arrest in hypothermia (En-Nia et al., 2005; Lu et al., 2005; Matsumoto et al., 2005). The slower growth rate was attributed to faster accumulation of G_1-specific cell cycle inhibitors $p16^{Ink4a}$ and $p21^{Kip1}$. Conversely, overexpression of YB-1 in the MCF-7 breast cancer cell line grown in soft agar resulted in increase in size and number of colonies (Sutherland et al., 2005). Accordingly, YB-1 is frequently overexpressed in various tumours (summarised in Table II), and in highly proliferative tissues, such as the developing and regenerating liver (Grant and Deeley, 1993), infarcted heart (Kamalov et al., 2005) and colorectal epithelial glands (Shibao et al., 1999). Moreover, in cancer tissues, YB-1 often shows nuclear localisation, which correlates with tumour progression and is a poor prognostic factor (Kuwano et al., 2004) (see also Table II). Nuclear YB-1 expression is linked with multidrug resistance and the activation of expression of the multidrug resistance 1 (*MDR1*) gene encoding the transmembrane ATP binding cassette transporter (Kuwano et al., 2004). YB-1 has been also implicated in positive regulation of promoters of other genes associated with growth and metastasis, such as matrix metalloproteinase 2 (Mertens et al., 1997; Mertens et al., 2002), topoisomerase II α (Shibao et al., 1999), cyclin A and B1 (Jurchott et al., 2003), and DNA polymerase α (En-Nia et al., 2005), as well as downregulation of growth arrest factor p53 (Lasham et al., 2003) and pro-apoptotic Fas (Lasham et al., 2000).

Cancer type	References
breast carcinoma	Bargou et al., 1997*; Fujita et al., 2005*; Janz et al., 2002*; Rubinstein et al., 2002
colorectal cancer	Shibao et al., 1999
hepatocellular carcinoma	Yasen et al., 2005*
non-small cell lung carcinoma	Gessner et al., 2004; Shibahara et al., 2001*; Yao et al., 2002
osteosarcoma	Oda et al., 1998*
ovarian carcinoma	Kamura et al., 1999*; Yahata et al., 2002*
prostate cancer	Gimenez-Bonafe et al., 2004*
synovial sarcoma	Oda et al., 2003*
thyroid anaplastic carcinoma	Ito et al., 2003*

Table II. YB-1 is upregulated in various cancers. Asterisks mark reports in which nuclear localisation of YB-1 was reported and associated with the multidrug resistance and/or poor clinical outcome.

The YB-1 protein is implicated in resistance to genotoxic stress. Depletion of MSY-1 in embryonic stem cells or mouse embryonic fibroblasts increases sensitivity to cisplatin and mitomycin C, and to oxidative stress (Lu et al., 2005; Shibahara et al., 2004). Consistently, elevated YB-1 levels in a number of drug resistant cell lines are linked with increased resistance to DNA damaging agents (Ohga et al., 1996). Thus, concentration of YB-1 appears to correlate inversely with cellular sensitivity to DNA cross-linking in cancer cells and there is an evidence for YB-1 playing a role in DNA repair. YB-1 interacts with proliferating cell nuclear antigen (PCNA) (Ise et al., 1999) and p53 (Okamoto et al., 2000), proteins essential for DNA repair. Moreover, it preferentially binds to single stranded, abasic and cisplatin-modified DNA and posses 3'→5' exonuclease activity (Hasegawa et al., 1991; Ise et al., 1999; Izumi et al., 2001). It has been suggested that YB-1 brings p53 to the damage site, as p53 alone is not capable to interact with modified nucleic acids (Izumi et al., 2001), and as a DNA chaperone structurally organises the repair machinery.

1.2.3 Y-box protein 2

Y-box protein 2 is a cytoplasmic protein expressed exclusively in germ cells in the mouse (Gu et al., 1998), human (Kohno et al., 2006; Tekur et al., 1999), and frog (Tafuri and Wolffe, 1990). Translational regulation represents the major mechanism of gene regulation in germ cell differentiation and early embryogenesis. During spermatogenesis, diploid spermatogonia undergo the meiotic division, differentiate into haploid spermatids and eventually spermatozoa. This process is accompanied by vast cellular growth, morphogenesis and reorganisation of the nucleus. The mRNAs encoding proteins involved in the final step of differentiation, particularly packaging of DNA, are synthesised in large quantities and maintained silent until the protein product is required (Kleene, 2003). The growth of the oocyte is also associated with accumulation of large quantities of mRNAs, which are translationally repressed until the last step of differentiation and then fertilisation. Particularly rich in stored mRNAs are amphibian oocytes, in which translation of maternally deposited mRNAs supports protein production throughout multiple divisions during early development until zygotic gene expression is turned on. Mouse MSY2 functions in translational repression and stabilisation of mRNAs in both male and female germ cells (Herbert and Hecht, 1999; Yu et al., 2001; Yu et al., 2002), while its *Xenopus* orthologue, FRGY2, is a major protein of oocyte mRNPs (Deschamps et al., 1992), which mediates stabilisation and translational repression of stored mRNAs (Bouvet and Wolffe, 1994; Matsumoto et al., 1996; Tafuri and Wolffe, 1993; Yurkova and Murray, 1997). The MSY2 protein constitutes approximately 0.7 and 2% of the total soluble protein in the maturating sperm and in the oocyte, respectively (Yang et al., 2005a; Yu et al., 2001). Function of Y-box protein 2 appears to be essential for germ cells, as absence of MSY2 results in male and female infertility (Yang et al., 2005b; Yu et al., 2004). Reduction of MSY2 leads to general reduction of protein synthesis (Yu et al., 2004), likely due to mRNA destabilisation.

MSY2 binds to the YRS of the protamine 1 mRNA, and this sequence is responsible for proper repression of the message in elongating spermatids *in vivo* (Giorgini et al., 2001). Protamines are small arginine-rich proteins that are involved in chromatin condensation in the nucleus of spermatozoa, and protamine mRNAs are not translated until cessation of transcription in elongated spermatids (Kleene, 2003; Steger, 2001). Moreover, MSY2 and FRGY2 posses moderate sequence specifity for the YRS *in vitro* and in yeast three-hybrid

assay (Bouvet et al., 1995; Giorgini et al., 2001; Matsumoto et al., 1996; Yu et al., 2001), hence it was concluded that this motif targets mRNAs for MSY2-mediated silencing. However, a recent report in which a set of MSY2 bound messages was identified, suggested that there is no apparent consensus sequence *in vivo* (Yang et al., 2005a). Notably, the promoters of corresponding genes contain Y-box sequences, suggesting that MSY2, similarly as FRGY2 (Bouvet and Wolffe, 1994; Ranjan et al., 1993), might be associated with messages concomitantly with transcription. Although MSY2 and its orthologues in human and frog are localised predominantly in the cytoplasm (Kohno et al., 2006; Ranjan et al., 1993; Yu et al., 2001), chromatin immunoprecipitation (ChIP) from male germ cells revealed MSY2 association with Y-boxes of germ cell specific genes, but not cell growth and maintenance genes, whose mRNAs are not bound by MSY2 and are immediately translated (Yang et al., 2005a). Similarly as for YB-1, mRNA binding might play a role in cytoplasmic retention of Y-box protein 2, as the RNA binding activity of MSY2 is required for its cytoplasmic localisation (Yu et al., 2003). Likewise, the CTD contains sequences responsible for the cytoplasmic localisation, since deletion mutants are localised in the nucleus (Yoshida et al., 2006b; Yu et al., 2003).

Human dbpC shows wide expression in malignancies, particularly in testicular seminomas and ovarian dysgerminomas but also in many cancer cells in other organs (Kohno et al., 2006), although in normal tissues dbpC is restricted to germ cells. Notably, even tumours classified as negative based on the abundance of dbpC expression, showed scattered dbpC-positive cells. It has been suggested that dbpC belongs to a growing group of germ cell specific factors designated as cancer/testis (CT) antigens, whose upregulation results in aberrant expression of germline genes and leads to immortalisation, aneuploidy, migration and metastasis of cancer cells (Kohno et al., 2006; Simpson et al., 2005). As the CT antigens are often detected in spermatogonia or spermatogonial stem cells, and the expression of the CT antigens is frequently found in only a small proportion of cells in cancer tissues, it is plausible that some of the CT antigens could be stem cell markers for tumour stem cells (Simpson et al., 2005). dbpC in cancer tissues, as well as in germ cell tumour cell lines, was found exclusively in the cytoplasm (Kohno et al., 2006; Yoshida et al., 2006b), suggesting that the main function of dbpC is related to the stability of mRNA and translational regulation rather than transcription.

1.2.4 Y-box protein 3

Mouse MSY3 (also designed MSY4/YB3), rat YB2/RYB-a, and human dbpA are highly expressed in the testis (Davies et al., 2000; Ito et al., 1994; Iuchi et al., 2001; Kohno et al., 2006; Mastrangelo and Kleene, 2000). Moderate levels of expression are found in trophoblast, skeletal muscle and heart, and low in the kidney, brain and retina. Alternative splicing leads to expression of two forms of the protein, different in the CTD in all species analysed (see Figure IV, p. 19), yet functional differences between these splice variants were not reported.

Y-box protein 3 is a translational repressor in germ cells

Expression of Y-box protein 3 in testes is detected in spermatogenic cells from pachytene spermatocytes until elongating spermatids (Davies et al., 2000; Iuchi et al., 2001; Kohno et al., 2006; Mastrangelo and Kleene, 2000). MSY3 is one of the major proteins present in cytoplasmic stored mRNPs, and, in concert with MSY2, specifically binds and represses the protamine 1 mRNA (Davies et al., 2000; Giorgini et al., 2002; Giorgini et al., 2001; Mastrangelo and Kleene, 2000). Notably, prolonged expression of MSY3 in

spermatids, and hence extended translational repression of messages encoding for proteins playing a role in sperm morphogenesis, leads to the disruption of spermatogenesis and sterility with severe defects in sperm morphology (Giorgini et al., 2002). In this study, authors also speculated that MSY3-mediated repression requires the YRS, since analysis of several mRNAs showed that only mRNAs which contained the YRS were affected. MSY3 might play a general role in repression and packaging of mRNAs in germ cells, as its expression in oocytes has been reported (Davies et al., 2000).

Y-box protein 3 in proliferation and transcription

The canine Y-box protein 3 was identified in the MDCK epithelial cell line based on the interaction with the SH3 domain of the tight junction protein ZO-1, and therefore designated ZO-1-associated nucleic acid binding protein (ZONAB) (Balda and Matter, 2000). In epithelial cell lines, overexpression of ZONAB, but also of human dbpA, induces cell proliferation and results in increased cell density in mature monolayers, whereas depletion of ZONAB reduces cell density and proliferation (Balda et al., 2003; Sourisseau et al., 2006). Moreover, manipulation of the level of ZONAB interferes with cyst formation by MDCK cells in 3-D cultures (Sourisseau et al., 2006), suggesting it functions in epithelial tissue morphogenesis. The subcellular localisation and function of ZONAB depend on the cell density: at a low cell density, a pool of ZONAB is nuclear and acts as a transcription factor, while at high cell densities, ZONAB relocates from the nucleus to the cytoplasm and junctions, where it interacts with ZO-1 (Balda and Matter, 2000) and RalA, a member of the Ras superfamily of small GTPases (Frankel et al., 2005). Nuclear ZONAB/dbpA, via binding to Y-box sequences, activates expression of cyclin D1 and PCNA (Sourisseau et al., 2006), and negatively regulates the activity of the *ErbB-2* promoter (Balda and Matter, 2000). ZO-1 is believed to inhibit ZONAB by cytoplasmic sequestration. Since ZONAB also binds cyclin dependent kinase 4 (Cdk4), the cytoplasmic retention of ZONAB results in reduced nuclear Cdk4, thereby inhibiting G_1/S transition (Balda et al., 2003). Additionally, dbpA directly inhibits the kinase activity of Cdk4 and neuron-specific Cdk5 *in vitro* (Moorthamer et al., 1999).

Consistent with the role of ZONAB in promoting cell proliferation, rat RYB-a and mouse MSY3 are highly expressed in the foetal and regenerating liver, whereas its expression is undetectable in the adult intact tissue (Ito et al., 1994; Kajino et al., 2001). Notably, dbpA is associated with advanced stages of hepatocellular carcinoma and its nuclear localisation is linked with poor prognosis for patients (Yasen et al., 2005). dbpA was found as a target of transcription factor E2F, which is often elevated in cancer tissues (Arakawa et al., 2004). Moreover, ZONAB signalling is positively regulated by the heat shock protein 110/Apg-2, which competes with ZONAB for binding to ZO-1 (Tsapara et al., 2006), and was found to be upregulated in hepatocellular and pancreatic carcinomas (Gotoh et al., 2004; Nakatsura et al., 2001).

MSY3 in the nervous system

In the adult central nervous system, MSY3 was detected in oligodendrocytes and astrocytes throughout the brain, as well as in retinal neurons, where it colocalises with ZO-1 and ZO-2 at gap junctions (Ciolofan et al., 2006; Penes et al., 2005). The function of the protein in this context, however, has not been investigated.

1.3 Aims of this study

Persistence of multipotent progenitors throughout development is essential for the generation of cellular diversity; in the adult organism somatic stem cells as descendants of embryonic progenitors continue to produce differentiated progeny for tissue renewal, repair and plasticity. All major signalling pathways are implicated in the control of stem cell decisions, but what are the inherent mechanisms that rule proliferation and maintenance of stem cells? In particular, deregulation of gene expression in transformation and cancer provides cues as to the intrinsic regulation of proliferation and differentiation. With this in mind, Y-box proteins, as multifunctional coordinators for the control of gene expression in the nucleus and the cytoplasm, in homeostasis and pathology, are excellent candidates for such factors.

This study aims to examine the expression of MSY3 in the developing murine nervous system and elucidate its putative role in the regulation of proliferation and differentiation of neural progenitors. Two following premises are at the base of this study: i) MSY3 promotes proliferation of epithelial cells in a manner opposite to junctional protein ZO-1; ii) neuroepithelial cells downregulate some of the epithelial features before the switch from proliferation to neurogenesis, simultaneously upregulating expression of ZO-1.

A separate project aimed to reveal whether the asymmetric distribution of the antiproliferative Tis21 protein during the cell division could be associated with distinct fates of the daughter cells. Specifically, it was speculated that the daughter cell which inherited the protein upon the cytokinesis would become a neuron or a basal progenitor. This project was conducted during the first year of my thesis work and is presented in the first part of the *Results*, which reflects the chronological order. However, as this study was not continued, it is not considered in the *Discussion* section.

2 RESULTS

PART I

2.1 Asymmetric distribution of the Tis21 protein during mitosis

In animal development there are numerous examples of cell fate specification by the asymmetric distribution of fate determinants upon the mitosis (reviewed in: Betschinger and Knoblich, 2004). Since it was observed that the immunoreactivity of the affinity purified K4 antibody, which was raised against the Tis21 protein, exhibited an asymmetric distribution during the cytokinesis in cultured neuroepithelial cells (Lilla Farkas, unpublished results), the attempt to reveal the link between this distribution and the cell fate was undertaken.

2.1.1 Distribution of the K4 immunoreactivity in cultures of neuroepithelial cells

To confirm the original finding, neuroepithelial cell clusters derived from the embryonic day 10.5 (E10.5) telencephalon and cultured in defined media in a presence of bFGF were stained with the K4 antibody. Indeed, in some mitotic figures an asymmetric distribution of the immunoreactivity could be observed (Figure 1 A). The frequency of an unequal distribution of the K4 immunoreactivity was lower (4.6%; n=136 cells) than previously observed (40%), perhaps due to different preparation of cultures.

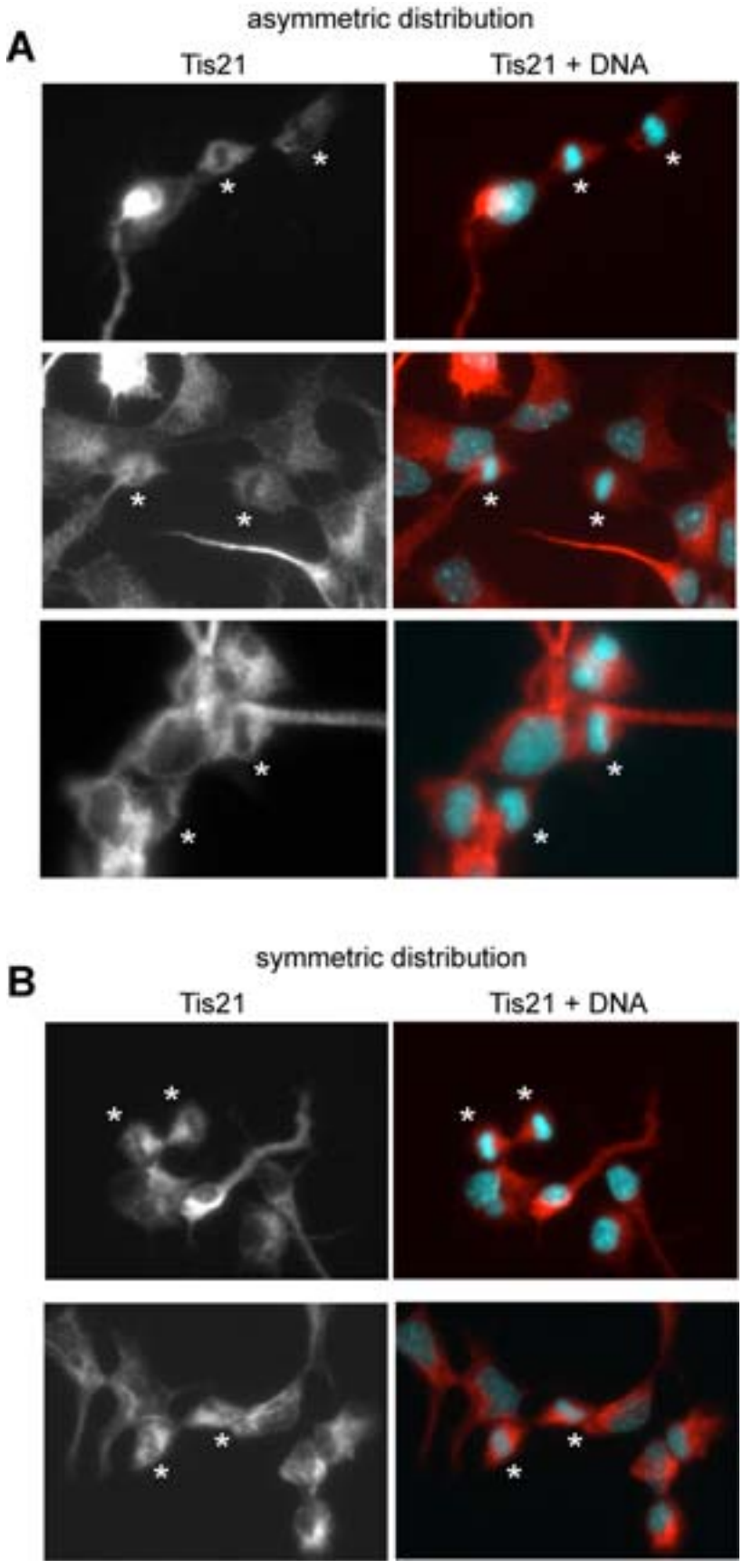

Figure 1. Distribuiton of the K4 immunoreactivity at the cytokinesis *in vitro*. Neuroepithelial cell cluster cultures grown in a presence of bFGF were stained with the K4 antibody directed against Tis21 (red). Nuclei are visualised with DAPI (cyan). Cells in the cytokinesis are marked by asterisks. Examples of (**A**) asymmetric and (**B**) symmetric distribution of the K4 immunoreactivity.

2.1.2 *Specifity of the K4 antibody*

Before investigating the distribution of Tis21 in the neuroepithelium, the monospecifity of the K4 antibody for the Tis21 protein was tested. The rabbit polyclonal K4 antiserum was raised against a peptide corresponding to the C-terminal 12 amino acids of the mouse Tis21 and affinity purified. As no immunostaining was observed in rat E13 embryos, which also express Tis21, it was concluded that the substitution of Ala-155 of the mouse Tis21 by a threonine in the rat protein destroys the K4 epitope and hence the antibody recognises only the Tis21 protein.

In immunoblotting of COS7 cells transfected with the Tis21 expression plasmid, but not of control mock transfected cells, the K4 antibody recognised a 17 kDa band corresponding to the molecular weight of the Tis21 protein (Figure 2 A, left panel). The same band was recognised by the second antibody against Tis21 (Figure 2 A, right panel). Similarly, Tis21-transfected cells were immunoreactive in fluorescent staining (Figure 2 B). Therefore, the K4 antibody can recognise the Tis21 protein in misexpressing cells, as previously reported (Iacopetti et al., 1999).

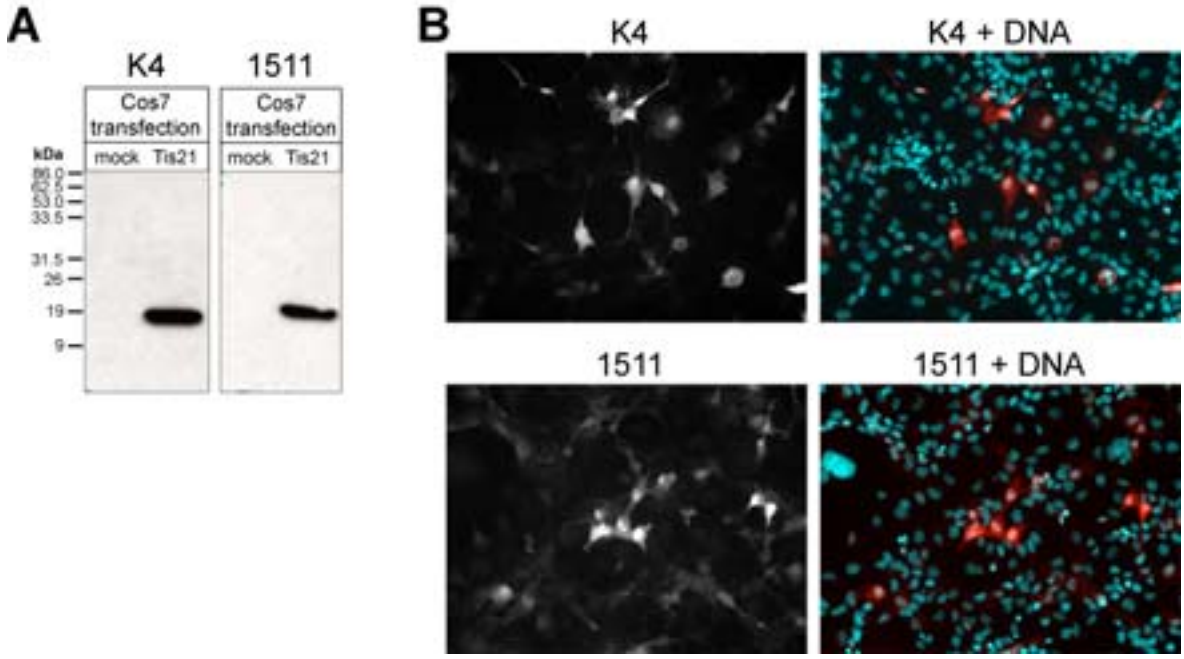

Figure 2. K4 antibody recognises Tis21 ectopically expressed in Cos7 cells. Cos7 cells were transfected with the Tis21 expression plasmid or mock transfected as a control. The Tis21 protein was detected either by (**A**) immunoblotting, or (**B**) immunofluorescence, using the K4 or 1511 antibodies, which were raised against peptides residing in the C-terminal domain of Tis21 (Iacopetti et al., 1999). Both antibodies recognise a band of approximately 17 kDa, only when the Tis21 plasmid was included. In (B) nuclei are visualised with DAPI (cyan); magnification, 400x.

The K4 antibody was applied on sections from E10.5 mouse and E12 rat embryos employing two protocols, which differed in time of treatment with Triton X-100, a non-ionic detergent used to permeabilise cells. In the first protocol, 0.3% Triton X-100 was applied for 15 min at the beginning of the procedure, whereas in the second protocol the detergent was used additionally in a blocking step and during incubation with antibodies. Interestingly, a pattern of the K4 immunoreactivity in both species differed significantly according to the staining protocol. By applying Triton X-100 throughout the staining, the expected gradient of immunoreactivity corresponding to neurogenesis, as well as a intensive

labelling in the neuronal layers, were observed in the mouse tissue (Figure 3A, and data not shown). No staining in the rat could be detected using this protocol (Figure 3B). Short Triton X-100 treatment of mouse sections, however, resulted in even staining throughout the neuroepithelium without a gradient (Figure 3 C, and data not shown). In contrast, when this protocol was used for the rat tissue, the ventricular zone exhibited staining in a gradient which parallel the onset of neurogenesis (Figure 3 D and data not shown). The subcellular pattern of staining was similar to that observed in the mouse, although the signal was weaker. Additionally, strong immunoreactivity in neurons could be observed (data not shown). It is important to note that the original conclusion that the K4 immunoreactivity, and hence the Tis21 protein, marks neurogenic progenitors was based upon the immunostaining pattern revealed using 0.1% Triton X-100 throughout the staining procedure (Iacopetti et al., 1999). Therefore, for all subsequent experiments 0.3% Triton X-100 was used for all steps of immunostaining.

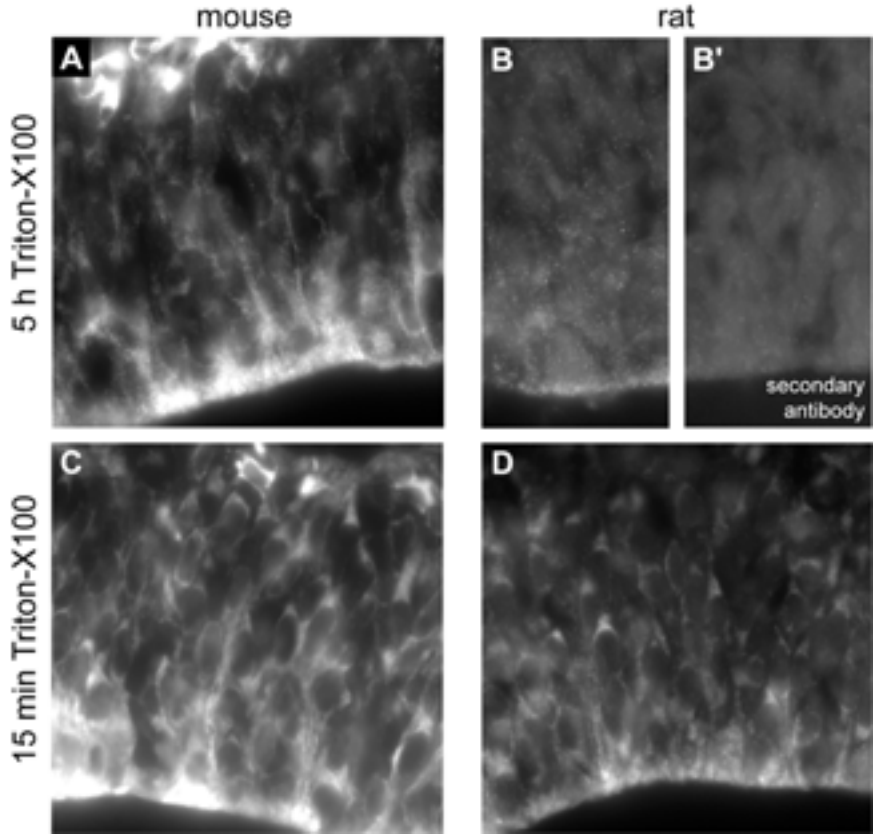

Figure 3. The K4 immunoreactivity in the mouse and rat tissue differs according to time of the Triton X-100 treatment. Saggital cryosections from the E10.5 mouse (**A**,**C**), and E12 rat telencephalon (**B**,**D**), which are equivalent stages of development, were stained with the K4 antibody. Apical is towards bottom. (**A**,**B**,**B'**) In a presence of 0.3% Triton X-100 during the whole procedure, the K4 antibody stains neuroepithelial cells and neurons in the mouse neural tube (A), whereas in the rat tissue gives a negative signal (B); (**B'**) shows a control without the primary antibody. (**C**,**D**) The short treatment with Triton X-100 yields even staining in the mouse neuroepithelium, and staining in the rat tissue similar to that observed in mouse upon longer treatment with this detergent. Magnification, 1000x.

Next, the K4 antibody was applied on sections from homozygous Tis21 knock-in embryos, in which the first exon of the *Tis21* gene was substituted by GFP sequence followed by a polyadenylation (polyA) signal. In this transgenic animal no full length Tis21 protein could be detected by immunoblotting (Haubensak, 2002; Haubensak et al., 2004). Surprisingly, the overall and subcellular pattern of staining was indistinguishable from wild

type mouse embryos (Figure 4). Since the second exon of the *Tis21* gene is still present in the genome and little amount of longer mRNA containing this exon, probably as a result of read through the single polyA signal, can be detected by RT-PCR (Ji Feng Fei, personal communication) it cannot be excluded that the N-terminally truncated Tis21 protein is still expressed in the neuroepithelium by unknown mechanism and hence recognised by the K4 antibody.

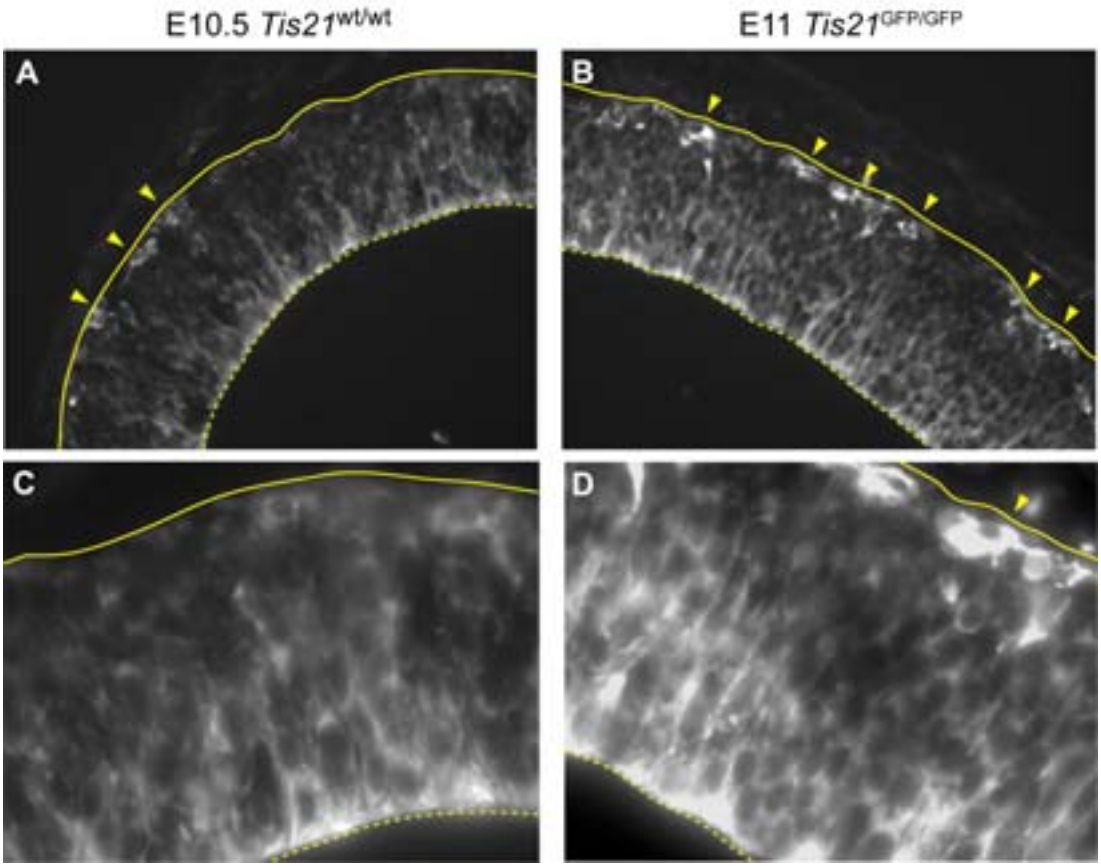

Figure 4. The K4 immunoreactivity in Tis21 homozygous knock-in mouse embryos is not diminished. (**A**,**C**) Sections from E10.5 wild type; and (**B**,**D**) E11 *Tis21*$^{GFP/GFP}$ embryos were stained with the K4 antibody. Despite the lack of the full-length protein in the homozygous knock-in embryos, the K4 immunoreactivity exhibits pattern identical to the wild type tissue with differential staining in the ventricular zone cells and strong labelling of neurons (arrowheads). Continuous and dashed lines delineate the pial and ventricular surfaces, respectively. Magnification: (A,B) 400x; (C,D) 1000x.

To further characterise the specifity of the K4 antibody, it was applied on sections from E11.5 heterozygous *Tis21*-GFP embryos and the fluorescence staining was investigated by confocal microscopy. If the K4 antibody specifically recognises Tis21 it should be present only in GFP positive cells. As shown in Figure 5, this is not the case. In addition to double positive K4$^+$/GFP$^+$ (filled arrowheads) and double negative K4$^-$/GFP$^-$ cells (empty arrows), both the K4$^+$/GFP$^-$ (empty arrowheads) and K4$^-$/GFP$^+$ (filled arrows) progenitor cells could be observed.

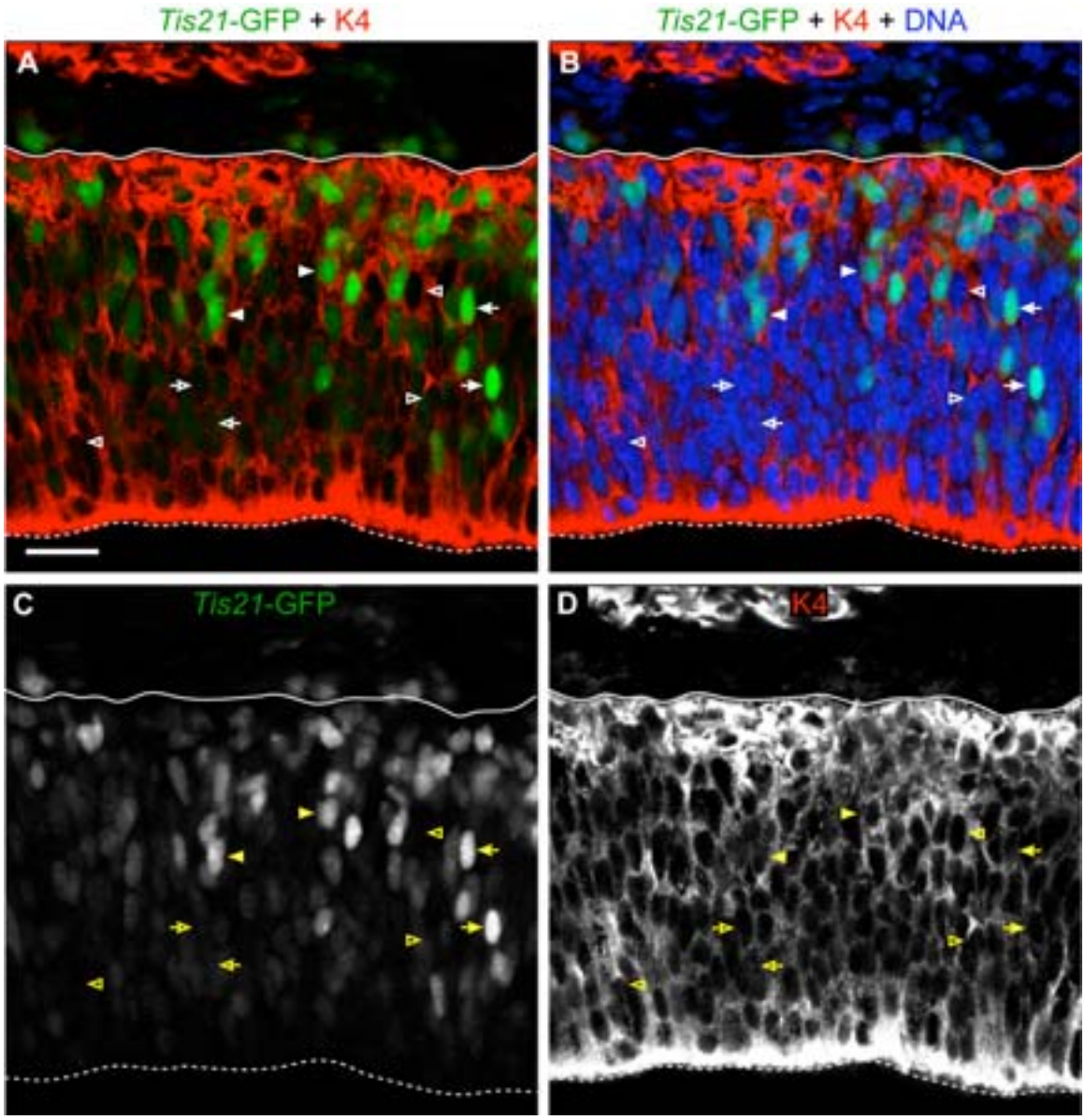

Figure 5. The K4 immunoreactivity does not overlap with *Tis21*-GFP. Sections from the E11.5 heterozygous *Tis21*-GFP mouse embryo were stained with the K4 antibody (red). Nuclei are visualised with DAPI (blue). GFP (green) carries a nuclear localisation signal and is expressed from the *Tis21* locus, reflecting expression of the *Tis21* mRNA. All four combinations of fluorescence can be observed: *filled arrowheads*, $K4^+/GFP^+$; *empty arrowheads*, $K4^+/GFP^-$; *filled arrows*, $K4^-/GFP^+$; *empty arrows*, $K4^-/GFP^-$. Images are single optical sections (1μm). Continuous and dashed lines delineate the pial and ventricular surfaces, respectively. Scale bar equals 20 μm.

Although slightly shorter half life of the *Tis21* mRNA compare to the *GFP* mRNA has been recorded (Ji Feng Fei, unpublished results), it is unlikely that the revealed discrepancy between GFP fluorescence and the K4 immunoreactivity results from different half-lives of the GFP and Tis21 proteins, because both last sufficiently long to be inherited by newborn neurons (Haubensak et al., 2004; Iacopetti et al., 1999). Moreover, since GFP is inserted into the *Tis21* locus, its expression is driven by endogenous regulatory sequences, and as a consequence it reflects precisely the *Tis21* mRNA expression (Haubensak, 2002; Haubensak et al., 2004), excluding the possibility that the endogenous protein can be detected before GFP. Taken together, it is plausible that the K4 antibody cross-reacts with other protein than Tis21, and therefore is not suitable to detect Tis21 in the neuroepithelium.

2.1.3 Distribution of the K4 immunoreactivity in the neuroepithelium

Regardless the nature of the K4 epitope, its distribution in mitotic figures *in vivo* was investigated by confocal microscopy in proliferating and neurogenic progenitors, as identified by GFP expression in heterozygous *Tis21*-GFP embryos. It is believed that the GFP positive progenitors which divide at the apical surface of the neuroepithelium undergo neurogenic asymmetric divisions (Haubensak et al., 2004; Kosodo et al., 2004), therefore, if unequal distribution of the K4 epitope is to be a cell fate determinant, it should be observed in GFP positive cells. As shown in Figure 6, the K4 immunoreactivity was present as a diffused weak staining in the cytoplasm and also strongly associated with lateral membranes and junctions, whereas the staining in cultured cells was mainly cytoplasmic (compare with Figure 1). The cytoplasmic staining did not exhibit an unequal distribution in GFP positive (n=5), as well as in GFP negative cells (n=3). It was not possible to conclude about the distribution of the lateral staining, since it could not be assigned to a particular cell.

To summarise, although the K4 immunoreactivity was unequally distributed during the mitosis in some of *in vitro* cultured neuroepithelial cells, the pattern of immunostaining observed *in vivo* was distinct. This dissimilarity can be attributed to the difference in the staining protocol used for tissue sections and cell cultures, as the latter were stained applying only a short treatment with Triton X-100 or other permeabilising agents (0.2% saponin, acetone). Several other antisera and affinity purified antibodies raised against Tis21 during time of this work also did not yield a specific signal. Thus, this project was not continued.

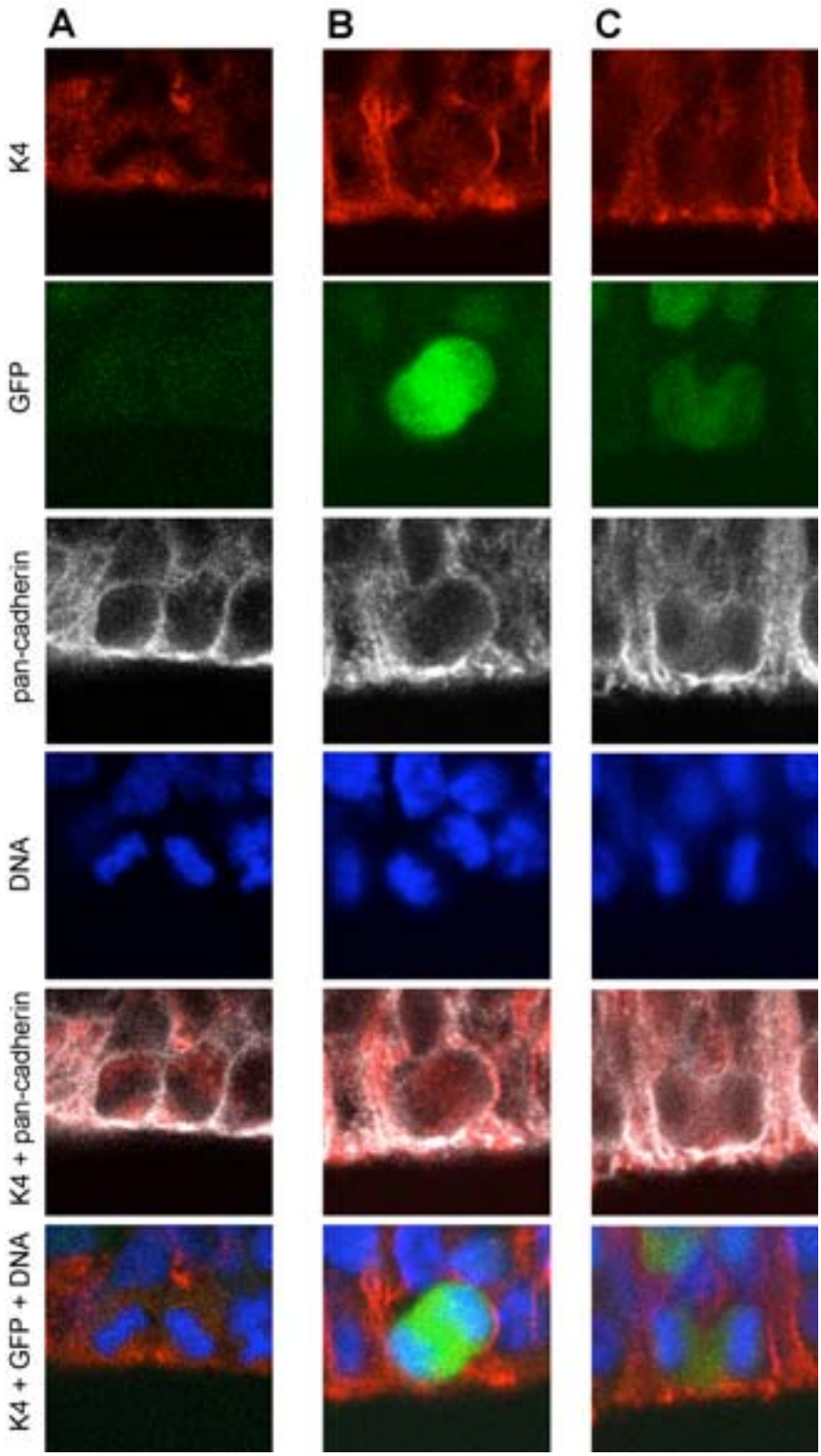

Figure 6. Distribution of the K4 immunoreactivity in mitotic cells *in vivo*. Cryosections from E11.5 heterozygous *Tis21*-GFP embryos were stained with K4 (red), and pan-cadherin (white) antibodies. Nuclei are visualised with DAPI (blue). (**A**) proliferative division, as marked by absence of GFP. (**B**,**C**) GFP-positive neurogenic asymmetric divisions. GFP is localised in the cytoplasm despite its nuclear localisation signal as a result of nuclear envelope breakdown upon mitosis. The K4 immunoreactivity is diffused in the cytoplasm and is strong at lateral membranes marked by pan-cadherin staining, without apparent asymmetric distribution. Images are maximum intensity projections from several optical sections.

PART II

2.2 Characterisation of the expression of mouse Y-box protein 3 (MSY3) during central nervous system development

2.2.1 Two splice variants of the MSY3 protein are expressed in the developing embryo

To study the MSY3 protein in the mouse central nervous system, a panel of antibodies directed against this protein was generated and characterised (for details see *Materials and Methods*). In immunoblotting of protein extracts from mouse embryos, all antibodies recognised a similar set of immunoreactive bands of approximately 58-60 and 47 kDa (Figure 7 A, red arrows). Although predicted molecular weights for the long and short MSY3 isoform are 38.8 and 30.7 kDa, respectively, Y-box proteins due to a high content of basic amino acids and asymmetric structure tend to migrate at much higher molecular weights (Tafuri and Wolffe, 1991). Moreover, migration pattern of the canine ZONAB protein is very similar (Balda and Matter, 2000). Pre-immune sera (Figure 7 A, lanes 1, 3, 5) or a non-related serum (Figure 7 B, lane 1) did not reveal such a pattern of immunoreactivity.

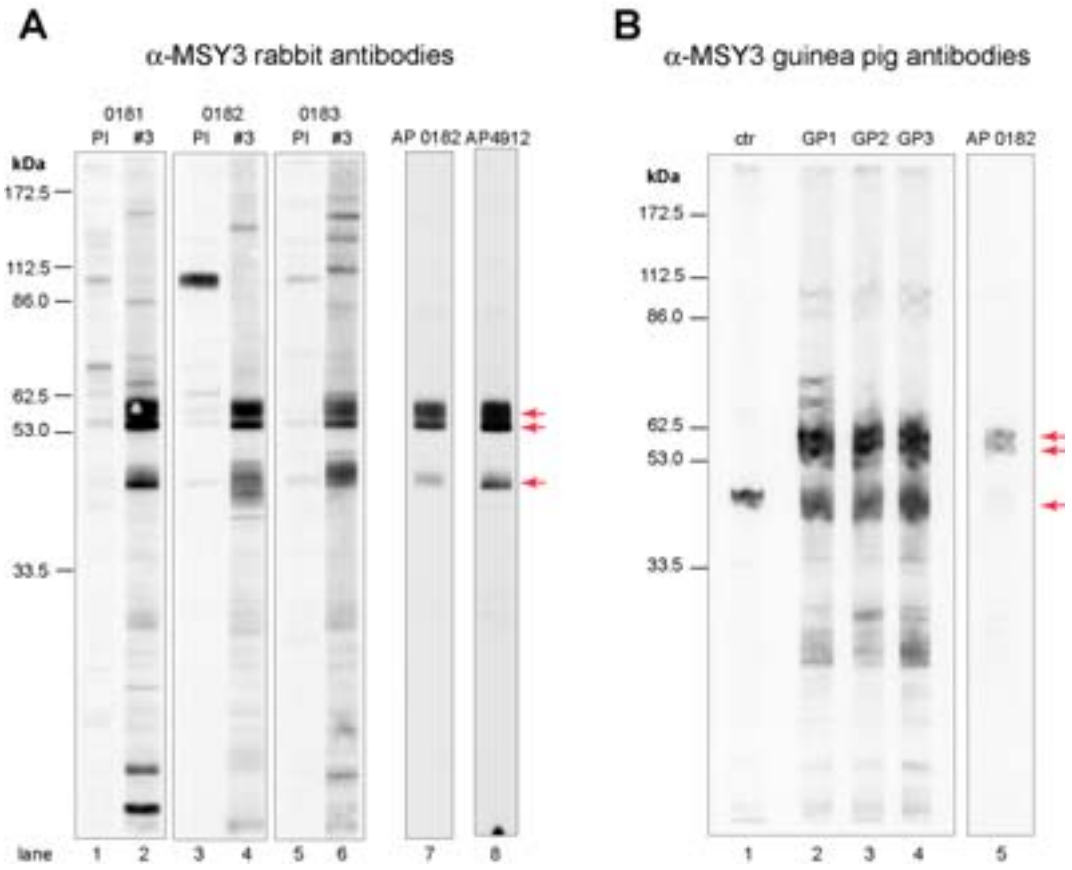

Figure 7. Characterisation of antibodies against the MSY3 protein. Protein lysate from (**A**) E9.5, or (**B**) E10.5 embryos was analysed by immunoblotting using antibodies directed against the MSY3 protein as follows: (**A**) Rabbit polyclonal antisera from the third bleed (#3, lanes 2, 4, 6) and the corresponding pre-immune sera (PI, lanes 1, 3, 5); affinity purified serum 0182 (lane 7); and affinity purified rabbit polyclonal antibody AP4912 (lane 8). (**B**) A control guinea pig serum (lane 1) and three guinea pig antisera (lanes 2-4); the AP0182 rabbit antibody is shown as a control (lane 5). Arrows indicate immunoreactive bands recognised by all antibodies. The additional, weaker bands do not relate to the

MSY3 protein, as the corresponding proteins are not immunoprecipitated with anti-MSY3 antibodies and are not routinely detected on immunoblots. The position of prestained apparent molecular weight markers is indicated.

To evaluate whether these bands correspond to the MSY3 protein, HeLa cells were transiently transfected with expression plasmids carrying cDNA corresponding to either the short or long MSY3 splice variant, and analysed by immunoblotting along with the protein extract from mouse embryos. Indeed, as shown in Figure 8, the AP4912 antibody recognised bands migrating at 47 kDa and 58-60 kDa in cells transfected with the short or long MSY3 variant, respectively (Figure 8, lanes 2 and 3, red arrows). No band was detected in cells transfected with the empty vector (Figure 8, lane 1). Notably, the same set of immunoreactive bands was observed in the extract prepared from E9.5 mouse embryos (Figure 8, right panel lane 4), with the long splice variant of MSY3 being the major form. It is interesting to note that in each case the antibody recognised doublets of immunoreactive bands, possibly due to phosphorylation of MSY3. The identical pattern of immunoreactive bands was observed with the AP0182 antibody (data not shown).

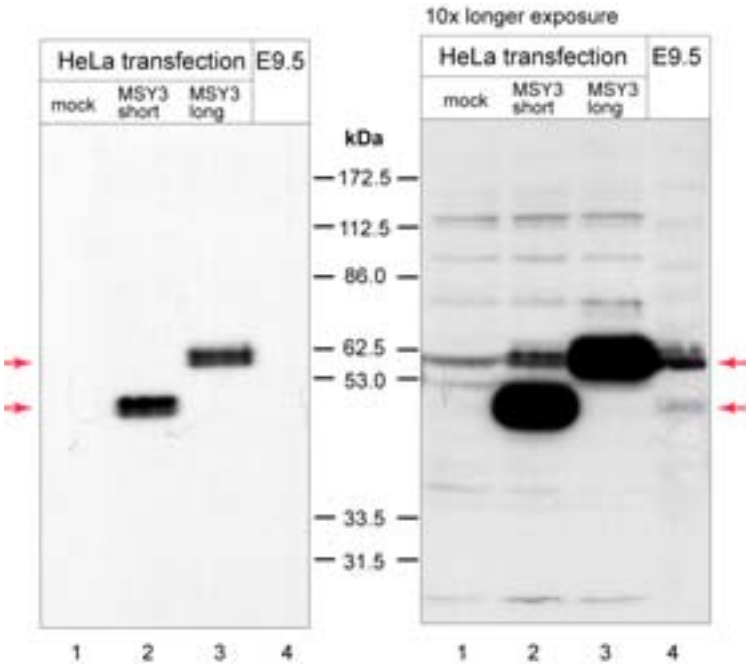

Figure 8. Both splice variants of MSY3 are expressed in the mouse embryo. Detergent extracts from HeLa cells transiently transfected with the expression vector encoding short or long splice variant of the MSY3 cDNA (lanes 2 and 3), or the empty vector as a negative control (mock, lane 1), and from E9.5 embryos (lane 4) were analysed by immunoblotting with the affinity purified antibody AP4912 against MSY3. The right panel shows 10-times longer exposure of the same membrane as the left panel. Arrows indicate bands corresponding to the MSY3 protein isoforms. The position of prestained apparent molecular weight markers is indicated.

2.2.2 *Expression of MSY3 is associated with neuronal progenitors*

We first asked whether MSY3 is expressed in the developing CNS. Double staining for MSY3 and a marker of new-born neurons, βIII-tubulin, revealed that MSY3 is expressed in the germinal zone (Figure 9, red) but not in the neuronal layer (Figure 9, green). Within the neuronal layer, blood vessels, as identified by morphology, are also brightly stained (Figure 9 and Figure 12, arrowheads). Since blood vessels often trap antibodies nonspecifically, it cannot be concluded that this staining reflects presence of the MSY3 protein. MSY3 was

also expressed in most other tissues between E10.5 and E12.5, namely skin, mesenchyme, heart, somites and peripheral ganglia (Figure 12, and data not shown; see also Lu et al., 2006).

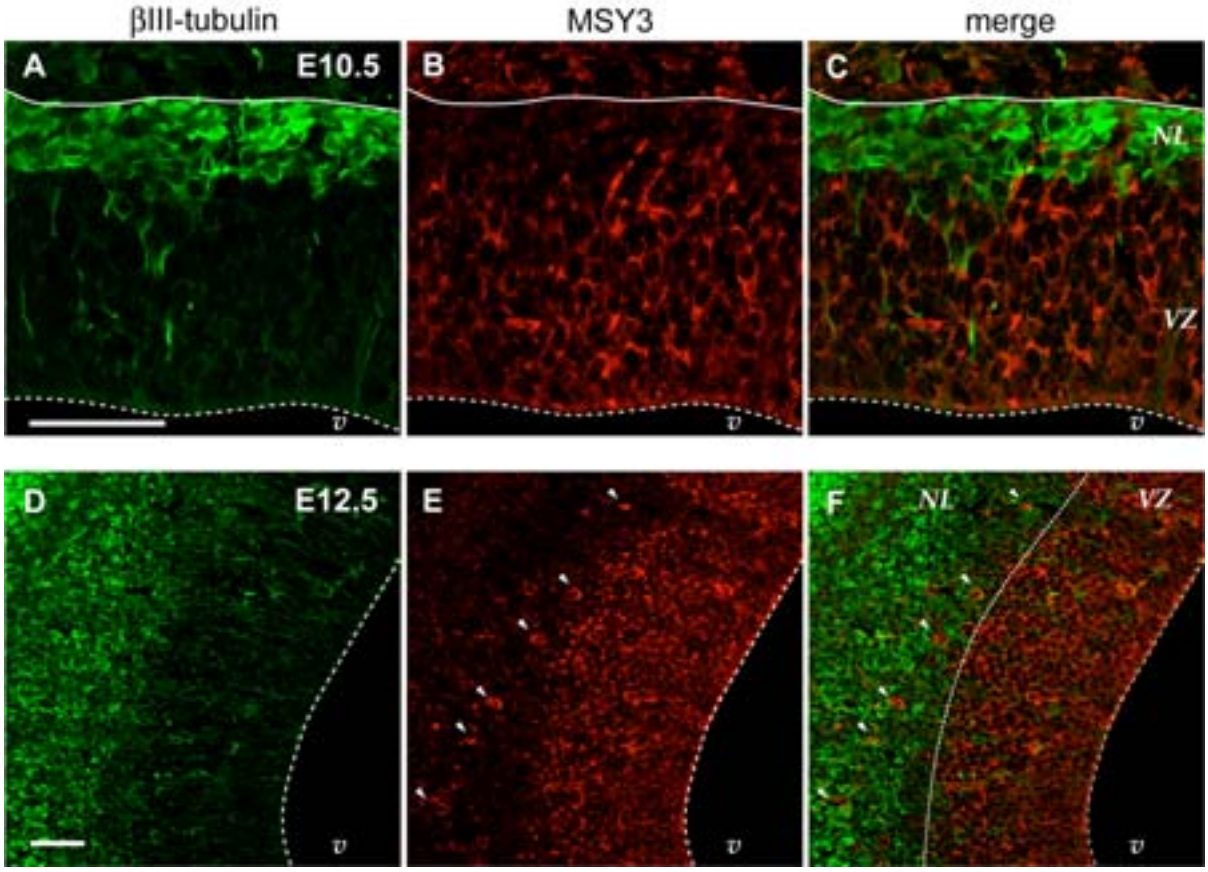

Figure 9. MSY3 is expressed in progenitors, but absent from neuronal layer. Transverse cryosections through a mouse rhombencephalon at E10.5 (**A-C**), and diencephalon at E12.5 (**D-F**), stained for neuronal marker, βIII-tubulin (green), and MSY3 (red). MSY3 expression is confined to the ventricular zone (*VZ*), where progenitors reside. Neuronal layers (*NL*, demarcated by dotted line in F) at different stages of embryogenesis are negative for MSY3. Images are single optical sections (1 μm). Continuous and dashed lines delineate the pial and ventricular surfaces, respectively; *v*, ventricle; arrowheads point to stained blood vessels within the neuronal layer; scale bars equal 50 μm.

To investigate further expression of MSY3 in progenitors, the sections of the telencephalon from E8, E11.5 and E14 embryos were analysed by colabelling with the RC2 monoclonal antibody. The RC2 antibody stains radially oriented cells with the soma in the ventricular zone and the process reaching the pia as early as E9.5 (Gadisseaux et al., 1992; Misson et al., 1988). The RC2 immunoreactivity is associated with intermediate filaments, and most likely indicates posttranslational modification of nestin (Chanas-Sacre et al., 2000).

At the neural plate stage, i.e. at E8, MSY3 was expressed in all neuroepithelial and ectodermal cells (Figure 10 A, and data not shown). No RC2 staining could be detected at this time point (Figure 10 B). At E11.5 and E14.5, RC2 labelled radially oriented cells showing little overlap with the MSY3 immunoreactivity (Figure 10 G,K). This apparent lack of colocalisation could be explained by a different subcellular localisation of both antigens. Whereas MSY3 is perinuclear, RC2 stains intermediate filaments. Indeed, higher magnification images revealed that most of MSY3 positive cells are also stained for RC2, which is particularly evident in rounded mitotic cells (Figure 10 O, open arrowhead). However, not all RC2 positive cells express also MSY3 (Figure 10 O, arrows).

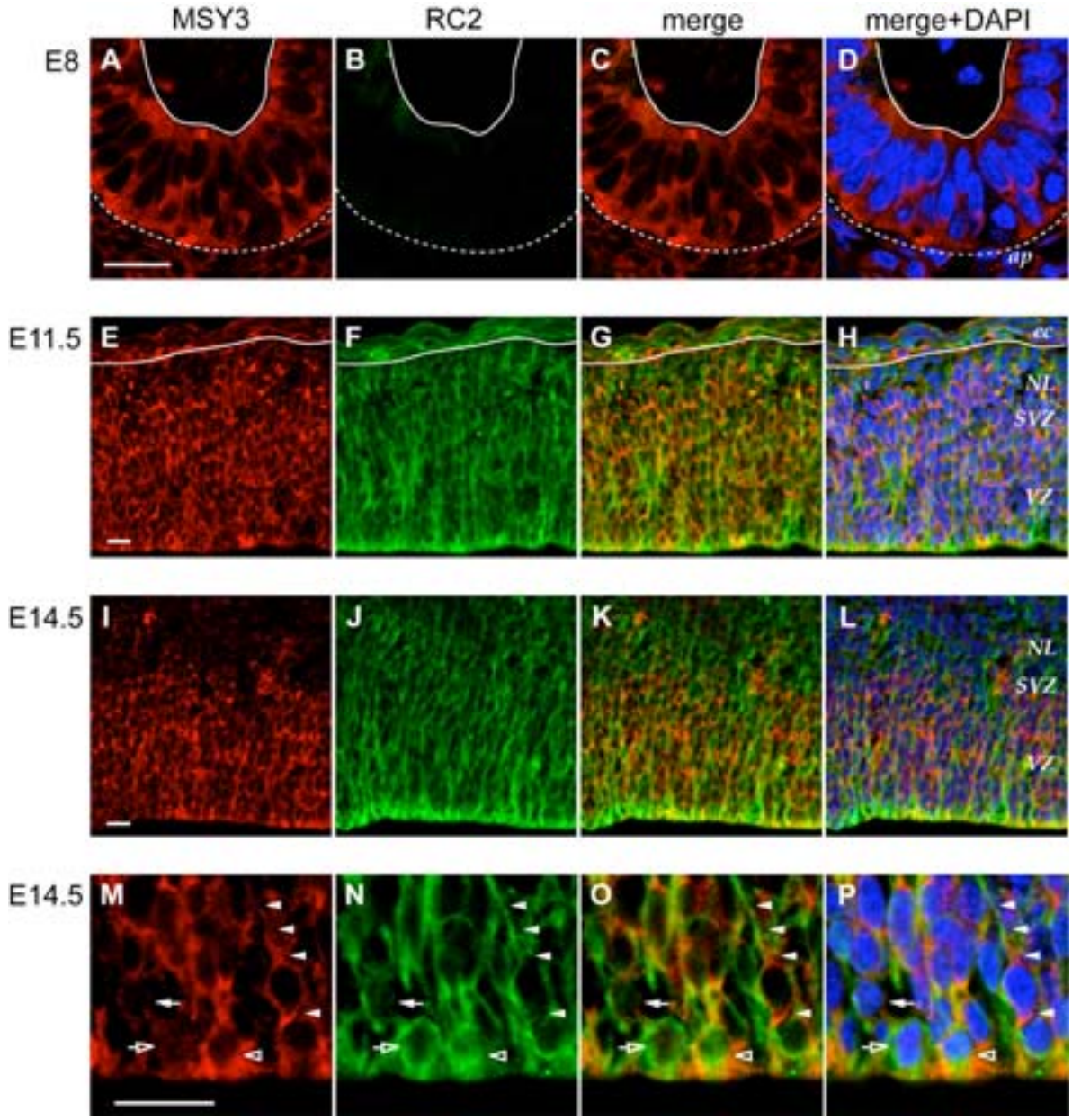

Figure 10. MSY3 is expressed in a subset of RC2 positive progenitors. Cryosections through (**A-D**) the prospective forebrain at E8, (**E-H**) the lateral telencephalon at E11.5, and (**I-P**) the lateral cortex at E14.5, stained for MSY3 (red) and RC2 (green). Nuclei were visualised with DAPI (blue). (**A-D**) MSY3 is expressed before the onset of RC2 expression. (**E-L**) At E11.5 and E14.5, the RC2 antibody labels radial cells. Note that RC2 gives a filament-like staining and MSY3 stains mainly the perinuclear cytoplasm. (**M-P**) As seen at higher magnification, RC2 positive progenitors are also MSY3 immunoreactive (arrowheads). MSY3 is not expressed in all RC2 positive cells (arrows). Mitotic cells at the apical surface are indicated by empty arrow and arrowhead. Images are single optical sections (A-L, 2 μm; M-P, 1.5 μm). Apical surface is towards bottom. The continuous and dashed lines delineate pial and ventricular surfaces, respectively. *ap*, apical; *NL*, neuronal layer; *VZ*, ventricular zone; *SVZ*, subventricular zone. Scale bars indicate 20 μm.

Similar results were obtained from a preparation of acutely dissociated cells from telencephali of E11.5 embryos. 8 h after plating, vast majority of MSY3 positive cells was positive for progenitor marker nestin (97%, n=89; Figure 11 A-D), and simultaneously most of nestin immunoreactive cells was positive for RC2 (93%, n=42; Figure 11 E-H). The coexpression of nestin and the RC2 antigen in the same progenitors has already been reported, and both antigens are associated with proliferating cells (Chanas-Sacre et al., 2000; Hartfuss et al., 2001).

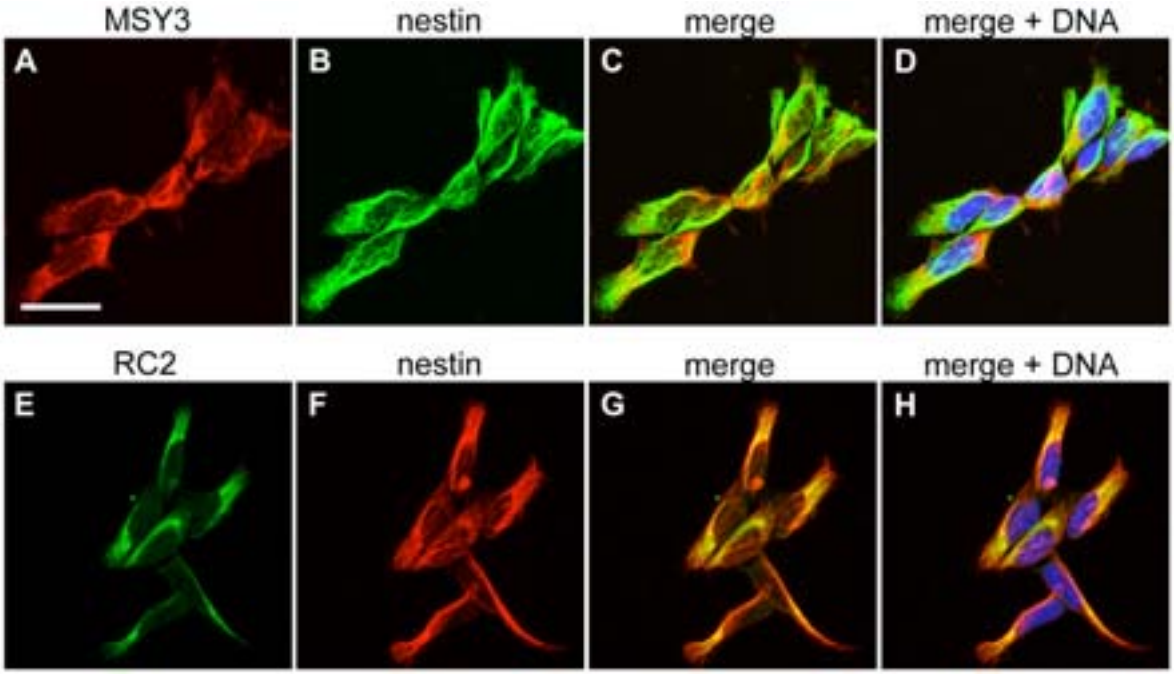

Figure 11. Colocalisation of MSY3, nestin and RC2 in acutely dissociated cells. Cells were fixed 8 h after plating and double immunostained for (**A-D**) MSY3 and nestin, or (**E-H**) nestin and RC2, as indicated in the figure. Nuclei are visualised by DAPI (blue). Note that the MSY3 expressing cells also contain nestin, and nestin immunoreactive cells express also RC2. Images are maximum intensity projections of Z-stacks. Scale bar equals 20 μm.

2.2.3 *Expression of the MSY3 protein in the developing CNS is downregulated in temporal and spatial correlation with neurogenesis*

Expression of MSY3 was analysed further with regard to the wave of neurogenesis in the developing mouse brain. The onset, and termination, of neurogenesis proceeds in a posterior to anterior gradient in brain vesicles, i.e. from the hindbrain to the telencephalon, and in the spinal cord from rostral to caudal. Thus, already at E8.5 some neurons are born in the ventral hindbrain and midbrain, at E9 in the spinal cord, by E9.5-10 in the diencephalon, and at E10.5 in the rostral telencephalon. Furthermore, in the telencephalon, the longitudinal neurogenic gradient proceeds from anterior towards posterior, whereas transverse gradients set from the ventrolaterall towards dorsomedial telencephalon, as well as ventromedially (Bayer and Altman, 1991; Gardette et al., 1982; Haubensak, 2002; Haubensak et al., 2004; McConnell, 1981; Nornes and Carry, 1978).

Two regions of the developing mouse brain along its rostrocaudal axis, i.e. the telencephalon and rhombencephalon, of various developmental stages were analysed by immunostaining on transverse cryosections derived from *Tis21*-GFP embryos (Figure 12). Since *Tis21*-GFP marks neurogenic, but not proliferating, progenitors, it is a useful tool to visualise progression of neurogenesis. As reported previously (Haubensak et al., 2004), in the rostral telencephalon, first GFP positive cells appear at E10.5 (Figure 12 C), and by E15.5 they reach 60% fraction of the progenitor cells in this region. Notably, the MSY3 immunoreactivity decreases in the telencephalon starting at E11.5 (Figure 12 F), and is dramatically down-regulated at E12.5 (Figure 12 H), when a significant proportion (ca. 20%) of progenitor cells generate neurons. Later, between E14 and E18, MSY3 expression remains at constant low level in the germinal zone (Figure 12 J).

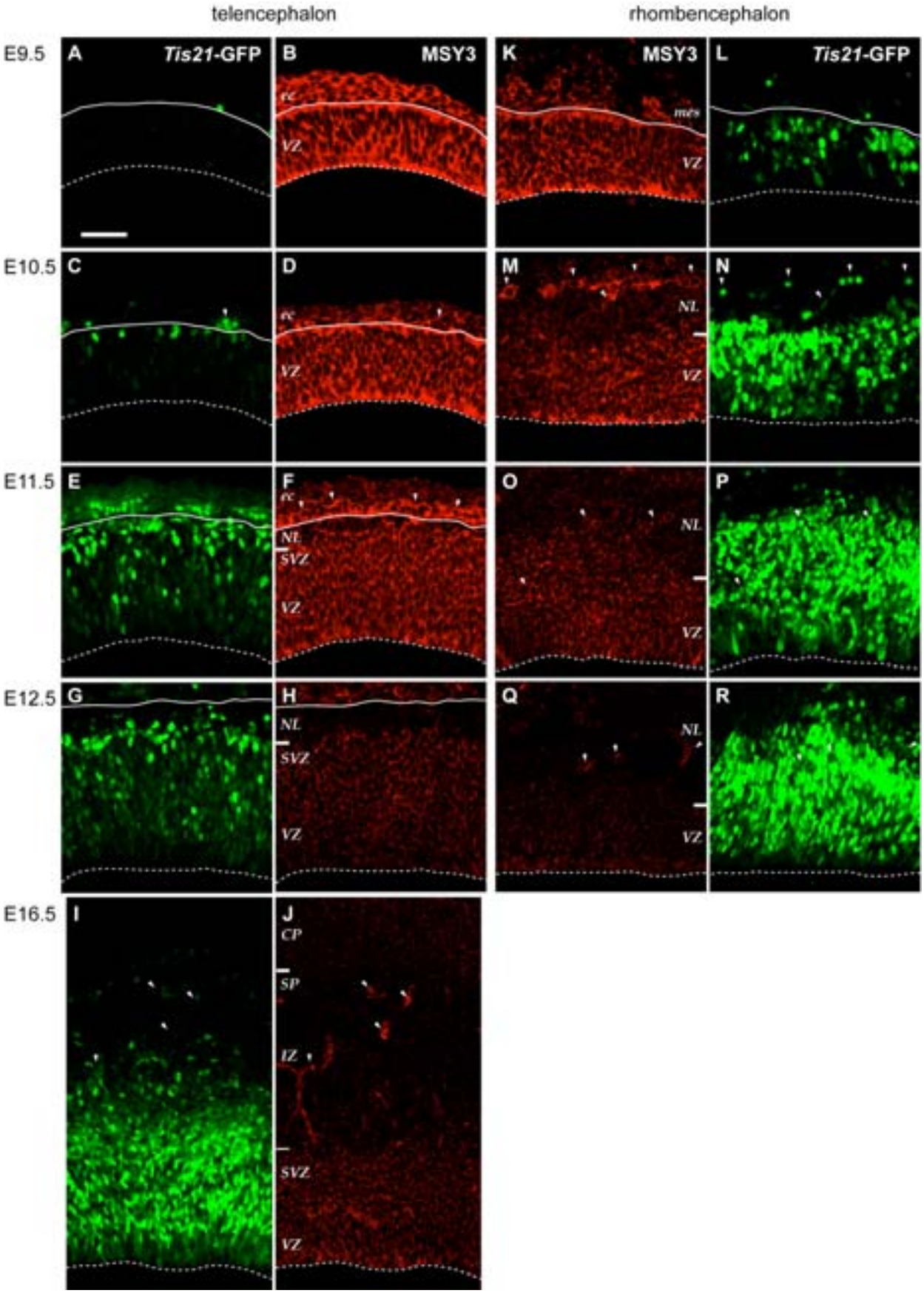

Figure 12. Spatial and temporal expression of MSY3 in the heterozygous *Tis21*-GFP mouse embryos. Transverse cryosections through (**A-J**) the rostral telencephalon, and (**K-R**) lateral rhombencephalon, at indicated developmental stages were stained for MSY3 (red, middle panels). Images are single optical sections (3 μm) acquired with the same settings in the middle of a tissue section. Ventricle is towards bottom. GFP carries a nuclear localisation signal and marks neurogenic progenitor cells (green, right and left panels). Note that MSY3 immunostaining is decreasing with

development, and is lower in the rhombencephalon than in the telencephalon at each developmental stage, in inverse pattern to *Tis21*-GFP. The MSY3 labelling is detected also in the surface ectoderm (*ec*), and mesenchyme (*mes*). The continuous and dashed lines delineate the pial and ventricular surfaces, respectively. *NL*, neuronal layer; *VZ*, ventricular zone; *SVZ*, subventricular zone; *CP*, cortical plate; *IZ*, intermediate zone; *arrows*, blood vessels; scale bar equals 50 μm.

In the brain, first neurons are born in the rhombencephalon, and already at E9.5 many cells in this region are *Tis21*-GFP positive (Figure 12 L). Remarkably, for each developmental time point analysed, the MSY3 immunoreactivity is lower in the rhombencephalon than in the telencephalon (compare left and right panels in Figure 12).

MSY3 expression declines also in relation to the ventrodorsal gradient of neurogenesis, which is particularly striking in the rhombencephalon at E10.5 onwards. As illustrated in Figure 13, the MSY3 immunoreactivity appears lower in more ventral region (Figure 13 A, towards left), where neurogenesis is more advanced than dorsally (Figure 13 B,C). Moreover, in the telencephalon, MSY3 is downregulated in ventrolateral to dorsomedial gradient (Figure 17 A, p.47), corresponding to the neurogenic wave (Bayer and Altman, 1991).

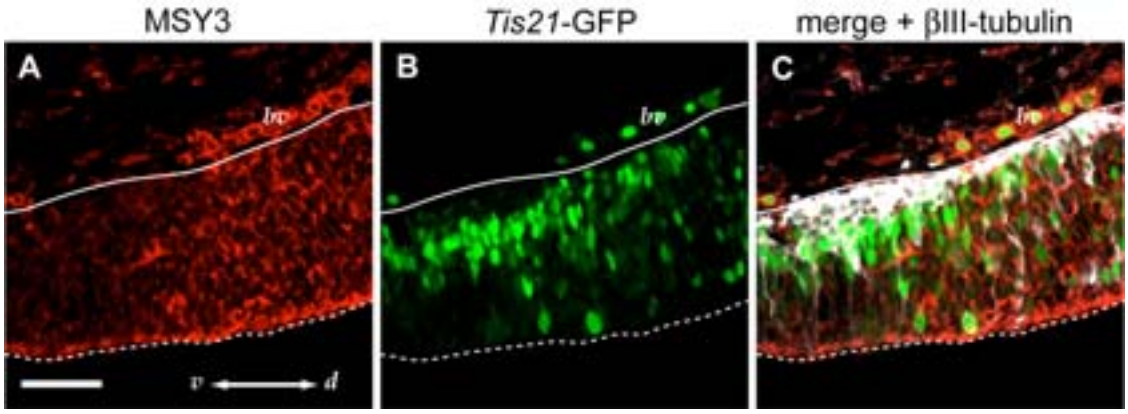

Figure 13. MSY3 is down-regulated in a ventral to dorsal gradient. A transverse cryosection through the ventro-lateral rhombencephalon of the E10.5 heterozygous *Tis21*-GFP embryo stained with antibodies against MSY3 and βIII-tubulin. Ventral is towards left. Neurogenesis proceeds in ventral-to-dorsal gradient, as visualised by abundance of *Tis21*-GFP positive progenitors (B, green), and accumulation of neurons (C, white). Images are single optical sections (4 μm). Dashed and continuous lines indicate the ventricular and pial surfaces, respectively; *bv*, blood vessel; scale bar, 50 μm.

To corroborate the immunostaining data, MSY3 expression was analysed by immunoblotting. Protein extracts were prepared from whole E8.5 embryos, or telencephali and hindbrains dissected out from embryos aged between E9.5 and E14.5, and from the adult brain. As shown in Figure 14, MSY3 is strongly expressed at E8.5 and at E9.5 in the telencephalon, when only few neurons are born. With the onset of neurogenesis, however, MSY3 is progressively downregulated, being below the detection level in the adult brain. In agreement with immunostaining, at any given stage this downregulation is more prominent in the hindbrain than in the telencephalon.

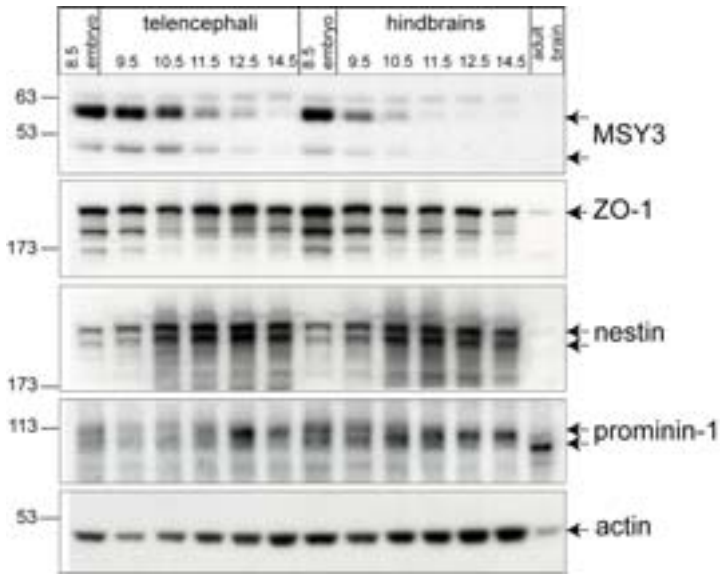

Figure 14. MSY3 is downregulated at the onset of neurogenesis. 20 μg of protein extracts prepared from E8.5 embryos and from telencephali or hindbrains at indicated developmental stages, and from the adult brain, were analysed by immunoblotting with antibodies against proteins expressed in neuronal progenitors, i.e. MSY3 (AP4912), ZO-1, nestin, prominin-1, as well as actin, as indicated. Note that only MSY3 is downregulated during the neurogenic period. The position of prestained apparent molecular weight markers is indicated.

Since neurons, which do not express MSY3, accumulate with the progression of neurogenesis, it could be argued that the MSY3 level is constant in progenitors and observed down-regulation of MSY3 is accounted for by diluting a protein fraction derived from progenitors by other cell types. Therefore, it is of importance that other proteins expressed in progenitors, but not in neurons, i.e. zonula occludens-1 (ZO-1), nestin and prominin-1 (Aaku-Saraste et al., 1996; Hatakeyama et al., 2004; Hockfield and McKay, 1985; Lendahl et al., 1990; Weigmann et al., 1997), do not exhibit such downregulation in time and space (Figure 14). The expression of nestin actually increases between E9.5 and E10.5, and remains constant, as previously reported (Hockfield and McKay, 1985). Only the increase in actin immunoreactivity is likely resulting from changes in cellular composition of the samples.

Taken together, the MSY3 protein is downregulated precisely at the onset of neurogenesis. Importantly, the reported pattern was seen with all antibodies against MSY3.

2.2.4 MSY3 is not expressed in specialised regions of the neural tube

After the closure of the neural tube, cells at its dorsal and ventral aspects form the morphologically distinct roof and floor plate, which specify and pattern the neural tissue along the dorsoventral axis (Fuccillo et al., 2006; Liu and Niswander, 2005; Placzek and Briscoe, 2005). Remarkably, MSY3 expression is very low in some of these regions. In the E12.5 brain, derivatives of, and tissues located immediately to, the embryonic dorsal midline, namely the lamina terminalis (Figure 15 D-F), anlage of the choroid plexus (Figure 15 G-I), and the cortical hem (Figure 15 J,K) are devoid of MSY3 expression. At earlier stages, i.e. E10.5-E11.5, MSY3 expression in equivalent regions is lower than in a surrounding tissue (data not shown). In the spinal cord, already at E10.5 MSY3 is not expressed in the floor plate (Figure 15 A-C).

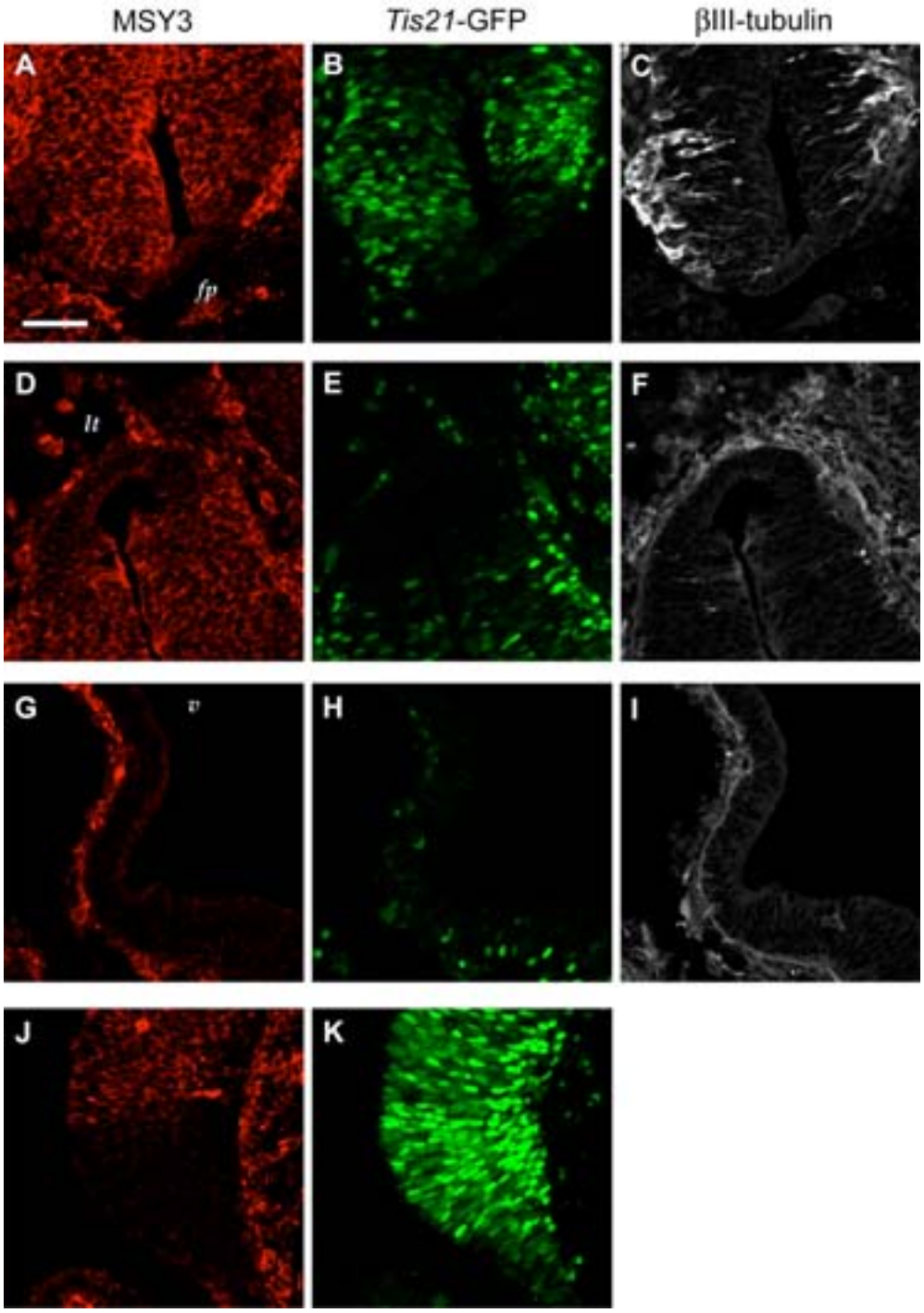

Figure 15. MSY3 is not expressed in non-neurogenic regions of the neural tube and in the cortical hem. Transverse cryosections of heterozygous *Tis21*-GFP embryos stained with antibodies against MSY3 (red) and βIII-tubulin (white). (**A-C**) the E10.5 spinal cord; (**D-F**) the E12.5 hypothalamus; (**G-K**) the E12.5 medial telencephalon showing the anlage of the choroid plexus (G-I) and the cortical hem (J,K). The floor plate (*fp*), lamina terminalis (*lt*) and choroid plexus, which contain post-mitotic cells and do not generate neurons, as seen by absence of *Tis21*-GFP positive progenitors (green) and neurons, are negative for MSY3. Dorsal is towards up. Images are single optical sections (4 μm for A-I, 3 μm for J,K). *v*, ventricle. Scale bar equals 50 μm.

Cells of the floor and roof plate, including the lamina terminalis, do not generate neurons, which can also be seen by absence of *Tis21*-GFP positive progenitors and βIII-tubulin positive neurons. It is important to note that by the time of the analysis these cells has largely withdrawn from the cell cycle (Baek et al., 2006; Kahane and Kalcheim, 1998).

Bilaterally, from the cells of the dorsal midline in the anterior telencephalon, and prosteriorly from cells near the dorsal midline, develops the cortical hem (Currle et al., 2005; Hebert et al., 2003). The hem, through expression of multiple members of Wnt and BMP families, is indispensable for development of abutting regions: laterally the hippocampus, and medially the telencephalic choroid plexus epithelium (Grove et al., 1998; Lee et al., 2000; Yoshida et al., 2006a). This region is a source of reelin-positive Cajal-Retzius cells (CR), which migrate out onto the surface of the cortex, playing an essential role in proper layering (Takiguchi-Hayashi et al., 2004; Yoshida et al., 2006a). Notably, by E12.5, i.e. when MSY3 is downregulated, generation of CR cells is largely accomplished, and the hem is composed of thinning neuroepithelium, which shrinks further until E16.5 (Takiguchi-Hayashi et al., 2004; Yoshida et al., 2006a).

The choroid plexus produces the cerebrospinal fluid and its epithelium is the only nonneural tissue that develops from the neural tube. It differentiates at three locations: in the hindbrain roof, anterior diencephalic roof and bilaterally at dorsomedial edges of the telencephalon (Currle et al., 2005; Hebert et al., 2003). Transition of the choroid plexus epithelium into a simple columnar to cuboidal cells contiguous with adjacent pseudostratified neuroepithelium is complete at the time of analysis (Sturrock, 1979), its cells being mostly postmitotic (Hebert et al., 2003).

Thus, it becomes evident that in the neural tube MSY3 expression is associated solely with highly proliferative and not differentiated cell types.

2.2.5 *MSY3 expression in neurogenic versus proliferating progenitors*

Because proliferating and neurogenic progenitors co-exist in the ventricular zone, and MSY3, although downregulated, is still expressed when neurogenesis is ongoing, it was interesting to determine in which of these populations the MSY3 protein is present. To address this question, MSY3 immunostaining and *Tis21*-GFP fluorescence in the lateral midbrain and ventral telencephalon of E11.5 heterozygous embryos were compared as explained in *Material and Methods* and in Figure 16. Single cells in the neuroepithelium were delineated by concanavalin A staining, as described previously (Noctor et al., 2002). Concanavalin A is a lectin, which binds α-mannopyranosyl and α-glucopyranosyl in the ER and on the cell surface (Figure 16 A,B). Following, the cells were graded for the MSY3 immunoreactivity as strong, middle and weak (Fig. 16 D,D'; red, yellow and blue arrows, respectively), and for the *Tis21*-GFP fluorescence as strong, middle, weak or none (Figure 16 E,E'; white, pale green, dark green and grey circles).

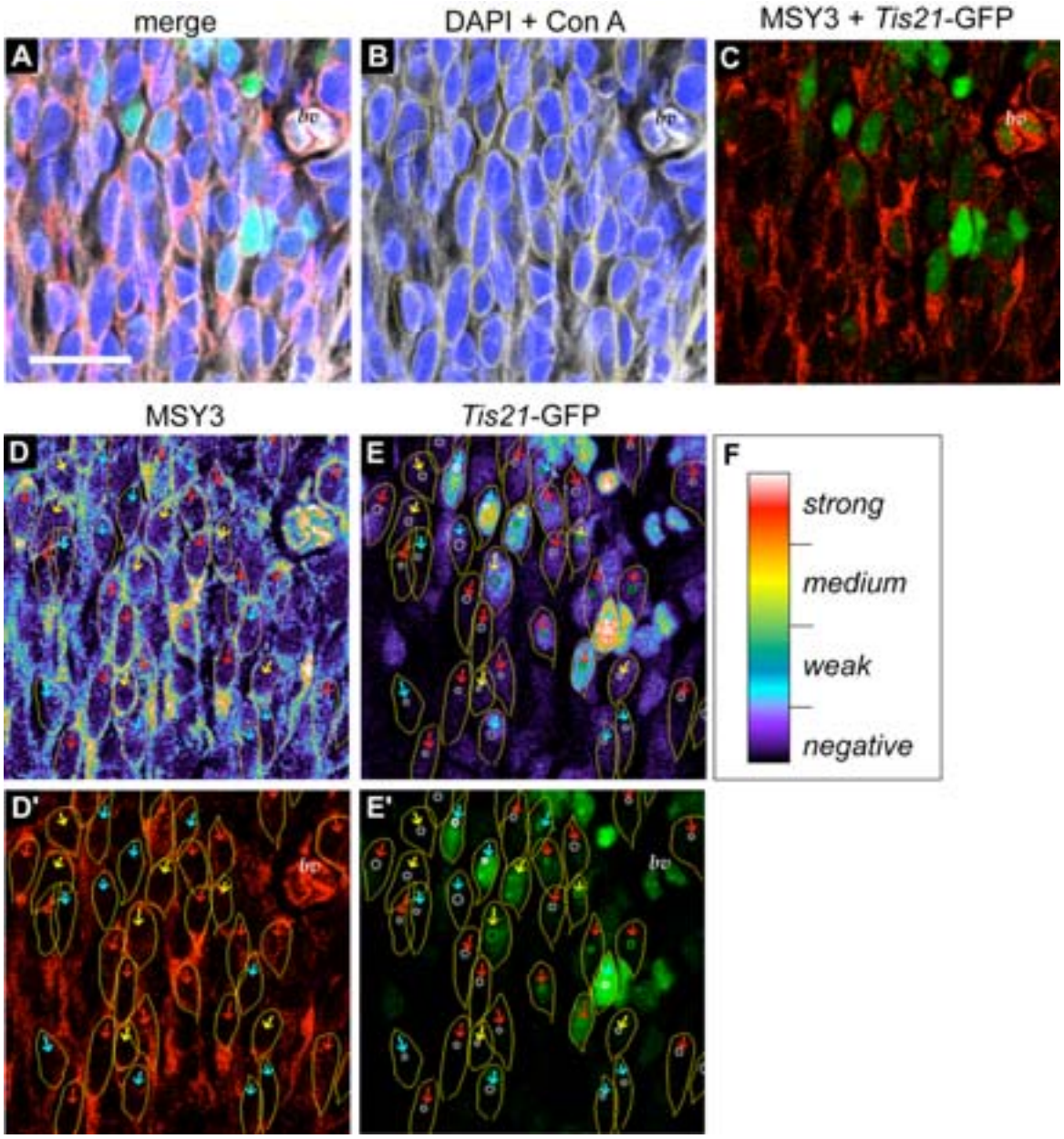

Figure 16. Analysis of MSY3 expression in neurogenic versus proliferating progenitors. (**A**) Coronal cryosections of E11.5 heterozygous *Tis21*-GFP embryos were stained with MSY3 (red) and concanavalin A, (Con A; white), nuclei were visualised by DAPI (blue). (**B**) Single cells were identified in several consecutive optical sections based on Con A and DAPI staining and delineated with yellow line. Note that for clarity a single optical section of 1 μm is shown, and several cells - whose overlay, but not the cell body, is visible - are present in other optical sections. (**C**) Merge for MSY3 and *Tis21*-GFP. (**D**,**D'**) Delineated cells were scored for MSY3 immunofluorescence using the rainbow scale (F) as strong (red arrows), middle (yellow arrows) and weak (blue arrows). (**E**,**E'**) Delineated and marked for MSY3 cells were then scored for *Tis21*-GFP fluorescence using the rainbow scale (F) as strong (white circle), medium (absent from this section), weak (dark green circles) and negative (grey circles). Scale bar equals 20 μm.

As summarised in Table 1, for the lateral midbrain, majority of cells that express high levels of *Tis21*-GFP, simultaneously express low levels of MSY3 (74%). This tendency does not reflect the abundance of the latter in the whole population, which is about one-third (32%). Cells expressing lower level of *Tis21*-GFP show random pattern of MSY3 expression. In the ventral telencephalon, however, no inverse regulation of the two proteins could be observed. Notably, in the ventral telencephalon fewer cells are weakly stained for

MSY3, than in the midbrain (15% vs. 32%), which is in agreement with the general pattern of MSY3 downregulation along the rostrocaudal axis of the embryo.

EGFP / MSY3	strong	medium	weak	none	**total MSY3**
	lateral midbrain				
strong	2	9	51	124	186 (42%)
medium	5	11	32	66	114 (26%)
weak	20	14	32	72	141 (32%)
	ventral telencephalon				
strong	1	5	27	100	133 (52%)
medium	5	5	27	48	85 (33%)
weak	1	4	9	24	38 (15%)

Table 1. Semiquantitative analysis of MSY3 and *Tis21*-GFP expression levels. Each cell was assigned two estimated values: MSY3 immunoreactivity (rows; strong, medium and weak) and *Tis21*-GFP fluorescence (columns; strong, medium, weak or none) as shown in Figure 16. Numbers represent cell counts for each category, pooled from total of four sections per region from two age-matched embryos. The last column (*total MSY3*) gives the total number of cells scored for MSY3 as strong, medium and weak; in brackets the percentage of cells in a given category over the total number of cells is indicated. Whereas in the lateral midbrain strongly *Tis21*-GFP positive cells are largely week for MSY3, no such correlation could be observed in the ventral telencephalon.

Thus, although a general pattern of MSY3 expression is inversely regulated to *Tis21*-GFP, present data, albeit suggestive for some regions, is not sufficient to conclude that MSY3 is specifically excluded from the neurogenic progenitors.

2.2.6 MSY3 is down-regulated in radial glia

MSY3 expression was analysed during the transition of neuroepithelial cells to radial glia. Only radial glia express markers characteristic to differentiated astrocytes, such as GLAST (astrocyte-specific glutamate transporter) and BLBP (brain lipid binding protein). GLAST expression is broader than BLBP and most, if not all, BLBP positive cells express also GLAST (Anthony et al., 2004; Hartfuss et al., 2001). MSY3 expression in GLAST positive radial glia was examined by immunostaining on sections from E12.5 embryos (Figure 17). At this stage, the onset of GLAST and BLBP expression in the telencephalon appears in correlation with the initiation of neurogenesis and radial glia directed neuronal migration (Anthony et al., 2004; Gotz and Huttner, 2005; Hartfuss et al., 2001).

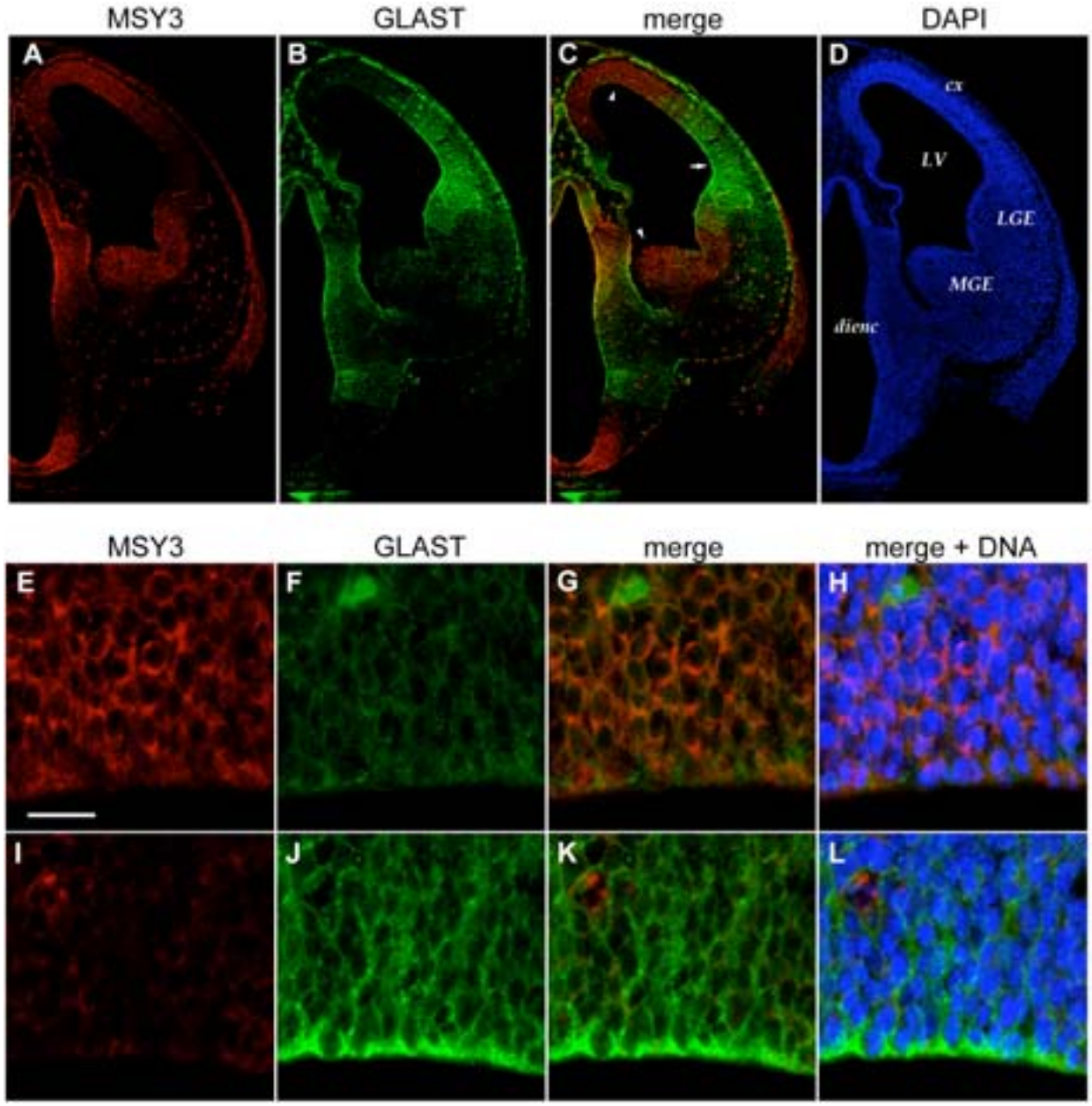

Figure 17. MSY3 expression is downregulated during the transition from neuroepithelial to radial glial progenitors. Immunostaining for MSY3 (red) and GLAST (green) on a transverse cryosection through the E12.5 brain. Nuclei are visualised with DAPI. (**A-D**) Downregulation of MSY3 proceeds in a lateral to caudomedial gradient (arrow), which corresponds to the onset of GLAST expression (arrowheads). Image is a composite of single optical sections (3 µm). (**E-H**) and (**I-L**) are enlarged images of the rostral and caudolateral cortex, respectively. *cx*, cortex; *dienc*, diencephalon; *LGE*, lateral ganglionic eminence; *MGE*, medial ganglionic eminence; *LV*, lateral ventricle. Scale bar equals 20 µm (E-L).

As reported previously, GLAST staining in the telencephalon appeared in a rostrolateral to caudomedial gradient (Figure 17 B,C, arrowheads) (Anthony et al., 2004). Moreover, in regions where GLAST expression was initiated, all radial glia were GLAST immunoreactive (Figure 17 J). Notably, MSY3 expression decreases in an opposite gradient (Figure 17 A,C, arrow). Both antigens colocalise only in a narrow domain of the diencephalon. As the onset of GLAST expression defines the transition from neuroepithelial cells to radial glia, MSY3 is downregulated upon this switch.

2.2.7 *Expression of MSY3 in Hes5-GFP transgenic mouse line*

In the developing rodent CNS, the expansion and maintenance of self-renewal of progenitors requires Notch signalling. First Notch-dependent precursors appear at E8.5 with onset of its expression (de la Pompa et al., 1997; Hitoshi et al., 2002; Hitoshi et al., 2004; Reaume et al., 1992). After E8.5 onward, bHLH transcription factors Hes1 and Hes5 are essential effectors of Notch signalling. The onset of *Hes5* expression coincides with that of *Notch* and *Delta* (de la Pompa et al., 1997; Hatakeyama and Kageyama, 2006), and in the *RBP-J* null embryos, in which the Notch signalling is abolished, *Hes-5* is not expressed (de la Pompa et al., 1997). Therefore, the *Hes5* gene regulatory sequences can be utilised to visualise activation of Notch signalling.

MSY3 expression in relation to Notch signalling was investigated by immunostaining in *Hes5*-GFP transgenic embryos (kindly provided by Onur Basak and Verdon Taylor, Freiburg). In this reporter line, GFP expression is entirely dependent on Notch. The GFP expression pattern, in contrast to the previously reported *Hes5*-EGFP line (Ohtsuka et al., 2006), precisely reproduces that of the endogenous *Hes5* mRNA. The onset of GFP expression commences in a gradient preceding by approximately 1 day the onset of neurogenesis. By E11.5 it is expressed in progenitor cells throughout the entire brain, except for the diencephalon and midbrain at the rostral and dorsal extremities, respectively (Figure 18 B,F). Once induced, GFP expression is homogenous among progenitors in a given region. Then, as a consequence of lateral inhibition, scattered progenitors are selected for differentiation and downregulate *Hes5*-GFP. As presented in Figure 18, MSY3 and *Hes5*-GFP expression overlaps, particularly in the lateral and ventral telencephalon (Figure 18, empty arrows). However, in the cortical hem, where GFP expression is particularly strong, MSY3 is virtually absent (Figure 18, empty arrowheads). In the midbrain, diencephalon, and caudal ganglionic eminence the onset of GFP expression is accompanied by downregulation of MSY3 (Figure 18, solid arrowheads; and Figure 19 for higher magnification). Inversely, regions showing strong MSY3 immunostaining are still negative or weak for GFP (Figure 18, solid arrows; Figure 19).

Figure 18. Expression of MSY3 in the *Hes5*-GFP transgenic embryo. Coronal cryosections of the E11.5 *Hes5*-GFP embryo, in which GFP expression driven from the *Hes5* promoter is a marker of active Notch signalling, were stained for MSY3 (red) and GFP (green). (**A-C**) rostral, and (**D-F**) caudal sections. (**A-C**) In the telencephalon, expression of MSY3 and GFP are partially overlapping (open arrows) except for the cortical hem (open arrowheads). (**D-F**) In the diencephalon, and also the caudal telencephalon, strong MSY3 labelling coincides with low GFP expression (arrows); in reverse, induction of Notch signalling is accompanied by downregulation of MSY3 (arrowheads). Images are composites of single optical sections (3 μm). *dienc*, diencephalon; *mb*, midbrain; *tel*, telencephalon. Scale bar equals 300 μm.

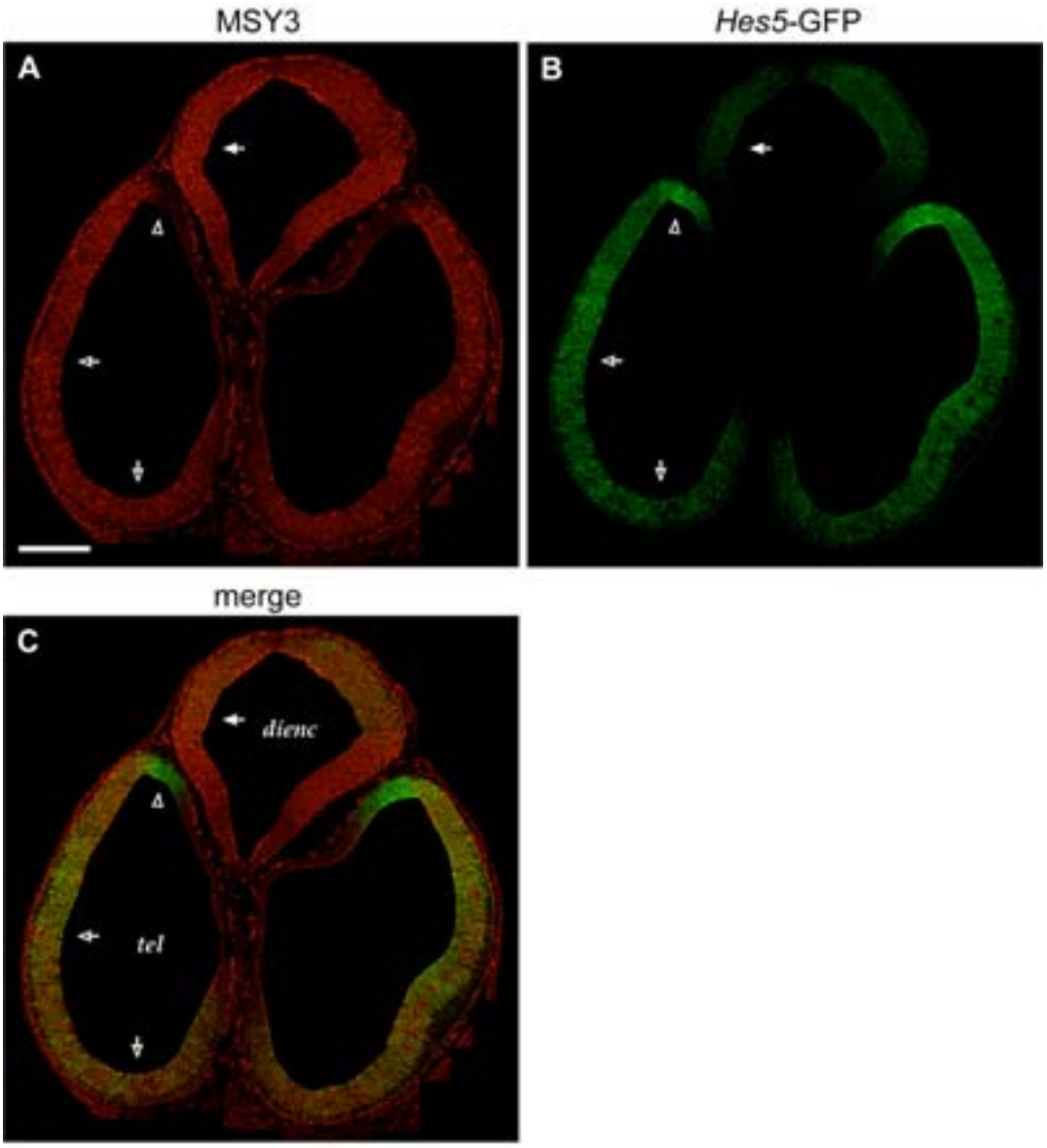
MSY3
Hes5-GFP
A
B
merge
C
dienc
tel

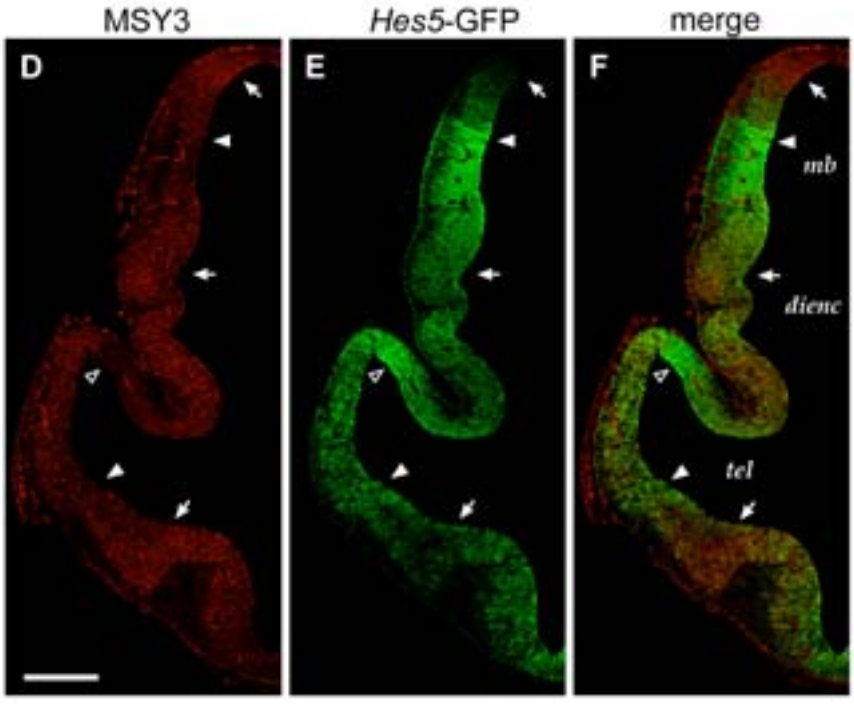
MSY3
Hes5-GFP
merge
D
E
F
mb
dienc
tel

Interestingly, in the areas located between the regions of strong and weak Notch activation, such as the dorsolateral midbrain and diencephalon, it was frequently observed that scattered groups of cells which begin to express GFP simultaneously downregulate MSY3 (Figure 19 G-I, arrows). It is likely that these cells are clonally related, since after the division daughter cells often remain in a close contact (Cai et al., 1997b). Such clusters of cells are coupled via gap junctions, and are synchronised with respect to the cell cycle and interkinetic nuclear migration (Cai et al., 1997b; Lo Turco and Kriegstein, 1991; Pearson et al., 2005).

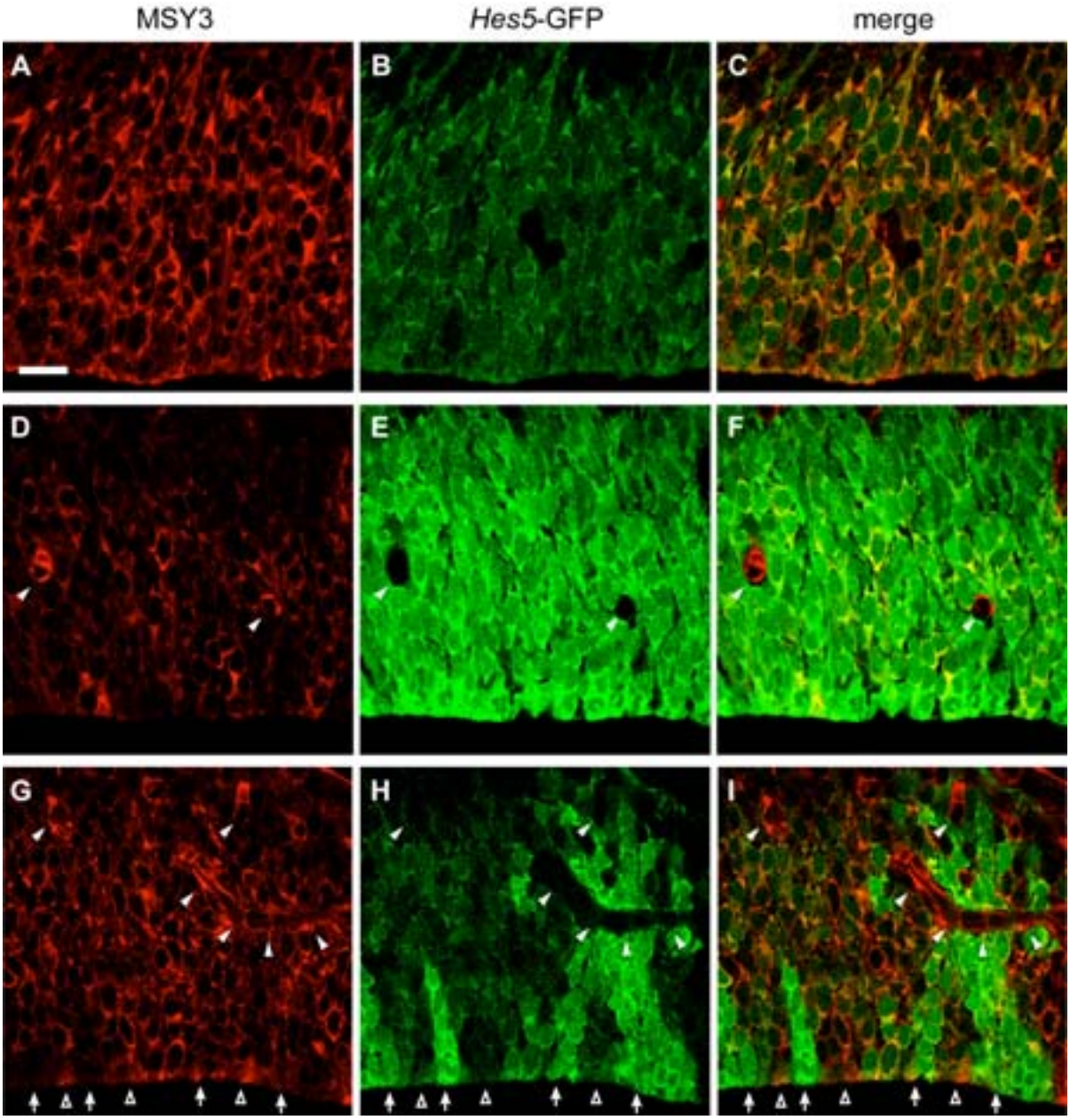

Figure 19. Onset of expression of *Hes5*-GFP in the midbrain coincides with downregulation of MSY3. Cryosections of the E11.5 *Hes5*-GFP embryo through (**A-C**) the dorsal midbrain, (**D-F**) the ventrolateral midbrain, and (**G-I**) dorsolateral midbrain, were stained for MSY3 (red) and GFP (green). Images are single optical sections (1 μm) acquired with the same settings; (A-F) were acquired from the same tissue section. Induction of *Hes5*-GFP is coupled with downregulation of MSY3, also in individual cells (G-I, arrows). Cells with weak Notch activation remain strongly immunoreactive for MSY3 (G-I, empty arrowheads). Ventricle is towards bottom. *small arowheads*, blood vessels. Scale bar equals 20 μm.

Progenitors downregulate Notch signalling with commitment to differentiation. Because the expression of MSY3 correlates with proliferation, it was plausible that cells with low levels of Notch signalling also express MSY3 to a lesser extent. To test this hypothesis, MSY3 expression was examined at a cellular resolution in the ventral telencephalon of E11.5 *Hes5*-GFP embryos. In this area, individual cells express variable levels of *Hes5*-GFP. As shown in Figure 20, all four possible combinations of fluorescent labelling could be detected (i.e. GFP+/MSY3+, GFP+/MSY3-, GFP-/MSY3+, and GFP-/MSY3-) at random frequencies. Thus, there is no apparent correlation between MSY3 expression and Notch signalling.

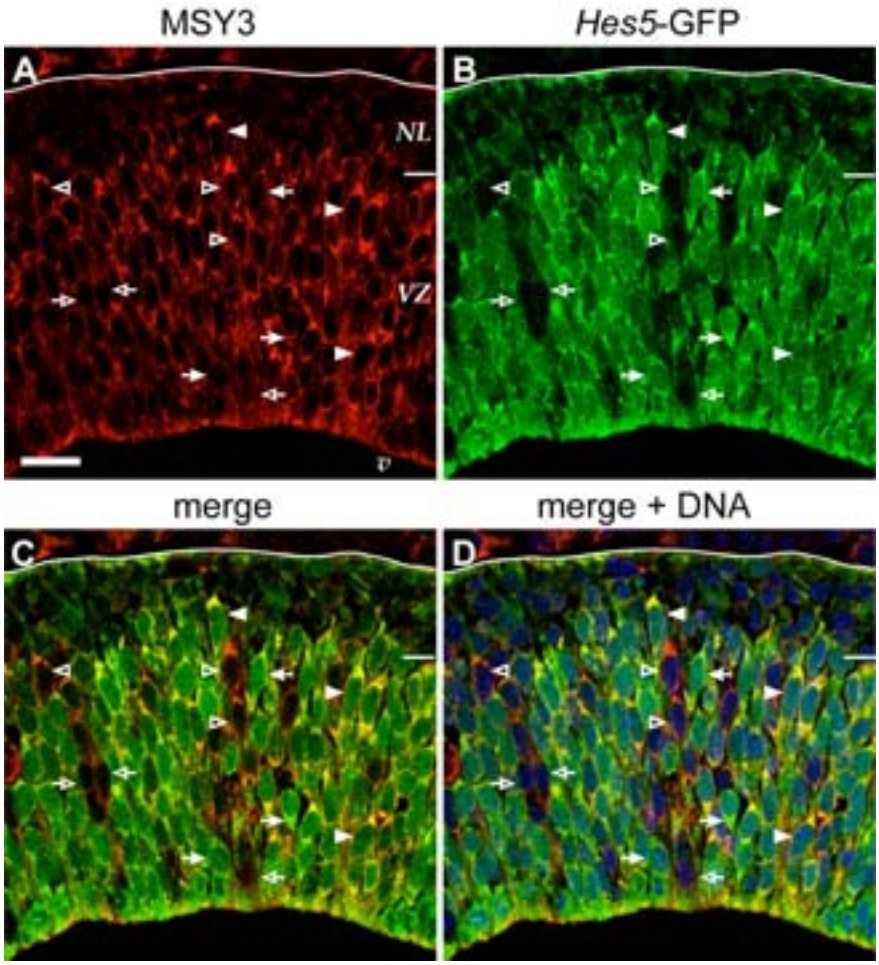

Figure 20. Expression of MSY3 does not correlate with Notch signalling in individual cells after the onset of neurogenesis. Cryosections through the ventral telencephalon of the *Hes5*-GFP embryo at E11.5 were stained for MSY3 (red) and GFP (green). All four possible combinations of expression of both proteins can be detected. Progenitors that downregulated Notch signalling no longer express GFP from the *Hes5* promoter, and show low or high MSY3 immunoreactivity (open arrows and arrowheads, respectively). Among progenitors with high levels of Notch signalling, MSY3 is also expressed at the low or high levels (solid arrows and arrowheads, respectively). Lines delineate the pial surface. *NL*, nuclear layer; *VZ*, ventricular zone. Scale bar equals 20 μm.

2.2.8 MSY3 expression is not reduced in Notch1-deficient progenitors

Expression of MSY3 is downregulated coincidentally with an increase in neurogenic divisions in the neuroepithelium, yet neither a cellular comparison with *Tis21*-GFP expression or Notch signalling could by far prove this correlation in individual cells. If downregulation of MSY3 is a part of a differentiation process, it should also be induced

prematurely when precocious neurogenesis is triggered experimentally. To test this hypothesis, MSY3 expression was analysed after conditional ablation of *Notch1* in ventricular zone progenitors, which causes the premature onset of neurogenesis.

Conditional ablation of *Notch1* gene using Cre-Lox system allows to circumvent the developmental arrest and early lethality of *Notch1* null embryos (Swiatek et al., 1994). Recombination between LoxP sites flanking the first coding exon of *Notch1* results in a null allele restricted to cells which express the Cre recombinase (Radtke et al., 1999). For this study, homozygous Floxed Notch1 mice were crossed with a transgenic line expressing Cre in the midbrain-hindbrain boundary from the *Engrailed2* promoter enhancer (Lütolf et al., 2002; Zinyk et al., 1998). In addition, the Floxed Notch1 line is combined with the R26R allele, which consists of the Floxed PGK neo cassette inserted into the ROSA26 locus and downstream a *β-galactosidase* gene. Cre-mediated recombination leads to expression of β-galactosidase, thus allowing to follow the fate of Cre-expressing cells and their progeny (Soriano, 1999). The midbrain-hindbrain region regulate anterior-posterior pattering and formation of the caudal midbrain and the cerebellum (Hidalgo-Sanchez et al., 2005; Reifers et al., 1998). Cre recombination starts at E9, and by E10 cells in the cerebellar primordium show drastic reduction of *Notch1* and *Hes5* expression, accompanied by upregulation of Notch1 ligands *Dll1* (Delta-like) and *Dll3*, which are normally expressed in differentiating cells (Lütolf et al., 2002). Furthermore, ectopic expression of a proneural genes *Math 1* and *Mash1* at E10, followed by upregulation of *Tis21*-GFP at E11.5, indicate the premature initiation of a differentiation program. Nonetheless, the Notch1-deficient cells do not complete differentiation but instead are eliminated by apoptosis (Lütolf et al., 2002; and Verdon Taylor, unpublished data).

MSY3 expression was examined in Notch-depleted cells at E11.5 on transverse sections through the midbrain-hindbrain boundary. Expression of β-galactosidase confirmed efficient Cre-recombination in the medial cerebellar primordium, as previously reported (Figure 21 A,B, arrow) (Lütolf et al., 2002). Surprisingly, however, MSY3 expression was not affected (compare Figure 21 C and D). Therefore, it can be concluded that downregulation of MSY3 is not an early marker of differentiation.

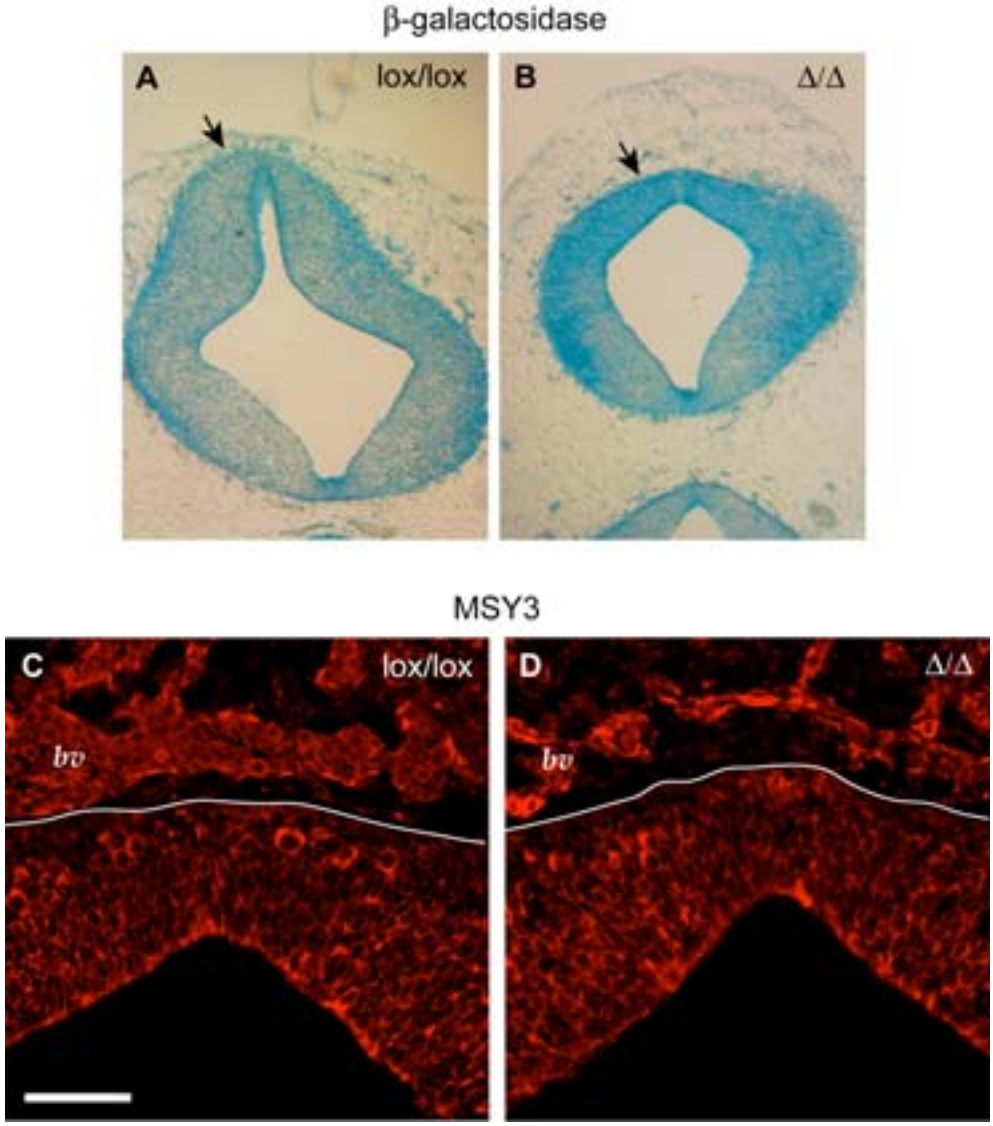

Figure 21. MSY3 expression is not affected in Notch1-deficient progenitors. Transverse cryosections through the midbrain-hindbrain region E11.5 embryos stained for (**A,B**) β-galactosidase, and (**C,D**) MSY3. Dorsal is up. Expression of Cre from the *Engrailed2* promoter enhancer results in generation of a null *Notch1* allele and also allows for expression of β-galactosidase from the reporter ROSA26 locus. (**A,B**) Despite strong background staining resulting from prolonged incubation with the X-gal staining solution, β-galactosidase expression can be detected in the medial cerebellar primordium of *En2*-Cre expressing embryos (arrow in B), but not in the *En2*-Cre negative neural tube (arrow in A). (**C,D**) MSY3 expression is not altered in Notch1 mutant embryo (**Δ/Δ**) as compared with wild type (lox/lox). Images in (C,D) are single optical sections (1.9 μm). Continuous line delineates the pial surface. *bv*, blood vessels. Scale bar equals 50 μm.

2.2.9 Subcellular localisation of MSY3

It has been previously reported that the canine and human orthologues of MSY3 (ZONAB and dbpA/CSDA) in epithelial cell lines colocalise at tight junctions with zonula ocludens-1 (ZO-1) (Balda and Matter, 2000; Sourisseau et al., 2006). Moreover, in the proliferating subconfluent cells, ZONAB/dbpA is present in the nucleus, where it acts as a transcription factor for genes encoding growth related proteins (see *Introduction*). In attempt to understand MSY3 function in the neuroepithelial cells, first its subcellular localisation was investigated by light and electron microscopy.

Sections from embryos at E8 and at E10.5, i.e. prior and at the onset of neurogenesis, were stained for MSY3 and ZO-1. Before the closure of the neural tube, the

neuroepithelium consists of columnar cells which elongate and form a pseudostrarified epithelium as progenitor cells expand. This process is accompanied by bringing closer junctional complexes and morphological changes within the apical plasma membrane (Marzesco et al., 2005). As presented in Figure 22, ZO-1 immunostaining appeared at junctions with a honey comb pattern, visible on single optical sections as puncta at the apical side of neuroepithelial cells. At both stages, MSY3 immunoreactivity was reduced at junctions compare to the adjacent cytoplasm (Figure 22, arrows). The same pattern of expression was observed also later, at E12 (data not shown), throughout the neuroepithelium. Moreover, MSY3 was never detected in the nucleus.

Immunogold electron microscopy confirmed that the MSY3 immunoreactivity is present throughout the cytoplasm (Figure 23). In agreement with fluorescence data, MSY3 was not found in the nucleus or at junctions. In some sections, MSY3 appeared associated with the endoplasmic reticulum (ER), although without enrichment in this subcellular compartment.

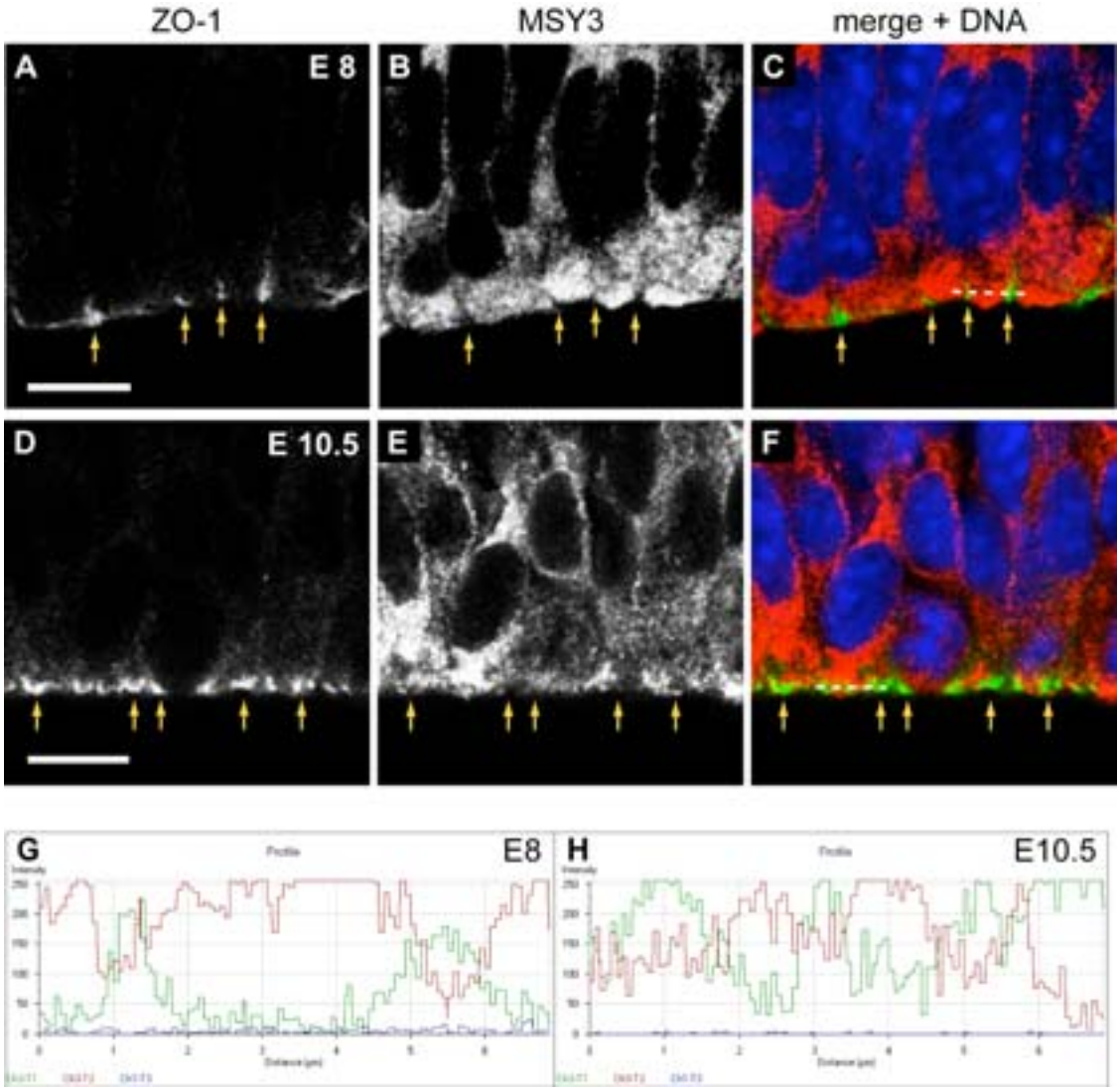

Figure 22. MSY3 subcellular distribution in the mouse neuroepithelium. Cryosections through (**A-C**) the prospective forebrain at E8, and (**D-F**) the telencephalon at E10.5, were stained for ZO-1 (green) and MSY3 (red). DNA was visualised with DAPI (blue). The apical surface is towards bottom. The MSY3 immunoreactivity is not detected in the nucleus nor is concentrated at junctions (arrows). (**G**,**H**) Fluorescence intensity profiles for ZO-1 (green curve) and MSY3 (red curve) along the regions indicated by dashed lines in (C) and (F). Note that picks of ZO-1 immunofluorescence coincide with falls in the MSY3 staining. Images are single optical sections (1 μm). Scale bar equals 10 μm.

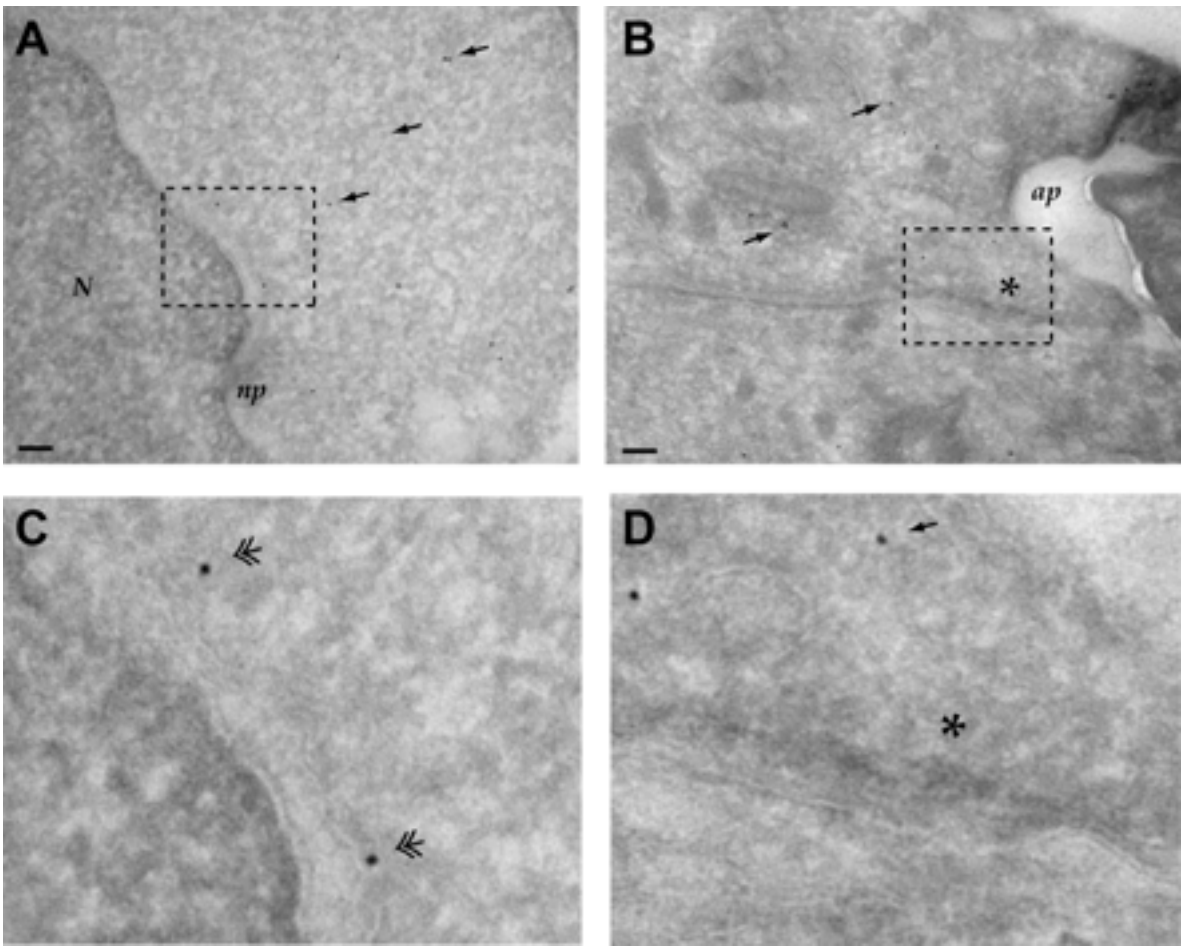

Figure 23. Immunogold electron microscopy shows the cytoplasmic localisation of MSY3. Ultrathin sections of the E10.5 telencephalon were stained for MSY3 followed by protein A-10 nm gold. Arrows indicate some of the immunogold particles. (**A**) MSY3 is detected throughout the cytoplasm, but not in the nucleus (*N*), (**B**) or at the junctional complexes (asterisk). (**C**,**D**) Enlargement of boxed areas in (A) and (B). Some of the gold particles are associated with ER (double-headed arrows). *ap*, apical; *N*, nucleus; *np*, nuclear pore. Scale bar equals 100 nm.

The subcellular localisation of MSY3 appears to be different in neuroepithelial cells than reported previously for its orthologues in epithelial cell lines, yet it cannot be excluded that the epitope recognised by the antibodies is masked in the tissue. However, the same pattern of expression was observed when: i) two independent antibodies were used, one directed against the whole N-terminal domain; ii) different fixation (1-4% PFA or 4% PFA + 0.1% glutaraldehyde) or permeabilisation (0.2% saponin, 0.3 % Triton X-100 or 0.01% SDS) methods were employed. Additionally, the guinea pig GP2 antiserum against the mouse MSY3 protein can detect tight junction associated and nuclear forms of ZONAB in MDCK cells (Karl Matter, personal communication).

2.3 Manipulation of the MSY3 protein levels in the neuroepithelium

2.3.1 Knockdown of MSY3 in proliferating progenitors

The developmental profile of MSY3 expression would suggest that it is involved in maintenance of symmetric proliferative divisions of progenitor cells, and/or its downregulation is necessary for a differentiation process. To test directly whether MSY3 is essential for proliferation of precursors, its expression in progenitors was reduced by RNA interference *in vivo* prior to the onset of neurogenesis.

Endonuclease prepared small interfering RNAs (esiRNAs; a mixture of short interfering RNAs) directed against MSY3 were electroporated in one side of the brain of E9.5 embryos, along with a reporter GFP plasmid. Expression of GFP indicates the electroporated region and enables to follow the fate of targeted cells. After electroporation, embryos developed in a whole embryo culture for 48 h. Immunostaining revealed robust reduction of the MSY3 protein in the targeted region (Figure 24 A,C; upper left panels) when compared to the control non-electroporated side (Figure 24 A,C; upper right panels) of the neural tube or embryos electroporated with luciferase esiRNAs (Figure 24 B,D). GFP positive cells were similarly distributed between the ventricular zone and neuronal layer after MSY3 knockdown and in control embryos (Figure 24 A,B; bottom panels). The thickness of the neuronal layer or contribution of targeted cells to neuronal progeny were not altered, despite targeting of a large proportion of progenitors (Figure 24 A,B; middle panels). Moreover, MSY3 knockdown did not promote ectopic neurogenesis in the rostral diencephalon, which do not generate neurons at examined age (Figure 24 C,D; middle panels). Thus, downregulation of MSY3 did not trigger the cell cycle exit of neuroepithelial cells.

Because endogenous downregulation of MSY3 parallels the switch of neuroepithelial cells to radial glia, it is plausible that knockdown of MSY3 would induce radial glia, which are normally absent in the E11.5 telencephalon. However, radial glia marker GLAST was not upregulated in the targeted area (data not shown).

Next, the abundance of basal progenitors was examined. To date, basal progenitors can be identified unambiguously based on their abventricular mitosis, therefore phosphohistone 3 positive mitotic figures at the basal aspect of the ventricular zone were quantified in targeted and control hemispheres. After downregulation of MSY3, the number of abventricular mitoses in the targeted area per section (4.7±2.1 SD; n=14 sections) was similar to the control hemisphere (4.6±1.5 SD; n=14). Therefore, MSY3 downregulation also did not promote symmetric terminal divisions via basal progenitors.

Taken together, although applied technique resulted in strong reduction of MSY3 in the germinal ventricular zone, performed analysis did not reveal an alteration in a proliferative potential or lineage of MSY3-dpeleted progenitors.

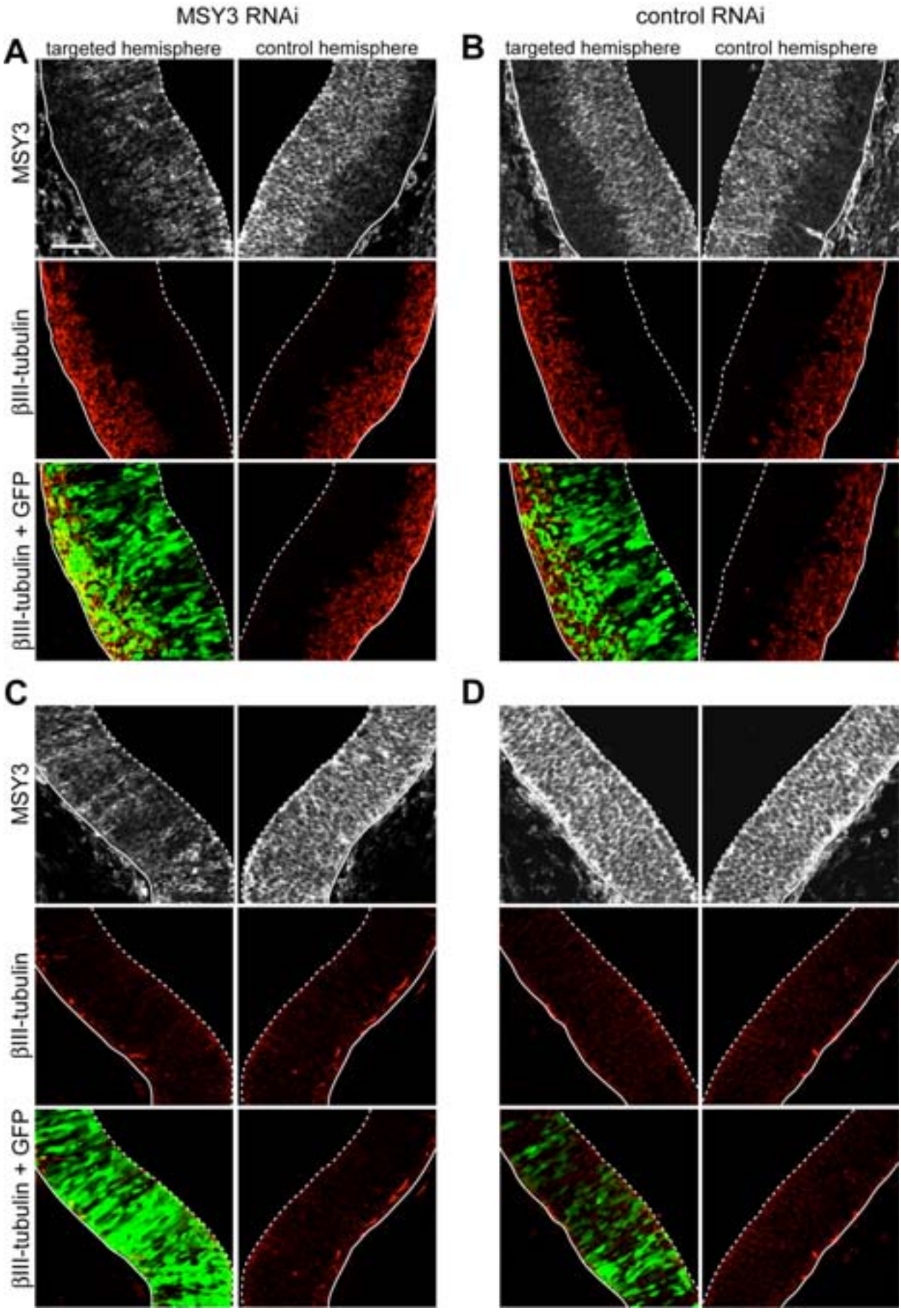

Figure 24. Konckdown of MSY3 by esiRNAs does not increase neurogenesis. Brains of E9.5 embryos were electroporated with esiRNAs directed against MSY3 (**A,C**) or luciferase as a control (**B,D**) along with the GFP reporter

plasmid, followed by development in a whole embryo culture for 48 h. Coronal cryosections through (**A,B**) the basal telencephalon, and (**C,D**) the rostral diencephalon were stained for MSY3 (white) and βIII-tubulin (red). The targeted hemisphere, as identified by GFP fluorescence (green) shows remarkable decrease of MSY3 expression compared to the control hemisphere (right panels) or control embryos (B,D). Electroporated cells of targeted and control embryos are similarly distributed in the ventricular zone and neuronal layer, suggesting that proliferation and differentiation of progenitor cells was not perturbed. Expression of a neuronal marker βIII-tubulin appears not altered, and no ectopic neurons are generated upon MSY3 knockdown in the rostral diencephalon (C). Images are single optical sectios (3 μm). Dorsal is up; continous and dashed lines delineate the pial and ventricular surfaces, respectively. Scale bar equals 50 μm.

2.3.2 Overexpression of MSY3 in progenitors undergoing neurogenic divisions

In a second approach to reveal a potential role of MSY3 in proliferation or differentiation, the protein was ectopically expressed in progenitors after the onset of neurogenesis. The MSY3 and reporter monomeric red fluorescent protein (mRFP) expression plasmids were electroporated in the lateral telencephalon of embryos at E10.5 or E12.5. This two developmental time points enable, respectively: i) to maintain expression of MSY3 through the period it is being physiologically downregulated; and ii) to introduce and maintain MSY3 at the time it is already reduced. The electroporated embryos developed for 36 and 48 h in whole embryo culture or *in utero*, respectively.

Electroporated cells, marked by mRFP fluorescence, showed strong expression of MSY3 in both experimental conditions (Figure 25 C,E and Figure 26 C, green), which confirmed previously reported high ratio of coelectroporation (Saito and Nakatsuji, 2001). Subset of targeted cells reside in the ventricular zone and exhibit elongated morphology of neuroepithelial/radial glia precursors. At the time of analysis – i.e. at E12 and E14.5 when electroporation was performed at E10.5 or at E12.5, respectively – neurogenesis is advanced. When mRFP alone was misexpressed, a large proportion of electroporated cells left the ventricular zone and accumulated in the forming neuronal layer at E12 (Figure 25 B) or migrated into the intermediate zone and the cortical plate at E14.5 (Figure 25 D). Additionally, at E14.5 electroporated cells underwent tangential migration from the lateral intermediate zone towards the basal telencephalon in the lateral cortical stream (Figure 26 D and data not shown) (Bayer and Altman, 1991; McCarthy et al., 2001). Indistinguishable distribution and abundance of mRFP expressing cells in the outer layers were observed also in control embryos (Figure 25 A, and Figure 26 C). In addition, mRFP positive cells in the neuronal layers express a neuronal marker βIII-tubulin (Figure 25 A, and data not shown). It is important to note that in the employed method only progenitor cells which are facing the ventricle, but not neurons, can receive DNA. Thus all neurons expressing mRFP are derived from cycling precursors. Overexpression of MSY3 at E10.5 also did not perturb expression of *Tis21*-GFP by E12 in the lateral cortex or ganglionic eminences (compare the control and targeted hemisphere in Figure 25 A and B; and data not shown).

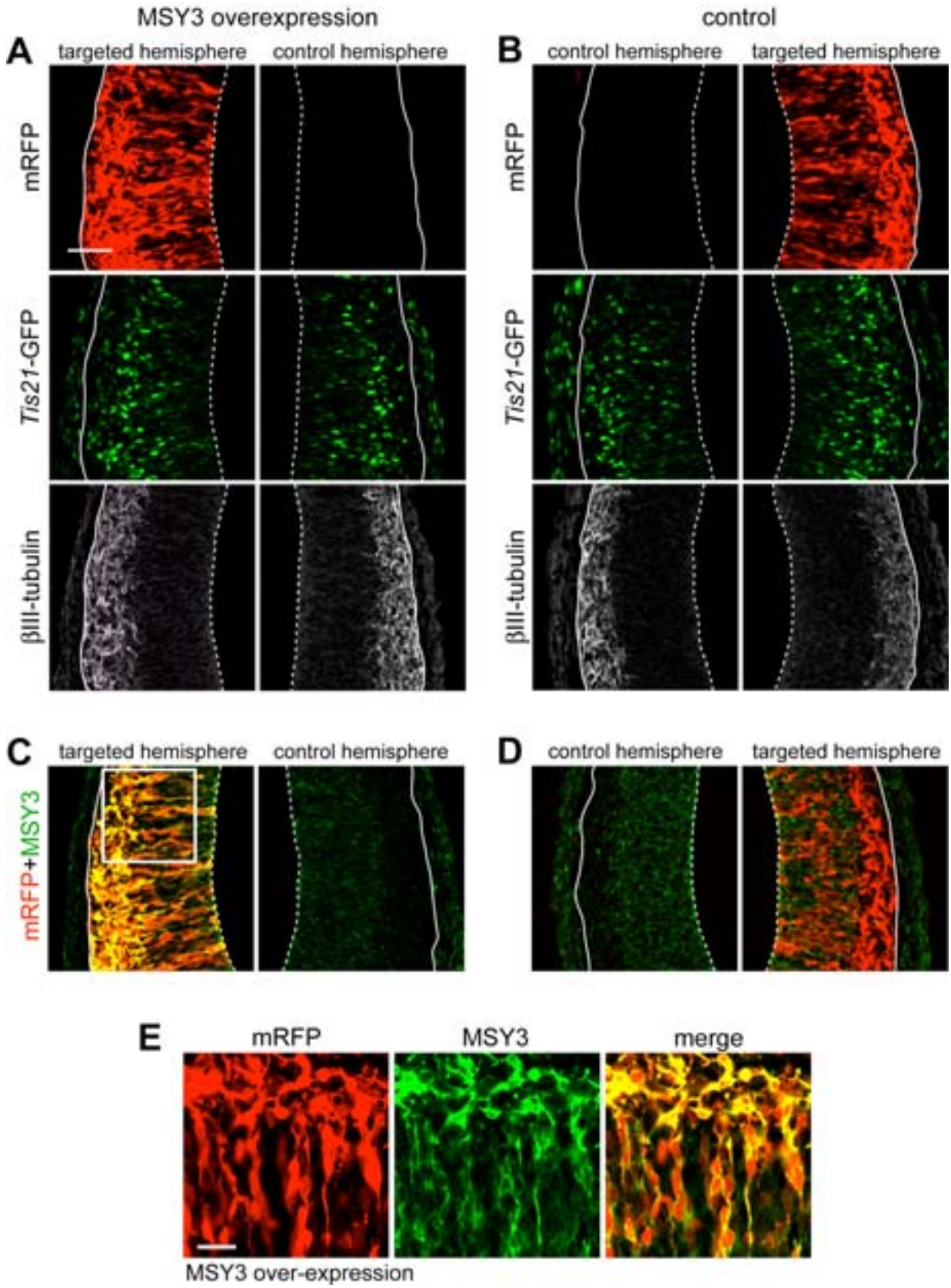

Figure 25. Overexpression of MSY3 at E10.5 does not prevent neurogenic divisions. Heterozygous *Tis21*-GFP embryos were electroporated at E10.5 with the MSY3 expression plasmid together with the mRFP reporter plasmid (**A**,**C**,**E**), or with the mRFP plasmid alone as a control (**B**,**D**), and developed for 36 h in whole embryo culture. Coronal cryosections through the lateral telencephalon were stained for βIII-tubulin (A,B, white), or MSY3 (C-E, green). (**A**,**B**) In the ventricular zone, many GFP positive cells indicate neurogenic divisions, which show similar pattern after MSY3 overexpression and in control embryos (middle panels). Many targeted cells reside in the neuronal layer (upper panels) and express βIII-tubulin (bottom panels). (**C**-**E**) mRFP positive cells show elevated MSY3 immunostaining (green)

compared to the non-electroporated controlateral hemisphere only when MSY3 plasmid was included. (**E**) enlargement of boxed area in (C). Images are single optical sections (2 μm). Continuous and dashed lines delineate the pial and ventricular surfaces, respectively. Scale bar equals (A-D) 50 μm, (E) 20 μm.

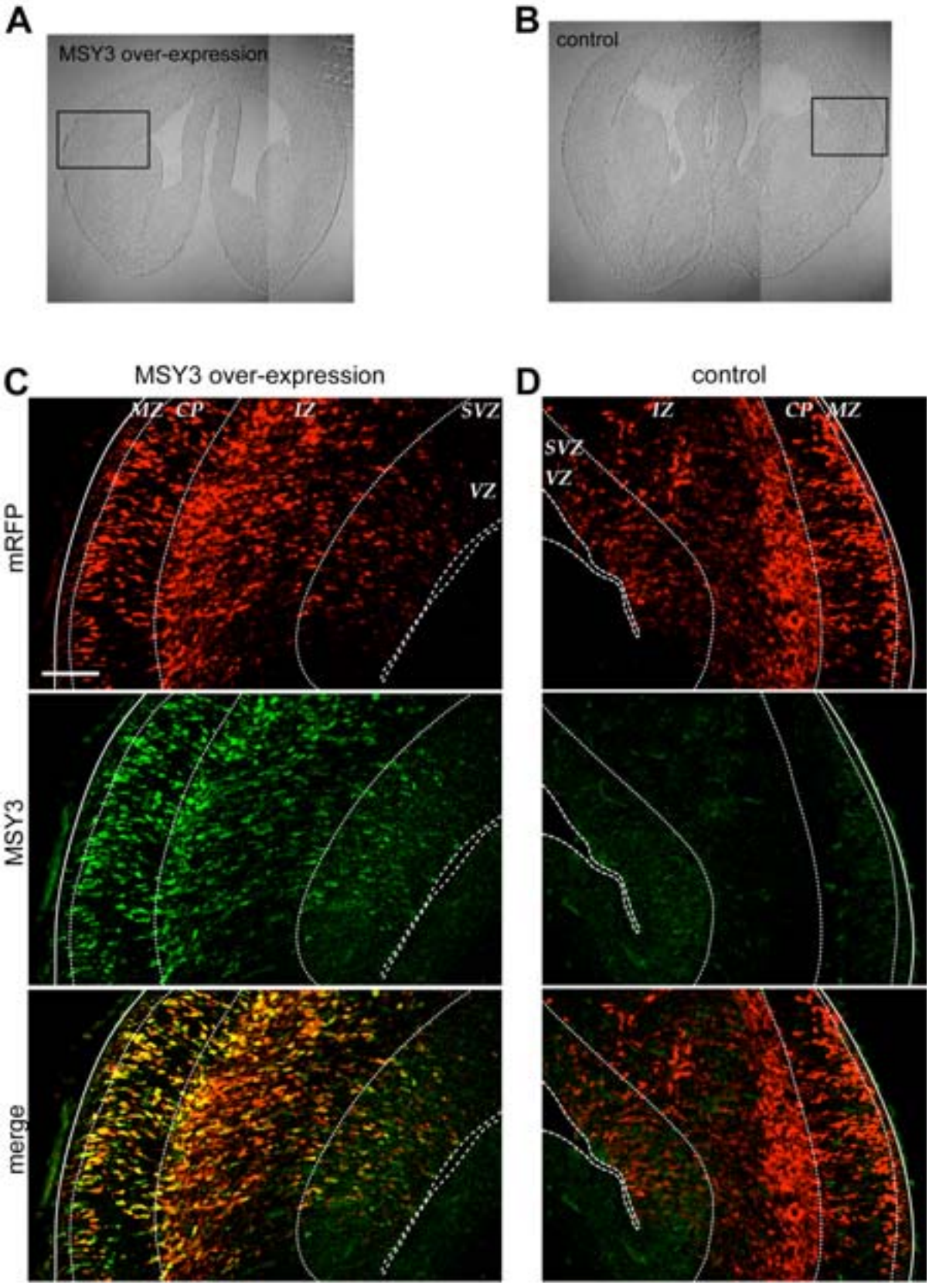

Figure 26. Overexpression of MSY3 at E12.5 does not affect the fate of progenitors. Embryos were electroporated at E12.5 with the MSY3 expression plasmid together with the mRFP reporter plasmid (**A**,**C**), or with the mRFP plasmid

alone as a control (**B**,**D**), and were allowed to develop for 48 h *in utero*. (**A**,**B**) Phase contrast images of coronal cryosections, boxes indicate regions shown in (C,D). (**C**,**D**) Targeted cells show strong immunostaining for MSY3 (green), which colocalises with mRFP (yellow in C) and is not observed in control electroporation (D). mRFP positive cells in both conditions are located in the germinal ventricular and subventricular zone (*VZ*, *SVZ*) or migrated into the intermediate zone (*IZ*) and the cortical plate (*CP*) delineated with dotted lines. Images are single optical sections (3 μm). Dorsal is up. Continuous and dashed lines indicate the pial and ventricular surfaces, respectively. *CP*, cortical plate; *IZ*, intermediate zone; *MZ*, marginal zone; *SVZ*, subventricular zone; *VZ*, ventricular zone. Scale bar equals 100 μm.

In conclusion, overexpression of MSY3 did neither maintain or revert progenitors to undergo proliferative instead of neurogenic divisions. Because virtually all neurons derived from targeted cells also express MSY3 from the ubiquitous CAGGS promoter used in this experiment, it suggests that maintained expression of this protein did not interfere with neuronal differentiation and/or their response to environmental cues which guide migration.

2.4 MSY3 expression in progenitor cells in neurospheres

Isolated progenitor cells derived from the embryonic neuroepithelium or from adult germinal zones can proliferate *in vitro* in a presence of bFGF or EGF as free-floating aggregates called neurospheres (Gritti et al., 1999; Gritti et al., 1996; Reynolds and Weiss, 1996), which consist of relatively rare stem cells and fast proliferating but more restricted transient amplifying cells (Reynolds and Rietze, 2005). Neurospheres may be dissociated and subcultured repeatedly, this feature being used to evaluate the maintenance and expansion of neural stem and progenitor cells. Thus, the neurosphere assay offers an alternative, and due to prolonged culture time more sensitive, method to address the role of MSY3 in maintenance and proliferation of progenitor cells.

Expression of MSY3 was analysed by immunofluorescence in EGF-dependent neurospheres derived from the postnatal brain (P1). During growth, the neurosphere acquires a three-dimensional structure with proliferating cells present towards the edge, whilst more differentiated cells are found in the centre, along with apoptotic and necrotic cells (Campos, 2004; Lobo et al., 2003). Neurospheres after several passages were grown for 2, 3 and 5 days, and immunostained for MSY3 (Figure 27), as well as markers for progenitors (nestin), astrocytes (GFAP) and neurons (βIII-tubulin and neurofilament-160) (Figure 27; Figure 28). While most of cells expressed MSY3 after 2 days of culture (Figure 27 A,C), only a subset of cells at the periphery are immunoreactive in spheres grown for 5 days (Figure 27 E,G). Neurospheres grown for 3 days exhibited a transition pattern (not shown). Strongly positive cells were found mainly on the surface of neurospheres. Strikingly similar pattern of expression was observed for nestin (Figure 27 B,F), yet not all nestin positive cells were also immunoreactive for MSY3 (Figure 27 C,G). Additionally, MSY3 was found in some, but not all, mitotic figures (Figure 27 A,D; and Figure 28 B; arrows and arrowheads, respectively).

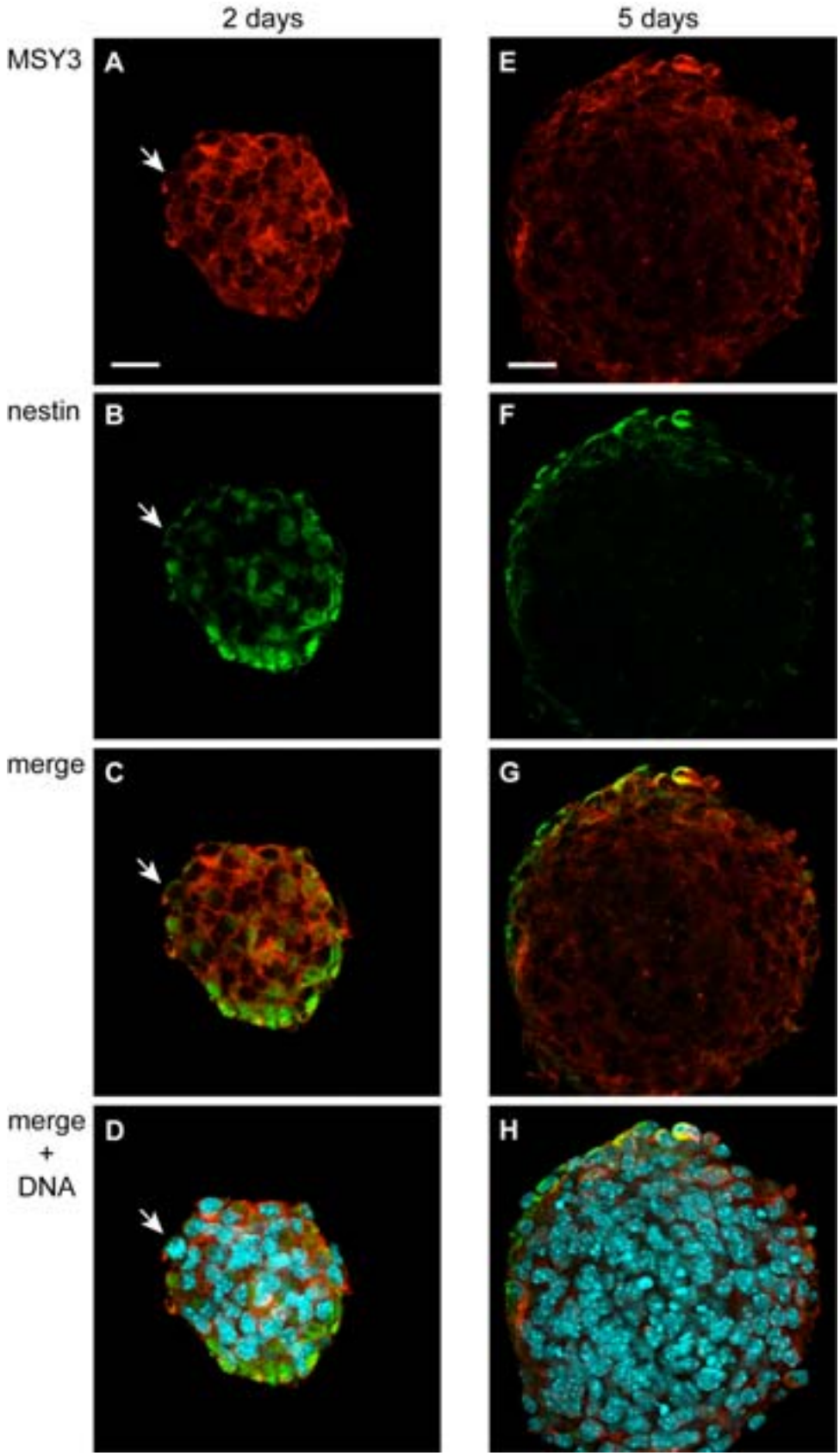

Figure 27. MSY3 is expressed in nestin positive progenitors in neurospheres. Neurospheres were grown in EGF-supplemented medium for 2 (**A-D**), and 5 days (**E-F**), and stained in suspension for MSY3 (A,E) and nestin (B,F). Nuclei are visualised with DAPI (D,H, cyan). After 2 days, most of cells in the neurosphere are nestin positive progenitors, and after 5 days they become restricted to the periphery. MSY3 expression exhibits a similar pattern and is absent from differentiated and apoptotic cells residing in the centre of older neurospheres. Moreover, it can be observed in some mitotic figures (arrow). Images are single optical sections (1 μm) through the middle of a neurosphere. Scale bar equals 20 μm.

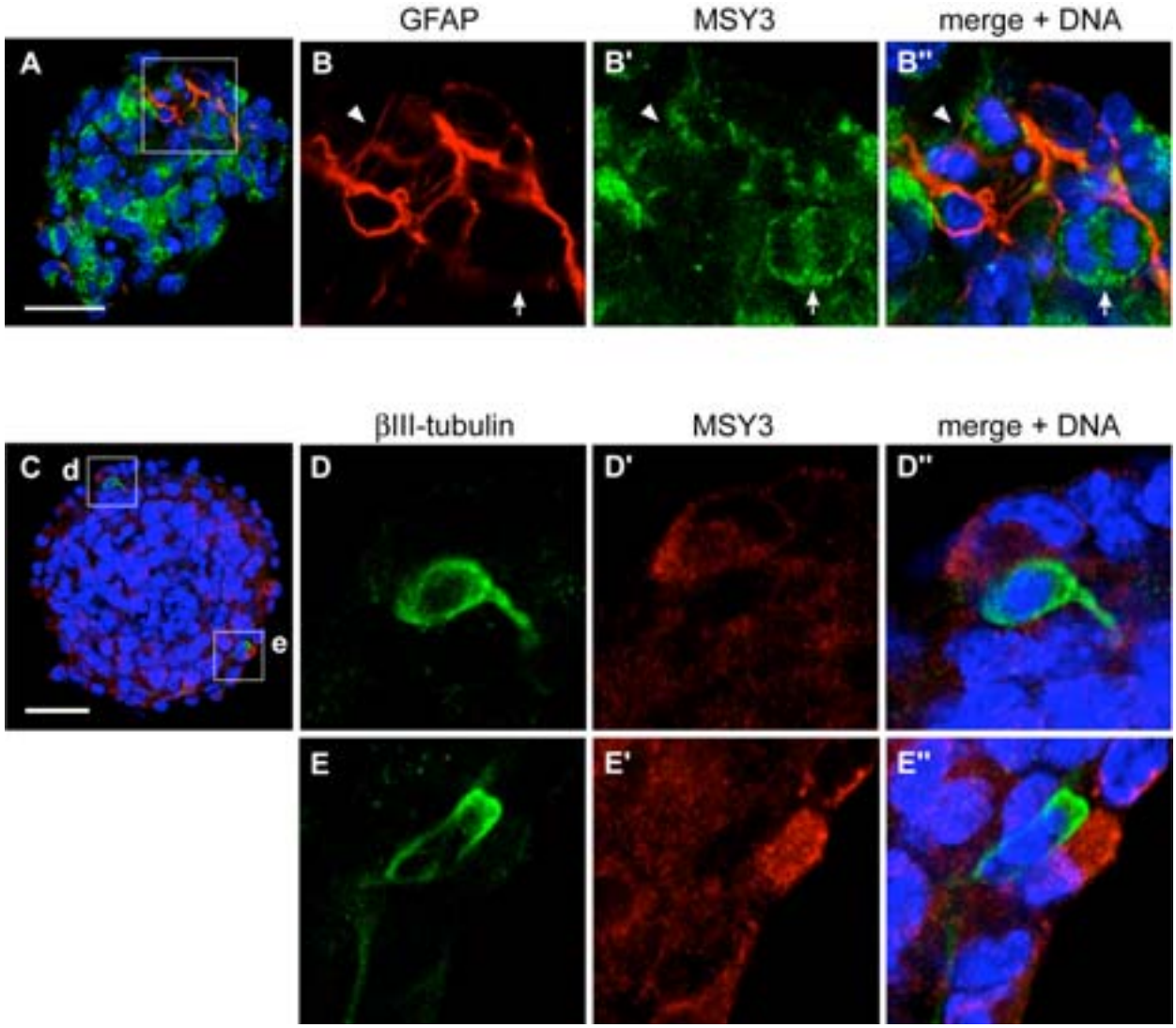

Figure 28. MSY3 is not expressed in differentiated cells in neurospheres. (**A**-**B"**) Neurospheres were grown in EGF-supplemented medium for 3 days and stained for MSY3 and GFAP; or (**C**-**E"**) for 5 days and stained for MSY3 and βIII-tubulin, as indicated. Nuclei are visualised with DAPI (blue). (**B**-**B"**), (**D**-**D"**), and (**E**-**E"**) are enlargement of the areas boxed in (A) and (C). MSY3 is largely excluded from GFAP positive astrocytes and βIII-tubulin stained neurons, though adjacent cells show strong MSY3 expression. Arrows and arrowheads indicate two mitotic figures, which show variable levels of the MSY3 immunoreactivity. Images are single optical sections (1 μm) through the middle of a neurosphere. Scale bars equal 20 μm.

Expression of MSY3 was also largely excluded from GFAP-positive astrocytes (Figure 28 A-B") and neurons (Figure 28 C-E"), the latter present only in neurospheres cultured for 5 days. These data implicate that MSY3 is associated with proliferating progenitor cells not only *in vivo*, but also *in vitro*.

2.4.1 Knockdown of MSY3 in neurospheres

In order to downregulate MSY3 in neurospheres, RNAi triggered by small hairpin RNAs (shRNAs) was employed. To maintain high expression of interfering RNAs and achieve efficient knockdown in proliferative cells, hairpins were expressed in a context of natural microRNA precursor sequences (mir-30). Such a strategy allows proper processing by Drosha and Dicer and yields higher levels of silencing compare to conventional shRNAs (Dickins et al., 2005; Silva et al., 2005). Interfering RNAs complementary to the MSY3

mRNAs at position 647, 1077 and 1363 were chosen, the last one being located in the 3'UTR (Figure 29 A). To evaluate their performance, hairpin constructs driven by the U6 promoter were transiently transfected into Neuro-2A cells, which endogenously express MSY3. Immunoblotting of protein extracts prepared 2 days post-transfection revealed that expression of hairpins MSY3-1077 and MSY3-1363 resulted in efficient depletion of MSY3 (Figure 29 B), whereas expression of the control luciferase hairpin or the GFP plasmid alone did not affect the expression levels of MSY3.

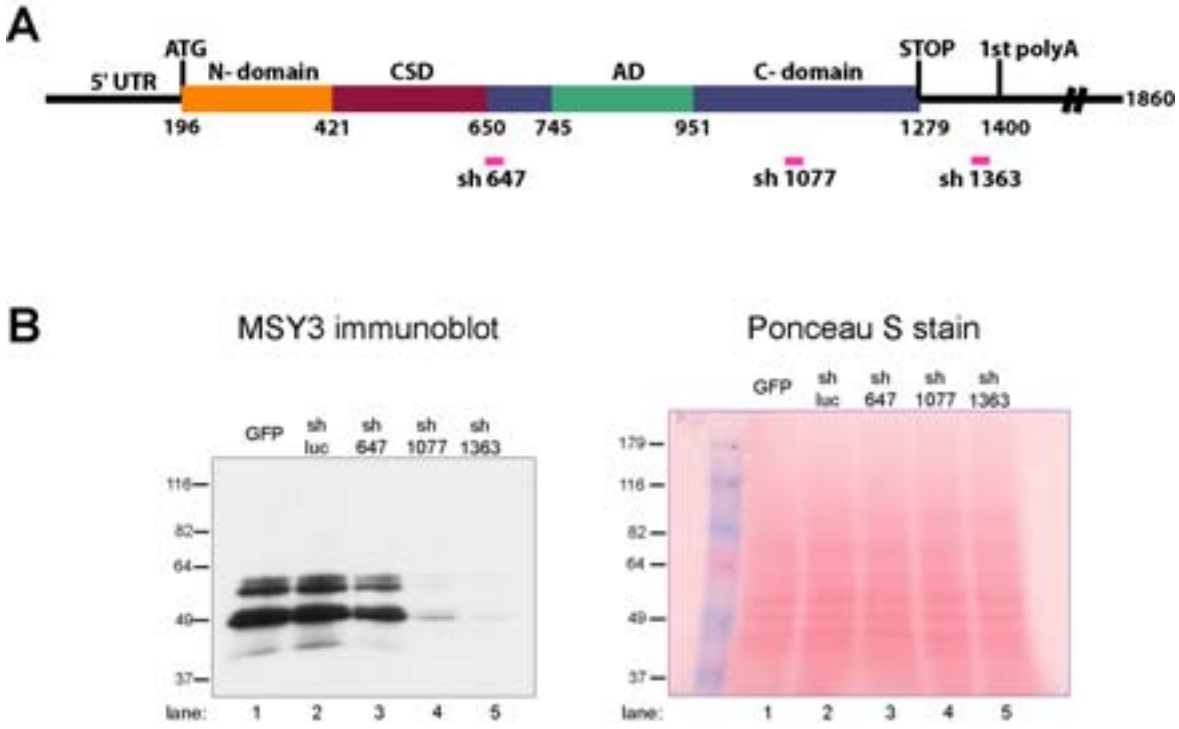

Figure 29. shRNAs design and performance. (**A**) Scheme depicts the positions of shRNAs target sites on the MSY3 message. (**B**) Protein lysates from Neuro-2A cells transiently transfected with a GFP plasmid alone (lane 1), with MSY3 shRNAs as shown in (A) (lanes 3-5), or with control luciferase shRNA (lane 2), were analysed by immunoblotting for MSY3 expression. Hairpins 1077 and 1363 (lanes 4 and 5) triggered efficient knockdown of the MSY3 protein 2 days after transfection. Ponceau S staining of the same membrane shows equal protein loading.

MSY3-1077, -1363 and luciferase shRNAs were inserted into the pAAV-hrGFP plasmid. This plasmid contains hrGFP, a codon optimised green fluorescent protein derived from *Renilla* and distinct from the GFP protein commonly used, which serves as a lineage tracer. In a preliminary experiment these constructs were transfected into neurospheres grown for 1 day. 3 days after transfection, neurospheres were fixed, stained for MSY3 along with nestin, GFAP or βIII-tubulin/NF-160 lineage markers and examined by confocal microscopy (Figure 30). Approximately 23% of control transfected cells were positive for MSY3 (n=119 cells; 10 neurospheres) (Figure 30 A-D, arrow), whereas only 3% of cells transfected with MSY3-1363 shRNA construct (n=162 cells; 8 neurospheres) showed MSY3 immunofluorescence, which was never strong, indicating high efficiency of silencing (Figure 30 E-H, arrowheads). Some of cells transfected with MSY3-1077 shRNA were positive for MSY3 and therefore not included in further analysis.

Double labelling for nestin and MSY3 (Figure 30 A-H) revealed that a large proportion of control transfected and targeted cells comprises nestin positive progenitors (control 89%, n=46 cells of 4 neurospheres; MSY3 knockdown 69%, n=91 cells of 4 neurospheres), and

in the control transfection almost half of them was also positive for MSY3 (48%). MSY3 positive but nestin negative cells were not detected, in agreement with previous observations that MSY3 labels a subpopulation of progenitor cells. GFAP stains mostly cellular processes, which complicates colocalisation analysis. Nevertheless, 29 and 18% of transfected cells in control and MSY3 knockdown neurospheres, respectively, appeared positive for GFAP (control n=73 cells of 6 neurospheres; MSY3 knockdown n=71 cells of 5 neurospheres). All GFAP positive astrocytes were negative for MSY3 (Figure 30 I-P). Since EGF-dependent neurospheres do not generate many neurons, 3 days after transfection very few neurospheres contained single βIII-tubulin positive cells in both experimental conditions.

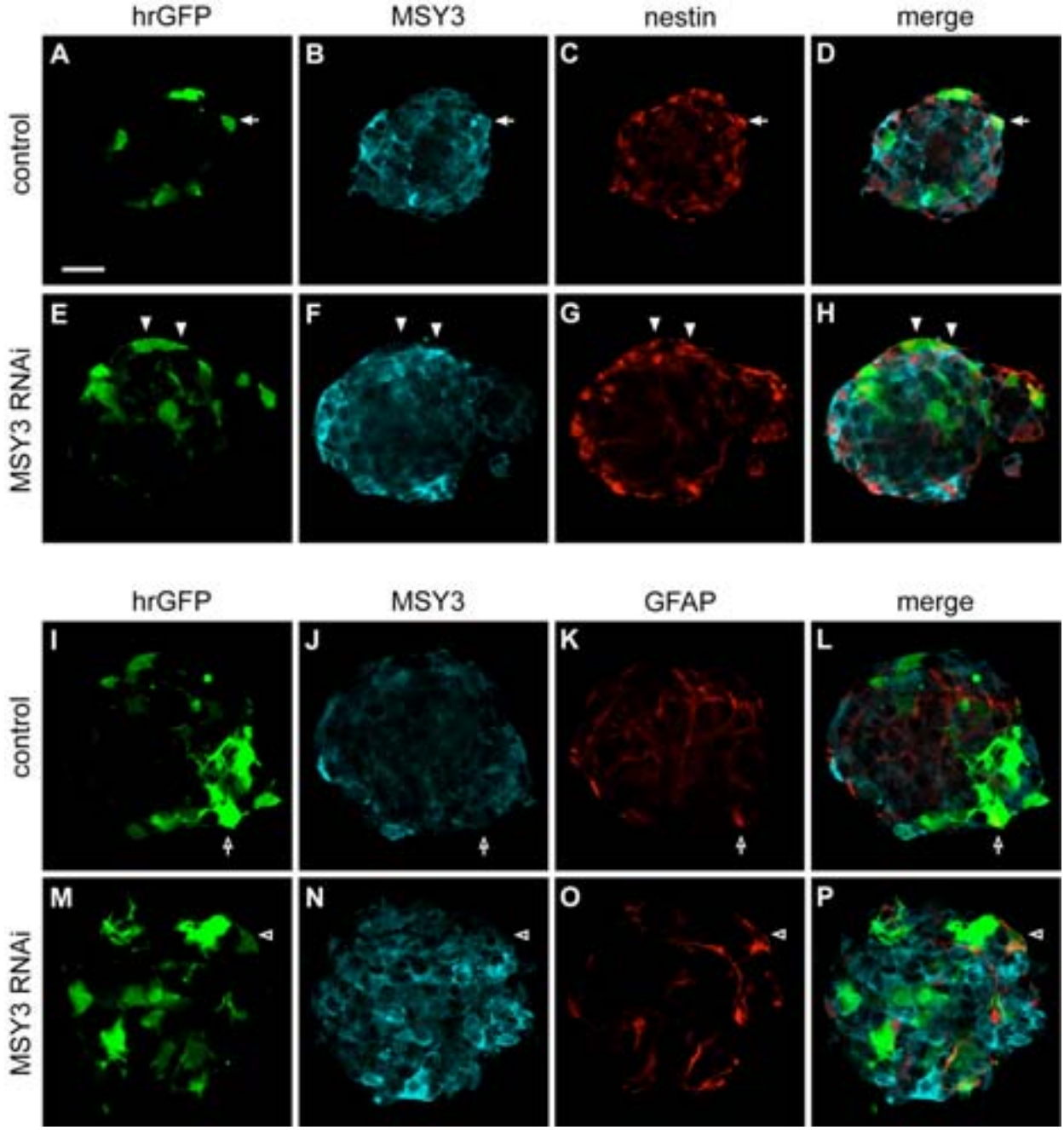

Figure 30. MSY3 knockdown in neurospheres. Neurospheres were transfected with the pAAV-hrGFP vector carrying either (**A-D** and **I-L**) luciferase shRNA as a control, or (**E-H** and **M-P**) MSY3 shRNA-1363, and were stained for MSY3 and nestin (A-H) or GFAP (I-P) three days post-transfection. Transfected cells are identified by hrGFP

expression. (**A-H**) A subset of control transfected cells is double positive for nestin and MSY3 (arrow), whereas MSY3-1363 targeted cells do not show MSY3 immunostaining (arrowheads). (**I-P**) GFAP positive transfected cells do not express MSY3 and are observed in the control and after MSY3 knockdown (empty arrows and arrowheads). Images are single optical sections (1 μm) through the middle of neurospheres. Scale bar equals 20 μm.

This experiment demonstrates that using designed strategy it is possible to transfect progenitor cells and downregulate MSY3 in neurospheres. Differences in ratios of nestin and GFAP positive cell populations between the control and MSY3 knockdown are likely to account for by a variability observed among neurospheres and a relatively small number of spheres analysed. Nonetheless, MSY3 knockdown did not induce neuronal differentiation in the neurospheres cultured in presence of EGF.

2.5 Expression of MSY3 in the postnatal brain

Generation of new neurons persists in the adult brain in the SVZ (subventricular zone) of the lateral ventricle and in the hippocampal dentate gyrus. Since MSY3 is present in neurospheres derived from the postnatal brain, it is likely that also *in vivo* progenitors in the adult neurogenic regions express MSY3. To test this hypothesis, the expression pattern of MSY3 was investigated by immunostaining in brains obtained from heterozygous *Tis21*-GFP mice at different time points after birth.

In both germinal niches, cells along the lineage from stem cells to differentiated neurons express different set of molecular markers. The putative astrocytic stem cells show staining for GFAP, as well as for nestin and vimentin (Doetsch et al., 1997; Kronenberg et al., 2003; Seri et al., 2001). Transient amplifying neuronal precursors are initially nestin positive, but with lineage progression exhibit increasingly differentiated phenotypes, namely expression of microtubule binding protein doublecortin (Dcx) and polysialylated neural adhesion cell molecule (PSA-NCAM), followed by loss of nestin (Brown et al., 2003; Doetsch et al., 1997; Kronenberg et al., 2003; Seri et al., 2004). Expression of doublecortin is downregulated when cells are acquiring the mature phenotype (Brown et al., 2003).

Shortly after birth, expression of MSY3 was detected neither in the SVZ (Figure 31 A-C) nor in the dentate gyrus (Figure 32 B). However, at the end of the second postnatal week (P13), MSY3 became reexpressed in both germinal zones (Figure 31 E; Figure 32 E) and persisted until adulthood (P5W) (Figure 31 H; Figure 32 K).

In the SVZ, MSY3 was detected in clusters of cells above the ependyma, and almost entirely overlapped with Dcx, indicating that it is expressed in transient amplifying precursors. Since no Dcx-negative and MSY3-positive cells close to the ventricle could be detected, MSY3 is not present in the SVZ astrocytes, which do not stain for Dcx (Brown et al., 2003). Furthermore, MSY3 was largely excluded from *Tis21*-GFP positive cells. Postnatally, the *Tis21*-GFP expression labels a subpopulation of Dcx-positive precursors at their terminal divisions and is inherited by newborn neurons (Allessio Attardo and Klaus Fabel, personal communication). Interestingly, the pattern of MSY3 expression coincides with anatomical transition between the embryonic ventricular zone and the adult SVZ (Tramontin et al., 2003). At birth, radial glia are still present in the ventricular zone of the lateral ventricle and continue to generate neurons. Accordingly, radially arrayed progenitors in the ventricular zone of P4 mice were positive for Sox2 transcription factor, which is expressed in VZ progenitor cells (Figure 31 C) (Ferri et al., 2004). Lack of MSY3 in the postnatal VZ is consistent with its downregulation in radial glia during embryonic development. However, during the next two weeks radial glia progressively transform into

ependymal cells and astrocytes, and the adult anatomy of the SVZ is established (Tramontin et al., 2003).

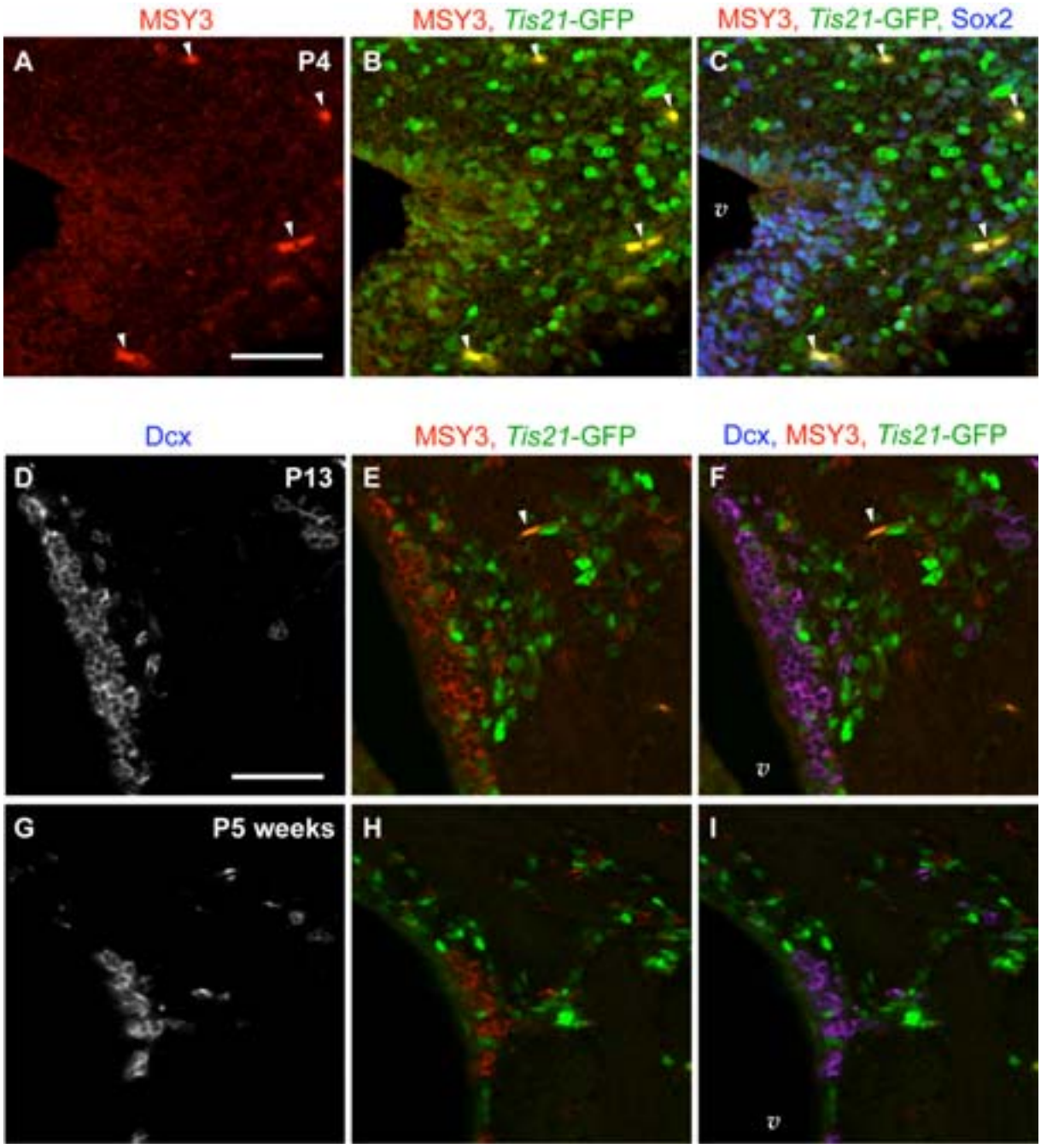

Figure 31. MSY3 is expressed in transient amplifying precursors in the adult SVZ. Coronal sections through the lateral ventricle derived from heterozygous *Tis21*-GFP mice at different time points after birth were stained for MSY3 and a progenitor cell marker Sox2 or doublecortin (Dcx), as indicated in the figure. (**A-C**) At day 4, Sox2 is expressed by radial glia progenitors in the remaining VZ, however, MSY3 is not expressed at this age. (**D-F**) At day 13, MSY3 is coexpressed with Dcx, which marks transient amplifying precursors and young neurons. Only few MSY3 positive cells express *Tis21*-GFP. (**G-I**) At 5 weeks the number of MSY3/Dcx-positive cells decreased and does not overlap with *Tis21*-GFP. *v*, ventricle; *arrowheads*, unspecific fluorescence of blood vessels. Images are single optical sections (1 μm). Scale bars equal 50 μm.

In the dentate gyrus, similarly as in the SVZ, MSY3 was detected in the Dcx-labelled transient amplifying precursors (Figure 32 D-L), being downregulated in cells expressing

Tis21-GFP. The appearance of MSY3 positive cells also coincides with establishment of the adult hippocampal germinal zone (Altman and Bayer, 1990a).

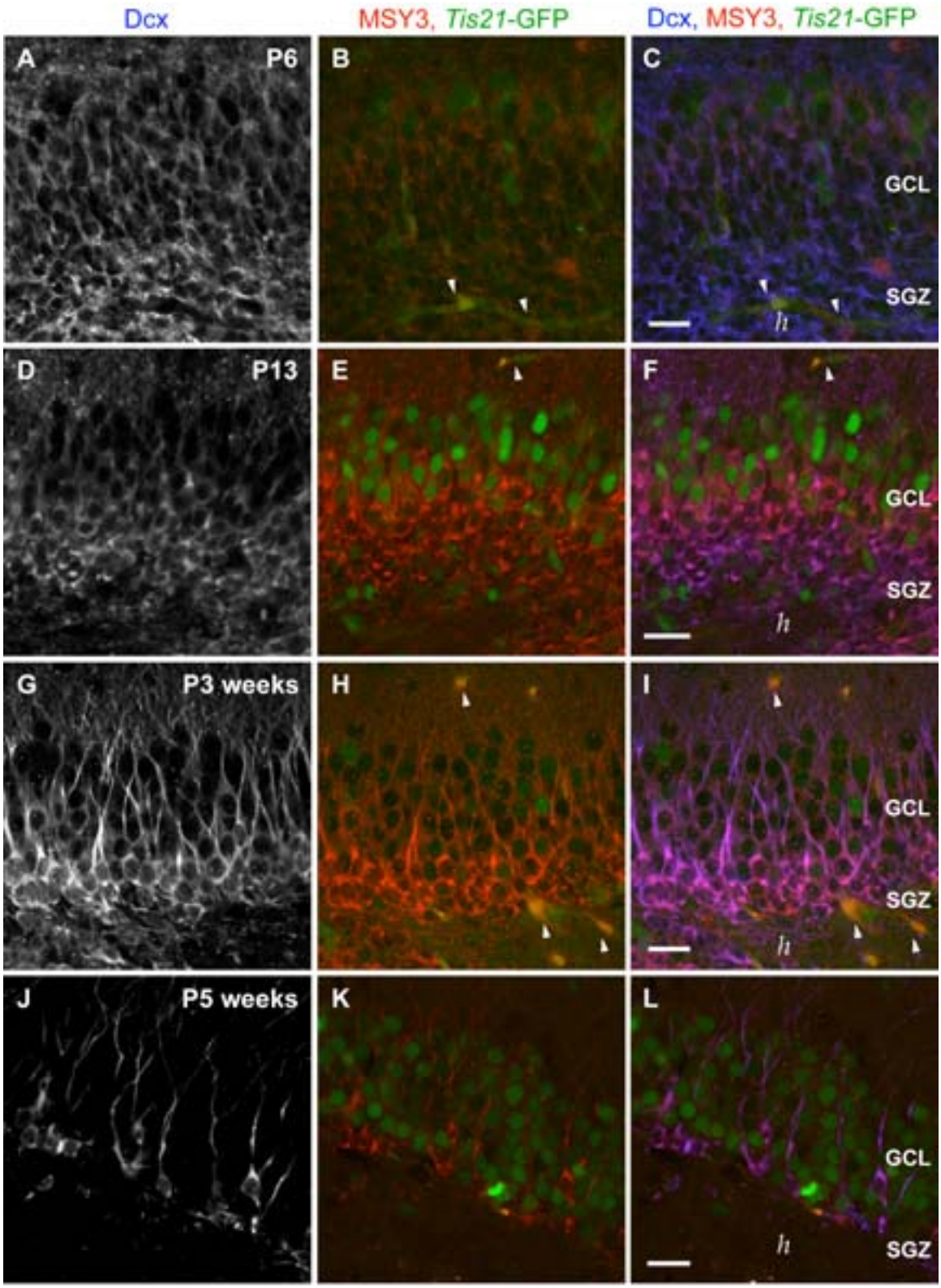

Figure 32. MSY3 is expressed in transient amplifying precursors in the dentate gyrus. Coronal sections of the hippocampus derived from heterozygous *Tis21*-GFP mice at different time points after birth were stained for MSY3 and doublecortin (Dcx), as indicated in the figure. Stem cells of the dentate gyrus reside at the base of the granular cell layer (*GCL*) forming the subgranular zone (*SGZ*). In the GCL the newborn cells localise interiorly, whereas earlier born cells are found on the outside. (**A-C**) During the first postnatal week, progenitor cells from the embryonic SVZ migrate

to the dentate gyrus to populate the hilus (*h*) and SGL, and granule cells undergo differentiation. MSY3 is not detected at this time point. (**D-L**) During following weeks, MSY3 becomes expressed in Dcx-positive cells (**D-I**) and persist until the adulthood (**J-L**). MSY3 and *Tis21*-GFP expression patterns are largely exclusive, particularly in older animals. *h*, hilus; *arrowheads*, unspecific fluorescence of blood vessels. Images are single optical sections (1 μm). Scale bars equal 20 μm.

At two weeks some of the *Tis21*-GFP expressing cells were positive for MSY3 in both neurogenic regions (Figure 31 E, Figure 32 E), however, with time these populations became exclusive (Figure 31, Figure 32 H,K). To summarise, MSY3 is expressed in proliferating transient amplifying precursors in the adult neurogenic zones and is downregulated as cells are entering a differentiation program. The abundance of labelled cells decreased with time, which is in agreement with the decrease of neuronal production with age (Emsley et al., 2005).

Surprisingly, during the first two postnatal weeks MSY3 was transiently re-expressed in the pyramidal neurons in the neocortex (Figure 33 A-D) and CA fields of the hippocampus (data not shown). It is important to note that until E18 cortical neurons are negative for MSY3 (Figure 9; Figure 12 J; data not shown). Eventually, in juvenile (P3W) and adult (P6W) brains MSY3 was not detected (Figure 33 E, F; data not shown).

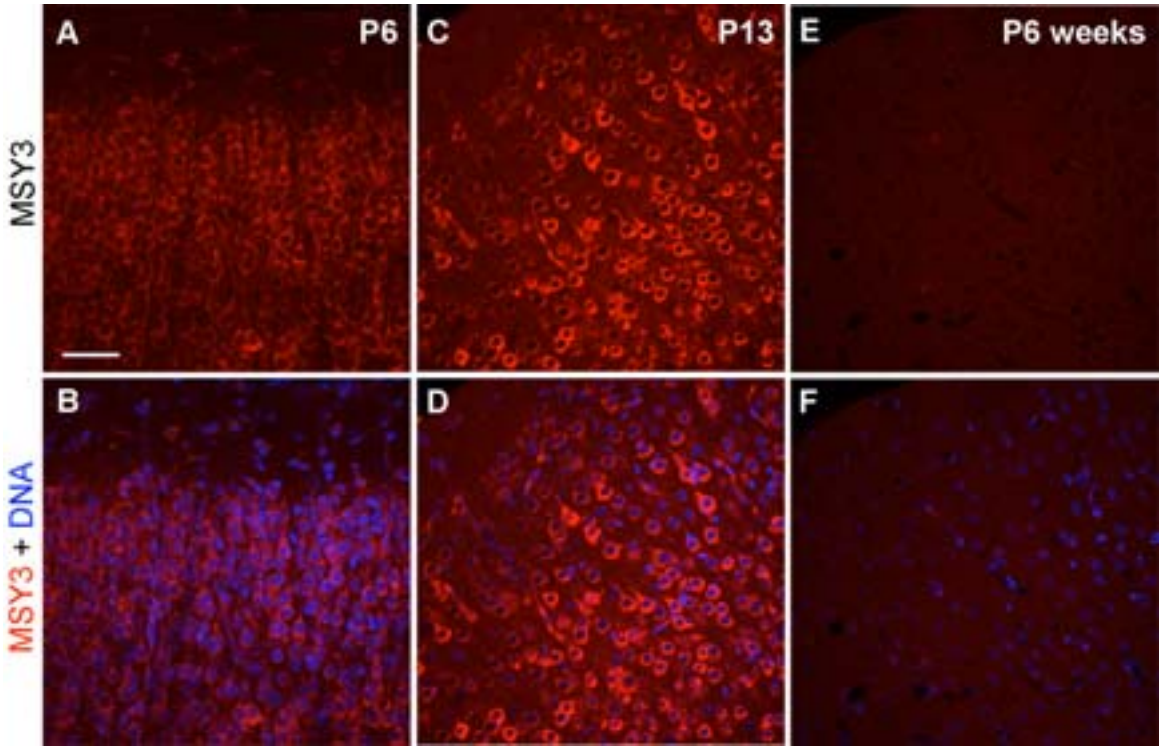

Figure 33. MSY3 is transiently expressed in cortical neurons after birth. Coronal sections through the frontal cortex derived from heterozygous *Tis21*-GFP mice at different time points after birth were stained for MSY3 (red), nuclei were visualised with DAPI (blue). (**A**,**B**) and (**C**,**D**) MSY3 is expressed in pyramidal neurons during two first postnatal weeks. (**E**,**F**) In the adult cortex, MSY3 is not detected. Dorsal is up. Images are single optical sections (1 μm). Scale bar equals 50 μm.

2.6 Biochemical characterisation of MSY3

2.6.1 MSY3 is recovered in RNase A-sensitive complexes

Since MSY3 was detected solely in the cytoplasm applying immunostaining (Figure 22; Figure 23), its subcellular localisation was further analysed by differential centrifugation. Fractions enriched in nuclei (NE), mitochondria and membranes (P15), polysomes/ribosomes and microsomes (P100), and cytosol (S100) were prepared from E10.5 embryonic brains or whole embryo homogenates, and analysed by immunoblotting for MSY3. Most of the MSY3 protein was found in the P100 fraction and only small amounts were detected in other fractions, indicating that MSY3 is included in a large complex in the cytoplasm (Figure 34 A).

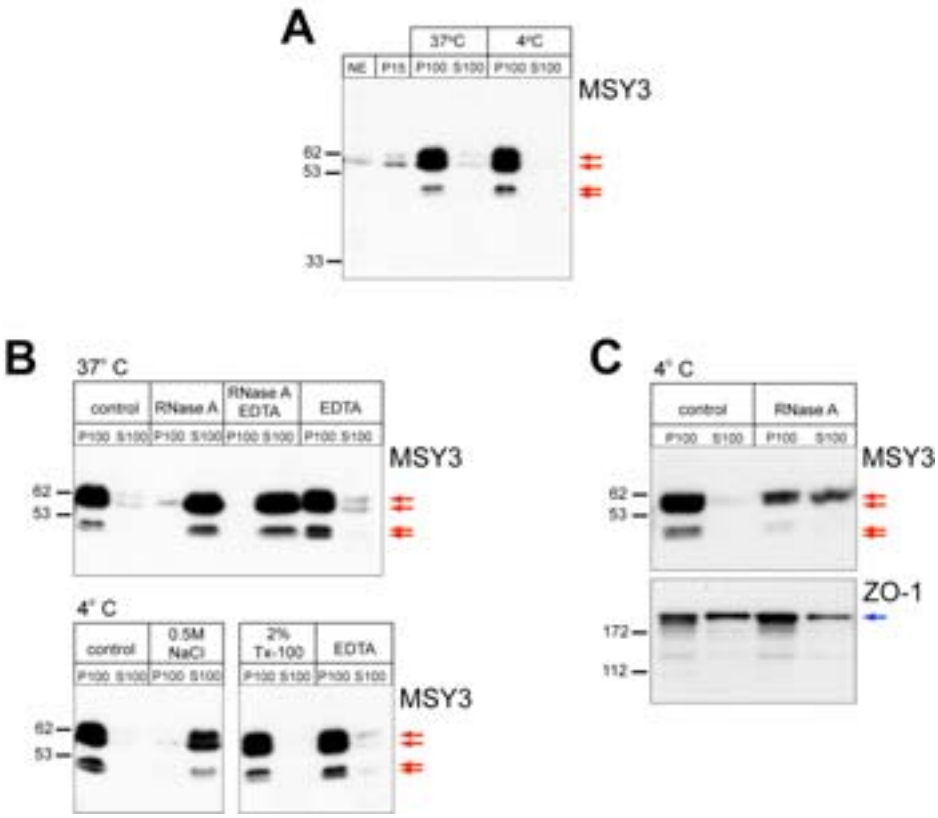

Figure 34. Subcellular distribution of MSY3 protein upon fractionation of homogenate prepared from E10.5 mouse embryos depends on RNA integrity. Homogenate from (**A-B**) whole embryos, or (**C**) embryonic brains at E10.5, was subjected to differential centrifugation to yield fractions enriched in nuclei (NE), membranes and mitochondria (P15), microsomes, ribosomes and polyribosomes (P100), and cytosol (S100). An equal proportion of each fraction was analysed by immunoblotting for MSY3 and in (C) for ZO-1. (**A**) MSY3 is recovered mostly in the P100 fraction. (**B**) Upper panel: treatment of the postmitochondrial supernatant (S15) with 1 mg/ml RNase A at 37ºC in absence or presence of 25 mM EDTA, but not with EDTA alone, released MSY3 to the S100 supernatant; bottom panel: the postmitochondrial supernatant was treated with 0.5 M NaCl, 2% Triton X-100, or 25 mM EDTA at 4ºC; only high salt affects sedimentation of MSY3 into the P100 fraction. (**C**) The P100 pellet was treated with RNase A at 4ºC, resulting only in partial release of MSY3 into the supernatant. ZO-1, which is also recovered in the P100 fraction, is not affected by the RNase A treatment.

Given that MSY3 is pelletable upon ultracentrifugation, the question arises about the nature of the MSY3-containing complexes. Y-box proteins are characterised as translational regulators, and the P100 fraction contains various ribonucleoprotein particles (RNPs). In

the cytoplasm, translationally silenced mRNA is associated with non-ribosomal particles (free mRNPs), whereas translationally active mRNA species are associated with ribosomes. To test directly whether sedimentation of MSY3 in the P100 fraction depends on RNA, the postmitochondrial supernatant (S15) was treated with RNase A or EDTA and ultracentrifuged. Immunoblot analysis showed that after the RNase A treatment at 37ºC virtually all MSY3 protein is recovered in the supernatant, which was not altered by presence of EDTA (Figure 34 B). The RNase A treatment at 4ºC releases only 30-50% of MSY3 into the supernatant (Figure 34 C), suggesting that at the physiological temperature the enzyme is more active or that unwinding of RNA exposes it to the cleavage. The control incubation at 37ºC in the absence of RNase A did not affect MSY3 sedimentation (Figure 34 A,B). Moreover, the distribution of ZO-1, which was also found in the P100 fraction was not perturbed by the RNase A treatment (Figure 34 C). MSY3 was released in the supernatant also upon a treatment with high salt (0.5 M NaCl) (Figure 34 B), which disrupts many protein-protein interactions and releases majority of proteins from mRNA, but preserves polysomes (Auerbach and Pederson, 1975; Corbin et al., 1997; Kumar and Lindberg, 1972). On the contrary, in a presence of EDTA, which dissociates ribosomes into subunits, thus releases mRNA from polysomes (Henshaw, 1968), MSY3 remained in the P100 fraction (Figure 34 B). Distribution of MSY3 into the P100 fraction was also resistant to 2% Triton X-100 solubilisation (Figure 34 B), suggesting that sedimentation of MSY3 was not due to association with membranes.

2.6.2 MSY3 co-fractionates with translating ribosomes

To further characterise the MSY3-containing complexes, the embryo postmitochondrial supernatant was fractionated on a sucrose gradient and fractions were analysed for MSY3 by immunoblotting (Figure 35). MSY3 was distributed in fractions 3 to 8 from the top of the gradient (Figure 35 A). Ribosomal RNA showed similar distribution, suggesting that some of the MSY3 protein is associated with polysomes. In agreement with this hypothesis, in response to the EDTA treatment MSY3 shifted to lighter fractions, alike ribosomal RNA (Figure 35 B). Upon the RNase A digestion MSY3 was found free floating on the top of the gradient (Figure 35 C). The RNA digestion was not complete under this condition, as short RNA species could be detected in fractions 3-6. Notably, MSY3 was found in corresponding fractions, whereas complete digestion of RNA results in a complete shift into a soluble fraction (see Figure 34 B; and data not shown). Because RNase A cleaves single stranded RNA, these partly protected RNA species must be highly structured or assembled with proteins and likely represent ribosomal RNA (Auerbach and Pederson, 1975), suggesting that in this fractions MSY3 turns to be associated with rRNA. Such unspecific interaction was already reported for YB-1 (Nekrasov et al., 2003).

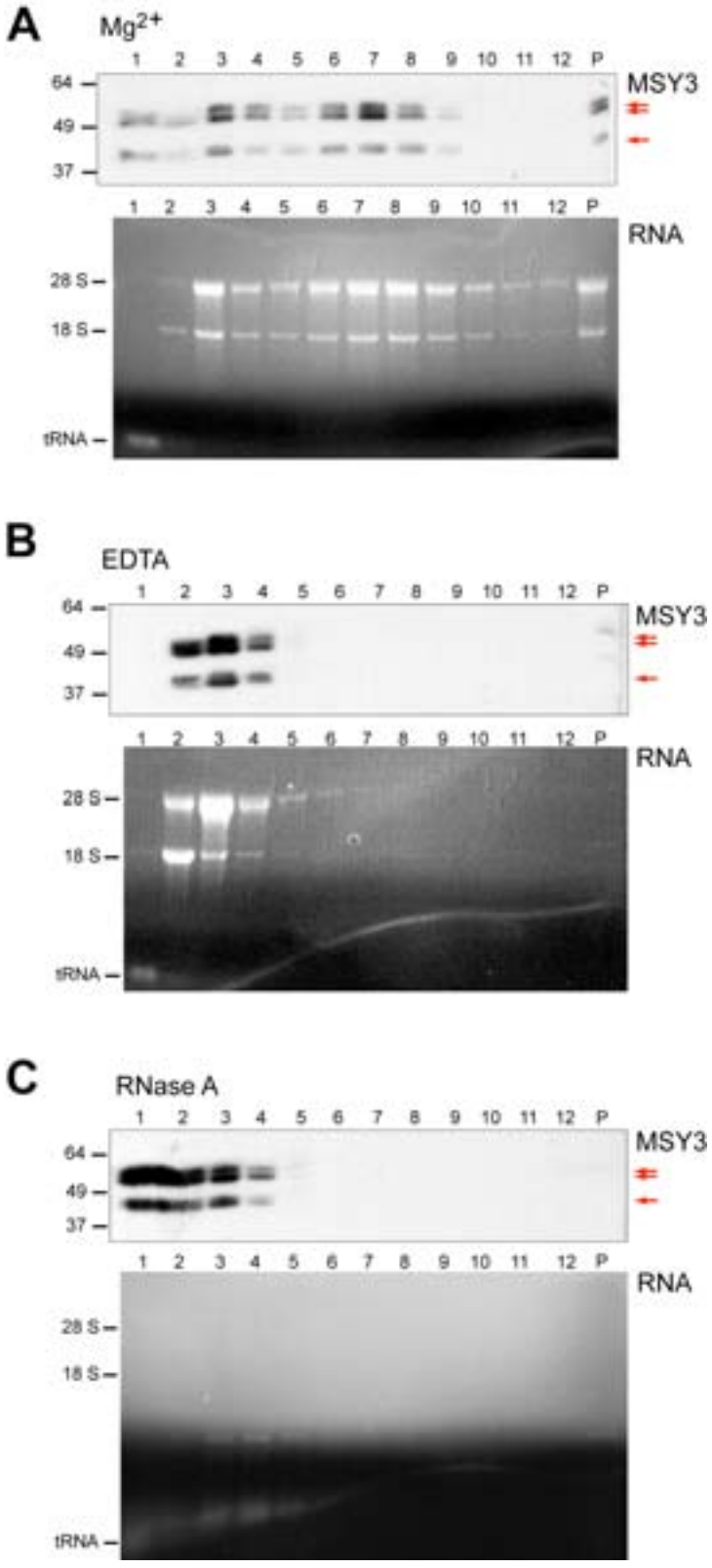

Figure 35. MSY3 co-fractionates with ribosomal/polyribosomal fractions. The postmitochondrial supernatant from E10.5 embryos was centrifuged on a 15-50% linear sucrose gradient. Fractions 1 to 12 were collected from the top to the bottom and equal proportions of each fraction and the pellet (P) were analysed by immunoblotting with an antibody against MSY3 (upper panels, arrows). Extracts were prepared (**A**) in a presence of Mg^{2+}, or pre-treated with (**B**) 25 mM EDTA, or (**C**) 1 mg/ml RNase A. Bottom panels show the ethidium bromide staining of RNA extracted from each fraction. The position of prestained apparent molecular markers is indicated.

In order to confirm polysomal association of MSY3, the translation process was disrupted with puromycin, which causes premature chain termination by acting as an analogue of the 3' terminal end of aminoacyl-tRNA and thereby inhibits protein synthesis. Neuro-2A cells or embryos in whole embryo culture were treated with puromycin for 3 and 4 h, respectively, and postmitochondrial supernatant obtained from them was fractionated on a sucrose gradient. Immunoblotting analysis revealed that after the puromycin treatment, MSY3 partly shifted from heavy to lighter fractions in Neuro-2A cells and to a lesser extent in embryos (Figure 36). Similar shift was observed for the S6 ribosomal protein and for ribosomal RNA, and also after the EDTA treatment of Neuro-2A cells. Such a behaviour is characteristic for proteins associated with actively translating ribosomes (Stefani et al., 2004). It is likely that the puromycin treatment of embryos was less effective because penetration of the drug into tissue is not as efficient as in monolayer of cultured cells. Additionally, embryos cultured in a presence of puromycin showed bloody effusions and slower heartbeat than in the control, indicating toxicity, which did not permit longer incubation times. Interestingly, in control Neuro-2A cells, the MSY3 distribution is bimodal with two peaks corresponding to a large ribosome/large mRNP fractions (fractions 2-3) and to small polyribosomes (fraction 6). This phenomenon was not observed in the embryo.

Thus, MSY3 in the neuroepithelium, as well as in the neuroblastoma cell line, is partly associated with translating ribosomes, suggesting the role in regulation of translation.

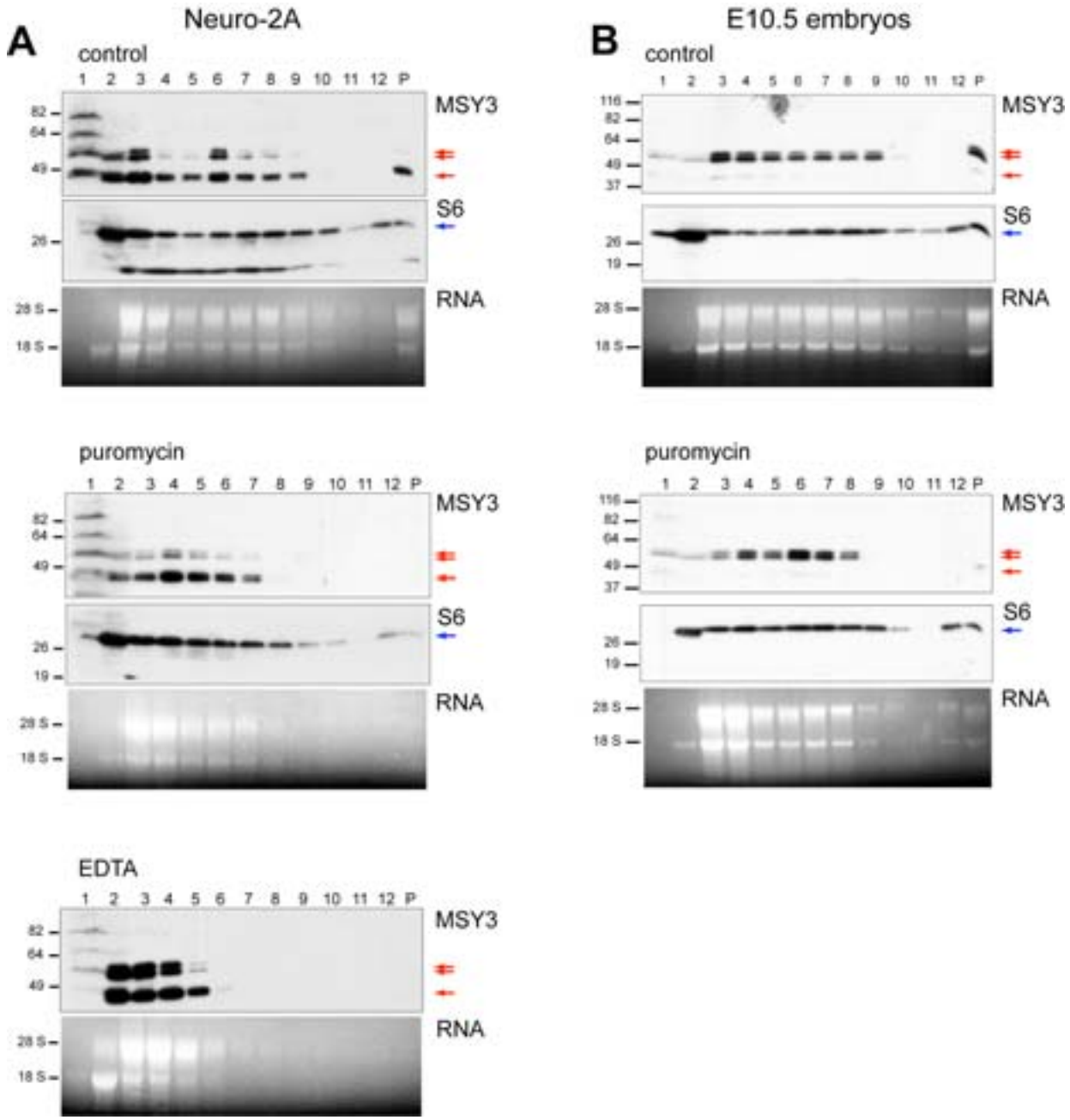

Figure 36. MSY3 associates with actively translating polyribosomes. (**A**) Neuro-2A cells, or (**B**) E10.5 embryos, were cultured in control conditions or treated with 100 μg/ml puromycin for 3 and 4 h before lysis, and analysed on sucrose density gradients as in Figure 35. Immunoblotting was performed with antibodies against MSY3 and the ribosomal protein S6. In (A) a sample pre-treated with 25 mM EDTA is shown as a control.

2.6.3 MSY3 co-immunoprecipitates with RNA and YB-1

To investigate what RNA species and proteins are associated with MSY3, immunoprecipitation was employed. The MSY3 protein was immunoprecipitated from Neuro-2A cells or E9.5 embryos in a presence of Mg^{2+} or EDTA with the GP2 antiserum against MSY3, but not with a control serum (Figure 37 A). Remarkably, the MSY3 antibody precipitated also RNA in both treatment conditions (Figure 37 B). Most of RNA detected in the MSY3 immunoprecipitate constitutes ribosomal RNA, but a smear on the gel suggests a presence of mRNA. However, after addition of EDTA, partial degradation of RNA was

observed, also in the unbound fraction. It is plausible that EDTA renders RNA susceptible to RNases by opening its secondary structure and disrupting association with proteins.

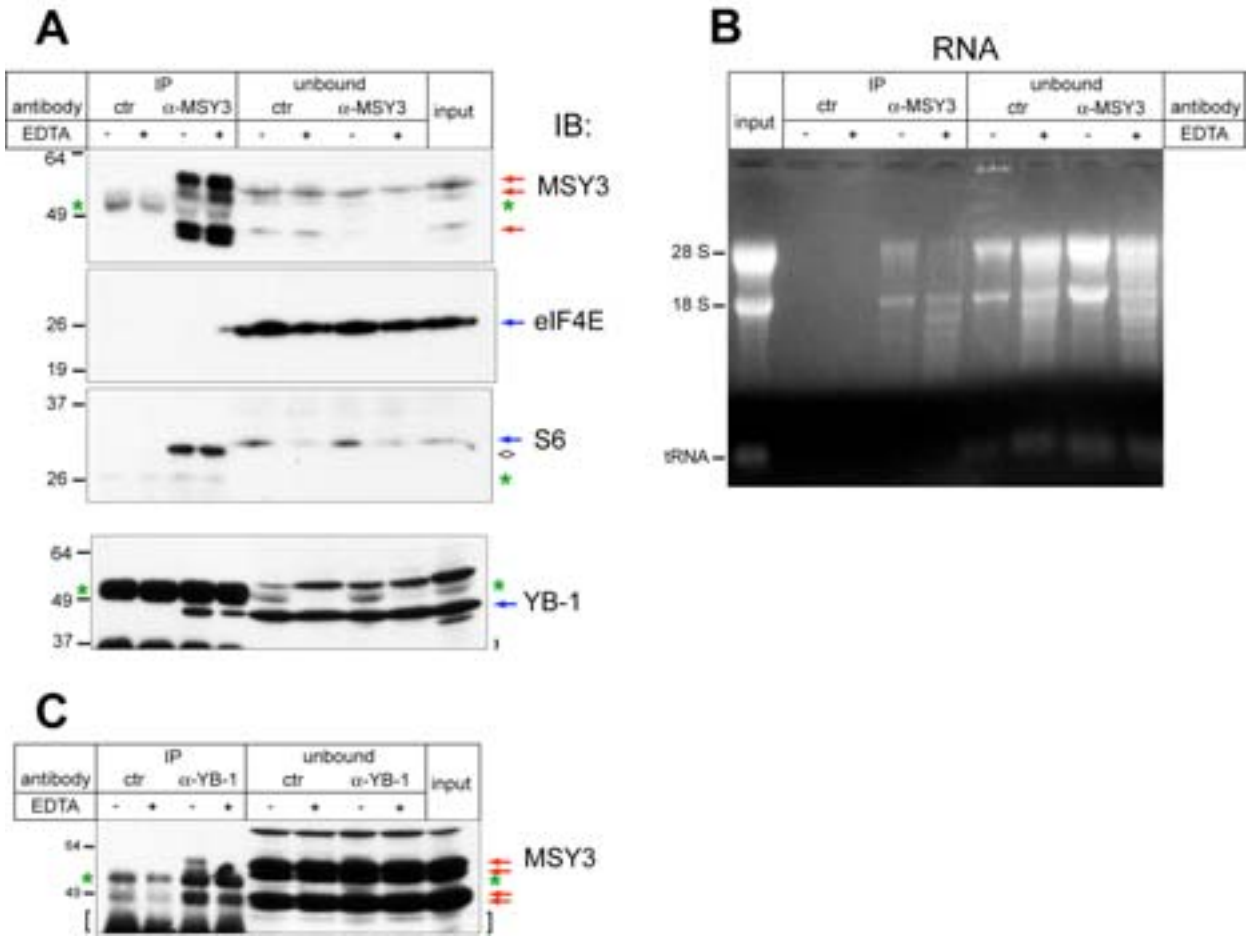

Figure 37. MSY3 co-immunoprecipitates with RNA and YB-1. MSY3 was immunoprecipitated from Neuro-2A cell lysate in a presence of Mg^{2+} or EDTA. (**A**) 10% of bound fractions (IP) and 3% of unbound and input protein lysate were analysed by immunoblotting for MSY3, eIF4E, and S6 ribosomal protein, or under the same experimental conditions for YB-1, as indicated. YB-1 can be co-immunoprecipitated with MSY3. Arrows indicate analysed proteins; asterisks mark unspecific bands of IgG; diamond points to an unspecific band recognised by all antibodies after longer exposure times; brackets indicate unspecific bands recognised by secondary antibodies after use of protein A sepharose. (**B**) Ethidium bromide staining of RNA extracted from 50% of bound fractions and 5% of the unbound and input lysate. MSY3 co-imunoprecipitates with RNA, in particular with rRNA. A smear and low molecular bands visible in EDTA-treated samples likely result from partial degradation of RNA. (**C**) YB-1 was immunoprecipitated from Neuro-2A cell lysate and analysed as in (A). A weak band corresponding to the molecular weight of MSY3 can be detected. The position of prestained molecular marker is indicated on the left.

After immunoprecipitation of MSY3 from 40 embryos (3 litters) in a presence of Mg^{2+}, 4 μg of RNA could be recovered from the bound fraction, which constitutes approximately 2.8% of the input. Efficiency of RNA co-immunoprecipitation suggests that i) MSY3 associates with ample rRNA species by direct or indirect association with ribosome itself, or it binds to a large range of mRNAs; and ii) MSY3 is an abundant protein. In support for the latter notion, similar amounts of RNA could be recovered from bound fractions after immunoprecipitation of MSY3 and YB-1 (data not shown), an mRNPs major protein present in the cell in molar amounts similar to ribosomal proteins (Davydova et al., 1997). MSY3 also co-immunoprecipitates with YB-1, and this association was weaker in a presence of EDTA (Figure 37 A,C), suggesting it is mediated primarily by binding to the same RNA

molecule, possibly mRNA, further supporting the hypothesis that MSY3 is involved in translation. Surprisingly, neither ribosomal protein S6 or eIF4E were detected in the MSY3 immunoprecipitate (Figure 37 A). The question whether MSY3 binds RNA directly and what are its target messages awaits further investigation.

2.6.4 *Manipulation of MSY3 levels does not influence total translation rates*

To determine if levels of MSY3 would affect the rate of total protein synthesis, MSY3 was downregulated or elevated in Neuro-2A cells by transient transfection of esiRNAs or the MSY3 expression plasmid, respectively (Figure 38 A,B). 48 h post-transfection, the total protein synthesis rate was measured by quantifying the incorporation of ^{35}S-labelled amino acids for 10, 20 and 30 min. As presented in Figure 38, neither knockdown nor upregulation of MSY3 affected global translation.

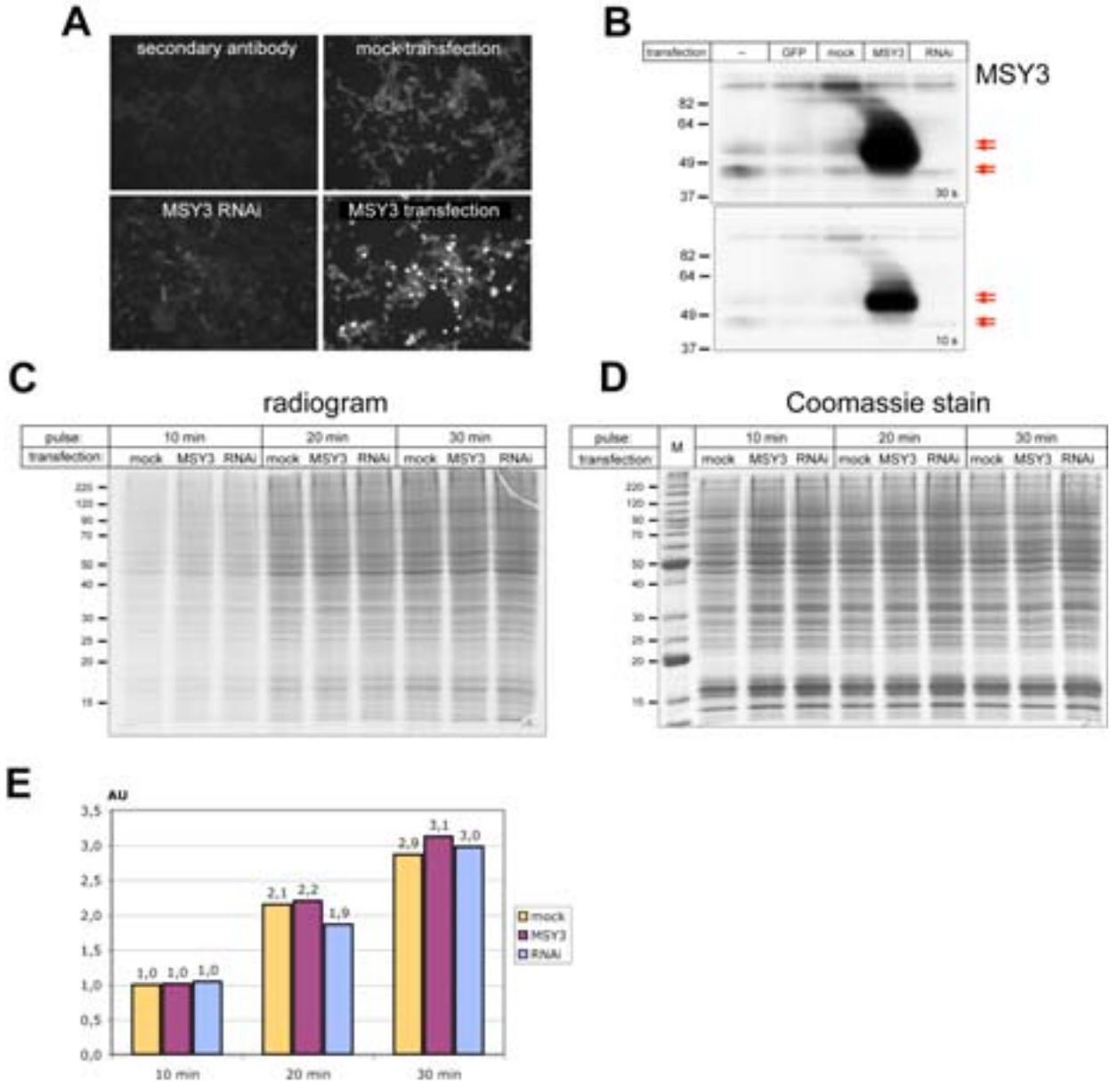

Figure 38. Manipulating the MSY3 protein levels does not affect global protein synthesis rates. Neuro-2A cells were either mock transfected or transfected with MSY3 esiRNAs or MSY3 expression plasmid and analysed 48 h

post-transfection by: (**A**) immunofluorescence; (**B**) immunoblotting with antibody against MSY3. In (A) the upper left panel shows staining without the primary antibody. In (B) two exposures (10 s and 30 s) of the same membrane are shown. (**C-E**) Neuro-2A cells were pulse-labelled with ^{35}S for 10, 20 and 30 min and protein extracts were analysed by 12% SDS-PAGE and radiography (C); (D) shows Coomassie stain of the same gel. *M*, the molecular weight markers. (**E**) Quantification of the radiogram shown in (C); an arbitrary value 1.0 was attributed to the signal in the first lane, bars represent relative intensity of the signal normalised to the amount of loaded protein quantified after Coomassie staining.

2.6.5 *Developmental downregulation of the MSY3 protein is not shared by all proteins involved in translation regulation*

With increased cell cycle length and differentiation, which occur in the course of neurogenesis, it is plausible that neuroepithelial cells downregulate their translational apparatus and protein synthesis rates. Hence, downregulation of MSY3, which coincides with these processes, might be a general feature of the translational machinery. To evaluate this hypothesis, developmental profile of expression of some other proteins involved in translation was analysed, namely eukaryotic initiation factor 4E (eIF4E), Y-box protein 1 (YB-1/p50) and fragile X mental retardation protein (FMRP). eIF4E is a limiting factor for translation initiation and its level, as well as the phosphorylation state, are tightly coupled with cellular need for protein synthesis, therefore it is a good sensor for monitoring the state of the translation machinery in context of proliferation and differentiation. FMRP is an RNA binding protein, which acts as a translational repressor, possibly in the microRNA pathway. The loss of the *fmr1* gene, which encodes the FMRP protein, results in defective neuronal differentiation and *in vitro* in increased neuronal production at the expense of glia (Castren et al., 2005). Its function is indispensable for neurons, though FMRP is also highly expressed in progenitors (Abitbol et al., 1993). In patients, absence of FMRP protein causes mental retardation (fragile X syndrome) (Bagni and Greenough, 2005; Khandjian et al., 2004). YB-1 was included in the analysis as another member of the Y-box family. Interestingly, expression of these proteins was not downregulated during development (Figure 39).

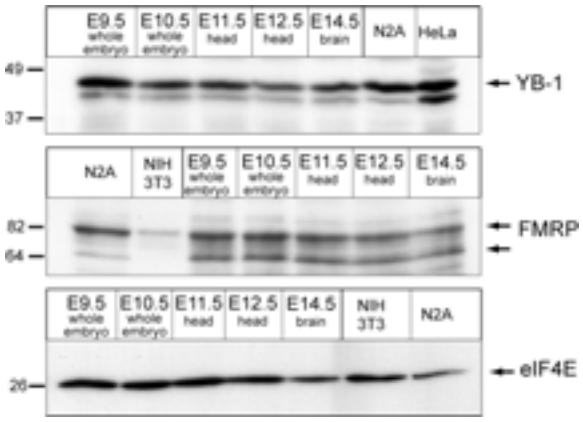

Figure 39. Developmental expression of eIF4E, YB-1 and FMRP in the mouse embryo. 40 μg of protein lysates prepared from embryos at indicated developmental stages was analysed by immunoblotting with antibodies against eIF4E, YB-1 and FMRP, as indicated. Equal amount of protein lysates from various cell lines were loaded as a control. The position of prestained apparent molecular weight markers is shown.

3 DISCUSSION

The aim of this work was to understand whether MSY3 could play a role in formation of the nervous system, particularly in maintenance of proliferation of neural progenitors. It is illustrated here that the expression of the MSY3 protein is related to proliferative divisions of neuronal precursors in embryogenesis, but also in the adult brain. The presented work provides some hints as to possible role of MSY3 in neural progenitors.

3.1 Expression of MSY3 in the central nervous system coincides with proliferation

3.1.1 MSY3 expression is downregulated in spatiotemporal correlation with neurogenesis

It has been shown here that the MSY3 protein in the developing CNS is associated solely with progenitor cells and not neurons. Firstly, the protein is abundantly expressed in the neuroepithelium before the onset of neurogenesis (Figure 10; Figure 14). Secondly, after the onset of neurogenesis, MSY3 is confined to the ventricular zone, but absent from neuronal layers (Figure 9). Thirdly, in acutely dissociated cells it is restricted to nestin-positive progenitors (Figure 11).

In the course of neurogenesis, neuroepithelial cells switch from proliferative to neurogenic divisions, and the proportion of the latter is progressively increasing (Cai et al., 2002; Haubensak et al., 2004; Takahashi et al., 1996). Concurrently, expression of MSY3 declines, which was shown by two independent approaches: morphologically, i.e. using immunofluorescence and confocal microscopy, and biochemically. Specifically, it was revealed that the reduction of MSY3 expression proceeds with known gradients of neurogenesis: i) from caudal to rostral along the anteroposterior axis of the brain (Figure 12; Figure 14); ii) from ventral do dorsal (Figure 13); iii) in the telencephalon from rostrolateral to caudomedial (Figure 17); iv) in the cortical hem prior to other regions (Figure 15). In addition, by E12.5 MSY3 was absent from specialised regions of the neural tube, namely the floor plate, the roof plate, and the choroid plexus epithelium, which are largely composed of non-proliferating cells (Figure 15). In contrast, highly proliferative neuroepithelium immediately adjacent to these areas is strongly positive for MSY3. Thus, a general pattern of MSY3 expression coincides with proliferative divisions of neuroepithelial cells.

Nonetheless, at the beginning of neurogenesis MSY3 did not appear to be downregulated in neurogenic progenitors compare to proliferative ones at a single cell resolution (Figure 16). Expression of MSY3 was examined by confocal microscopy using *Tis21*-GFP heterozygous knock-in embryos, in which GFP expression marks cells that generate neurons (Haubensak et al., 2004). However, this analysis had large technical limitations and in this regard is only preliminary. First, progenitor cells are highly elongated and juxtaposed in the ventricular zone, consequently immunostaining of only little portion of the cytoplasm surrounding the nucleus could be estimated, neglecting the apical and basal processes. Second, confocal microscopy does not allow quantifying the real intensity of immunostaining, because of its narrow range of light detection for any given settings. Third,

lateral scattering and unequal penetration of antibodies in a tissue section cause more superficial optical slices to appear brighter than deeper ones, therefore, are also interfering with the estimation. This important question could be addressed more profoundly by FACS analysis.

3.1.2 MSY3 is downregulated upon the switch from neuroepithelial to radial glia cells

Neural progenitor cells pass through stereotyped patterns of gene expression during development, and distinct antigenic profiles are characteristic of particular developmental stages and progenitor types (Anthony et al., 2004; Gotz and Huttner, 2005; Hartfuss et al., 2001; Malatesta et al., 2003). It was shown here that the MSY3 downregulation parallels the developmental progression of GLAST induction (Figure 17). Since the onset of BLBP and GLAST expression defines the transition from neuroepithelial cells to radial glia, MSY3 appears to be specifically downregulated in radial glia.

3.1.3 MSY3 is downregulated at the onset of Notch signalling activation

It has been presented here, using the transgenic *Hes5*-GFP mouse line, in which GFP expression is dependant on active Notch signalling (Basak and Taylor, 2006), that MSY3 is reduced concomitantly with the initiation of Notch signalling (Figure 18). Furthermore, such downregulation was observed also in individual cells (Figure 19).

Neuroepithelial cells during development change their dependence on *Hes* genes and Notch signalling. Neural induction and initial expansion of the neuroectoderm occurs in absence of both. At E7.5 in mouse, i.e. at the neurula stage, the neuroepithelium starts to express *Hes1* and *Hes3*, while Noch1 is absent (Hatakeyama and Kageyama, 2006; Hitoshi et al., 2004). Around E8.5 *Hes3* expression is gradually downregulated in a ventral to dorsal gradient, which corresponds to induction of *Notch1*, its ligand *Dll1*, and *Hes5* (Allen and Lobe, 1999; de la Pompa et al., 1997; Hatakeyama et al., 2004; Hatakeyama and Kageyama, 2006; Hitoshi et al., 2004). Thus, early progenitor cells proceed from Notch- and Hes-independent, to Notch-independent and Hes-dependent, and finally Notch- and Hes-dependent characteristics. This sequence was recapitulated also *in vitro* (Hitoshi et al., 2002; Hitoshi et al., 2004). Once induced, Notch promotes, and is necessary for, progenitor maintenance (Kageyama et al., 2005; Louvi and Artavanis-Tsakonas, 2006). However, loss of *Hes* genes, which is accompanied by precocious neurogenesis, is associated also with accelerated *Notch1* expression (Hatakeyama and Kageyama, 2006), and active Notch not only supports progenitor maintenance, but also transforms them into later progenitor type, radial glia (Dang et al., 2006; Gaiano et al., 2000). In addition, expression of BLBP, a radial glia marker, is dependent on Notch signalling (Anthony et al., 2005; Patten et al., 2006). Therefore it has been suggested that Notch signalling is associated with the switch of neuroepithelial cells from proliferative to asymmetric divisions, and necessary for progenitors while neurogenic cues are present (Hatakeyama and Kageyama, 2006).

Downregulation of MSY3 expression in the ventricular zone is not complete and progenitors maintain medium to low levels of MSY3 labelling throughout the neurogenic period. Comparison of MSY3 immunofluorescence with *Hes5*-GFP at a single cell resolution after the onset of neurogenesis did not reveal the correlation between the MSY3 expression and Notch signalling (Figure 20). During the neurogenic period, Notch signalling is essential for the maintenance of progenitors and inhibition of neurogenesis (Alexson et al., 2006; de la Pompa et al., 1997; Lütolf et al., 2002). Furthermore *Hes5*-GFP negative

progenitors are not capable of self-renewal *in vitro* (Basak and Taylor, 2006), hence *Hes5*-GFP expression is likely to be a marker of self-renewing progenitors. This would suggest that medium versus low levels of the MSY3 protein are not indicating whether progenitor cells undergo self-renewing divisions or terminal symmetric neurogenic divisions. Nevertheless, it is not formally excluded that *Hes5*-GFP-negative, but MSY3-positive progenitors undergo Notch-independent self-renewing divisions, for example by virtue of expressing *Hes1* under the control of Wnt signalling (Issack and Ziff, 1998).

Consistently, MSY3 expression was not affected in *Notch1*-deficient progenitors in the cerebellar primordium (Figure 21), which prematurely express markers of neuronal commitment, i.e. *Mash1* and *Math1* proneural genes, Notch ligands *Dll1* and *Dll3*, as well as *Tis21*-GFP (Lütolf et al., 2002). However, these progenitors do not differentiate into mature neurons, but instead commit programmed cell death (Lütolf et al., 2002).

Altogether, downregulation of MSY3 concomitantly with Notch activation is coherent with its reduction in radial glia and switch of ventricular zone progenitors to asymmetric divisions. After this transition, the level of MSY3 seems not to distinguish between neurogenic asymmetric and terminal divisions, identified by the lack of *Hes5*-GFP, but also by expression of *Tis21*-GFP. However, these analyses were performed at E11.5, when majority of cells still expresses MSY3; it is plausible that at later time points such a correlation exists.

3.1.4 Expression of MSY3 after the onset of neurogenesis

Although there are differences in the MSY3 immunolabelling intensity between individual cells, brightly labelled progenitors are rare in the ventricular zone from E12.5-E13 onwards (Figure 12). Since throughout the neurogenic period a pool of progenitors undergoes symmetric proliferative divisions (Cai et al., 2002; Haubensak et al., 2004; Miyata et al., 2004), the association of MSY3 with proliferation appears questionable. However, several studies employing retroviral labelling and time lapse microscopy showed that after the onset of neurogenesis the ventricular zone is a mosaic of specialised precursor cells and relatively infrequent multipotent stem cells. Already at E9.5 many of ventricular zone progenitors seem to be restricted to glial or neuronal fates (McCarthy et al., 2001). In the telencephalon, there is no significant number of progenitors that would undergo symmetric proliferative divisions for several cell cycles as very few large clones can be retrovirally labelled during the early and mid- phase of neurogenesis (Cai et al., 2002; Halliday and Cepko, 1992; Walsh and Cepko, 1988; Walsh and Cepko, 1992; Walsh and Cepko, 1993), and the size of clones decreases with time (Cai et al., 2002). Similarly, in time lapse studies of organotypic slice cultures from embryos in mid- to late neurogenesis, it was revealed that a relatively small fraction of progenitors (21-23%) undergoes symmetric proliferative divisions with both daughter cells staying in the ventricular zone (Miyata et al., 2001; Miyata et al., 2004; Noctor et al., 2004). Furthermore, *in vitro*, less than 10% of E10 progenitors are stem cells, which generate more restricted precursor cells attributed to glial or neuronal lineages; moreover, this capability is reduced with developmental progression (Davis and Temple, 1994; Qian et al., 1998; Qian et al., 2000).

All told, proliferative progenitor cells before and after the onset of neurogenesis seem not equivalent, and this change in potential is accompanied by downregulation of MSY3. Other parameter that is not equal between the proliferative fraction of early progenitors, i.e. before and at the onset of neurogenesis, and in the mid-neurogenesis is the cell cycle length, which increases by approximately 36% from E10.5 until E14.5 (Calegari et al., 2005a).

Therefore, it could be concluded that a high level of MSY3 expression marks a fast proliferating sub-population of symmetrically dividing progenitors. Figure 40 summarises the relation of MSY3 expression in a lineage of progenitor cells in the developing CNS.

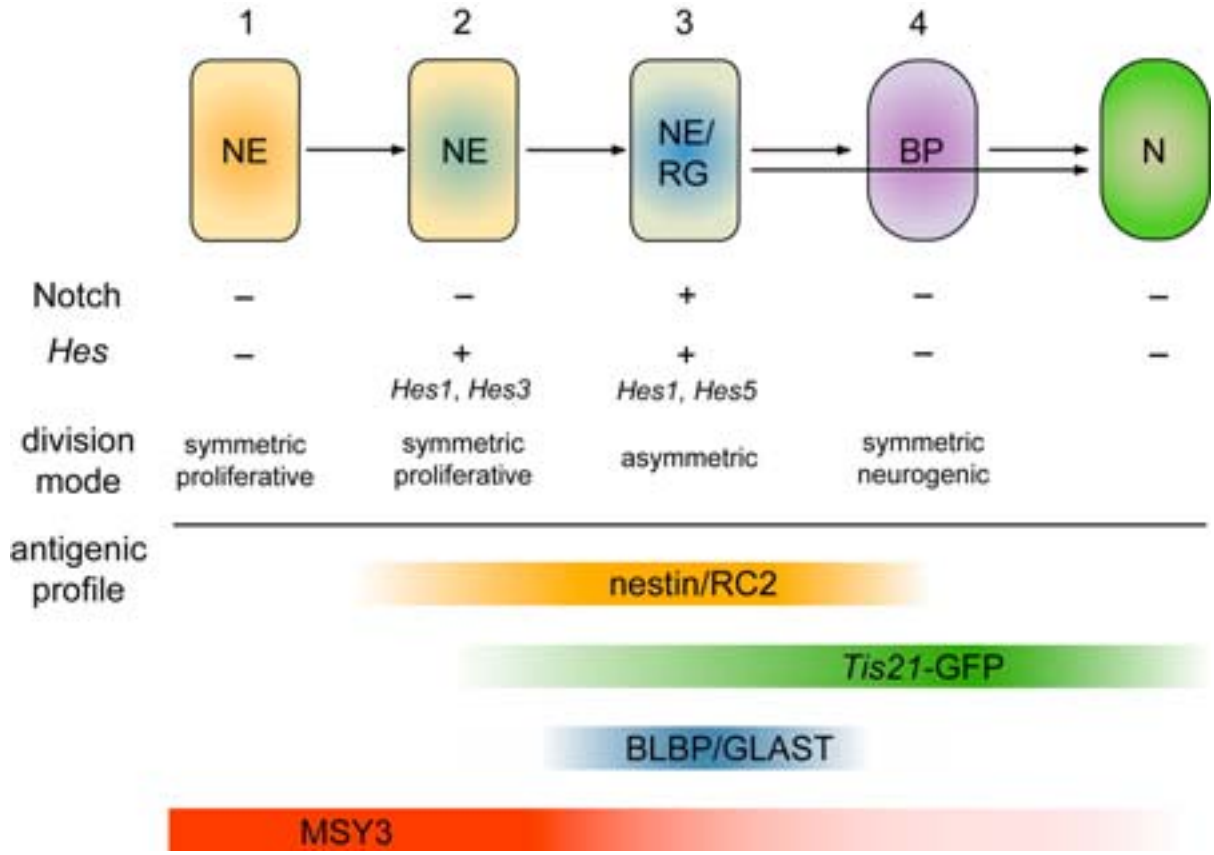

Figure 40. MSY3 is downregulated during transition from proliferating to neurogenic divisions of progenitor cells. Neural progenitor cells change their characteristics over time (Hatakeyama and Kageyama, 2006): **1**) Initially, neuroepithelial cells (NE) proliferate in absence of *Notch* and *Hes* expression. **2**) At E7.5-E8.5, neuroepithelial cells initiate expression of the *Hes3* and *Hes1* genes, simultaneously becoming dependent on the presence of anti-neurogenic action of Hes transcription factors (Hatakeyama et al., 2004; Hatakeyama and Kageyama, 2006). At this time, progenitors undergo symmetric proliferative divisions and express high levels of MSY3 protein, which is present in the neuroepithelium before nestin. **3**) At the onset of neurogenesis, expression of *Hes* genes, and therefore progenitor maintenance, becomes dependent on Notch signalling (de la Pompa et al., 1997), which is accompanied by reduction of the MSY3 protein. Following, progenitor cells upregulate radial glial markers, such as BLBP and GLAST (Anthony et al., 2004; Hartfuss et al., 2001), and downregulate MSY3 to low levels, which persist in the ventricular zone by the end of the neurogenic period. Most of radial glial (RG) cells undergo asymmetric divisions (Miyata et al., 2004; Noctor et al., 2001). **4**) Neuroepithelial and radial glial cells give rise to basal progenitors (BP) (Miyata et al., 2004; Noctor et al., 2004), which express *Tis21*-GFP (Haubensak et al., 2004) and variable levels of MSY3 protein at the onset of neurogenesis. MSY3 is absent from neurons (N), which are postmitotic cells. *NE*, neuroepithelial cell; *RG*, radial glial cell; *BP*, basal progenitor; *N*, neuron.

3.1.5 Expression of MSY3 in transient amplifying precursors of the adult brain

Preliminary results indicate that in the postnatal and adult brain, MSY3 expression sets in the germinal zones while they are acquiring the mature organisation, i.e. at the end of the second week (Figure 31; Figure 32). MSY3 was detected in the transient amplifying progenitors, as suggested by the overlapping pattern of MSY3 and Dcx (doublecortin) expression. Dcx labels highly proliferating precursors and migrating neurons, but not mature neurons or astrocytic stem cells (Brown et al., 2003; Kempermann et al., 2004). Remarkably, in both regions MSY3 is not present in the *Tis21*-GFP-positive cells. Thus, as

in the embryo MSY3 is downregulated while whole population of progenitor cells is progressing in development and being gradually restricted in lineage and proliferation competence, in the adult germinal zones it declines with the lineage progression and differentiation from a precursor cell to a neuron. To confirm that MSY3 is not present in differentiated cells, other markers of maturating neuroblasts and fully differentiated neurons should be used, such as Prox-1, NeuN, Calbindin and Calretinin in the dentate gyrus, and βIII-tubulin in the SVZ (Doetsch et al., 1997; Kempermann et al., 2004). Proliferative state of MSY3 labelled cells could be established employing BrdU. Although not tested directly, the presented data suggests that MSY3 is absent from GFAP-positive astrocytes, given it is limited to Dcx-positive cells.

After birth, both the lateral ventricle wall and the dentate gyrus undergo radical histological rearrangements. In the lateral ventricle, radial glia of the embryonic ventricular zone transform into ependymal cells and subventricular zone astrocytes (Tramontin et al., 2003). In the dentate gyrus, majority of proliferative cells found in the hilus and derived originally from the embryonic subventricular zone differentiate into granule neurons by the end of the third postnatal week, expanding the thickness of the granule cell layer (Altman and Bayer, 1990a). The remaining progenitors populate the subgranular zone and generate locally new granule cells. Thus, in both germinal zones MSY3 is not expressed during time of increased cell differentiation, instead its expression is reestablished with appearance of transient amplifying population.

Although the picture emerges, in which expansion of progenitors via symmetric proliferative divisions and expression of MSY3 in the embryonic and adult brain are linked, it has to be emphasised that particularly in the hippocampus proliferation of transient amplifying cells is limited (Brown et al., 2003; Hayes and Nowakowski, 2002; Seri et al., 2001). The average cell cycle length of proliferating cells in the murine dentate gyrus was estimated as 12-14 h (Hayes and Nowakowski, 2002); similar average cell cycle length is characteristic for progenitors of E13-E14 developing cerebral cortex, which is after the MSY3 is downregulated (Takahashi et al., 1995). The average cell cycle length of progenitors in the rat subventricular zone appears even longer, being estimated as 14 h (Smith and Luskin, 1998) or 19 h (Zhang et al., 2006). However, it is difficult to compare the relative intensity of MSY3 immunostaining in embryonic and adult tissues because of differences in the molecular composition (e.g. extracellular matrix content or protein-protein interactions) and processing for staining (see *Materials and Methods*), which may influence antigen accessibility.

3.1.6 Expression of MSY3 in neurospheres

Stem and progenitor cells isolated from embryonic or adult germinal zones have capacity to proliferate and self-renew in *in vitro*, forming free-floating aggregates of proliferating and differentiating cells called neurospheres (Gritti et al., 1996; Reynolds and Rietze, 2005; Reynolds and Weiss, 1996). Here it was shown that MSY3 is expressed in a subset of nestin-positive precursors of neurospheres grown in EGF-containing medium. The population of nestin expressing cells is heterogeneous, containing stem cells with theoretically infinitive self-renewal capacity and proliferating precursors (Lendahl et al., 1990; Reynolds and Rietze, 2005; Reynolds and Weiss, 1996; Suslov et al., 2002), however molecular markers to unambiguously discriminate between these different populations of proliferating cells are currently not available. Hence, the heterogeneity of MSY3 expression in the nestin-positive precursors remains unexplained. It is noteworthy that the majority of EGF-dependent neurospheres is derived from the transient amplifying precursors rather

than *bona fide* stem cells, at least in the ventricular zone (Doetsch et al., 2002), and it is the former that expresses MSY3 *in vivo*. Therefore, it could be speculated that *in vitro* MSY3 is expressed in fast proliferating precursors.

Neural stem cells can be cultured in a presence of EGF or bFGF. EGF and bFGF act on separate populations of embryonic neural progenitors stimulating their growth and renewal by independent mechanisms (Tropepe et al., 1999). bFGF-responsive stem cells emerge earlier in development (around E8.5) than EGF-responsive stem cells (around E13.5), and the latter can be derived from bFGF-grown neurospheres (Hitoshi et al., 2002; Hitoshi et al., 2004; Tropepe et al., 1999). Given that primary bFGF-responsive progenitors cells exhibit longer cell cycle than EGF-responsive cells *in vitro*, which likely reflects distinct proliferative kinetics of progenitors *in vivo* (Martens et al., 2000), it would be interesting to compare MSY3 expression in these two cell populations. If MSY3 is linked with fast growth, it should be expressed at a lower level in neurospheres grown bFGF-containing medium.

3.1.7 Expression of MSY3 in other cell types of the central nervous system

Surprisingly, during the two first postnatal weeks, MSY3 was found in cortical neurons with pyramidal morphology (Figure 33). This is in contrast to earlier absence of this protein in cortical neurons during the whole neurogenic period (Figure 9; Figure 12). During maturation of the nervous system, immature neurons are selected for survival or undergo apoptosis, establish synaptic connections and associate with glia (Rao and Jacobson, 2005). Any of these processes could require function of MSY3. However, the ability of MSY3 to inhibit Cdk5 kinase *in vitro* is in this context of particular interest (Moorthamer et al., 1999). Cdk5 is functionally a brain specific serine/threonine kinase (Tsai et al., 1993) and *Cdk5*-null embryos demonstrate block of neuronal migration (Gilmore et al., 1998) and, as a consequence, inverted pattern of cortical layering (i.e. outside-in). It is plausible, that MSY3 could inhibit Cdk5 in young neurons of the cortical plate once they reached the proper position. Nevertheless, such a role would only be auxiliary, as MSY3-overexpressing neurons during embryogenesis do not fail to migrate (see next section). On the other hand, the overexpression of MSY3 was performed between E12.5 and E14.5, i.e. at the emergence of the cortical plate (Bayer and Altman, 1991), and a block of neuronal migration into the cortical plate of the *Cdk5* knockout embryos occurs shortly after splitting the preplate into the marginal zone and the subplate, therefore the early cortical plate start to form (Gilmore et al., 1998). Thus, to evaluate a putative role of MSY3 in neuronal migration, misexpression of MSY3 ought to be performed at later stages.

Another cell type, which is not related to neuronal progenitors and expresses high levels of MSY3 protein appears as bipolar cells in the neuronal layers of the ventral portion of the hindbrain and spinal cord at E12.5, and at E14.5 in the thalamus (data not shown). These cells are not labelled by βIII-tubulin antibody, therefore unlikely represent neurons. Although the nature of these cells awaits further investigation, the spatiotemporal pattern of their appearance suggests they might be oligodendrocyte precursors (Thomas et al., 2000). It is interesting to note that oligodendrocyte precursors are proliferative progenitors (Ono et al., 2001; Yuan et al., 2002), and *in vitro* embryonic glial progenitors undergo vast expansion before maturation into glia (Qian et al., 2000).

3.2 MSY3 is not an essential player in the control of precursor proliferation

MSY3 is expressed in proliferating progenitors, being downregulated when they switch to neurogenic divisions. But is the high level of MSY3 expression causally related to cellular proliferation or is just a marker associated with rapid cell growth? This question was addressed here by acutely manipulating the level of MSY3 in the neuroepithelium.

Premature downregulation of MSY3 in the neuroepithelium between E9.5 and E11.5 employing RNAi did not affect proliferation of targeted cells, based on the following observations: i) similar proportion of targeted cells remained in the ventricular zone in the control and RNAi-induced embryos; ii) RNAi did not promote ectopic neurogenesis in the regions of the neural tube that do not generate neurons at analysed developmental time point, such as the rostral diencephalon; iii) downregulation of MSY3 did not induce radial glia prematurely; iv) the abundance of basal progenitors did not increase.

Furthermore, overexpression of MSY3 at E10.5 or E12.5 for 36 or 48 h, respectively, did not affect the cell cycle exit, differentiation or commitment of targeted cells: i) overexpressing cells at both developmental ages contribute to neuronal production similarly as progenitors targeted with a control plasmid only; ii) MSY3 overexpression did not reduce the number of *Tis21*-EGFP positive cells; iv) position of MSY3-overexpressing and control neurons within the neuronal layers exhibited indistinguishable pattern.

Together, these results indicate that, within the scope of the experiments, neither is MSY3 indispensable for the maintenance of progenitor proliferation, nor is its downregulation obligatory to enter a differentiation pathway. Therefore, the MSY3 protein is not a decisive node governing proliferation or differentiation in the neuroepithelium. In agreement, Lu and colleagues reported recently generation of the *MSY3* knockout mouse (Lu et al., 2006). The *MSY3* null animals are viable, and gross anatomical examination revealed that the major organs, including brain, show similar morphologies and sizes as wild type littermates. MSY3 appears essential only in the testis, as *MSY3*-deficient males exhibit degeneration of seminiferous tubules and increased spermatocyte apoptosis, which lead to reduced fertility.

Nonetheless, MSY3 might play a supplementary fine-tuning role in maintenance of progenitor cells in proliferation. It is not excluded that *MSY3* null mice exhibit mild alteration of neural development, e.g., a premature onset of neurogenesis, a change of cell cycle kinetics or a difference in cortical layering, which might be revealed by thorough examination.

Given that MSY3 is expressed *in vitro*, the neurosphere assay could offer a quantitative analysis of proliferative capacities of MSY3-deficient progenitors (Alexson et al., 2006; Reynolds and Rietze, 2005): i) neurospheres can be repetitively passaged and this ability reflects self-renewal property of neural stem cells; ii) the number of secondary spheres obtained after dissociation of a single sphere provides an estimation of the number of proliferative divisions, as only cells that divide symmetrically can expand the number of secondary spheres; iii) the average number of cells per a neurosphere allows to deduce proliferation rates of progenitors; iv) BrdU incorporation might provide additional cues as to the cell cycle kinetics and proliferation. The downregulation of MSY3 in progenitor cells by shRNA in a preliminary experiment provides a tool to address some of these questions. The plasmid used in this experiment can be packaged into adeno-associated viral particles, which infect neural progenitors with high efficiency (Verdon Taylor, personal communication). However, it needs to be mentioned that the integration of an adenovirus into the cellular DNA is rare and the adenoviral genome stays episomal being inherited only

by one daughter cell upon the division. Therefore, the adenoviral infection is not suitable to assay the stem cell maintenance, which requires prolonged culture. Alternatively, neurospheres could be prepared from the *MSY3* null mice.

3.3 Towards the cellular function of MSY3

3.3.1 Subcellular localisation of MSY3

Y-box proteins are multifunctional regulators of gene expression at the level of transcription and translation, and often are linked with proliferation and cancer (see *Introduction*). In agreement, the MSY3 orthologues in the dog (ZONAB) and human (dbpA) epithelial cell lines, acting as transcription factors, promote G_1/S transition, hence increase proliferation and final cell density in mature monolayers (Balda et al., 2003; Sourisseau et al., 2006). In neural progenitor cells, the MSY3 protein, as investigated by subcellular fractionation (Figure 34), immunofluorescence (Figure 22) and immunoelectron microscopy (Figure 23), was detected throughout the cytoplasm, and unlike ZONAB/dbpA was not found in the nucleus or at junctions.

Nuclear localisation of ZONAB/dbpA is linked with its function in promoting proliferation (Balda and Matter, 2000; Sourisseau et al., 2006). However, ZONAB/dbpA is localised to the nucleus only in subconfluent cells, and translocates to the cytoplasm as cells form functional tight junctions and cease proliferation (Balda and Matter, 2000). In the developing neural tube, neuroepithelial cells are linked by adherence/tight junctions to form continuous tissue, yet, unlike the mature monolayer of MDCK cells, are highly proliferative. The proposed pro-proliferative action of MSY3 in progenitor would rather employ other mechanism than transcriptional regulation. Nevertheless, it cannot be excluded that a minute fraction of the protein localises to the nucleus and exerts its function as a transcription factor. Despite cytoplasmic localisation and function as an mRNA binding protein, the other member of the Y-box family, MSY2, is associated with certain Y-box-containing promoters in germ cells, possibly linking transcription with mRNA storage (Yang et al., 2005a). The cytoplasmic localisation of MSY3 in neuroepithelial cells could also be mediated by RNA binding. Work presented here shows that the MSY3 protein in the developing mouse embryo, as well as in the Neuro-2A cell line, is associated with RNA. In various cell lines, cytoplasmic retention of another Y-box protein YB-1 is attributed to mRNA binding (Bader et al., 2003; Bader and Vogt, 2005; Sorokin et al., 2005). The YB-1 nuclear localisation is induced by stress or is a peculiarity of transformed cell lines and cancer tissues. In this regard, MDCK cells are also immortal cell line, and nuclear expression of ZONAB might image a tumour state.

The interaction of ZONAB/dbpA with ZO-1 and RalA at tight junctions is believed to sequester the protein from the nucleus, thereby inhibiting its function as a transcription factor (Balda and Matter, 2000; Frankel et al., 2005). Moreover, junctional ZONAB sequesters from the nucleus its binding partner, Cdk4 (Balda et al., 2003). Despite high levels of expression of ZO-1 and MSY3 in the neuroepithelium shown here, these two proteins do not colocalise in progenitor cells. However, ZONAB shows also diffuse cytoplasmic staining, and to visualise junctional association of ZONAB, MDCK cells are pre-treated with Triton X-100 prior to the fixation, which partly extracts the cytoplasmic pool of the protein (Balda and Matter, 2000; Frankel et al., 2005). Therefore, it is not excluded that ZONAB, and hence MSY3, inactivation mediated by ZO-1 is not direct and

independent of ZONAB junctional localisation. Given the ability of MSY3 to bind mRNA it is also possible that specific localisation of ZONAB/dbpA mediates tethering of messages to junctions and local protein synthesis.

Progenitor cells are coupled via adherens and tight junctions (Aaku-Saraste et al., 1996; Chenn et al., 1998; Hatakeyama et al., 2004), though closure of the neural tube is accompanied by remodelling of thight junctions: loss of occludin expression is coupled with loss of paracellular barrier (Aaku-Saraste et al., 1996). Simultaneous upregulation of ZO-1 expression has been reported in the chick neural tube (Aaku-Saraste et al., 1996); nevertheless, biochemical analysis presented here (Figure 14), as well as confocal microscopy (Figure 22) did not reproduce such a phenomenon in the mouse neuroepithelium. Though, the immunofluorescence staining on cross-sections presented by Aaku-Saraste and colleagues might be misleading, as during transition from columnar to elongated pseudostratified epithelium, separate punctae of junctions are brought in the proximity and appear as a continuous line under the epifluorescent microscope. This gross morphological change, however, may not reflect amount of the ZO-1 protein associated with each individual cell.

Two isoforms of ZO-1 result from alternative splicing and differ by internal 80 amino acid domain, termed α (Balda and Anderson, 1993; Willott et al., 1992). ZO-1α^- is associated with structurally dynamic junctions, such as junctions of endothelial cells, Sertoli cells and podocytes, whereas ZO-1α^+ is associated with less dynamic junctions of epithelial cells (Balda and Anderson, 1993). Interestingly, mouse neuroepithelium expresses mostly ZO-1α^- isoform, as indicated by immunoblotting in comparison with the extract prepared from the liver (data not shown), which expresses both ZO-1 isoforms (Balda and Anderson, 1993). Although not confirmed by RT-PCR or isoform-specific antibodies, this preliminary finding further supports the notion that neuroepithelial tight junctions are not equivalent of the mature junctions of epithelial cells. The assembly of tight junctions during the early pre-implantation development is a step-wise process that initiates from recruitment of the ZO-1α^- isoform and rab13 upon the E-cadherin adhesion (Fleming et al., 2000; Sheth et al., 1997; Sheth et al., 2000). The final phase in the tight junction formation requires ZO-1α^+ isoform, which is indispensable for junctional localisation of occludin (Furuse et al., 1994; Sheth et al., 1997). Notably, both proteins are absent from the neuroepithelial cells. It is plausible that only ZO-1α^+ isoform supports junctional localisation of ZONAB/dbpA/MSY3. Indeed, in MCF-10A-JB cells, which lack functional tight junctions, dbpA is not present at cell contacts, while in the MCF-10A-95 subclone, which forms functional tight junctions, dbpA colocalises with ZO-1 at the cell periphery (Sourisseau et al., 2006). The MCF-10A-JB clone express ZO-1 and occludin at junctions in a non-continuous punctuate pattern.

In the adult brain and retina, MSY3 protein localises at glial and neuronal gap junctions, respectively (Ciolofan et al., 2006; Penes et al., 2005). In these studies, the antibody directed against the C-terminus of MSY3 showed sparse puncta of immunoreactivity when applied on MSY3-overexpressing HeLa cells (Ciolofan et al., 2006). However, the anti-MSY3 antibodies reported here, which were raised against the N-terminal domain, in MSY3-overexpressing HeLa cells recognise granular staining throughout the cytoplasm, resembling that in the neuroepithelium or Neuro-2A cells (data not shown). It is therefore plausible that differential accessibility of the epitopes located in the N- or C-terminus of MSY3 contributes to a different apparent subcellular localisation. Since the corresponding antibody against the C-terminal domain of MSY3 is now commercially available, it will be possible to address this issue.

3.3.2 MSY3 associates with actively translating ribosomes – does it bind mRNA?

Subcellular fractionation (Figure 34), immunoprecipitation (Figure 37) and polysomal analysis (Figure 35; Figure 36) performed in this study revealed that the MSY3 protein in the developing embryo, as well as in Neuro-2A cells, is associated with RNA and on a sucrose density gradient co-fractionates with ribosomes and actively translating polysomes.

Disruption of polysomes by EDTA or puromycin results in a shift of MSY3 to fractions containing ribosomal subunits. Two possible explanations of this result come in hand. Firstly, MSY3 could be bound to the ribosome itself, and, secondly, to be associated with mRNA released from the polysomes. It is important to note that the EDTA-dissociated mRNAs, though separated from ribosomes, are associated with proteins and have a similar sedimentation coefficient to ribosomal subunits (Henshaw, 1968). Indeed, the protein content of EDTA- or puromycin-dissociated mRNPs comprises about 60% of the weight of the complexes (Henshaw, 1968; Kumar and Lindberg, 1972; Perry and Kelley, 1968), therefore it is plausible that sedimentation of MSY3 is caused by association with mRNA. Majority of MSY3 in germ cells is bound directly to stored mRNA, devoid of ribosomes (Davies et al., 2000). The immunoprecipitation of MSY3 in a presence of EDTA revealed its association with rRNA, yet in this condition rRNA was partially degraded and most probably released from the ribosome, suggesting that this interaction is unspecific, as it was reported for YB-1 (Nekrasov et al., 2003). To investigate whether MSY3 associates with ribosome or mRNA in proliferating cells, oligo(dT)-cellulose can be used to separate the components of EDTA-dissociated polysomes into an unbound ribosome fraction and a fraction retained by the resin that contains mRNA associated with proteins (Corbin et al., 1997; Lindberg and Sundquist, 1974).

High salt environment results in removal of more than 50% of proteins from polysomal mRNPs, nevertheless, polysomes remain intact (Kumar and Lindberg, 1972). MSY3 is solubilised by treatment with 0.5 M NaCl, implicating it does not act as an mRNP core protein, such as YB-1 or PABP, which retain binding to mRNA in high salt (Auerbach and Pederson, 1975; Lindberg and Sundquist, 1974). It is unknown whether MSY3 binds RNA directly or association with RNA is mediated by a protein. To solve this question, MSY3 could be immunoprecipitated under stringent conditions from [^{3}H]-uridine labelled cells after UV-crosslinking and partial RNase digestion. Radioactive labelling of MSY3 would indicate that the protein binds directly to mRNA, since only molecules in direct contact can be covalently crosslinked by UV.

3.3.3 What is the role of MSY3 in translation?

Translation of mRNA into protein represents the final step in the gene expression pathway (for review see: Gebauer and Hentze, 2004). Two general modes of translational control are utilised by cells: the global control, in which translation of most mRNAs in the cell is regulated; and mRNA-specific control, whereby the translation of a defined group of mRNAs is modulated by binding of regulatory protein complexes to specific elements present in the messages, usually in their 3' or 5' UTRs (Gebauer and Hentze, 2004; Kuersten and Goodwin, 2003).

Overexpression or downregulation of MSY3 in Neuro-2A cells did not affect global protein synthesis rates. This result, however, does not exclude possibility that MSY3 acts as a general translational regulator. The global translation regulation in eukaryotic cells is achieved mostly by modification of levels and activity of translation initiation factors (Gebauer and Hentze, 2004; Gingras et al., 1999; Richter and Sonenberg, 2005). Translation

of nuclear-encoded mRNAs requires binding of rate-limiting eIF4E to the mRNA cap structure. eIF4E subsequently recruits the scaffolding protein eIF4G and the RNA helicase eIF4A, which facilitates the ribosome binding and scanning along the 5' UTR towards the initiation codon. The requirement for eIF4E binding and eIF4A helicase activity is proportional to the degree of mRNA 5' secondary structure, and messages with extensive secondary structure in their 5' UTRs are less competitive for translation initiation (Kornack and Rakic, 1998; Koromilas et al., 1992; Svitkin et al., 2001). Computational analysis of 5' UTRs of human genes revealed that the class of mRNAs which contain lengthy untranslated regions with a high degree of secondary structure consists of mRNAs encoding transcription factors, growth factors and their receptors, proto-oncogens, and other regulatory proteins which are poorly translated under normal conditions (Davuluri et al., 2000). Thus, this class of mRNAs is a primary target for the translational control. Consequently, an increase in eIF4E amount or activity does not lead to elevated rates of global translation (Saghir et al., 2001), but instead results in increased translation of a subset of mRNAs (Graff and Zimmer, 2003). In this context, it is tempting to speculate that MSY3, through its RNA chaperoning functions characteristic to Y-box proteins, supports translation of non-competitive, highly structured mRNAs.

Importantly, removal or overexpression of YB-1 does not affect the global translation rate (Davydova et al., 1997; Lu et al., 2005), despite the fact that YB-1 is a major mRNP protein (Evdokimova et al., 1995) and its loss affects cell growth and is lethal for embryos (En-Nia et al., 2005; Lu et al., 2005; Matsumoto et al., 2005). Instead, overexpression of YB-1 represses translation of reporter mRNAs (Bader et al., 2003; Bader and Vogt, 2005; Davydova et al., 1997; Evdokimova et al., 2001), or influences protein synthesis in cell-free systems (Evdokimova et al., 1998; Nekrasov et al., 2003; Pisarev et al., 2002).

Lu and colleagues in the aforementioned work (Lu et al., 2006) presented that double *YB-1/MSY3* null embryos showed more severe developmental defects than animals deficient in *YB-1* only. *YB-1* null embryos die perinatally, whereas embryonic death of double knockout embryos occurs between E8.5 and E11.5. Since at E11.5 expression of the MSY3 protein declines, this data indicate that MSY3 can rescue functions of YB-1 during early embryogenesis (when it is expressed), and suggest that both proteins share similar function(s). Moreover, YB-1 can be co-immunoprecipitated together with MSY3, as shown here. Co-immunoprecipitation is partly abolished by presence of EDTA, hence suggesting that it is mediated by mRNA.

Since MSY3 displays very specific expression profile in the developing CNS, being present only in proliferative progenitors (with minor exceptions), as compared to YB-1, which is also highly expressed in neurons (Funakoshi et al., 2003; and data not shown), it is possible that MSY3 modulates the function of YB-1. MSY3 could also act additively with YB-1, or have an additional separate function important for development. It is to be mentioned that YB-1 forms large multimeric complexes, and dimerisation is mediated by the C-terminal domain (CTD) (Skabkin et al., 2004; Tafuri and Wolffe, 1991). Interestingly, the CTD of MSY3 expressed in *E. coli* as a GST-fusion protein aggregates (data not shown), therefore it is not formally excluded that the MSY3 could heterodimerise with YB-1 via their CTDs. To investigate whether YB-1 associates directly with MSY3, immunoprecipitation could be carried in the presence of RNase. To get an insight into relation of MSY3 and YB-1, it would be essential to compare polysomal profile of YB-1, as well as a set of YB-1-bound mRNAs, before and after MSY3 developmental downregulation, or in the *MSY3* null background.

Identification of MSY3-bound mRNAs could provide a cue as to the function of MSY3. Since MSY3 can be efficiently co-immunoprecipitated with RNA, determination of bound

transcripts by microarray analysis, or UV-cross link and immunoprecipitation (CLIP) (Ule et al., 2003), followed by cloning of bound messages, are experimentally feasible. It might also be valuable to compare the set of messages bound by MSY3 to that associated with YB-1.

In germ cells, MSY3 contributes to packaging and silencing of mRNA, with minor fraction associated with polysomes (Davies et al., 2000), whereas in the embryo most of the MSY3 protein is associated with translating polysomes. A dual role in translation regulation has been assigned to YB-1, which at high molar ratios represses translation, whereas low levels of YB-1 are indispensable for translation initiation (Evdokimova et al., 1998). By analogy, it is plausible that stoichiometry of MSY3 to mRNA determines whether the protein supports or represses translation. Nonetheless, the polysomal association of MSY3 does not ultimately indicate that it is complexed with non-repressed messages. Inhibition of translation after the initiation step was observed in a variety of systems in which 3' UTRs regulate translation. These include silencing of the IL-1β mRNA in human monocytes (Kaspar and Gehrke, 1994) and the brain creatine kinase (CKB) mRNA in the rat (Shen et al., 2003), whereas in the *Drosophila* the unlocalised nanos and oskar mRNAs are regulated at a step after translation initiation (Braat et al., 2004; Clark et al., 2000). The mechanisms employing postinitiation repression might be common, since miRNAs cosediment with polysomes in worms and mammalian cells (Kim et al., 2004; Nelson et al., 2004; Olsen and Ambros, 1999). In *C. elegans*, the lin-14 and lin-28 mRNAs are repressed at a postinitiation stage by the lin-4 miRNA (Olsen and Ambros, 1999; Seggerson et al., 2002). Also, imperfectly complementary short RNAs, which mimic miRNAs, repress translation after the initiation in mammalian cells (Petersen et al., 2006). Importantly, repressed mRNAs show the polysomal sedimentation profile and are engaged in translational elongation, as shown by puromycin sensitivity. Furthermore, FMRP protein, which has been shown to repress translation (Laggerbauer et al., 2001; Li et al., 2001; Mazroui et al., 2002), is present in polysomes, which are sensitive to puromycin (Corbin et al., 1997; Khandjian et al., 2004; Stefani et al., 2004). FMRP is also part of the RISC complex in *Drosophila* (Caudy et al., 2002), and in mammalian cells (Jin et al., 2004).

Given that YB-1 can interact with FMRP (Ceman et al., 2000), it would be important to check whether the FMRP protein or members of the Argonaute family, key molecules in miRNA- and RNAi-mediated silencing (Carmell et al., 2002), co-immunoprecipitate with MSY3. It should also be noted that miRNA pathway and Argonaute proteins are recently emerging as determinants for the developmental control and stem cell decisions (Carmell et al., 2002; Cheng et al., 2005).

3.3.4 How could translation affect neurogenesis?

Availability of eIF4E is believed to be critical for translational activation of non-competitive mRNAs, which encode growth-related or anti-apoptotic proteins (Graff and Zimmer, 2003). Consistently, overexpression of eIF4E induces transformation (Avdulov et al., 2004; De Benedetti and Rhoads, 1990; Lazaris-Karatzas et al., 1990) and parallels enhanced translation of the reporter and endogenous messages with highly structured 5' UTRs, such as those encoding Myc, FGF, ornithine decarboxylase (ODC), cyclin D1, VEGF and *yes* src-like kinase (Defatta and De Benedetti, 2003; Graff and Zimmer, 2003). These effects can be counteracted by elevating the levels of inhibitory eIF4E binding proteins (4E-BPs) (Avdulov et al., 2004), which either sequester eIF4E from mRNAs or disrupt its binding to eIF4G (Richter and Sonenberg, 2005). In patients, upregulation of translation initiation factors and disregulation of ribosome biogenesis coincides with malignancy (Rosenwald, 2004; Ruggero and Pandolfi, 2003). Growth factors,

hormones and mitogen stimuli potently activate mRNA translation, largely through activation of the phosphatidylinositol 3-kinase (PI3K) pathway (Ruggero and Sonenberg, 2005). Thus, translational regulation is linked to cell growth and may represent one of the mechanisms by which proliferative divisions and fast cell cycle of progenitor cells are controlled.

Of importance is that the developmental profile of MSY3 expression seems not to reflect downregulation of the general translation apparatus, including another Y-box protein YB-1. These preliminary findings, however, require validation. Since not only does the activity of the translation machinery relay on the total amount of initiation factors, but also on their phosphorylation state and availability, levels of phosphorylated eIF4E and the ribosomal protein S6, as well as expression profile and phosphorylation of 4E-BPs, should be monitored.

Given that MSY3 developmental expression coincides with expansion of neuroepithelial cells, it is suggestive that MSY3 promotes proliferation and/or inhibits differentiation of progenitors by regulating translation. If so, several mechanisms could be envisaged. First, MSY3 might repress translation of mRNAs encoding differentiation factors. In the second scenario, MSY3 facilitates translation of growth- and cell division-associated mRNAs. Third, it should not be ignored that the short cell cycle of neuroepithelial cells prior to neurogenesis, i.e. of approximately 8 h, requires rapid growth, hence efficient synthesis of structural proteins. Although overexpression of MSY3 in the cell line did not affect general translation, it is not excluded that MSY3 in neuroepithelial cells non-selectively enhances global translation. Discovery of MSY3-bound messages and, possibly, its role in translation, might provide a clue as to which of these scenarios could apply during central nervous system development.

3.4 Concluding remarks

This work identified the murine MSY3 protein as a "pan-proliferative" marker of neural progenitor cells in the embryonic and adult brain. Expression of MSY3 relates to the fast cell cycle progression rather than being a stem cell feature. The presented data provide a suggestion that MSY3 and, by analogy, human dbpA could be used to identify proliferating cell populations throughout the nervous system also in regeneration and cancer. In this regard, it is interesting that MSY3 has common molecular characteristics in the developing embryo and the neuroblastoma cell line. Although multiple proteins involved in translation are elevated during cell proliferation, MSY3 is distinct as it is not present in differentiated neurons, which are also characterised by high metabolism and expression of YB-1. Therefore, despite the lack of an evident phenotype in MSY3-deficient progenitors and embryos, revealing molecular interactors of MSY3 in neuroepithelial cells could provide a specific link between translational machinery and cell cycle progression in development and pathology.

4 MATERIALS AND METHODS

4.1 Standard materials

4.1.1 Technical equipment

centrifuges	Beckman Coulter, Avanti J-25
	Beckman Coulter, Optima MAX Ultracentrifuge
	Beckman Coulter, Optima LE-80K Ultracentrifuge
	Heraeus, Megafuge 1.0R
	Eppendorf, centrifuge 5415R
balances	Sartorius, BL 3100
	Sartorius, BP 121S
water bath	GFL
gradient maker	Labconco, with SG-30 Hoefer unit
DNA gel chamber	EMBL
protein gel chamber	Sigma, E5889
	Sigma, Z37
semi-dry transfer system	CTI, Idstein, Germany, 11SD-1 with glass electrodes
power supply	Amersham Pharmacia Biotech, EPS 301
	Hoefer, EPS 2A2000
speedvac	Jouan, RC10.22/RCT60
gel dryer	Heto, GD-2
vacuum pumps	Vacumbrand GmbH
sonicator	Bandelin Electronic, Berlin, UW200
homogeniser	Eurostar Digital, IKA-WERKE
film developer	Kodak
cell culture hood	The Baker Company, SterilGARD III Advance
cell culture incubator	Heraeus, HeraCell (copper)
whole embryo culture incubator	R.K.I. Ikemoto, Tokyo, 10-0310
anaesthesia system	VetEquip, Pleasanton, California
needle puller	Sutter Instrument Co., USA, P-97
pneumatic pico pump	World Precision Instruments, PV 820
electro square porator	BTX Genetronics, Inc., San Diego, ECM 830
cell electroporator	Biorad, GenePulser II
cryostat	Microtome

ultra-cryostat	Leica, ultracut UCT/FCS
light microscopes	Olympus, SZX12 (dissection)
	Olympus, BX61 (epifluorescence; bright field)
	Zeiss LSM, Axiovert 200, LSM 510 AIM
electron microscope	Morgagni, FEI, The Nederlands
pipettes	Gilson

4.1.2 Chemicals

All standard chemicals were purchased from Invitrogen, Merck (Darmstadt), Roth (Karlsruhe) or Sigma, at analysis (p.a.) quality.

DNA standards	Invitrogen
	MBI Fermentas
Enzymes (molecular biology)	MBI Fermentas
	New England Biolabs
	Promega (Liga Fast)
	Roche
Trizol LS	Invitrogen
Glycogen	Q-Biogene
RNase A	Qiagen
GST-RNase III	MPI-CBG Protein Facility
RNase Inhibitors	Invitrogen
	Promega
Puromycin	Sigma
Pre-stained protein standards	Invitrogen
	Sigma
Protease inhibitor cocktail (for mammalian tissue)	Sigma
Glutathione sepharose	Amersham Biosciences
Protein A sepharose	Amersham Biosciecnes
Protein G sepharose	Amersham Biosciences
ECL detection solutions	Amersham Biosciences
	Pierce
Cell culture media and supplements	Gibco Invitrogen
Trypsin	Gibco Invitrogen

Accutase	PAA laboratories
DNase I type IV	Roche
hrEGF	Sigma
	R&D
Laminin	Sigma
Poly-L-lysine	Sigma
Lipofectamine 2000	Invitrogen
Salmon sperm DNA	Invitrogen
L-[^{35}S]methionine, L-[^{35}S]cysteine mix	PerkinElmer
Rat serum (whole embryo culture)	Charles River (Japan)

4.1.3 Kits

BCA Protein Assay Kit	Pierce
EndoFree Plasmid Maxi Kit	Qiagen
MEGAscript T7 Kit	Ambion
Plasmid Maxi Kit	Qiagen
QIAprep Spin Miniprep Kit	Qiagen
QIAquick Gel Extraction Kit	Qiagen
TOPO-cloning Kit	Invitrogen

4.1.4 Gradient SDS-PAGE protein gels

NuPage 4-12% Bis-Tris Gel	Invitrogen
NuPage Running Buffer	Invitrogen

4.1.5 Membranes

Nitrocellulose Protan BA pore size 0.45 µm	Schleicher & Schuell
PVDF Immobilion-P pore size 0.45 µm	Milipore

4.1.6 Films

ECL Hyperfilm Hyperfilm	Amersham Bioscience

4.1.7 Bacterial strains

DH5α: F-, ϕ80d*lac*ZΔM15, Δ(*lacZYA-argF*)U169, *deo*R, *recA*1, *endA*1, *hsd*R17(rk-, mk+), *pho*A, *sup*E44, λ-, *thi*-1, *gyrA*96, *relA*1

BL21: ***F-, ompT, gal, dcm, lon, hsdS$_B$(r_B-m_B-) λ(DE3)***

HB101 (Promega): F-, *thi*-1, *hsdS*20 (r_B-, m_B-), *supE*44, *recA*13, *ara*-14, *leuB*6, *proA*2, *lacY*1, *gal*K2, *rpsL*20 (str^r), *xyl*-5, *mtl*-1

TOP10 (Invitrogen)F-, *mcr*A Δ(*mrr-hsd*RMS-*mcr*BC), ϕ80*lac*ZΔM15, Δ*lac*X74, *rec*A1, *ara*D139, *gal*U, *gal*K, Δ(*ara-leu*)7697, *rps*L (Str^R), *end*A1, *nup*G

DH10b pir116 (Open Biosystems):F-, *end*A1, *rec*A1, *gal*U, *gal*K, *deo*R, *nup*G, *rps*L, Δ*lac*X74, Φ80*lac*ZΔM15, *ara*D139, Δ(*ara,leu*)7697, *mcr*A, Δ(*mrr-hsd*RMS-*mcr*BC), *Umc*C::*pir*116-*Frt*, λ-

4.1.8 Cell lines

COS7: Adherent fibroblast-like cell line derived from the kidney of an African green monkey. This line was constructed from the CV-1 cell line by transformation with the origin defective mutant of SV40 encoding for the wild type T antigen. Contains T antigen, retains complete permissiveness for lytic growth of SV40, supports the replication from SV40 ori.

HeLa: The adherent epitheloid cell line derived from cervical cancer cells taken from Henrietta Lacks, who died from her cancer in 1951.

Neuro-2A: The adherent neuroblastoma clone established by R. J. Klebe and F. H. Ruddle from a spontaneous brain tumour of a strain A albino mouse.

NIH-3T3: The adherent fibroblast cell line of highly contact-inhibited cells was established from the NIH Swiss mouse embryo cultures. The established NIH-3T3 line was subjected to more than 5 serial cycles of subcloning in order to develop a subclone with morphologic characteristics best suited for transformation assays.

4.1.9 Animals

For this work following mouse strains were used:

NMRI wild type mice were purchased from Harlan and used for biochemical analyses, cryosections and whole embryo cultures.

C57BL6 wild type mice were used for *in utero* electroporations and neurosphere preparation.

***Tis21*-EGFP** mice strain in C57BL6 background, in which the protein-encoding portion of the exon 1 of the *Tis21* gene was replaced by EGFP carrying nuclear localisation signal (Haubensak et al., 2004). In this study heterozygous embryos were used for cryosections and whole embryo culture.

***Hes5*-EGFP** transgenic mice strain in C57BL6 background was obtained from Verdon Taylor and Onur Basak (Freiburg). This line was established by genomic insertion of the construct, in which EGFP is driven from the 1.6 kb promoter region of the *Hes5* gene. The RBP-J proximal site in the promoter and the *Hes5* 3'UTR confer activation by Notch-1 and

a proper expression pattern that corresponds to the *Hes5* mRNA (Verdon Taylor, unpublished data).

En2-Cre* x Floxed *Notch1 *Notch1* cerebellar knock-out embryos were kindly provided by Verdon Taylor (Lütolf et al., 2002). The first coding exon of the *Notch1* gene was flanked by LoxP sequences to generate the Floxed *Notch1* allele and the *Notch1* null allele after Cre-induced recombination (Radtke et al., 1999). This line was crossed to the *En2-Cre* transgenic line, in which the Cre recombinase is expressed from the *engrailed-2* promoter enhancer and therefore is restricted to the neuroepithelium of the midbrain-hindbrain boundary. For cell fate tracing, the ROSA26-R Cre-reporter line (*R26R*) was used in a combination with the *En2-Cre* transgene and Floxed *Notch1* alleles. The *R26R* comprises the Floxed PGK prmoter driving a neomycin cassette containing three polyadenylation sequences and the *lacZ* gene with polyadenylation site introduced into the ROSA26 locus by homologous recombination. Cre-mediated recombination deletes the PGK neo cassette and results in constitutive expression of β-galactosidase (Soriano, 1999).

All mice were maintained on a 12 h light/dark cycle. Time pregnant females were obtained by overnight mating and the noon of a day when a vaginal plug was designated embryonic day 0.5 (E0.5).

4.1.10 Vectors

pAAV-hrGFP (Stratagene)	Adeno-associated viral vector expressing from the CMV promoter the hrGFP low-toxicity green fluorescent protein derived originally from from *Renilla* and codon optimised for mammalian cells. left ITR; CMV promoter fused with β-globin intron; hrGFP; hGH polyA; right ITR; f1 ori; ampiciline resistance gene; pUC ori
pCAGGS2 (Christio Goridis, Paris)	Mammalian expression vector based on the hybrid chicken β-actin/rabbit β-globin promoter fused to the CMV-IE enhancer sequence. CMV-IE, chicken β-actin promoter and exon I, rabbit β-globin intron II/exon III splice acceptor site; MCS; rabbit β-globin polyA; SV40 ori; pUC13 ori; ampiciline resistance gene
pCAGGS2-EGFP (Christo Goridis, Paris)	pCAGGS2 vector that drives expression of EGFP.
pCAGGS2-mRFP	pCAGGS2 vector that drives expression of mRFP (monomeric red fluorescent protein).
pGEX-M7	Procaryotic chemically inducible expression vector for construction of fusion proteins with the GST (glutathione S-transferase) moiety at the amino-terminus. *tac* promoter; GST gene; PreScission and TEV proteases

	sites; MCS; ampiciline resistance gene; origin of replication; lac I^q repressor
pGL2 (Promega)	Mammalian expression vector that drives expression of *Photinus pyralis* luciferase gene from the SV40 promoter/enhancer. ampicilin resistance gene; fi ori; SV40 promoter; luciferase gene; SV40 small t antigen intron; SV40 polyA; SV40 enhancer; ori *Col*E1
pJ4 (J.P. Magaud and J.P. Rouault, Lyon)	Mammalian expression vector containing the 1.8-kb *Sma*I-*Acc*I fragment of the mouse *Tis21* gene in the backbone of the pME18S vector under the control of the SRa promoter.
pSM2 (Open Biosystems)	Retroviral replication defective mammalian vector for efficient expression of shRNA-mirs in the backbone of primary mir30 mi-RNA. Provides also puromycine resistance for selection. LTR; U6 promoter; mir5'; shRNA cloning site; mir3'; U6 terminator; chloramphenicol resistance gene; *phosphoglycerate-kinase-1* (PGK) promoter, puromycine resistance gene; sinLTR; RK6γ ori; f1 ori T; kanamycin resistance gene
pSM2-luc (Open Biosystems)	pSM2 vector that drives expression of shRNA against luciferase

4.1.11 Clones

IRAK p961D1855Q2 (RZPD)	MSY3 N-truncated long splice variant; in the pCMV-SPORT6 backbone
IMAG p998F169447Q3 (RZPD)	MSY3 short splice variant with the deletion of nucleotide 810 of the open reading frame; in the pCMV-SPORT6 backbone

4.1.12 Oligonucleotides

Sequencing primers

	Sequence (5' – 3')	Name
P1	GCC CAG ATG GAG TTC CTG TAG	YB3 (469-489) F
P2	GGT CCA CGG CGC CTG CCA TAG	YB3 (536-556) R

P3	TCG GCT TCT GGC GTG TGA C	pCAGGS 5' 1 (1597-1615)
P4	CTC TAG AGC CTC TGC TAA C	pCAGGS 5' 2 (1622-1640)
P5	TTA GCC AGA AGT CAG ATG CTC	pCAGGS 3' (1880-1860)
P6	GTT ATG TAA CGC GGA ACT CC	CMV-R 83
P7	GGA CGA AAC ACC GTG CTC GC	pSM2-F (2476)
P8	TTC TGC GAA GTG ATC TTC CG	pSM2-R (2808)

Cloning primers

	Sequence (5' – 3')	Name
P9	GGA TCC GGC TTG AGC GAG GCG GGC GA	5'YB3-N-Bam
P10	CTC GAG CTA CGC GTC CTC GCC GCC CG	3'YB3-N-Xho
P11	GGA TCC ATT GGG GAG ATG AAG GA	5'YB3-C-Bam
P12	CTC GAG CCA GGG TCA CTC GGC ACT	3'YB3-C-Xho
P13	GGC CGC AAC TGG ATC CGA CTA	AAV-NotBamMlu 5'
P14	CGC GTA GTC GGA TCC AGT TGC	AAV-NotBamMlu 5'
P15	TCG AGC TGT TGA CAG TGA GCG ACC AGA TGG A GT TCC TGT AGA ATA GTG AAG CCA CAG ATG TAT TCT ACA GGA ACT CCA TCT GGG TGC CTA CTG CC T CGG	hp 647-F
P16	AAT TCC GAG GCA GTA GGC ACC CAG ATG GAG T TC CTG TAG AAT ACA TCT GTG GCT TCA CTA TTC TAC AGG AAC TCC ATC TGG TCG CTC ACT GTC AA C AGC	hp 647-R
P17	TCG AGC TGT TGA CAG TGA GCG AGA GAG GCT G AA GAC AAA GAA ATA GTG AAG CCA CAG ATG TA T TTC TTT GTC TTC AGC CTC TCC TGC CTA CTG CC T CGG	hp 1077-F
P18	AAT TCC GAG GCA GTA GGC AGG AGA GGC TGA A GA CAA AGA AAT ACA TCT GTG GCT TCA CTA TTT CTT TGT CTT CAG CCT CTC TCG CTC ACT GTC AAC AGC	hp 1077-R

P19	TCG AGC TGT TGA CAG TGA GCG ACA CGA CCT TA C CAA CAC CAA ATA GTG AAG CCA CAG ATG TAT T TG GTG TTG GTA AGG TCG TGG TGC CTA CTG CC T CGG	hp 1363-F
P20	AAT TCC GAG GCA GTA GGC ACC ACG ACC TTA CC A ACA CCA AAT ACA TCT GTG GCT TCA CTA TTT G GT GTT GGT AAG GTC GTG TCG CTC ACT GTC AAC AGC	hp 1363-R

esiRNA primers

	Sequence (5' – 3')	Name
P21	TAA TAC GAC TCA CTA TAG GGT GTA GTT GAA GGA GAA AAG GGT GC	T7-5'-YB3_bis
P22	AAT TAA CCC TCA CTA AAG GGT TGC CAT CTT GTG AAA CAG CG	T3-3'-YB3_bis
P23	TAA TAC GAC TCA CTA TAG GGC CTC AAC GCT GTT TCA CAA GAT G	T7 5' YB3_ter
P24	TAA TAC GAC TCA CTA TAG GGT TTG GTG TTG GTA AGG TCG TGG	T7 3'YB3_ter
P25	TAA TAC GAC TCA CTA TAG GGA GAG CAA CTG CAT AAG G	Fluc-T7 F
P26	TAA TAC GAC TCA CTA TAG GGA GAA TCT GAC GGC AGG CAG T	Fluc-T7 R
P27	CGT AAT ACG ACT CAC TAT AGG GTG AGC AAG GGC GAG GA	T7 EGFP F
P28	CGT AAT ACG ACT CAC TAT AGG GTA CAG CTC GTC CAT GCC GA	T7 EGFP R

4.1.13 Antibodies

Primary antibodies

Antigen	Description	Dilution	Supplier/ Reference
actin	mouse mAb clone AC-40	1:5000 (IB)	Sigma
βIII-tubulin	mouse mAb clone SDL.3D10	1:500 – 1:800 (IF)	Sigma
cadherin, pan-	mouse mAb clone CH-19	1:300 (IF)	Sigma
Dcx	goat polyclonal	1:100 (IF)	Santa Cruz Biotechnology
eIF4E	rabbit polyclonal	1:1000 (IB)	Cell Signaling
FMRP	mouse mAb	1.7 µg/ml (IB)	Developmental

	clone 7G1-1		Studies Hybridoma Bank
GFAP	mouse mAb G-A-5	1:300 (IF)	Sigma
GFP	rabbit polyclonal	1:500 (IF) 1:5000 (IB)	Transduction Laboratories
GFP	rabbit polyclonal	1:500 (IF)	Molecular Probes
GLAST	guinea pig antiserum	1:2000 – 1:4000 (IF)	Chemicon
MSY3	AP4912 rabbit polyclonal, aff. pur.	1:5000 (IF, IB)	Karl Matter
MSY3	AP0182 rabbit polyclonal, aff. pur.	1:1000 (IB)	see below and *Results*
MSY3	guinea pig antiserum GP2	1:10,000 (IF, IB) 1:50 (EM) 1:1000 (IP)	see below and *Results*
nestin	mouse mAb clone Rat-401	hybridoma supernatant 1:10 (IF)	Developmental Studies Hybidoma Bank
nestin	rabbit polyclonal, aff. pur.	1:1000 (IF) 1:5000 (IB)	Eva Aaku-Saraste
neurofilament 160	mouse mAb clone RMO044	1:50 (IF)	Sigma
phospho-histone 3	rabbit polyclonal	1:300 (IF)	Upstate
RC2	mouse mAb	1:200 – 1:300 (IF)	Developmental Studies Hybridoma Bank
ribosomal protein S6	rabbit mAb	1:1000 (IB)	Cell Signalling
Tis21/BTG2	K4 rabbit polyclonal, aff. pur.	1:4000 (IF) 1:1000 (IB)	(Iacopetti et al., 1999)
Tis21/BTG2	1511 rabbit polyclonal, aff. pur.	1:10,000 (IB)	(Iacopetti et al., 1999)
YB-1	rabbit polyclonal	1:500 (IB) 5 μg/ml = 1:100 (IP)	Abcam
YB-1	rabbit polyclonal	1:200 (IB)	Cell Signalling
ZO-1 ZO-1	mouse mAb clone ZO1-1A12 rabbit polyclonal	1:500 (IF) 1:2000 – 1:5000 (IB) 1:2000 (IB)	Zymed Zymed
α-mannopyranosyl α-glucopyranosyl	Concanavalin A Lectin Alexa 649 conjugate	50 μg/ml	Molecular Probes

Secondary antibodies

Description	Conjugate	Dilution	Supplier
Goat α guinea pig IgG	HRP	1:5000 – 1:20,000 (IB)	Jackson ImmunoResearch
Goat α guinea pig IgG	Alexa 488	1:1000 – 1:1400 (IF)	Molecular Probes
Goat α guinea pig IgG	Alexa 594	1:1000 – 1:1400 (IF)	Molecular Probes
Goat α guinea pig IgG	Alexa 649	1:1000 – 1:1400 (IF)	Molecular Probes
Donkey α guinea pig IgG	Cy3	1:2000 (IF)	Jackson ImmunoResearch
Goat α mouse IgG	HRP	1:5000 – 1:20,000 (IB)	Jackson ImmunoResearch
Donkey α mouse IgG	Alexa 594	1:1000 – 1:1400 (IF)	Molecular Probes
α mouse IgM	Cy2	1:2000 (IF)	Jackson ImmunoResearch
Goat α mouse IgG	Cy2	1:2000 (IF)	Jackson ImmunoResearch
Goat α mouse IgG	Cy3	1:2000 (IF)	Jackson ImmunoResearch
Goat α mouse IgG	Cy5	1:2000 (IF)	Jackson ImmunoResearch
Goat α mouse IgG	Cy5.5	1:1000 (IF)	Biotrend Chemikalien
Donkey α rabbit IgG (min. cross-reaction)	HRP	1:5000 – 1:20,000 (IB)	Jackson ImmunoResearch
Goat α rabbit IgG	HRP	1:5000 – 1:20,000 (IB)	Jackson ImmunoResearch
Donkey α rabbit IgG	Alexa 594	1:1000 (IF)	Molecular Probes
Goat α rabbit IgG	Cy2	1:2000 (IF)	Jackson ImmunoResearch
Goat α rabbit IgG	Cy3	1:2000 (IF)	Jackson ImmunoResearch
Goat α rabbit IgG	Cy5	1:2000 (IF)	Jackson ImmunoResearch
Donkey α rat IgG	HRP	1:5000 (IB)	Jackson ImmunoResearch
Protein A	10 nm gold		J. Slot, Utrecht University, The Netherlands

EM: electron microscopy; IF: immunofluorescence; IP: immunoprecipitation; IB: immunoblot. All secondary antibodies used for immunofluorescence are minimal cross-reaction to other species.

4.1.14 Buffers, stock solutions and media

Buffers and solutions for bacterial cultures

LB-medium	10g/L Bacto-Trypton 5g/L Bacto-Yeast-Extract 10g/L NaCl pH 7.0
LB-agar	15g/L Bacto-Agar in LB-medium
Ampicilin (100x)	100 mg/ml in H_2O
Chloramphenicol (100x)	40 mg/ml in ethanol
Kanamycin (300x)	100 mg/ml in H_2O

Buffers and media for cell culture

10x PBS	13.7 M NaCl (80 g) 27 mM KCl (2 g) 14 mM KH_2PO_4 (2.4 g) 0.1 M Na_2HPO_4 (14.4 g) H_2O to 1l adjust pH to 7.4 with HCl
Complete medium I (COS7, HeLa, primary neuroepithelial culture)	Dulbecco's Modified Eagle Medium 4.5 g/l glucose 2 mM L-glutamine, 1 mM sodium pyruvate 100 U/ml penicillin (1x) 100 µg/ml streptomycin (1x) 10% FCS
Complete medium II (NIH3T3 and Neuro-2A)	Dulbecco's Modified Eagle Medium 1 g/l glucose 2 mM L-glutamine, 1 mM sodium pyruvate 100 U/ml penicillin (1x) 100 µg/ml streptomycin (1x) 10% FCS
Neurosphere culture medium	Dulbecco's Modified Eagle Medium:Nutrient Mix F-12 (1:1) 2 mM dipeptid L-alanyl-L-glutamine (GlutaMAX I) 1x B27 (1:50)

	10 ng/ml hrEGF do not sterile filter after addition of B27
Trypsin-versene	0.25% trypsin w/o EDTA diluted in 1x versene salt solution
Papain-mix	30 U/ml papain 0.24 mg/ml cysteine 40 µg/ml DNase I type IV in Leibovitz L-15 Medium sterile filter
Trypsin inhibitor-mix	45 mg Ovomucoid trypsine inhibitor 21 mg BSA 390 µl DNase I type IV (40 mg/ml stock) 39 ml Leibovitz L-15 Medium sterile filter, can be stored for 1 week
Freezing medium	10% DMSO in FCS

Buffers and media for whole embryo culture

PB1 (dissection medium)	Dulbecco's PBS 100 U/ml penicillin (1x) 100 µg/ml streptomycin (1x) 10% FCS
WEC (culture medium)	10 ml rat serum 2 mg/ml glucose 1 mM sodium pyruvate (1x) 100 U/ml penicillin (1x) 100 µg/ml streptomycin (1x) sterile filter

Buffers and solutions for immunostaining

Tissue cryo-solution	250 ml glycerol 250 ml ethylene glycol 500 ml 0.2 M phosphate buffer, pH 7.4
Blocking buffer I (cryosections)	10% FCS in PBS
Blocking buffer II (cells)	5% FCS 1% BSA in PBS

Blocking buffer III	10% donkey serum 0.15% Triton X-100 in PBS
Incubation buffer III	3% donkey serum 0.15% Triton X-100 in PBS
DAPI (2000x)	1 mg/ml in H_2O
Moviol mounting medium	6 g Moviol 4-88 (Calbiochem) 15 g of glycerol (microscopy grade) stir to mix add 15 ml of H_2O, incubate overnight add 30 ml of 0.2 M Tris-Cl pH8.5 heat to 50ºC for 10 min clarify by centrifugation at 5000 x*g* for 15 min

Buffers and solutions for electron microscopy

Fixation buffer	4% paraformaldehyde 0.1% glutaraldehyde in 100 mM phosphate buffer, pH 7.4
Infiltration buffer	2.3 M sucrose in phosphate buffer, pH 7.4
Cryosection buffer	1.3 M sucrose 1% methylcellulose in phosphate buffer, pH 7.4
Contrasting solution	1% glutaraldehyde 0.3% uranylacetate 1.8% methylcellulose

Buffers and solutions for β-galactosidase staining

β-galactosidase staining buffer	Mix before use: 10 mM $K_3Fe(CN)_6$ (from 100 mM stock) 10 mM $K_4Fe(CN)_6x3H_2O$ (from 100 mM stock) 2 mM Mg 0.5% Triton X-100 in H_2O
X-gal stock	40 mg/ml 5-bromo-4-chloro-3-indolyl-beta-D-galactopyranoside

	in DMSO (keep at –20ºC)

Buffers and solutions for DNA agarose gel electrophoresis

10x TBE	0.89 M Tris 0.89 M boric acid 20 mM EDTA pH 8.0
50x TAE	2 M Tris 1 M acetic acid 100 mM EDTA pH 8.5
ethidium bromide (20,000x)	5 mg/ml in H_2O

Buffers and solutions for RNA agarose gel electrophoresis

10x MOPS	200 mM MOPS 50 mM sodium acetate 10 mM EDTA pH 7.0
1.2% RNA agarose gel	1.2 g agarose 72 ml H_2O boil until agarose dissolves, cool to 60ºC 10 ml 10x MOPS 18 ml formaldehyde (37%) 5 µl ethidium bromide (5 mg/ml stock)
5x sample buffer	4 ml 10x MOPS 3084 µl formamide 720 µl formaldehyde (37%) 2 ml glycerol 80 µl EDTA (0.5 M) bromophenol blue

Buffers and solutions for protein SDS-polyacrylamide gel electrophoresis

10x SDS-PAGE running buffer	250 mM Tris-HCl 1.9 M glicine 1% SDS pH 8.8	30.25 g/l 143.25 g/l 20 g/l
4x resolving gel buffer	1.5 M Tris-HCl 0.4% SDS pH 8.8	18.17 g/100 ml 0.4 g/100 ml

4x stacking gel buffer	0.5 M Tris-HCl 0.4% SDS pH 6.8	6.05 g/100 ml 0.4 g/100 ml
6x Laemmli sample buffer	0.35 M Tris-HCl 10% SDS 30% glycerol 9.3% DTT bromophenol blue pH 6.8	7 ml 0.5 M Tris-HCl/10 ml 1 g/10 ml 3 ml/10 ml 0.93 g/ml 1.2 mg
AMBA	30% acrilamide 0.8% bisacrilamide	
Coomassie super-stain	10% acetic acid 50% methanol 0.1% Coomassie blue	100 ml/l 500 ml/l 1 g/l
Destain	10% acetic acid 25% isopropanol	100 ml/l 25 ml/l

Buffers and solutions for immunoblotting

Anode buffer I	0.3 M Tris 20% methanol pH 10.4	36.3 g/l 200 ml/l
Anode buffer II	25 mM Tris 20% methanol pH 10.4	3 g/l 200 ml/l
Cathode buffer	25 mM Tris 40 mM 6-amino-n-caproic acid 20% methanol pH 9.4	3 g/l 5.24 g/l 200 ml/l
Blocking solution	5% skimmed milk 0.2% Tween-20 in PBS	
Washing solution	0.2% Tween-20 in PBS	

Buffers and solutions for protein isolation and immunoprecipitation

Homogenisation buffer I (TKM)	50 mM triethanolamine-HCl pH 7.8 0.25 M sucrose 50 mM KCl 5 mM $MgCl_2$

	1 mM DTT (add before use from 100 mM stock)
Homogenisation buffer II (NIM)	20 mM Tris-HCl pH 7.5 0.25 M sucrose 50 mM KCl 5 mM $MgCl_2$ 1 mM DTT (add before use from 100 mM stock)
Homogenisation buffer III (polysomal analysis)	20 mM Tris-HCl pH 7.5 100 mM KCl 5 mM $MgCl_2$
Polysomal sucrose buffer I	20 mM Tris-HCl pH 7.5 15% sucrose 100 mM KCl 5 mM $MgCl_2$
Polysomal sucrose buffer II	20 mM Tris-HCl pH 7.5 50% sucrose 100 mM KCl 5 mM $MgCl_2$
Sucrose density barrier	20 mM Tris-HCl pH 7.5 2.3 M sucrose 50 mM KCl 5 mM $MgCl_2$
RIPA lysis buffer	50 mM Tris-HCl pH 8.0 150 mM NaCl 1.0% NP-40 0.5% deoxycholic acid (DOC) 0.1% SDS
NP-40 lysis buffer	50 mM Tris-HCl pH 7.8 1.0% NP-40 150 mM KCl 5 mM $MgCl_2$
NP-40 hypotonic lysis buffer	50 mM Tris-HCl pH 7.8 1.0% NP-40 10 mM KCl 5 mM $MgCl_2$
Wash buffer A	10 mM Tris-HCl pH 7.5 0.2 % NP-40 150 mM KCl 5 mM $MgCl_2$
Wash buffer C	10 mM Tris-HCl pH 7.5

5 mM $MgCl_2$

Buffers and solutions for GST-fusion protein purification

Elution buffer	50 mM HEPES pH 8.0 300 mM NaCl 10 mM glutathione

Buffers and solutions for endonuclease-prepared small interfering RNAs preparation

Digestion buffer	20 mM Tris-HCl pH 7.9 5% glycerol 140 mM NaCl 2.7 mM KCl 5 mM $MgCl_2$ 0.5 mM EDTA 1 mM DTT (add before use from 100 mM stock)
Equilibration buffer	20 mM Tris-HCl pH 8.0 300 mM NaCl 1 mM EDTA
Wash buffer	20 mM Tris-HCl pH 8.0 400 mM NaCl 1 mM EDTA
Elution buffer	20 mM Tris-HCl pH 8.0 520 mM NaCl 1 mM EDTA

4.2 Methods

4.2.1 Preparation and purification of plasmid DNA

DNA was prepared and purified in a small (mini-prep) or large (maxi-prep) scale using kits from Qiagen, following the manufacturer's instructions. For embryo injection or cell transfection, the EndoFree plasmid maxi kit was used, followed by additional step of purification by ethanol precipitation in a presence of 2.5 M ammonium acetate.

4.2.2 Plasmid construction

MSY3 cDNAs

Two EST clones IMAG p988F169447Q3 and IRAK p961D1855Q2, containing part of the long and short splice variants of mouse MSY3, were combined to generate by restriction

digestion the full-length cDNA of both variants. To obtain the long splice variant, the *Eco*RI-*Eco*NI fragment of the IRAK p961D1855Q2 clone was ligated into the *Eco*RI-*Eco*NI digested IMAG p988F169447Q3. The short splice variant was obtained by subcloning the *PpuM*I-*Nhe*I fragment from IMAGE p988F169447Q3 into the *PpuM*I-*Nhe*I digested IRAK p961D1855Q2. The resulting cDNA clones were completely sequenced and named pCMV-SPORT6-MSY3-L and pCMV-SPORT6-MSY3-S.

MSY3 expression vectors

The eukaryotic expression plasmids pCAGGS2-MSY3-L and pCAGGS2-MSY3-S containing the entire CDS of the long and short YB3 splice variant, respectively, were obtained by subcloning of the *Xho*I/*Xba*I cDNA fragments released from either pCMV-SPORT6-MSY3-L or pCMV-SPORT6-MSY3-S plasmids into the modified pCAGGS2 expression vector opened with *Xho*I and *Nhe*I. In pCAGGS2-MSY3-L-UTR and pCAGGS2-MSY3-S-UTR vectors, the 3'UTR of MSY3 was excised by *NotI* and *BstEII* restriction enzymes, cohesive ends were blunted with Klenow exo– fragment and ligated.

GST-MSY3 fusion proteins vectors

The bacterial expression plasmids pGEX-MSY3-N and pGEX-MSY3-C containing cDNA fragments of MSY3, corresponding to amino acids 2S-74A and 261I-361E, fused in-frame to the glutathione S-transferase (GST) were constructed by PCR amplification using Herculase DNA polymarase (Roche) from the IRAK p961D1855Q2 and IMAG p988F169447Q3 clones using P9/P10 and P11/P12 oligonucleotides, respectively. The thermal cycle profile employed 2 min denaturation step at 95ºC followed by 30 amplification cycles (1 min of denaturation at 95ºC, 30 s of annealing at 60ºC and x s of extension at 68 ºC). The resulting PCR products were digested with *BamH*I-*Xho*I restriction enzymes, whose sites were introduced in the oligonucleotides, and cloned into the corresponding sites of the pGEX-7M vector.

Small interfering RNA vectors

Hairpin constructs containing small interfering RNAs directed against the MSY3 mRNA at positions 647, 1077 and 1363 (the MSY3 5'UTR extends 194 bp before the ATG codon and was here included for numbering) were obtained by insertion of annealed oligonucleotide pairs P15/P16, P17/P18 and P19/P20, respectively, into the *Xho*I-*Eco*RI digested pSM2 vector. The hairpin expression cassette, consisting of the U6 promoter, mir30 sequences with a hairpin and the U6 terminator, was then inserted upstream of the CMV promoter in the pAAV-hrGFP vector. First, a *BamH*I restriction site was introduced into the pAAV-hrGFP vector opened with *Not*I and *Mlu*I by insertion of annealed oligonucleotides P13/P14, generating the pAAV-hrGFP-B vector. Subsequently, the *BamH*I-*Mlu*I restriction fragments from the pSM2-hp1077, pSM2-hp1363, and control pSM2-luc plasmids were ligated into the corresponding sites of the pAAV-hrGFP-B vector.

All constructs were confirmed by sequencing.

4.2.3 GST-fusion proteins production

BL21 bacteria carrying the pGEX-MSY3-N plasmid, encoding for glutathione S-transferase (GST) fused in frame to the N-terminal domain of MSY3 protein, were grown in 800 ml LB until OD_{600}=0.5. Fusion protein expression was induced with 0.2 mM isopropyl-1-thio-β-D-galactopyranoside (IPTG) for 2 h and bacteria collected by

centrifugation for 10 min at 6,000 x *g*. The pellet was resuspended in a total volume of 40 ml of PBS and frozen in liquid nitrogen. The cell suspension was thawed, the protease inhibitor cocktail added (Sigma; 1:500), and treated with 0.1 mg/ml of lysosyme for 30 min on ice, then bacteria were disrupted by sonication at 4ºC. The lysate was cleared by centrifugation at 112,000 x *g* for 1 h. GST-fusion proteins were precipitated with 500 µl of glutathione sepharose (Amersham), beads were washed 3 times in 10 ml of PBS, and loaded on a MicroSpin column (Biorad), GST-fusion proteins were eluted with 500 µl aliquots of the elution buffer containing 10 mM glutathione. Total of 4.4 mg of protein in 2 ml of the eluate was recovered.

Fusion of the C-terminal portion of the MSY3 protein to the GST protein, encoded in the pGEX-MSY3-C plasmid, was recovered in the pellet upon ultracentrifugation, due to precipitation in the inclusion bodies. Therefore this construct was not further used.

4.2.4 Generation of antibodies

Three rabbit polyclonal antisera, named 0181, 0182 and 0183, were raised against the peptide CGGTTLPQAAADAPA (with C added for the conjugation) corresponding to the amino acid residues 10 to 23 of the MSY3 protein; the 0182 antiserum was further affinity purified. Independently, the affinity purified rabbit antiserum against the identical peptide, and named AP4912, was obtained from Karl Matter (UCL, United Kingdom). Antisera GP1, GP2 and GP3 directed against the N-terminal domain of MSY3 (amino acids S2–A74) fused to the GST protein were raised in guinea pigs.

4.2.5 Whole embryo culture and electroporation

Preparation of embryos for the whole embryo culture was carried out at room temperature in pre-warmed PB1. Time-pregnant females were killed via cervical translocation, the uterus was removed and placed in PB1. E9.5 or E10.5 embryos were dissected under a dissection microscope free of decidua and Reichert's membrane, and yolk sac and amnion were opened exposing the embryo to the culture medium. Embryos were placed in 1.5-2 ml of WEC medium per embryo and cultured at 30 rpm in a continuous-flow atmosphere of 5% CO_2, in N_2, with O_2 in a proportion listed below.

time of culture	0 h	8 h	20 h	25 h	32 h	44 h
O_2	20%	20%	60%	60%	95% (or 60%)	95%
flow (ml/min)	50	75	50	75	50 (or 100 for 60%)	50

Before injection of nucleic acid and electroporation, embryos were allowed to recover in culture for 1-2 h. Embryos were immobilised in an agarose mold immersed in PB1 or Dulbecco's PBS and telencephalic vesicles were filled with PBS containing 0.01% fast green, 0.3 µg/µl plasmid DNA encoding for marker fluorescent protein, and 1.8 µg/µl of pCAGGS-MSY3-L or 1 µg/µl esiRNAs using a glass capillary controlled by a standard micromanipulator and connected to a pneumatic PicoPump. Immediately after injection, 5 square electric pulses of 25 V, 50 ms each, at 1 s intervals were delivered through tweezers-like electrodes placed at 1 cm distance. After electroporation, embryos were returned into culture and allowed to develop for 36 (E10.5) or 48 h (E9.5). At the end of this period, extraembryonic membranes and placenta were removed and embryos which expressed a

fluorescent marker were washed briefly with PBS and processed for immunohistochemistry as described below.

4.2.6 *In utero electroporation*

E12.5 pregnant mice were anaesthetised with isofluorane and injected sub-cutaneously with 0.03 mg/ml aqueous solution of buprenorfin (25 µl per 10 g body weight). Pregnant mouse was placed on a warmed stage and anasthaesia was sustained by constant delivery of isofluorane atmosphere through a nose cone. In order to access the embryos, the pregnant female was shaved and a 1.5-2 cm ventral midline incision was made through the skin and peritoneal muscle, through which the uterine horns were gently pulled out. The uterus was kept wet with pre-warmed Dulbecco's PBS during the operation time. The telencephalic vesicles of embryos were visualised by transillumination and approximately 2 µl of PBS containing 0.02% Fast Green, 0.3 µg/µl of pCAGGS-mRFP plasmid DNA, and 1.8 µg/µl of pCAGGS-MSY3-L or 1.4 µg/µl of pCAGGS-MSY3-L-UTR plasmid DNA was injected into the lateral ventricle through the uterus using a glass capillary connected to a pneumatic PicoPump. Immediately after injection, six square electric pulses of 30 V, 50 ms each at 1 s intervals were delivered using 1 mm diameter tweezers electrodes. After electroporation, the uterus was placed back in the abdomen, the mouse was sutured and allowed to recover on a warm platform. After 2 days, the animals were sacrificed and embryos which expressed a fluorescent marker were processed for immunohistochemistry as described below.

4.2.7 *Preparation of embryos for cryosectioning*

Time pregnant females were sacrificed via cervical translocation, and the uterus was removed. Embryos were dissected in chilled PBS free of diciduae and extraembryonic membranes, except for E8 embryos, which were only removed from the uterus. For E12.5 embryos, heads were cut off at the level of the otic pit/mandibular arch to allow better penetrance of solutions to the brain ventricles. For later stages of development, the brains were excised, leaving meaninges. Whole embryos, heads and brains were fixed over night at 4ºC in 2-4% paraformaldehyde in a phosphate buffer, pH 7.4, by immersion, with constant agitation. For β-galactosidase staining, embryos were fixed for 2 h in 0.2% glutaraldehyde and 2% paraformaldehyde. For electron microscopy, embryos were fixed in 0.1% GA and 4% PFA in a phosphate buffer, pH7.4. Except for electron microscopy, the tissue was then infiltrated with 30% sucrose in PBS for 24-48 h and frozen in Tissue-Tek O.C.T compound (Sakura Finetek). Embryos were cut on a cryostat (Microtome) to 14-20 µm sections.

4.2.8 *Preparation of postnatal brains for cryosectioning*

For brain collection, the pups until the third postnatal week (P3W) were sacrificed by cutting off the heads, brains removed and fixed for 24 h in 4% paraformaldehyde. Adult mice were anaesthetised with an intraperitoneal injection of a mixture of Ketamine and Xylazine and then intracardially perfused with 0.9% NaCl, followed by freshly prepared cold 4% paraformaldehyde in a phospate buffer, pH 7.4. The brains were removed and post-fixed overnight in 4% paraformaldehyde. All brains were infiltrated with 30% sucrose in PBS for 24 h. Sections were cut frozen using a sliding microtome to 40 µm thick sections, which were stored in the tissue cryo-solution at –20ºC.

4.2.9 Cell culture and transfection

Neuroepithelial cluster culture

Neuroepithelial clusters and dissociated cells were cultured in the Complete medium I (Dulbecco's Modified Eagle Medium with 4.5 g/l glucose, supplemented with 10% FCS, 100 U/ml penicillin and 100 μg/ml streptomycin) in a humidified incubator at 37°C under a 5% CO_2 atmosphere in 24-well plates.

Pregnant NMRI mice were sacrificed on gestational day 10 or 11 and embryos were harvested. The forebrains of embryos were dissected free of meaninges in ice-cold Leibovitz L-15 medium, washed with 10 ml of L-15 medium and trypsinised in 1 ml trypsin-EDTA 0.25% at 37ºC for 3-5 min with gentle agitation. To block the trypsin, 1 ml of complete medium containing 10% FCS was added. Cells were mechanically dissociated with fire-polished Pasteur pipette to yield suspensions of single cells or small clusters of 10-30 cells, as microscopically monitored. After trituration, cells were washed with 8 ml of the complete medium and collected by centrifugation for 3 min at 1000 rpm. Clusters and cells were diluted with the culture medium and plated at density 10^4-10^5 clusters or cells per well of 24-well plates on coverslips coated with 0.01% poly-L-lysine (Sigma) and 10 μg/ml laminin. Clusters and dissociated cells were processed for immunostaining after 24 and 8 h, respectively.

Neural stem cell (neurospheres) culture

Neural stem cells were grown as free-floating aggregates (neurospheres) in a humidified incubator at 37°C under 6% CO_2 atmosphere in Dulbecco's Modified Eagle Medium/Nutrient Mix F-12 (1:1), containing 1:50 B27 supplement and 10 ng/ml human recombinant EGF. Each second day of culture, $^1/_4$ - $^1/_3$ volume of fresh medium was added. Neurospheres were dissociated every 3-5 days, with sub-culture ratio of 1:3-1:5.

Preparation of neural stem cells was performed at room temperature under sterile conditions. P1-P9 animals were sacrificed by cutting off the heads, brains were removed and placed in the Leibovitz L-15 medium. Hemispheres were dissected free of meaninges, choroids plexus and olfactory bulb; placed in 300 μl of papain-mix : trypsin inhibitor-mix (1:1), minced with tweezers and incubated at 37ºC for 30-45 min. The cells were dissociated with a fire-polished Pasteur pipette in a presence of an additional 1 volume of the trypsin inhibitor. The cell suspension was then transferred to 9 ml of DMEM/F12 medium and spun for 5 min at 80 *x* g. After decanting the supernatant, cells were resuspended gently in 1 ml of culture medium and transferred to 3 ml of medium in a 25 ml flask.

For propagation, neurospheres were collected by centrifugation for 5 min at 80 *x* g, and incubated in 500 μl of trypsin-versene 0.25% for 6 min at 37ºC. To block the trypsin, 1 volume of trypsin inhibitor was added and cells were dissociated by trituration for 5 min through 1 ml pipette tip. Cells were washed with 8 ml of DMEM/F-12, spun for 5 min at 80 *x* g, resuspended in 1 ml of culture medium, and transferred to flasks at a 1:3-1:5 ratio.

Cos7 and HeLa cell lines

Cos7 cells were maintained in a humidified incubator at 37°C under a 5% CO_2 atmosphere in the Complete medium I.

Neuro-2A and NIH-3T3 cell lines

Neuro-2A cells were maintained in a humidified incubator at 37°C under a 5% CO_2 atmosphere in the Complete medium II.

Transfections

Transient transfections were achieved by electroporation or lipofection.

For electroporation, cells were trypsinised and $5x10^5$ cells were resuspended in 200 µl of complete medium with 15 mM HEPES pH 7.5. 50 µl of transfection mixture containing 210 mM NaCl, 30 µg of salmon sperm DNA and 5 µg of pCAGGS2, pCAGGS2-MSY3-L or pCAGGS2-MSY3-S plasmids was added to the cell suspension. Cells were electroporated at 950 µFD, 240 V using BioRad Gene Pulser II. After electroporation, cells were washed with complete medium containing 15 mM HEPES pH 7.5 and plated on 100-mm Petri-dishes. Cells were analysed by immunoblotting 36 h after transfection.

For lipofection, Lipofectamine 2000 reagent (Invitrogen) was used, according to the manufacturer's instructions. Briefly, 10^6 cells were plated on a 60-mm Petri dish the day before transfection in the complete medium without antibiotics. Before the transfection, medium was replaced by 2 ml serum-free OPTI-MEM I (Invitrogen). For each transfection, 5 µg of plasmid DNA and 2-3 µg of esiRNA was used, combined with 10-20 µl of lipofectamine.

4.2.10 Protein extract preparation

Tissue protein extracts

Tissue protein extracts were prepared from mouse embryos or adult brain. All steps were performed at 4°C. For the time-course analysis of YB3 expression, telencephali and hindbrains were dissected from embryonic brains in ice-cold PBS. Tissues were homogenized in RIPA buffer containing the protease inhibitor cocktail (Sigma; 1:500), lysed for 30 min, centrifuged at 10,000 x *g* for 10 min, and the supernatant collected.

Alternatively, whole embryos (E9.5), heads (E10.5-12.5) or brains (E14.5) were solubilised in 5 volumes of 1.2x Laemmli sample buffer containing the protease inhibitor cocktail (Sigma; 1:500) without DTT and bromophenol blue, which were added after protein quantification. Tissue was triturated with plastic pestle or 1 ml pipet tip, and the sample boiled for 15 min.

Protein concentration was determined using BCA Protein Assay Kit (Pierce Chemical Company) following the manufacturer's instructions, and 40 µg of each sample was analysed by SDS-PAGE and immunoblotting.

Cell protein extracts

HeLa cells grown on 100-mm Petri dishes were washed with ice-cold PBS, scraped from the dish in ice-cold PBS and centrifuged at 900 x *g* for 5 min. The cell pellets were lysed in 200 µl of RIPA buffer containing protease inhibitor cocktail (Sigma; 1:500) for 30 min at 4°C and detergent extracts obtained after centrifugation (10,000 x *g* for 10 min) were subjected to SDS-PAGE and immunoblotting.

Neuro-2A cells grown on 60-mm Petri dishes were washed twice with ice-cold PBS and solubilised directly in 500 µl of 1.2x Laemmli sample buffer containing protease inhibitor cocktail (Sigma; 1:1000), scraped and boiled for 15 min. 20-40 µl was analysed by SDS-PAGE and immunoblotting.

4.2.11 Differential centrifugation

The subcellular fractionation was performed at 4°C. Around 30 E10 – E11 mouse embryos (two to three litters) were dissected in ice-cold PBS and homogenised in a glass-Teflon Potter homogeniser (10 strokes at 1200 rpm) in the Homogenisation buffer I or II with addition of 40 U/ml ribonuclease inhibitor (Promega) and the protease inhibitor cocktail (Sigma; 1:200). The homogenate was centrifuged at 900 x *g* for 10 min resulting in the crude nuclei pellet and the supernatant, which was further centrifuged at 15,000 x *g* for 10 min to obtain the mitochondria-enriched fraction (P15) and the post-mitochondria supernatant (PMS). The PMS was divided in aliquots, and incubated at 37°C for 45 min without any additions or with 1 mg/ml RNase A (Qiagen), 25 mM EDTA, or 1 mg/ml RNase A and 25 mM EDTA; or alternatively at 4°C for 45 min in absence or presence of 0.5 M NaCl, 2% Triton X-100, or 25 mM EDTA. The reaction mixtures were than centrifuged at 100,000 x *g* for 2 h resulting in the P100 pellet and the S100 supernatant. Supernatants were subjected to methanol/chloroform precipitation and resuspended in SDS Laemmli sample buffer. The crude nuclei pellet was resuspended in the homogenisation buffer II, filtered by centrifugation through 35 μm mesh in a cell strainer cup tube (Falcon, BD Biosciences) at 1000 x *g*. The resulting pellet was resuspended in the Homogenisation buffer II containing 1.8 M sucrose, overlaid on a 2.3 M sucrose cushion in the same buffer, and centrifuged at 100,000 x *g* for 1 h. The supernatant and interphase were discarded and the nuclear pellet was resuspended in the homogenisation buffer. Equal proportions of each fraction were analysed by SDS-PAGE and immunoblotting.

4.2.12 Polyribosomal analysis

All steps were performed at 4°C. Around 40 E10.5 embryos were homogenised as described above in the Homogenisation buffer III with addition of 100 U/ml ribonuclease inhibitor (Invitrogen or Promega) and the protease inhibitor cocktail (Sigma; 1:300). The homogenate was centrifuged at 800 x g for 10 min and the supernatant was centrifuged further at 15,000 x g for 10 min. NP-40 was added to the supernatant to a final concentration of 1% to release ribosomes/polyribosomes from membranes. The supernatant was incubated for 2 h on ice without any additions, or with 25 mM EDTA or 1 mg/ml RNase A. The samples were overlaid on 11 ml of a 15-50% linear sucrose gradient prepared in the homogenisation buffer, and centrifuged at 100,000 x g for 2 h. 1 ml fractions were collected manually from the top of the gradient and the pellet was resuspended in 1 ml of the homogenisation buffer. 500 μl of each fraction was subjected to the methanol/chloroform precipitation in a presence of the haemoglobin carrier. 15% of each fraction was then analysed by SDS-PAGE and immunoblotting analysis. RNA was isolated from 100 μl of each fraction.

4.2.13 Immunoprecipitation

Immunoprecipitation was performed from an embryo tissue homogenate or Neuro-2A cells. All steps were carried out at 4ºC.

Around 40 E9.5 – E10 embryos were homogenised in the NP-40 lysis buffer containing 100 U/ml ribonuclease inhibitor (Invitrogen or Promega) and protease inhibitor cocktail (Sigma; 1:300). Alternatively 6-7 100-mm dishes of Neuro-2A cells at 60% confluency were washed twice with PBS and cells were scraped in 200 μl/dish of the NP-40 hypotonic lysis

buffer containing 100 U/ml ribonuclease inhibitor (Invitrogen or Promega) and the protease inhibitor cocktail (Sigma; 1:300). Salt was adjusted to 150 mM KCl and the cell suspension was passed 3 times through a 22 G needle. The homogenate, both from embryos and cells, was then incubated on ice for 30 min and cleared by centrifugation at 15,000 x g for 10 min. 5 µl of guinea pig GP2 anti MSY3 antiserum or control guinea pig serum, or 2.5 µg anti YB1 antibody (Abcam) or control rabbit IgG were added to 500 µl of homogenate and incubated with end-over-end agitation for 4 h. The immune complexes were incubated with 35 µl of Protein G Sepharose 4 Fast Flow (Amersham Biosciences) for 2 h with end-over-end agitation. The beads were collected by centrifugation at 3000 rpm and washed 3 times with NP-40 buffer, 3 times with washing buffer A and 2 times with washing buffer C. At last washing step, samples were divided in two and processed for protein extraction or RNA isolation. Proteins were extracted from beads by boiling for 5 min in Laemmli sample buffer. 1/4 of the sample was then analysed by immunoblotting.

4.2.14 Metabolic labelling

Neuro-2A cells were transfected on 60-mm Petri dishes with pCAGGS-GFP, pCAGGS-MSY3-L-UTR or esiRNAs directed against YB3 48 h before. 45 min prior labelling, complete medium was replaced by Dulbecco's Modified Eagle Medium without methionine and cysteine (Invitrogen) supplemented with 2 mM glutamine, 100 U/ml penicillin and 100 µg/ml streptomycin. Labelling was performed in 2 ml of the same medium containing 86 µCi/ml [^{35}S] methionine/cysteine (Perkin Elmer). After 10, 20, or 30 min cells were washed with ice-cold PBS and labelling was stopped by addition of 500 µl of 1.2x Laemmli sample buffer containing the protease inhibitor cocktail (Sigma; 1:1000). 20 µl of each sample was resolved by 12% SDS-PAGE followed by radiography.

4.2.15 Immunoblotting

Proteins were analysed by SDS-PAGE (typically 9% for MSY3) or for time-course analysis of MSY3 expression by gradient 4-12% NuPage gels (Invitrogen), and transferred to PVDF membranes using a semi-dry blotting system. After transfer, membranes were incubated over night at 4ºC in the blocking buffer. Proteins of interest were then detected by incubation with appropriate primary antibodies for 1.5 h at room temperature followed by horseradish peroxidase-conjugated secondary antibodies. All antibodies were diluted in the blocking buffer. Washing steps were performed for 1 h with several changes of the washing buffer. Immune complexes were visualised with extended duration chemiluminescence developing reagents (Pierce Chemical Company) on ECL films (Amersham Biosciences).

4.2.16 RNA isolation

After sucrose gradient analysis, RNA was isolated from 100 µl of each fraction. After immunoprecipitation, beads with immunocomplexes, 25 µl of total homogenate, homogenate with immune complexes (pre-IP) and unbound fractions were adjusted to 100 µl with wash buffer C. All samples were mixed with 3 volumes of Trizol LS (Invitrogen), frozen in liquid nitrogen and stored at -20°C until further processed.

To isolate RNA from cells, NIH3T3 cells were grown on 100-mm Petri dishes to 50-70% confluency. Cells were washed twice with ice-cold PBS, scraped in 1500 µl of PBS

and collected by centrifugation for 3 min at 2000 x *g*. Cells were resuspended in 200 µl of PBS, mixed with 3 volumes of Trizol LS and frozen in liquid nitrogen.

The RNA isolation was performed according to the manufacturer's instructions in presence of the glycogen carrier (1-2 µg/sample), and analysed by electrophoresis in 1.2% denaturing agarose gel.

4.2.17 Endonuclase preparation of small interfering RNAs (esiRNAs)

Fragments of MSY3, luciferase, and EGFP cDNAs were amplified by PCR using oligonucleotides P21/P22, P23/P24 (MSY3), P25/P26 (luciferase) and P27/P28 (EGFP). Transcription was performed from 16 µl of PCR product with MEGAScript T7 Kit (Ambion) following manufacturer's instructions, and RNA was annealed in thermal cycler as follows: 90ºC for 3 min, ramp to 70ºC with 0.1ºC/sec, 70ºC for 3 min, ramp to 50ºC with 0.1ºC/sec, 50ºC for 3 min, ramp to 25ºC with 0.1ºC/sec. dsRNA was partially digested to esiRNAs with length of about 18 to 25 bp with RNase III in the 200 µl of the digestion buffer at 37ºC for 2-4 h. esiRNAs were purified in two aliquots on 200 µl of Q-Sepharose (Amersham) equilibrated with Equilibration buffer, washed with 500 µl of the Wash buffer and eluted twice with 300 µl of the Elution buffer. esiRNAs were precipitated with isopropanol, washed with 70% ethanol and resuspended in PBS.

4.2.18 Immunohistochemistry and light microscopy

Immunofluorescence of fixed cells

Cells grown on coverslips were fixed for 15 min in 4% paraformaldehyde, washed with PBS, permeabilised with 0.3% Triton X-100 in PBS for 15 min or acetone for 3 min at –20ºC, quenched with 50 mM NH_4Cl in PBS, and incubated for 1 h in Blocking buffer I. Cells were incubated sequentially with primary and secondary antibodies for 3 and 1 h at room temperature, respectively. All antibodies were diluted in blocking buffer, and washing steps were performed in PBS. Coverslips were rinsed with water and mounted onto glass slides using Moviol solution.

Immunofluorescence of neurospheres

Neurospheres were fixed and stained in suspension, being collected by centrifugation for 5 min at 100 x *g* after each step. Neurospheres were fixed with 4% paraformaldehyde for 20 min, washed 3 times with PBS, permeabilised for 30 min with 0.3% Triton X-100 or 0.2% saponin, and free aldehyde groups were quenched for 30 min with 50 mM NH_4Cl in 1 ml of PBS. Neurospheres were then incubated with the Blocking buffer I for 1 h at room temperature. Incubation with primary and secondary antibodies was performed in 100 µl of blocking buffer, overnight at 4ºC and for 1.5 h at room temperature, respectively. DNA was labelled with DAPI (5 µg/ml). Neurospheres were washed with PBS and water, and mounted onto glass slides using Moviol solution.

Immunofluorescence of cryosections

Cryosections were rehydrated in PBS, permeabilised with 0.3% Triton X-100 in PBS for 15 min, quenched with 50 mM NH_4Cl in PBS, and incubated for 1 h in the Blocking buffer II. Optionally for this step, 0.3% Triton X-100 was added. Incubation with primary antibodies diluted in the blocking solution was performed overnight at 4°C. Sections were

washed with excess of PBS with agitation and incubated with the appropriate fluorochrome-conjugated secondary antibodies diluted in blocking buffer for 1 h at 37°C. DNA was labelled with DAPI (5 μg/ml) present together with secondary antibodies. Sections were rinsed with water and mounted using Moviol solution.

Sections derived from postnatal brains were stained free-floating. Sections were washed twice with Tris-buffered saline, pH 7.4 (TBS), permeabilised and blocked directly in the Blocking buffer III, followed by overnight incubation at 4ºC with primary antibodies diluted in the Incubation buffer III. Sections were washed three times in TBS, incubated with secondary antibodies for 4 h at room temperature, followed by staining with DAPI for 5 min. Sections were wet-mounted on glass slides using DABCO (1,4-diazabicyclo[2.2.2]octan) mounting medium.

β-galactosidase staining

Cryosections from embryos fixed with 2% paraformaldehyde and 0.2% glutaraldehyde were washed 3x for 15 min with pre-warmed at 37ºC β-galactosidase buffer followed by incubation with 1 mg/ml X-gal diluted in β-galactosidase buffer at 37ºC in a dark chamber. The chromogenic reaction was monitored under a microscope and stoped by washing with PBS. Sections were then rinsed with water and mounted using Moviol solution.

Microscopy

Labelled sections and cells were observed using a Zeiss Axiovert 200 M confocal laser scanning microscope or Olympus BX61 epifluorescent microscope. Zeiss LSM 510 AIM software, Adobe Photoshop and Adobe Illustrator (Adobe Systems, San Jose, CA) were used for data analysis and image processing.

For analysis of the MSY3 expression in various mice lines, as well as after overexpression and downregulation experiments, single optical slices of 2-4 μm were acquired in the middle of a tissue section using the same settings. A minimum of 3 embryos at each age or at each experimental condition was analysed. For analysis of the MSY3 subcellular and cellular distribution, in particular for comparison with Tis21-EGFP expression, Z-stacks of 1 μm slices at 0.5 μm intervals spanning the tissue section were acquired. Analysed were slices at 3 to 7 μm depth with respect to the tissue section surface.

4.2.19 Electron microscopy

Embryos fixed in 4% paraformaldehyde and 0.1% glutaraldehyde were cut into pieces, which were infiltrated with 10% gelatine at 37ºC, and embedded in 10% gelatine, followed by infiltration with 2.3 M sucrose at 4ºC. Specimens were quickly frozen in liquid N_2 and sectioned to 80 nm cryosections, which were collected in the Cryosection buffer. The gelatine was removed by incubation on a drop of PBS at 37ºC, and sections were subjected to immunolabelling with primary antibody, followed by protein A coupled to 10 nm gold particles. Sections were then treated for 10 min with the Contrasting solution and viewed in a Morganini electron microscope.

5 PRESENTATIONS AT CONFERENCES

ELSO Annual Meeting, Nice, 3–7 September 2004

"Down-regulation of YB3 during mammalian neurogenesis"
Anna N. Grzyb, Anne-Marie Marzesco, Maria S. Balda, Karl Matter and Wieland B. Huttner

Cortical Development: Neural Stem Cells To Neural Circuits, Santorini, 12-15 May

"Expression and characterisation of the YB3 protein during mouse neurogenesis"
Anna N. Grzyb, Anne-Marie Marzesco, Karl Matter and Wieland B. Huttner

ELSO Annual Meeting, Dresden, 3-7 September 2005

"Expression of Y-box protein 3 correlates with proliferation of neural progenitor cells during mouse neurogenesis"
Anna N. Grzyb, Anne-Marie Marzesco, Maria Balda, Karl Matter and Wieland B. Huttner

6 BIBLIOGRAPHY

Aaku-Saraste, E., Hellwig, A. and Huttner, W. B. (1996). Loss of occludin and functional tight junctions, but not ZO-1, during neural tube closure--remodeling of the neuroepithelium prior to neurogenesis. *Dev. Biol.* **180**, 664-79.

Aaku-Saraste, E., Oback, B., Hellwig, A. and Huttner, W. B. (1997). Neuroepithelial cells downregulate their plasma membrane polarity prior to neural tube closure and neurogenesis. *Mech. Dev.* **69**, 71-81.

Abitbol, M., Menini, C., Delezoide, A. L., Rhyner, T., Vekemans, M. and Mallet, J. (1993). Nucleus basalis magnocellularis and hippocampus are the major sites of FMR-1 expression in the human fetal brain. *Nat. Genet.* **4**, 147-53.

Alexson, T. O., Hitoshi, S., Coles, B. L., Bernstein, A. and van der Kooy, D. (2006). Notch signaling is required to maintain all neural stem cell populations--irrespective of spatial or temporal niche. *Dev. Neurosci.* **28**, 34-48.

Allen, T. and Lobe, C. G. (1999). A comparison of Notch, Hes and Grg expression during murine embryonic and post-natal development. *Cell. Mol. Biol. (Noisy-le-grand)* **45**, 687-708.

Altman, J. and Bayer, S. A. (1990a). Migration and distribution of two populations of hippocampal granule cell precursors during the perinatal and postnatal periods. *J. Comp. Neurol.* **301**, 365-81.

Altman, J. and Bayer, S. A. (1990b). Mosaic organization of the hippocampal neuroepithelium and the multiple germinal sources of dentate granule cells. *J. Comp. Neurol.* **301**, 325-42.

Altman, J. and Bayer, S. A. (1990c). Prolonged sojourn of developing pyramidal cells in the intermediate zone of the hippocampus and their settling in the stratum pyramidale. *J. Comp. Neurol.* **301**, 343-64.

Alvarez-Buylla, A. and Lim, D. A. (2004). For the long run: maintaining germinal niches in the adult brain. *Neuron* **41**, 683-6.

Alvarez-Buylla, A., Seri, B. and Doetsch, F. (2002). Identification of neural stem cells in the adult vertebrate brain. *Brain Res. Bull.* **57**, 751-58.

Anthony, T. E., Klein, C., Fishell, G. and Heintz, N. (2004). Radial glia serve as neuronal progenitors in all regions of the central nervous system. *Neuron* **41**, 881-90.

Anthony, T. E., Mason, H. A., Gridley, T., Fishell, G. and Heintz, N. (2005). Brain lipid-binding protein is a direct target of Notch signaling in radial glial cells. *Genes Dev.* **19**, 1028-33.

Arakawa, Y., Kajino, K., Kano, S., Tobita, H., Hayashi, J., Yasen, M., Moriyama, M. and Hino, O. (2004). Transcription of dbpA, a Y box binding protein, is positively regulated by E2F1: implications in hepatocarcinogenesis. *Biochem. Biophys. Res. Commun.* **322**, 297-302.

Artavanis-Tsakonas, S., Matsuno, K. and Fortini, M. E. (1995). Notch signaling. *Science* **268**, 225-32.

Auerbach, S. and Pederson, T. (1975). Phosphorylation of messenger RNA-bound proteins in HeLa cells. *Biochem. Biophys. Res. Commun.* **63**, 149-56.

Avdulov, S., Li, S., Michalek, V., Burrichter, D., Peterson, M., Perlman, D. M., Manivel, J. C., Sonenberg, N., Yee, D., Bitterman, P. B. et al. (2004). Activation of translation complex eIF4F is essential for the genesis and maintenance of the malignant phenotype in human mammary epithelial cells. *Cancer Cell* **5**, 553-63.

Bader, A. G., Felts, K. A., Jiang, N., Chang, H. W. and Vogt, P. K. (2003). Y box-binding protein 1 induces resistance to oncogenic transformation by the phosphatidylinositol 3-kinase pathway. *Proc. Natl. Acad. Sci. U S A* **100**, 12384-89.

Bader, A. G. and Vogt, P. K. (2005). Inhibition of protein synthesis by Y box-binding protein 1 blocks oncogenic cell transformation. *Mol. Cell. Biol.* **25**, 2095-106.

Baek, J. H., Hatakeyama, J., Sakamoto, S., Ohtsuka, T. and Kageyama, R. (2006). Persistent and high levels of Hes1 expression regulate boundary formation in the developing central nervous system. *Development* **133**, 2467-76.

Bagni, C. and Greenough, W. T. (2005). From mRNP trafficking to spine dysmorphogenesis: the roots of fragile X syndrome. *Nat. Rev. Neurosci.* **6**, 376-87.

Balda, M., Garrett, M. and Matter, K. (2003). The ZO-1-associated Y-box factor ZONAB regulates epithelial cell proliferation and cell density. *J. Cell Biol.* **160**, 423-32.

Balda, M. and Matter, K. (2000). The tight junction protein ZO-1 and an interacting transcription factor regulate ErbB-2 expression. *EMBO J.* **19**, 2024-33.

Balda, M. S. and Anderson, J. M. (1993). Two classes of tight junctions are revealed by ZO-1 isoforms. *Am. J. Physiol.* **264**, C918-24.

Bargou, R., Jurchott, K., Wagener, C., Bergmann, S., Metzner, S., Bommert, K., Mapara, M., Winzer, K., Dietel, M., Dorken, B. et al. (1997). Nuclear localization and increased levels of transcription factor YB-1 in primary human breast cancers are associated with intrinsic MDR1 gene expression. *Nat. Med.* **3**, 447-50.

Basak, O. and Taylor, V. (2006). Hes5 mediated NOTCH1 activity marks neural stem cells and/or radial glia during embryonic development. In *Embryonic and Somatic Stem Cells - Regenerative Systems for Cell and Tissue Repair*, (ed. V. ter Meulen and A. M. Wobus). Dresden, Germany.

Bayer, S. A. and Altman, J. (1991). Neocortical development. New York: Raven Press.

Ben-Arie, N., Bellen, H. J., Armstrong, D. L., McCall, A. E., Gordadze, P. R., Guo, Q., Matzuk, M. M. and Zoghbi, H. Y. (1997). Math1 is essential for genesis of cerebellar granule neurons. *Nature* **390**, 169-72.

Bentivoglio, M. and Mazzarello, P. (1999). The history of radial glia. *Brain. Res. Bull.* **49**, 305-15.

Berry, M. and Rogers, A. W. (1965). The migration of neuroblasts in the developing cerebral cortex. *J. Anat.* **99**, 691-709.

Bertrand, N., Castro, D. S. and Guillemot, F. (2002). Proneural genes and the specification of neural cell types. *Nat. Rev. Neurosci.* **3**, 517-30.

Betschinger, J. and Knoblich, J. A. (2004). Dare to be different: asymmetric cell division in Drosophila, C. elegans and vertebrates. *Curr. Biol.* **14**, R674-85.

Billon, N., Terrinoni, A., Jolicoeur, C., McCarthy, A., Richardson, W. D., Melino, G. and Raff, M. (2004). Roles for p53 and p73 during oligodendrocyte development. *Development* **131**, 1211-20.

Blader, P., Fischer, N., Gradwohl, G., Guillemot, F. and Strahle, U. (1997). The activity of neurogenin1 is controlled by local cues in the zebrafish embryo. *Development* **124**, 4557-69.

Bouvet, P., Matsumoto, K. and Wolffe, A. P. (1995). Sequence-specific RNA recognition by the Xenopus Y-box proteins. An essential role for the cold shock domain. *J. Biol. Chem.* **270**, 28297-303.

Bouvet, P. and Wolffe, A. P. (1994). A role for transcription and FRGY2 in masking maternal mRNA within Xenopus oocytes. *Cell* **77**, 931-41.

Braat, A. K., Yan, N., Arn, E., Harrison, D. and Macdonald, P. M. (2004). Localization-dependent oskar protein accumulation; control after the initiation of translation. *Dev. Cell.* **7**, 125-31.

Brown, J. P., Couillard-Despres, S., Cooper-Kuhn, C. M., Winkler, J., Aigner, L. and Kuhn, H. G. (2003). Transient expression of doublecortin during adult neurogenesis. *J. Comp. Neurol.* **467**, 1-10.

Butt, S. J., Fuccillo, M., Nery, S., Noctor, S. C., Kriegstein, A. R., Corbin, J. G. and Fishell, G. (2005). The temporal and spatial origins of cortical interneurons predict their physiological subtype. *Neuron* **48**, 591-604.

Cai, L., Hayes, N. L. and Nowakowski, R. S. (1997a). Local homogeneity of cell cycle length in developing mouse cortex. *J. Neurosci.* **17**, 2079-87.

Cai, L., Hayes, N. L. and Nowakowski, R. S. (1997b). Synchrony of clonal cell proliferation and contiguity of clonally related cells: production of mosaicism in the ventricular zone of developing mouse neocortex. *J. Neurosci.* **17**, 2088-2100.

Cai, L., Hayes, N. L., Takahashi, T., Caviness, V. S., Jr. and Nowakowski, R. S. (2002). Size distribution of retrovirally marked lineages matches prediction from population measurements of cell cycle behavior. *J. Neurosci. Res.* **69**, 731-44.

Calegari, F., Haubensak, W., Haffner, C. and Huttner, W. (2005a). Selective lenghtening of the cell cycle in the neurogenic subpopulation of neural progenitor cells during mouse brain development. *J Neurosci.* **in press**.

Calegari, F., Haubensak, W., Haffner, C. and Huttner, W. B. (2005b). Selective lengthening of the cell cycle in the neurogenic subpopulation of neural progenitor cells during mouse brain development. *J. Neurosci.* **25**, 6533-38.

Calegari, F. and Huttner, W. (2003). An inhibition of cyclin-dependent kinases that lengthens, but does not arrest, neuroepithelial cell cycle induces premature neurogenesis. *J. Cell Sci.* **116**, 4947-55.

Campbell, K. (2005). Cortical neuron specification: it has its time and place. *Neuron* **46**, 373-6.

Campbell, K. and Gotz, M. (2002). Radial glia: multi-purpose cells for vertebrate brain development. *Trends Neurosci.* **25**, 235-38.

Campos, L. S. (2004). Neurospheres: insights into neural stem cell biology. *J Neurosci Res* **78**, 761-9.

Canzoniere, D., Farioli-Vecchioli, S., Conti, F., Ciotti, M. T., Tata, A. M., Augusti-Tocco, G., Mattei, E., Lakshmana, M. K., Krizhanovsky, V., Reeves, S. A. et al. (2004). Dual control of neurogenesis by PC3 through cell cycle inhibition and induction of Math1. *J. Neurosci.* **24**, 3355-69.

Capowski, E. E., Esnault, S., Bhattacharya, S. and Malter, J. S. (2001). Y box-binding factor promotes eosinophil survival by stabilizing granulocyte-macrophage colony-stimulating factor mRNA. *J. Immunol.* **167**, 5970-76.

Cappello, S., Attardo, A., Wu, X., Iwasato, T., Itohara, S., Wilsch-Brauninger, M., Eilken, H. M., Rieger, M. A., Schroeder, T. T., Huttner, W. B. et al. (2006). The Rho-GTPase cdc42 regulates neural progenitor fate at the apical surface. *Nat. Neurosci.* **9**, 1099-107.

Carmell, M. A., Xuan, Z., Zhang, M. Q. and Hannon, G. J. (2002). The Argonaute family: tentacles that reach into RNAi, developmental control, stem cell maintenance, and tumorigenesis. *Genes Dev.* **16**, 2733-42.

Casarosa, S., Fode, C. and Guillemot, F. (1999). Mash1 regulates neurogenesis in the ventral telencephalon. *Development* **126**, 525-34.

Castren, M., Tervonen, T., Karkkainen, V., Heinonen, S., Castren, E., Larsson, K., Bakker, C. E., Oostra, B. A. and Akerman, K. (2005). Altered differentiation of neural stem cells in fragile X syndrome. *Proc. Natl. Acad. Sci. U S A* **102**, 17834-39.

Cau, E., Gradwohl, G., Casarosa, S., Kageyama, R. and Guillemot, F. (2000). Hes genes regulate sequential stages of neurogenesis in the olfactory epithelium. *Development* **127**, 2323-32.

Caudy, A. A., Myers, M., Hannon, G. J. and Hammond, S. M. (2002). Fragile X-related protein and VIG associate with the RNA interference machinery. *Genes Dev.* **16**, 2491-96.

Caviness, V. S., Jr., Goto, T., Tarui, T., Takahashi, T., Bhide, P. G. and Nowakowski, R. S. (2003). Cell output, cell cycle duration and neuronal specification: a model of integrated mechanisms of the neocortical proliferative process. *Cereb. Cortex* **13**, 592-98.

Caviness, V. S., Jr., Takahashi, T. and Nowakowski, R. S. (1995). Numbers, time and neocortical neuronogenesis: a general developmental and evolutionary model. *Trends Neurosci.* **18**, 379-83.

Cayouette, M. and Raff, M. (2003). The orientation of cell division influences cell-fate choice in the developing mammalian retina. *Development* **130**, 2329-39.

Cayouette, M., Whitmore, A. V., Jeffery, G. and Raff, M. (2001). Asymmetric segregation of Numb in retinal development and the influence of the pigmented epithelium. *J. Neurosci.* **21**, 5643-51.

Ceman, S., Nelson, R. and Warren, S. T. (2000). Identification of mouse YB1/p50 as a component of the FMRP-associated mRNP particle. *Biochem. Biophys. Res. Commun.* **279**, 904-8.

Chanas-Sacre, G., Thiry, M., Pirard, S., Rogister, B., Moonen, G., Mbebi, C., Verdiere-Sahuque, M. and Leprince, P. (2000). A 295-kDA intermediate filament-associated protein in radial glia and developing muscle cells in vivo and in vitro. *Dev. Dyn.* **219**, 514-25.

Chen, C. Y., Gherzi, R., Andersen, J. S., Gaietta, G., Jurchott, K., Royer, H. D., Mann, M. and Karin, M. (2000). Nucleolin and YB-1 are required for JNK-mediated interleukin-2 mRNA stabilization during T-cell activation. *Genes Dev.* **14**, 1236-48.

Cheng, L.-C., Tavazoie, M. and Doetsch, F. (2005). Stem cells: from epigenetics to microRNAs. *Neuron* **46**, 363-67.

Chenn, A. and McConnell, S. K. (1995). Cleavage orientation and the asymmetric inheritance of Notch1 immunoreactivity in mammalian neurogenesis. *Cell* **82**, 631-41.

Chenn, A. and Walsh, C. A. (2002). Regulation of cerebral cortical size by control of cell cycle exit in neural precursors. *Science* **297**, 365-9.

Chenn, A. and Walsh, C. A. (2003). Increased neuronal production, enlarged forebrains and cytoarchitectural distortions in beta-catenin overexpressing transgenic mice. *Cereb. Cortex* **13**, 599-606.

Chenn, A., Zhang, Y., Chang, B. T. and McConnell, S. K. (1998). Intrinsic polarity of mammalian neuroepithelial cells. *Mol. Cell. Neurosci.* **11**, 183-93.

Chitnis, A. and Kintner, C. (1996). Sensitivity of proneural genes to lateral inhibition affects the pattern of primary neurons in Xenopus embryos. *Development* **122**, 2295-301.

Ciani, L. and Salinas, P. C. (2005). WNTs in the vertebrate nervous system: from patterning to neuronal connectivity. *Nat. Rev. Neurosci.* **6**, 351-62.

Ciolofan, C., Li, X. B., Olson, C., Kamasawa, N., Gebhardt, B. R., Yasumura, T., Morita, M., Rash, J. E. and Nagy, J. I. (2006). Association of connexin36 and zonula occludens-1 with zonula occludens-2 and the transcription factor zonula occludens-1-associated nucleic acid-binding protein at neuronal gap junctions in rodent retina. *Neuroscience* **140**, 433-51.

Clark, I. E., Wyckoff, D. and Gavis, E. R. (2000). Synthesis of the posterior determinant Nanos is spatially restricted by a novel cotranslational regulatory mechanism. *Curr. Biol.* **10**, 1311-14.

Colas, J.-F. and Schoenwolf, G. C. (2001). Towards a cellular and molecular understanding of neurulation. *Dev. Dyn.* **221**, 117-45.

Coles, L. S., Bartley, A. M., Bert, A., Hunter, J., Polyak, S., Diamond, P., Vadas, M. A. and Goodall, G. J. (2004). A multi-protein complex containing cold shock domain (Y-box) and polypyrimidine tract binding proteins forms on the vascular endothelial growth factor mRNA. Potential role in mRNA stabilization. *Eur. J. Biochem.* **271**, 648-60.

Corbin, F., Bouillon, M., Fortin, A., Morin, S., Rousseau, F. and Khandjian, E. W. (1997). The fragile X mental retardation protein is associated with poly(A)+ mRNA in actively translating polyribosomes. *Hum. Mol. Genet.* **6**, 1465-72.

Coskun, V. and Luskin, M. B. (2001). The expression pattern of the cell cycle inhibitor p19(INK4d) by progenitor cells of the rat embryonic telencephalon and neonatal anterior subventricular zone. *J. Neurosci.* **21**, 3092-103.

Cremisi, F., Philpott, A. and Ohnuma, S.-i. (2003). Cell cycle and cell fate interactions in neural development. *Curr. Opin. Neurobiol.* **13**, 26-33.

Cunningham, J. J., Levine, E. M., Zindy, F., Goloubeva, O., Roussel, M. F. and Smeyne, R. J. (2002). The cyclin-dependent kinase inhibitors p19(Ink4d) and p27(Kip1) are coexpressed in select retinal cells and act cooperatively to control cell cycle exit. *Mol. Cell. Neurosci.* **19**, 359-74.

Currle, S. D., Cheng, X., Hsu, C.-m. and Monuki, E. S. (2005). Direct and indirect roles of CNS dorsal midline cells in choroid plexus epithelia formation. *Development* **132**, 3549-59.

Dang, L., Yoon, K., Wang, M. and Gaiano, N. (2006). Notch3 signaling promotes radial glial/progenitor character in the mammalian telencephalon. *Dev. Neurosci.* **28**, 58-69.

Davies, H. G., Giorgini, F., Fajardo, M. A. and Braun, R. E. (2000). A sequence-specific RNA binding complex expressed in murine germ cells contains MSY2 and MSY4. *Dev. Biol.* **221**, 87-100.

Davis, A. A. and Temple, S. (1994). A self-renewing multipotential stem cell in embryonic rat cerebral cortex. *Nature* **372**, 263-6.

Davuluri, R. V., Suzuki, Y., Sugano, S. and Zhang, M. Q. (2000). CART classification of human 5' UTR sequences. *Genome Res.* **10**, 1807-16.

Davydova, E. K., Evdokimova, V. M., Ovchinnikov, L. P. and Hershey, J. W. B. (1997). Overexpression in COS cells of p50, the major core protein associated with mRNA, results in translation inhibition. *Nucleic Acids Res.* **25**, 2911-16.

De Benedetti, A. and Rhoads, R. E. (1990). Overexpression of eukaryotic protein synthesis initiation factor 4E in HeLa cells results in aberrant growth and morphology. *Proc. Natl. Acad. Sci. U S A* **87**, 8212-16.

de la Pompa, J. L., Wakeham, A., Correia, K. M., Samper, E., Brown, S., Aguilera, R. J., Nakano, T., Honjo, T., Mak, T. W., Rossant, J. et al. (1997). Conservation of the Notch signalling pathway in mammalian neurogenesis. *Development* **124**, 1139-48.

Defatta, R. J. and De Benedetti, A. (2003). Translational upregulation of yes accompanies eIF4E-mediated oncogenic transformation. *Int. J. Oncol.* **23**, 1709-13.

Delalle, I., Takahashi, T., Nowakowski, R. S., Tsai, L. H. and Caviness, V. S., Jr. (1999). Cyclin E-p27 opposition and regulation of the G1 phase of the cell cycle in the murine neocortical PVE: a quantitative analysis of mRNA in situ hybridization. *Cereb. Cortex* **9**, 824-32.

Deschamps, S., Viel, A., Garrigos, M., Denis, H. and le Maire, M. (1992). mRNP4, a major mRNA-binding protein from Xenopus oocytes is identical to transcription factor FRG Y2. *J. Biol. Chem.* **267**, 13799-802.

Dickins, R. A., Hemann, M. T., Zilfou, J. T., Simpson, D. R., Ibarra, I., Hannon, G. J. and Lowe, S. W. (2005). Probing tumor phenotypes using stable and regulated synthetic microRNA precursors. *Nat. Genet.* **37**, 1289-95.

Didier, D. K., Schiffenbauer, J., Woulfe, S. L., Zacheis, M. and Schwartz, B. D. (1988). Characterization of the cDNA encoding a protein binding to the major histocompatibility complex class II Y box. *Proc. Natl. Acad. Sci. U S A* **85**, 7322-26.

Doetsch, F., Caille, I., Lim, D. A., Garcia-Verdugo, J. M. and Alvarez-Buylla, A. (1999a). Subventricular zone astrocytes are neural stem cells in the adult mammalian brain. *Cell* **97**, 703-16.

Doetsch, F., Garcia-Verdugo, J. M. and Alvarez-Buylla, A. (1997). Cellular composition and three-dimensional organization of the subventricular germinal zone in the adult mammalian brain. *J. Neurosci.* **17**, 5046-61.

Doetsch, F., Garcia-Verdugo, J. M. and Alvarez-Buylla, A. (1999b). Regeneration of a germinal layer in the adult mammalian brain. *Proc. Natl. Acad. Sci. U S A* **96**, 11619-24.

Doetsch, F., Petreanu, L., Caille, I., Garcia-Verdugo, J. M. and Alvarez-Buylla, A. (2002). EGF converts transit-amplifying neurogenic precursors in the adult brain into multipotent stem cells. *Neuron* **36**, 1021-34.

Durand, B., Gao, F.-B. and Raff, M. (1997). Accumulation of the cyclin-dependent kinase inhibitor p27/Kip1 and the timing of oligodendrocyte differentiation. *EMBO J.* **16**, 306-17.

Durand, B. and Raff, M. (2000). A cell-intrinsic timer that operates during oligodendrocyte development. *Bioessays* **22**, 64-71.

Dyer, M. A. and Cepko, C. L. (2001). p27Kip1 and p57Kip2 regulate proliferation in distinct retinal progenitor cell populations. *J. Neurosci.* **21**, 4259-71.

Emsley, J. G., Mitchell, B. D., Kempermann, G. and Macklis, J. D. (2005). Adult neurogenesis and repair of the adult CNS with neural progenitors, precursors, and stem cells. *Prog. Neurobiol.* **75**, 321-41.

En-Nia, A., Yilmaz, E., Klinge, U., Lovett, D. H., Stefanidis, I. and Mertens, P. R. (2005). Transcription factor YB-1 mediates DNA polymerase alpha gene expression. *J. Biol. Chem.* **280**, 7702-11.

Englund, C., Fink, A., Lau, C., Pham, D., Daza, R. A., Bulfone, A., Kowalczyk, T. and Hevner, R. F. (2005). Pax6, Tbr2, and Tbr1 are expressed sequentially by radial glia, intermediate progenitor cells, and postmitotic neurons in developing neocortex. *J. Neurosci.* **25**, 247-51.

Eriksson, P. S., Perfilieva, E., Bjork-Eriksson, T., Alborn, A. M., Nordborg, C., Peterson, D. A. and Gage, F. H. (1998). Neurogenesis in the adult human hippocampus. *Nat. Med.* **4**, 1313-7.

Evdokimova, V., Ruzanov, P., Anglesio, M. S., Sorokin, A., Ovchinnikov, L. P., Buckley, J., Triche, T. J., Sonenberg, N. and Sorensen, P. H. B. (2006a). Akt-mediated YB-1 phosphorylation activates translation of silent mRNA species. *Mol. Cell. Biol.* **26**, 277-92.

Evdokimova, V. M., Kovrigina, E. A., Nashchekin, D. V., Davydova, E. K., Hershey, J. W. B. and Ovchinnikov, L. P. (1998). The major core protein of messenger ribonucleoprotein particles (p50) promotes initiation of protein biosynthesis in vitro. *J. Biol. Chem.* **273**, 3574-81.

Evdokimova, V. M. and Ovchinnikov, L. P. (1999). Translational regulation by Y-box transcription factor: involvement of the major mRNA-associated protein, p50. *Int. J. Biochem. Cell Biol.* **31**, 139-49.

Evdokimova, V. M., Ovchinnikov, L. P. and Sorensen, P. H. B. (2006b). Y-box binding protein 1: providing a new angle on translational regulation. *Cell Cycle* **5**, 1143-47.

Evdokimova, V. M., Ruzanov, P., Imataka, H., Raught, B., Svitkin, Y., Ovchinnikov, L. P. and Sonenberg, N. (2001). The major mRNA-associated protein YB-1 is a potent 5' cap-dependent mRNA stabilizer. *EMBO J.* **20**, 5491-502.

Evdokimova, V. M., Wei, C.-L., Sitikov, A. S., Simonenko, P. N., Lazarev, O. A., Vasilenko, K. S., Ustinov, V. A., Hershey, J. W. B. and Ovchinnikov, L. P. (1995). The major protein of messenger ribonucleoprotein particles in somatic cells is a member of the Y-box binding transcription factor family. *J. Biol. Chem.* **270**, 3186-92.

Farah, M. H., Olson, J. M., Sucic, H. B., Hume, R. I., Tapscott, S. J. and Turner, D. L. (2000). Generation of neurons by transient expression of neural bHLH proteins in mammalian cells. *Development* **127**, 693-702.

Fargeas, C. A., Fonseca, A.-V., Huttner, W. B. and Corbeil, D. (2006). Prominin-1 (CD133): from progenitor cells to human disease. *Future Lipidol.* **1**, 213-25.

Fero, M. L., Rivkin, M., Tasch, M., Porter, P., Carow, C. E., Firpo, E., Polyak, K., Tsai, L.-H., Broudy, V., Perlmutter, R. M. et al. (1996). A syndrome of multiorgan hyperplasia with features of gigantism, tumorigenesis, and female sterility in p27(Kip1)-deficient mice. *Cell* **85**, 733-44.

Ferri, A. L., Cavallaro, M., Braida, D., Di Cristofano, A., Canta, A., Vezzani, A., Ottolenghi, S., Pandolfi, P. P., Sala, M., DeBiasi, S. et al. (2004). Sox2 deficiency causes neurodegeneration and impaired neurogenesis in the adult mouse brain. *Development* **131**, 3805-19.

Fishell, G. and Kriegstein, A. R. (2003). Neurons from radial glia: the consequences of asymmetric inheritance. *Curr. Opin. Neurobiol.* **13**, 34-41.

Fleming, T. P., Papenbrock, T., Fesenko, I., Hausen, P. and Sheth, B. (2000). Assembly of tight junctions during early vertebrate development. *Semin. Cell. Dev. Biol.* **11**, 291-99.

Fortini, M. E. and Artavanis-Tsakonas, S. (1994). The suppressor of hairless protein participates in notch receptor signaling. *Cell* **79**, 273-82.

Frankel, P., Aronheim, A., Kavanagh, E., Balda, M. S., Matter, K., Bunney, T. D. and Marshall, C. J. (2005). RalA interacts with ZONAB in a cell density-dependent manner and regulates its transcriptional activity. *EMBO J.* **24**, 54-62.

Fuccillo, M., Joyner, A. L. and Fishell, G. (2006). Morphogen to mitogen: the multiple roles of hedgehog signalling in vertebrate neural development. *Nat. Rev. Neurosci.* **7**, 772-83.

Fujita, T., Ito, K.-i., Izumi, H., Kimura, M., Sano, M., Nakagomi, H., Maeno, K., Hama, Y., Shingu, K., Tsuchiya, S.-i. et al. (2005). Increased nuclear localization of transcription factor Y-box binding protein 1 accompanied by up-regulation of P-glycoprotein in breast cancer pretreated with paclitaxel. *Clin. Cancer Res.* **11**, 8837-44.

Funakoshi, T., Kobayashi, S., Ohashi, S., Sato, T.-A. and Anzai, K. (2003). Isolation and characterization of brain Y-box protein: developmentally regulated expression, polyribosomal association and dendritic localization. *Mol. Brain Res.* **118**, 1-9.

Furuse, M., Itoh, M., Hirase, T., Nagafuchi, A., Yonemura, S., Tsukita, S. and Tsukita, S. (1994). Direct association of occludin with ZO-1 and its possible involvement in the localization of occludin at tight junctions. *J. Cell Biol.* **127**, 1617-26.

Gadisseaux, J. F., Evrard, P. H., Misson, J.-P. and Caviness Jr, V. S. (1992). Dynamic changes in the density of radial glial fibers of the developing murine cerebral wall: a quantitative immunohistological analysis. *J. Comp. Neurology* **322**, 246-52.

Gadisseux, J. F., Kadhim, H. J., van den Bosch de Aguilar, P., Caviness, V. S. and Evrard, P. (1990). Neuron migration within the radial glial fiber system of the developing murine cerebrum: an electron microscopic autoradiographic analysis. *Dev. Brain Res.* **52**, 39-56.

Gaiano, N., Nye, J. S. and Fishell, G. (2000). Radial glial identity is promoted by Notch1 signaling in the murine forebrain. *Neuron* **26**, 395-404.

Gal, J. S., Morozov, Y. M., Ayoub, A. E., Chatterjee, M., Rakic, P. and Haydar, T. F. (2006). Molecular and morphological heterogeneity of neural precursors in the mouse neocortical proliferative zones. *J. Neurosci.* **26**, 1045-56.

Garcia, A. D., Doan, N. B., Imura, T., Bush, T. G. and Sofroniew, M. V. (2004). GFAP-expressing progenitors are the principal source of constitutive neurogenesis in adult mouse forebrain. *Nat. Neurosci.* **7**, 1233-41.

Gardette, R., Courtois, M. and Bisconte, J. C. (1982). Prenatal development of mouse central nervous structures: time of neuron origin and gradients of neuronal production. A radioautographic study. *J. Hirnforsch.* **23**, 415-31.

Gebauer, F. and Hentze, M. W. (2004). Molecular mechanisms of translational control. *Nat. Rev. Mol. Cell. Biol.* **5**, 827-35.

Gessner, C., Woischwill, C., Schumacher, A., Liebers, U., Kuhn, H., Stiehl, P., Jurchott, K., Royer, H. D., Witt, C. and Wolff, G. (2004). Nuclear YB-1 expression as a negative prognostic marker in nonsmall cell lung cancer. *Eur. Respir. J.* **23**, 14-19.

Gilmore, E. C., Ohshima, T., Goffinet, A. M., Kulkarni, A. B. and Herrup, K. (1998). Cyclin-dependent kinase 5-deficient mice demonstrate novel developmental arrest in cerebral cortex. *J. Neurosci.* **18**, 6370-7.

Gimenez-Bonafe, P., Fedoruk, M. N., Whitmore, T. G., Akbari, M., Ralph, J. L., Ettinger, S., Gleave, M. E. and Nelson, C. C. (2004). YB-1 is upregulated during prostate cancer tumor progression and increases P-glycoprotein activity. *Prostate* **59**, 337-49.

Gingras, A.-C., Raught, B. and Sonenberg, N. (1999). eIF4 initiation factors: effectors of mRNA recruitment to ribosomes and regulators of translation. *Annu. Rev. Biochem.* **68**, 913-63.

Giorgini, F., Davies, H. and Braun, R. (2002). Translational repression by MSY4 inhibits spermatid differentiation in mice. *Development* **129**, 3669-79.

Giorgini, F., Davies, H. G. and Braun, R. E. (2001). MSY2 and MSY4 bind a conserved sequence in the 3' untranslated region of protamine 1 mRNA in vitro and in vivo. *Mol. Cell. Biol.* **21**, 7010-19.

Goto, T., Mitsuhashi, T. and Takahashi, T. (2004). Altered patterns of neuron production in the p27 knockout mouse. *Dev. Neurosci.* **26**, 208-17.

Gotoh, K., Nonoguchi, K., Higashitsuji, H., Kaneko, Y., Sakurai, T., Sumitomo, Y., Itoh, K., Subjeck, J. R. and Fujita, J. (2004). Apg-2 has a chaperone-like activity similar to Hsp110 and is overexpressed in hepatocellular carcinomas. *FEBS Lett.* **560**, 19-24.

Gotz, M. and Barde, Y.-A. (2005). Radial glial cells defined and major intermediates between embryonic stem cells and CNS neurons. *Neuron* **46**, 369-72.

Gotz, M. and Huttner, W. B. (2005). The cell biology of neurogenesis. *Nat. Rev. Mol. Cell. Biol.* **6**, 777-88.

Gowan, K., Helms, A. W., Hunsaker, T. L., Collisson, T., Ebert, P. J., Odom, R. and Johnson, J. E. (2001). Crossinhibitory activities of Ngn1 and Math1 allow specification of distinct dorsal interneurons. *Neuron* **31**, 219-32.

Graff, J. R. and Zimmer, S. G. (2003). Translational control and metastatic progression: enhanced activity of the mRNA cap-binding protein eIF-4E selectively enhances translation of metastasis-related mRNAs. *Clin. Exp. Metastasis* **20**, 265-73.

Grant, C. E. and Deeley, R. G. (1993). Cloning and characterization of chicken YB-1: regulation of expression in the liver. *Mol. Cell. Biol.* **13**, 4186-96.

Gritti, A., Frolichsthal-Schoeller, P., Galli, R., Parati, E. A., Cova, L., Pagano, S. F., Bjornson, C. R. and Vescovi, A. L. (1999). Epidermal and fibroblast growth factors behave as mitogenic regulators for a single multipotent stem cell-like population from the subventricular region of the adult mouse forebrain. *J. Neurosci.* **19**, 3287-97.

Gritti, A., Parati, E. A., Cova, L., Frolichsthal, P., Galli, R., Wanke, E., Faravelli, L., Morassutti, D. J., Roisen, F., Nickel, D. D. et al. (1996). Multipotential stem cells from the adult mouse brain proliferate and self-renew in response to basic fibroblast growth factor. *J. Neurosci.* **16**, 1091-100.

Grove, E. A., Tole, S., Limon, J., Yip, L.-w. and Ragsdale, C. W. (1998). The hem of the embryonic cerebral cortex is defined by the expression of multiple Wnt genes and is compromised in Gli3-deficient mice. *Development* **125**, 2315-25.

Gu, W., Tekur, S., Reinbold, R., Eppig, J. J., Choi, Y.-C., Zheng, J. Z., Murray, M. T. and Hecht, N. B. (1998). Mammalian male and female germ cells express a germ cell-specific Y-Box protein, MSY2. *Biol. Reprod.* **59**, 1266-74.

Guardavaccaro, D., Corrente, G., Covone, F., Micheli, L., D'Agnano, I., Starace, G., Caruso, M. and Tirone, F. (2000). Arrest of G(1)-S progression by the p53-inducible gene PC3 is Rb dependent and relies on the inhibition of cyclin D1 transcription. *Mol. Cell. Biol.* **20**, 1797-815.

Guillemot, F. (2005). Cellular and molecular control of neurogenesis in the mammalian telencephalon. *Curr. Opin. Cell. Biol.* **17**, 639-47.

Halliday, A. L. and Cepko, C. L. (1992). Generation and migration of cells in the developing striatum. *Neuron* **9**, 15-26.

Hartfuss, E., Galli, R., Heins, N. and Gotz, M. (2001). Characterization of CNS precursor subtypes and radial glia. *Dev. Biol.* **229**, 15-30.

Hasegawa, S. L., Doetsch, P. W., Hamilton, K. K., Martin, A. M., Okenquist, S. A., Lenz, J. and Boss, J. M. (1991). DNA binding properties of YB-1 and dbpA: binding to double-stranded, single-stranded, and abasic site containing DNAs. *Nucleic Acids Res.* **19**, 4915-20.

Hatakeyama, J., Bessho, Y., Katoh, K., Ookawara, S., Fujioka, M., Guillemot, F. and Kageyama, R. (2004). Hes genes regulate size, shape and histogenesis of the nervous system by control of the timing of neural stem cell differentiation. *Development* **131**, 5539-50.

Hatakeyama, J. and Kageyama, R. (2006). Notch1 expression is spatiotemporally correlated with neurogenesis and negatively regulated by Notch1-independent Hes genes in the developing nervous system. *Cereb. Cortex* **16 Suppl 1**, i132-37.

Haubensak, W. (2002). Analyse Neurone-generierender Zellteilungen im Neuroepithel der Maus. Inaugural Dissertation.

Haubensak, W., Attardo, A., Denk, W. and Huttner, W. (2004). Neurons arise in the basal neuroepithelium of the early mammalian telencephalon: a major site of neurogenesis. *Proc. Natl. Acad. Sci. U S A* **101**, 3196-201.

Haubst, N., Georges-Labouesse, E., De Arcangelis, A., Mayer, U. and Gotz, M. (2006). Basement membrane attachment is dispensable for radial glial cell fate and for proliferation, but affects positioning of neuronal subtypes. *Development* **133**, 3245-54.

Hayes, N. L. and Nowakowski, R. S. (2002). Dynamics of cell proliferation in the adult dentate gyrus of two inbred strains of mice. *Brain Res. Dev. Brain Res.* **134**, 77-85.

Hebert, J. M., Hayhurst, M., Marks, M. E., Kulessa, H., Hogan, B. L. and McConnell, S. K. (2003). BMP ligands act redundantly to pattern the dorsal telencephalic midline. *Genesis* **35**, 214-19.

Henrique, D., Hirsinger, E., Adam, J., Le Roux, I., Pourquie, O., Ish-Horowicz, D. and Lewis, J. (1997). Maintenance of neuroepithelial progenitor cells by Delta-Notch signalling in the embryonic chick retina. *Curr. Biol.* **7**, 661-70.

Henshaw, E. C. (1968). Messenger RNA in rat liver polyribosomes: evidence that it exists as ribonucleoprotein particles. *J. Mol. Biol.* **36**, 401-11.

Herbert, T. P. and Hecht, N. B. (1999). The mouse Y-box protein, MSY2, is associated with a kinase on non-polysomal mouse testicular mRNAs. *Nucleic Acids Res.* **27**, 1747-53.

Hidalgo-Sanchez, M., Millet, S., Bloch-Gallego, E. and Alvarado-Mallart, R.-M. (2005). Specification of the meso-isthmo-cerebellar region: the Otx2/Gbx2 boundary. *Brain Res. Rev.* **49**, 134-49.

Hirata, H., Ohtsuka, T., Bessho, Y. and Kageyama, R. (2000). Generation of structurally and functionally distinct factors from the basic helix-loop-helix gene Hes3 by alternative first exons. *J. Biol. Chem.* **275**, 19083-9.

Hitoshi, S., Alexson, T., Tropepe, V., Donoviel, D., Elia, A. J., Nye, J. S., Conlon, R. A., Mak, T. W., Bernstein, A. and van der Kooy, D. (2002). Notch pathway molecules are essential for the maintenance, but not the generation, of mammalian neural stem cells. *Genes Dev.* **16**, 846-58.

Hitoshi, S., Seaberg, R. M., Koscik, C., Alexson, T., Kusunoki, S., Kanazawa, I., Tsuji, S. and van der Kooy, D. (2004). Primitive neural stem cells from the mammalian epiblast differentiate to definitive neural stem cells under the control of Notch signaling. *Genes Dev.* **18**, 1806-11.

Hockfield, S. and McKay, R. D. (1985). Identification of major cell classes in the developing mammalian nervous system. *J. Neurosci.* **5**, 3310-28.

Holm, P. S., Bergmann, S., Jurchott, K., Lage, H., Brand, K., Ladhoff, A., Mantwill, K., Curiel, D. T., Dobbelstein, M., Dietel, M. et al. (2002). YB-1 relocates to the nucleus in adenovirus-infected cells and facilitates viral replication by inducing E2 gene expression through the E2 late promoter. *J. Biol. Chem.* **277**, 10427-34.

Honjo, T. (1996). The shortest path from the surface to the nucleus: RBP-J kappa/Su(H) transcription factor. *Genes Cells* **1**, 1-9.

Horton, S., Meredith, A., Richardson, J. A. and Johnson, J. E. (1999). Correct coordination of neuronal differentiation events in ventral forebrain requires the bHLH factor MASH1. *Mol. Cell. Neurosci.* **14**, 355-69.

Huttner, W. B. and Brand, M. (1997). Asymmetric division and polarity of neuroepithelial cells. *Curr. Opin. Neurobiol.* **7**, 29-39.

Huttner, W. B. and Kosodo, Y. (2005). Symmetric versus asymmetric cell division during neurogenesis in the developing vertebrate central nervous system. *Curr. Opin. Cell. Biol.* **17**, 648-57.

Iacopetti, P., Barsacchi, G., Tirone, F., Maffei, L. and Cremisi, F. (1994). Developmental expression of PC3 gene is correlated with neuronal cell birthday. *Mech. Dev.* **47**, 127-37.

Iacopetti, P., Michelini, M., Stuckmann, I., Oback, B., Aaku-Saraste, E. and Huttner, W. (1999). Expression of the antiproliferative gene TIS21 at the onset of neurogenesis identifies single neuroepithelial cells that switch from proliferative to neuron-generating division. *Proc. Natl. Acad. Sci. USA* **96**, 4639-44.

Ise, T., Nagatani, G., Imamura, T., Kato, K., Takano, H., Nomoto, M., Izumi, H., Ohmori, H., Okamoto, T., Ohga, T. et al. (1999). Transcription factor Y-box binding protein 1 binds preferentially to cisplatin-modified DNA and interacts with proliferating cell nuclear antigen. *Cancer Res.* **59**, 342-46.

Ishibashi, M., Ang, S., Shiota, K., Nakanishi, S., Kageyama, R. and Guillemot, F. (1995). Targeted disruption of mammalian hairy and Enhancer of split homolog-1 (HES-1) leads to up-regulation of neural helix-loop-helix factors, premature neurogenesis, and severe neural tube defects. *Genes Dev.* **9**, 3136-48.

Ishibashi, M., Moriyoshi, K., Sasai, Y., Shiota, K., Nakanishi, S. and Kageyama, R. (1994). Persistent expression of helix-loop-helix factor HES-1 prevents mammalian neural differentiation in the central nervous system. *EMBO J.* **13**, 1799-805.

Issack, P. S. and Ziff, E. B. (1998). Genetic elements regulating HES-1 induction in Wnt-1-transformed PC12 cells. *Cell Growth Differ.* **9**, 827-36.

Ito, K., Tsutsumi, K., Kuzumaki, T., Gomez, P., Otsu, K. and Ishikawa, K. (1994). A novel growth-inducible gene that encodes a protein with a conserved cold-shock domain. *Nucleic Acids Res.* **22**, 2036-41.

Ito, Y., Yoshida, H., Shibahara, K., Uruno, T., Nakano, K., Takamura, Y., Miya, A., Kobayashi, K., Yokozawa, T., Matsuzuka, F. et al. (2003). Y-box binding protein expression in thyroid neoplasms: its linkage with anaplastic transformation. *Pathol. Int.* **53**, 429-33.

Iuchi, Y., Kobayashi, T., Kaneko, T., Takahara, M., Ogino, T. and Fujii, J. (2001). Expression of a Y-box protein, YB2/RYB-a, precedes protamine 2 expression during spermatogenesis in rodents. *Molecular Human Reproduction* **7**, 1023-1031.

Izumi, H., Imamura, T., Nagatani, G., Ise, T., Murakami, T., Uramoto, H., Torigoe, T., Ishiguchi, H., Yoshida, Y., Nomoto, M. et al. (2001). Y box-binding protein-1 binds preferentially to single-stranded nucleic acids and exhibits 3'-->5' exonuclease activity. *Nucleic Acids Res.* **29**, 1200-7.

Janz, M., Harbeck, N., Dettmar, P., Berger, U., Schmidt, A., Jurchott, K., Schmitt, M. and Royer, H.-D. (2002). Y-box factor YB-1 predicts drug resistance and patient outcome in breast cancer independent of clinically relevant tumor biologic factors HER2, uPA and PAI-1. *Int. J. Cancer* **97**, 278-82.

Jin, P., Zarnescu, D. C., Ceman, S., Nakamoto, M., Mowrey, J., Jongens, T. A., Nelson, D. L., Moses, K. and Warren, S. T. (2004). Biochemical and genetic interaction between the fragile X mental retardation protein and the microRNA pathway. *Nat. Neurosci.* **7**, 113-7.

Junghans, D., Hack, I., Frotscher, M., Taylor, V. and Kemler, R. (2005). Beta-catenin-mediated cell-adhesion is vital for embryonic forebrain development. *Dev. Dyn.* **233**, 528-39.

Jurchott, K., Bergmann, S., Stein, U., Walther, W., Janz, M., Manni, I., Piaggio, G., Fietze, E., Dietel, M. and Royer, H.-D. (2003). YB-1 as a cell cycle-regulated transcription factor facilitating cyclin A and cyclin B1 gene expression. *J. Biol. Chem.* **278**, 27988-96.

Kageyama, R., Ohtsuka, T., Hatakeyama, J. and Ohsawa, R. (2005). Roles of bHLH genes in neural stem cell differentiation. *Exp. Cell Res.* **306**, 343-8.

Kahane, N. and Kalcheim, C. (1998). Identification of early postmitotic cells in distinct embryonic sites and their possible roles in morphogenesis. *Cell Tissue Research* **294**, 297-307.

Kajino, K., Yamamoto, T., Hayashi, J., Umeda, T., Takahara, T. and Hino, O. (2001). Recombination hot spots of hepatitis B virus genome binds to members of the HMG domain protein family and the Y box binding protein family; implication fo these proteins in genomic instability. *Intervirology* **44**, 311-316.

Kamalov, G., Varma, B. R., Lu, L., Sun, Y., Weber, K. T. and Guntaka, R. V. (2005). Expression of the multifunctional Y-box protein, YB-1, in myofibroblasts of the infarcted rat heart. *Biochem. Biophys. Res. Commun.* **334**, 239-44.

Kamura, T., Yahata, H., Amada, S., Ogawa, S., Sonoda, T., Kobayashi, H., Mitsumoto, M., Kohno, K., Kuwano, M. and Nakano, H. (1999). Is nuclear expression of Y box-binding protein-1 a new prognostic factor in ovarian serous adenocarcinoma? *Cancer* **85**, 2450-54.

Kaspar, R. L. and Gehrke, L. (1994). Peripheral blood mononuclear cells stimulated with C5a or lipopolysaccharide to synthesize equivalent levels of IL-1 beta mRNA show unequal IL-1 beta protein accumulation but similar polyribosome profiles. *J. Immunol.* **153**, 277-86.

Kato, H., Taniguchi, Y., Kurooka, H., Minoguchi, S., Sakai, T., Nomura-Okazaki, S., Tamura, K. and Honjo, T. (1997). Involvement of RBP-J in biological functions of mouse Notch1 and its derivatives. *Development* **124**, 4133-41.

Kay, J. N., Finger-Baier, K. C., Roeser, T., Staub, W. and Baier, H. (2001). Retinal ganglion cell genesis requires lakritz, a Zebrafish atonal Homolog. *Neuron* **30**, 725-36.

Kempermann, G., Jessberger, S., Steiner, B. and Kronenberg, G. (2004). Milestones of neuronal development in the adult hippocampus. *Trends Neurosci.* **27**, 447-52.

Khandjian, E. W., Huot, M.-E., Tremblay, S., Davidovic, L., Mazroui, R. and Bardoni, B. (2004). Biochemical evidence for the association of fragile X mental retardation protein with brain polyribosomal ribonucleoparticles. *Proc. Natl. Acad. Sci. U S A* **101**, 13357-62.

Kim, J., Krichevsky, A., Grad, Y., Hayes, G. D., Kosik, K. S., Church, G. M. and Ruvkun, G. (2004). Identification of many microRNAs that copurify with polyribosomes in mammalian neurons. *Proc. Natl. Acad. Sci. U S A* **101**, 360-65.

Kim, P., Helms, A. W., Johnson, J. E. and Zimmerman, K. (1997). XATH-1, a vertebrate homolog of Drosophila atonal, induces a neuronal differentiation within ectodermal progenitors. *Dev. Biol.* **187**, 1-12.

Kleene, K. C. (2003). Patterns, mechanisms, and functions of translation regulation in mammalian spermatogonic cells. *Cytogenet. Genome Res.* **103**, 217-24.

Klezovitch, O., Fernandez, T. E., Tapscott, S. J. and Vasioukhin, V. (2004). Loss of cell polarity causes severe brain dysplasia in Lgl1 knockout mice. *Genes Dev.* **18**, 559-71.

Kloks, C. P., Spronk, C. A., Lasonder, E., Hoffmann, A., Vuister, G. W., Grzesiek, S. and Hilbers, C. W. (2002). The solution structure and DNA-binding properties of the cold-shock domain of the human Y-box protein YB-1. *J. Mol. Biol.* **316**, 317-26.

Koch, J. (2000). Untersuchungen zur Plastizität der neuroepithelialien Basal Lamina im Laufe der Neurogenese der Maus. In *Inaugural Dissertation*, (ed. Universität Heilderberg.

Kohno, K., Izumi, H., Uchiumi, T., Ashizuka, M. and Kuwano, M. (2003). The pleiotropic functions of the Y-box-binding protein, YB-1. *Bioessays* **25**, 691-98.

Kohno, Y., Matsuki, Y., Tanimoto, A., Izumi, H., Uchiumi, T., Kohno, K., Shimajiri, S. and Sasaguri, Y. (2006). Expression of Y-box-binding protein dbpC/contrin, a potentially new cancer/testis antigen. *Br. J. Cancer* **94**, 710-16.

Koike, K., Uchiumi, T., Ohga, T., Toh, S., Wada, M., Kohno, K. and Kuwano, M. (1997). Nuclear translocation of the Y-box binding protein by ultraviolet irradiation. *FEBS Lett.* **417**, 390-94.

Kornack, D. R. and Rakic, P. (1998). Changes in cell-cycle kinetics during the development and evolution of primate neocortex. *Proc. Natl. Acad. Sci. U S A* **95**, 1242-6.

Kornack, D. R. and Rakic, P. (1999). Continuation of neurogenesis in the hippocampus of the adult macaque monkey. *Proc. Natl. Acad. Sci. U S A* **96**, 5768-73.

Koromilas, A. E., Lazaris-Karatzas, A. and Sonenberg, N. (1992). mRNAs containing extensive secondary structure in their 5' non-coding region translate efficiently in cells overexpressing initiation factor eIF-4E. *EMBO J.* **11**, 4153-58.

Kosodo, Y., Roper, K., Haubensak, W., Marzesco, A. M., Corbeil, D. and Huttner, W. B. (2004). Asymmetric distribution of the apical plasma membrane during neurogenic divisions of mammalian neuroepithelial cells. *EMBO J.* **23**, 2314-24.

Kronenberg, G., Reuter, K., Steiner, B., Brandt, M. D., Jessberger, S., Yamaguchi, M. and Kempermann, G. (2003). Subpopulations of proliferating cells of the adult hippocampus respond differently to physiologic neurogenic stimuli. *J. Comp. Neurol.* **467**, 455-63.

Kuersten, S. and Goodwin, E. B. (2003). The power of the 3' UTR: translational control and development. *Nat. Rev. Genet.* **4**, 626-37.

Kumar, A. and Lindberg, U. (1972). Characterization of messenger ribonucleoprotein and messenger RNA from KB cells. *Proc. Natl. Acad. Sci. U S A* **69**, 681-85.

Kuwano, M., Oda, Y., Izumi, H., Yang, S.-J., Uchiumi, T., Iwamoto, Y., Toi, M., Fujii, T., Yamana, H., Kinoshita, H. et al. (2004). The role of nuclear Y-box binding protein 1 as a global marker in drug resistance. *Mol. Cancer Ther.* **3**, 1485-92.

Ladomery, M. and Sommerville, J. (1994). Binding of Y-box proteins to RNA: involvement of different protein domains. *Nucleic Acids Res.* **22**, 5582-9.

Ladomery, M. and Sommerville, J. (1995). A role for Y-box proteins in cell proliferation. *Bioessays* **17**, 9-11.

Laggerbauer, B., Ostareck, D., Keidel, E.-M., Ostareck-Lederer, A. and Fischer, U. (2001). Evidence that fragile X mental retardation protein is a negative regulator of translation. *Hum. Mol. Genet.* **10**, 329-38.

Lardelli, M., Williams, R., Mitsiadis, T. and Lendahl, U. (1996). Expression of the Notch 3 intracellular domain in mouse central nervous system progenitor cells is lethal and leads to disturbed neural tube development. *Mech. Dev.* **59**, 177-90.

Lasham, A., Lindridge, E., Rudert, F., Onrust, R. and Watson, J. (2000). Regulation of the human fas promoter by YB-1, Puralpha and AP-1 transcription factors. *Gene* **252**, 1-13.

Lasham, A., Moloney, S., Hale, T., Homer, C., Zhang, Y. F., Murison, G. J., Braithwaite, A. W. and Watson, J. (2003). The Y-box-binding protein, YB1, is a potential negative regulator of the p53 tumor suppressor. *J. Biol. Chem.* **278**, 35516-23.

Lazaris-Karatzas, A., Montine, K. S. and Sonenberg, N. (1990). Malignant transformation by a eukaryotic initiation factor subunit that binds to mRNA 5' cap. *Nature* **345**, 544-47.

Lee, J. E., Hollenberg, S. M., Snider, L., Turner, D. L., Lipnick, N. and Weintraub, H. (1995). Conversion of Xenopus ectoderm into neurons by NeuroD, a basic helix-loop-helix protein. *Science* **268**, 836-44.

Lee, S. M., Tole, S., Grove, E. A. and McMahon, A. P. (2000). A local Wnt-3a signal is required for development of the mammalian hippocampus. *Development* **127**, 457-67.

Lendahl, U., Zimmerman, L. B. and McKay, R. D. (1990). CNS stem cells express a new class of intermediate filament protein. *Cell* **60**, 585-95.

Li, Z., Zhang, Y., Ku, L., Wilkinson, K. D., Warren, S. T. and Feng, Y. (2001). The fragile X mental retardation protein inhibits translation via interacting with mRNA. *Nucleic Acids Res.* **29**, 2276-83.

Lim, I. K. (2006). TIS21 (/BTG2/PC3) as a link between ageing and cancer: cell cycle regulator and endogenous cell death molecule. *J. Cancer. Res. Clin. Oncol.* **132**, 417-26.

Lim, I. K., Lee, M. S., Ryu, M. S., Park, T. J., Fujiki, H., Eguchi, H. and Paik, W. K. (1998). Induction of growth inhibition of 293 cells by downregulation of the cyclin E and cyclin-dependent kinase 4 proteins due to overexpression of TIS21. *Mol. Carcinog.* **23**, 25-35.

Lindberg, U. and Sundquist, B. (1974). Isolation of messenger ribonucleoproteins from mammalian cells. *J. Mol. Biol.* **86**, 451-68.

Liu, A. and Niswander, L. A. (2005). Bone morphogenic protein signalling and vertebrate nervous system development. *Nat. Rev. Neurosc.* **6**, 945-54.

Lo Turco, J. J. and Kriegstein, A. R. (1991). Clusters of coupled neuroblasts in embryonic neocortex. *Science* **252**, 563-66.

Lobo, M. V., Alonso, F. J., Redondo, C., Lopez-Toledano, M. A., Caso, E., Herranz, A. S., Paino, C. L., Reimers, D. and Bazan, E. (2003). Cellular characterization of epidermal growth factor-expanded free-floating neurospheres. *J. Histochem. Cytochem.* **51**, 89-103.

Lois, C. and Alvarez-Buylla, A. (1994). Long-distance neuronal migration in the adult mammalian brain. *Science* **264**, 1145-48.

Lois, C., Garcia-Verdugo, J.-M. and Alvarez-Buylla, A. (1996). Chain migration of neuronal precursors. *Science* **271**, 978-81.

Louvi, A. and Artavanis-Tsakonas, S. (2006). Notch signalling in vertebrate neural development. *Nat. Rev. Neurosci.* **7**, 93-102.

Lu, Z. H., Books, J. T. and Ley, T. J. (2005). YB-1 is important for late-stage embryonic development, optimal cellular stress responses, and the prevention of premature senescence. *Mol. Cell. Biol.* **25**, 4625-37.

Lu, Z. H., Books, J. T. and Ley, T. J. (2006). Cold Shock Domain Family Members YB-1 and MSY4 Share Essential Functions During Murine Embryogenesis. *Mol. Cell. Biol.*

Lütolf, S., Radtke, F., Aguet, M., Suter, U. and Taylor, V. (2002). Notch1 is required for neuronal and glial differentiation in the cerebellum. *Development* **129**, 373-85.

Lyons, D. A., Guy, A. T. and Clarke, J. D. W. (2003). Monitoring neural progenitor fate through multiple rounds of division in an intact vertebrate brain. *Development* **130**, 3427-36.

Ma, Q., Kintner, C. and Anderson, D. J. (1996). Identification of neurogenin, a vertebrate neuronal determination gene. *Cell* **87**, 43-52.

Malatesta, P., Hack, M. A., Hartfuss, E., Kettenmann, H., Klinkert, W., Kirchhoff, F. and Gotz, M. (2003). Neuronal or glial progeny: regional differences in radial glia fate. *Neuron* **37**, 751-64.

Manabe, N., Hirai, S., Imai, F., Nakanishi, H., Takai, Y. and Ohno, S. (2002). Association of ASIP/mPAR-3 with adherens junctions of mouse neuroepithelial cells. *Dev. Dyn.* **225**, 61-9.

Martens, D. J., Tropepe, V. and van Der Kooy, D. (2000). Separate proliferation kinetics of fibroblast growth factor-responsive and epidermal growth factor-responsive neural stem cells within the embryonic forebrain germinal zone. *J. Neurosci.* **20**, 1085-95.

Marzesco, A. M., Janich, P., Wilsch-Brauninger, M., Dubreuil, V., Langenfeld, K., Corbeil, D. and Huttner, W. B. (2005). Release of extracellular membrane particles carrying the stem cell marker prominin-1 (CD133) from neural progenitors and other epithelial cells. *J. Cell. Sci.* **118**, 2849-58.

Mastrangelo, M. and Kleene, K. (2000). Developmental expression of Y-box protein 1 mRNA and alternatively spliced Y-box protein 3 mRNAs in spermatogenic cells in mice. *Mol. Hum. Reprod.* **6**, 779-88.

Matsumoto, K., Meric, F. and Wolffe, A. P. (1996). Translational repression dependent on the interaction of the Xenopus Y-box protein FRGY2 with mRNA. Role of the cold shock domain, tail domain, and selective RNA sequence recognition. *J. Biol. Chem.* **271**, 22706-12.

Matsumoto, K., Tanaka, K. J. and Tsujimoto, M. (2005). An acidic protein, YBAP1, mediates the release of YB-1 from mRNA and relieves the translational repression activity of YB-1. *Mol. Cell. Biol.* **25**, 1779-92.

Matsumoto, K. and Wolffe, A. (1998). Gene regulation by Y-box proteins: coupling control of transcription and translation. *Trends Cell. Biol.* **8**, 318-23.

Matter, K. and Balda, M. S. (2003). Signalling to and from tight junctions. *Nat. Rev. Mol. Cell Biol.* **4**, 225-36.

Mazroui, R., Huot, M.-E., Tremblay, S., Filion, C., Labelle, Y. and Khandjian, E. W. (2002). Trapping of messenger RNA by Fragile X Mental Retardation protein into cytoplasmic granules induces translation repression. *Hum. Mol. Genet.* **11**, 3007-17.

McCarthy, M., Turnbull, D. H., Walsh, C. A. and Fishell, G. (2001). Telencephalic neural progenitors appear to be restricted to regional and glial fates before the onset of neurogenesis. *J. Neurosci.* **21**, 6772-81.

McConnell, J. A. (1981). Identification of early neurons in the brainstem and spinal cord. II. An autoradiographic study in the mouse. *J. Comp. Neurol.* **200**, 273-88.

Mertens, P. R., Harendza, S., Pollock, A. S. and Lovett, D. H. (1997). Glomerular mesangial cell-specific transactivation of matrix metalloproteinase 2 transcription is mediated by YB-1. *J. Biol. Chem.* **272**, 22905-12.

Mertens, P. R., Steinmann, K., Alfonso-Jaume, M. A., En-Nia, A., Sun, Y. and Lovett, D. H. (2002). Combinatorial interactions of p53, activating protein-2, and YB-1 with a single enhancer element regulate gelatinase A expression in neoplastic cells. *J. Biol. Chem.* **277**, 24875-82.

Minich, W. B., Maidebura, I. P. and Ovchinnikov, L. P. (1993). Purification and characterization of the major 50-kDa repressor protein from cytoplasmic mRNP of rabbit reticulocytes. *Eur. J. Biochem.* **212**, 633-38.

Mione, M. C., Cavanagh, J. F., Harris, B. and Parnavelas, J. G. (1997). Cell fate specification and symmetrical/asymmetrical divisions in the developing cerebral cortex. *J. Neurosci.* **17**, 2018-29.

Misson, J.-P., Edwards, M. A., Yamamoto, M. and Caviness Jr, V. S. (1988). Identification of radial glial cells within the developing murine central nervous system: studies based upon a new immunohistochemical marker. *Dev. Brain Res.* **44**, 95-108.

Miyata, T., Kawaguchi, A., Okano, H. and Ogawa, M. (2001). Asymmetric inheritance of radial glial fibers by cortical neurons. *Neuron* **31**, 727-41.

Miyata, T., Kawaguchi, A., Saito, K., Kawano, M., Muto, T. and Ogawa, M. (2004). Asymmetric production of surface-dividing and non-surface-dividing cortical progenitor cells. *Development* **131**, 3133-45.

Mizuguchi, R., Sugimori, M., Takebayashi, H., Kosako, H., Nagao, M., Yoshida, S., Nabeshima, Y., Shimamura, K. and Nakafuku, M. (2001). Combinatorial roles of olig2 and neurogenin2 in the coordinated induction of pan-neuronal and subtype-specific properties of motoneurons. *Neuron* **31**, 757-71.

Mizutani, K. and Saito, T. (2005). Progenitors resume generating neurons after temporary inhibition of neurogenesis by Notch activation in the mammalian cerebral cortex. *Development* **132**, 1295-304.

Moorthamer, M., Zumstein-Mecker, S. and Chaudhuri, B. (1999). DNA binding protein dbpA binds Cdk5 and inhibits its activity. *FEBS Lett.* **446**, 343-50.

Morrison, S. J. and Kimble, J. (2006). Asymmetric and symmetric stem-cell divisions in development and cancer. *Nature* **441**, 1068-74.

Nakatsura, T., Senju, S., Yamada, K., Jotsuka, T., Ogawa, M. and Nishimura, Y. (2001). Gene cloning of immunogenic antigens overexpressed in pancreatic cancer. *Biochem. Biophys. Res. Commun.* **281**, 936-44.

Nakayama, K., Ishida, N., Shirane, M., Inomata, A., Inoue, T., Shishido, N., Horii, I., Loh, D. Y. and Nakayama, K.-i. (1996). Mice lacking p27(Kip1) display increased body size, multiple organ hyperplasia, retinal dysplasia, and pituitary tumors. *Cell* **85**, 707-20.

Nekrasov, M. P., Ivshina, M. P., Chernov, K. G., Kovrigina, E. A., Evdokimova, V. M., Thomas, A. A. M., Hershey, J. W. B. and Ovchinnikov, L. P. (2003). The mRNA-binding protein YB-1 (p50) prevents association of the eukaryotic initiation factor eIF4G with mRNA and inhibits protein synthesis at the initiation stage. *J. Biol. Chem.* **278**, 13936-43.

Nelson, P. T., Hatzigeorgiou, A. G. and Mourelatos, Z. (2004). miRNP:mRNA association in polyribosomes in a human neuronal cell line. *Rna* **10**, 387-94.

Nguyen, L., Besson, A., Heng, J. I., Schuurmans, C., Teboul, L., Parras, C., Philpott, A., Roberts, J. M. and Guillemot, F. (2006). p27kip1 independently promotes neuronal differentiation and migration in the cerebral cortex. *Genes Dev.* **20**, 1511-24.

Nieto, M., Monuki, E. S., Tang, H., Imitola, J., Haubst, N., Khoury, S. J., Cunningham, J., Gotz, M. and Walsh, C. A. (2004). Expression of Cux-1 and Cux-2 in the subventricular zone and upper layers II-IV of the cerebral cortex. *J. Comp. Neurol.* **479**, 168-80.

Nieto, M., Schuurmans, C., Britz, O. and Guillemot, F. (2001). Neural bHLH genes control the neuronal versus glial fate decision in cortical progenitors. *Neuron* **29**, 401-13.

Noctor, S. C., Flint, A. C., Weissman, T. A., Dammerman, R. S. and Kriegstein, A. R. (2001). Neurons derived from radial glial cells establish radial units in neocortex. *Nature* **409**, 714-20.

Noctor, S. C., Flint, A. C., Weissman, T. A., Wong, W. S., Clinton, B. K. and Kriegstein, A. R. (2002). Dividing precursor cells of the embryonic cortical ventricular zone have morphological and molecular characteristics of radial glia. *J. Neurosci.* **22**, 3161-73.

Noctor, S. C., Martinez-Cerdeno, V., Ivic, L. and Kriegstein, A. R. (2004). Cortical neurons arise in symmetric and asymmetric division zones and migrate through specific phases. *Nat. Neurosci.* **7**, 136-44.

Nornes, H. O. and Carry, M. (1978). Neurogenesis in spinal cord of mouse: an autoradiographic analysis. *Brain Res.* **159**, 1-6.

Nose, A. and Takeichi, M. (1986). A novel cadherin cell adhesion molecule: its expression patterns associated with implantation and organogenesis of mouse embryos. *J. Cell Biol.* **103**, 2649-58.

Oda, Y., Ohishi, Y., Saito, T., Hinoshita, E., Uchiumi, T., Kinukawa, N., Iwamoto, Y., Kohno, K., Kuwano, M. and Tsuneyoshi, M. (2003). Nuclear expression of Y-box-binding protein-1 correlates with P-glycoprotein and topoisomerase II alpha expression, and with poor prognosis in synovial sarcoma. *J. Pathol.* **199**, 251-58.

Oda, Y., Sakamoto, A., Shinohara, N., Ohga, T., Uchiumi, T., Kohno, K., Tsuneyoshi, M., Kuwano, M. and Iwamoto, Y. (1998). Nuclear expression of YB-1 protein correlates with P-glycoprotein expression in human osteosarcoma. *Clin. Cancer Res.* **4**, 2273-7.

Ohga, T., Koike, K., Ono, M., Makino, Y., Itagaki, Y., Tanimoto, M., Kuwano, M. and Kohno, K. (1996). Role of the human Y box-binding protein YB-1 in cellular sensitivity to the DNA-damaging agents cisplatin, mitomycin C, and ultraviolet light. *Cancer Res.* **56**, 4224-28.

Ohnuma, S.-i. and Harris, W. A. (2003). Neurogenesis and the cell cycle. *Neuron* **40**, 199-208.

Ohtsuka, T., Imayoshi, I., Shimojo, H., Nishi, E., Kageyama, R. and McConnell, S. K. (2006). Visualization of embryonic neural stem cells using Hes promoters in transgenic mice. *Mol. Cell Neurosci.* **31**.

Ohtsuka, T., Ishibashi, M., Gradwohl, G., Nakanishi, S., Guillemot, F. and Kageyama, R. (1999). Hes1 and Hes5 as Notch effectors in mammalian neuronal differentiation. *EMBO J.* **18**, 2196-207.

Ohtsuka, T., Sakamoto, M., Guillemot, F. and Kageyama, R. (2001). Roles of the basic helix-loop-helix genes Hes1 and Hes5 in expansion of neural stem cells of the developing brain. *J. Biol. Chem.* **276**, 30467-74.

Okamoto, T., Izumi, H., Imamura, T., Takano, H., Ise, T., Uchiumi, T., Kuwano, M. and Kohno, K. (2000). Direct interaction of p53 with the Y-box binding protein, YB-1: a mechanism for regulation of human gene expression. *Oncogene* **19**, 6194-202.

Olsen, P. H. and Ambros, V. (1999). The lin-4 regulatory RNA controls developmental timing in Caenorhabditis elegans by blocking LIN-14 protein synthesis after the initiation of translation. *Dev. Biol.* **216**, 671-80.

Ono, K., Tsumori, T., Yokota, S. and Yasui, Y. (2001). Extensive proliferation of oligodendrocyte precursors in the parenchyma of the embryonic chick central nervous system. *Dev. Biol.* **231**, 77-86.

Parnavelas, J. G. (1999). Glial cell lineages in the rat cerebral cortex. *Exp. Neurol.* **156**, 418-29.

Parras, C. M., Schuurmans, C., Scardigli, R., Kim, J., Anderson, D. J. and Guillemot, F. (2002). Divergent functions of the proneural genes Mash1 and Ngn2 in the specification of neuronal subtype identity. *Genes Dev.* **16**, 324-38.

Patten, B. A., Sardi, S. P., Koirala, S., Nakafuku, M. and Corfas, G. (2006). Notch1 signaling regulates radial glia differentiation through multiple transcriptional mechanisms. *J. Neurosci.* **26**, 3102-8.

Pearson, R., Lüneborg, N. L., Becker, D. L. and Mobbs, P. (2005). Gap junctions modulate interkinetic nuclear movement in retinal progenitor cells. *J. Neurosci.* **25**, 10803-14.

Penes, M. C., Li, X. and Nagy, J. I. (2005). Expression of zonula occludens-1 (ZO-1) and the transcription factor ZO-1-associated nucleic acid-binding protein (ZONAB)-MsY3 in glial cells and colocalization at oligodendrocyte and astrocyte gap junctions in mouse brain. *Eur. J. Neurosci.* **22**, 404-18.

Perry, R. P. and Kelley, D. E. (1968). Messenger RNA-protein complexes and newly synthesized ribosomal subunits: analysis of free particles and components of polyribosomes. *J. Mol. Biol.* **35**, 37-59.

Petersen, C. P., Bordeleau, M. E., Pelletier, J. and Sharp, P. A. (2006). Short RNAs repress translation after initiation in mammalian cells. *Mol. Cell* **21**, 533-42.

Pisarev, A., Skabkin, M., Thomas, A., Merrick, W., Ovchinnikov, L. and Shatsky, I. (2002). Positive and negative effects of the major mammalian messenger ribonucleoprotein p50 on binding of 40 S ribosomal subunits to the initiation codon of beta-globin mRNA. *J. Biol. Chem.* **277**, 15445-51.

Placzek, M. and Briscoe, J. (2005). The floor plate: multiple cells, multiple signals. *Nat. Rev. Neurosci.* **6**, 230-40.

Qian, X., Goderie, S. K., Shen, Q., Stern, J. H. and Temple, S. (1998). Intrinsic programs of patterned cell lineages in isolated vertebrate CNS ventricular zone cells. *Development* **125**, 3143-52.

Qian, X., Shen, Q., Goderie, S. K., He, W., Capela, A., Davis, A. A. and Temple, S. (2000). Timing of CNS cell generation: a programmed sequence of neuron and glial cell production from isolated murine cortical stem cells. *Neuron* **28**, 69-80.

Radtke, F., Wilson, A., Stark, G., Bauer, M., van Meerwijk, J., MacDonald, R. H. and Aguet, M. (1999). Deficient T cell fate specification in mice with an induced inactivation of Notch1. *Immunity* **10**, 547-558.

Raffetseder, U., Frye, B., Rauen, T., Jurchott, K., Royer, H.-D., Jansen, P. L. and Mertens, P. R. (2003). Splicing factor SRp30c interaction with Y-box protein-1 confers nuclear YB-1 shuttling and alternative splice site selection. *J. Biol. Chem.* **278**, 18241-48.

Rakic, P. (1972). Mode of cell migration to the superficial layers of fetal monkey neocortex. *J. Comp. Neurol.* **145**, 61-83.

Rakic, P. (1995). A small step for the cell, a giant leap for mankind: a hypothesis of neocortical expansion during evolution. *Trends Neurosci.* **18**, 383-88.

Rallu, M., Corbin, J. G. and Fishell, G. (2002). Parsing the prosencephalon. *Nat. Rev. Neurosci.* **3**, 943-51.

Ranjan, M., Tafuri, S. R. and Wolffe, A. P. (1993). Masking mRNA from translation in somatic cells. *Genes Dev.* **7**, 1725-36.

Rao, M. S. and Jacobson, M. (2005). Developmental neurobiology, 4th edition. New York, Boston, Dordrecht, London, Moscow: Kluwer Academic/Plenum Publishers.

Reaume, A. G., Conlon, R. A., Zirngibl, R., Yamaguchi, T. P. and Rossant, J. (1992). Expression analysis of a Notch homoglogue in the mouse embryo. *Dev. Biol.* **154**, 377-87.

Reifers, F., Böhli, H., Walsh, E. C., Crossley, P. H., Stainier, D. Y. R. and Brand, M. (1998). Fgf8 is mutated in zebrafish acerebellar (ace) mutants and is required for maintenance of midbrain-hindbrain boundary development and somitogenesis. *Development* **125**, 2381-2395.

Reynolds, B. A. and Rietze, R. L. (2005). Neural stem cells and neurospheres--re-evaluating the relationship. *Nat. Methods* **2**, 333-6.

Reynolds, B. A. and Weiss, S. (1996). Clonal and population analyses demonstrate that an EGF-responsive mammalian embryonic CNS precursor is a stem cell. *Dev. Biol.* **175**, 1-13.

Reznikov, K., Acklin, S. E. and van der Kooy, D. (1997). Clonal heterogeneity in the early embryonic rodent cortical germinal zone and the separation of subventricular from ventricular zone lineages. *Dev. Dyn.* **210**, 328-43.

Richter, J. D. and Sonenberg, N. (2005). Regulation of cap-dependent translation by eIF4E inhibitory proteins. *Nature* **433**, 477-80.

Rosenwald, I. B. (2004). The role of translation in neoplastic transformation from a pathologist's point of view. *Oncogene* **23**, 3230-47.

Ross, S. E., Greenberg, M. E. and Stiles, C. D. (2003). Basic helix-loop-helix factors in cortical development. *Neuron* **39**, 13-25.

Rubinstein, D. B., Stortchevoi, A., Boosalis, M., Ashfaq, R. and Guillaume, T. (2002). Overexpression of DNA-binding protein B gene product in breast cancer as detected by in vitro-generated combinatorial human immunoglobulin libraries. *Cancer Res.* **62**, 4985-91.

Ruggero, D. and Pandolfi, P. P. (2003). Does the ribosome translate cancer? *Nat. Rev. Cancer* **3**, 179-92.

Ruggero, D. and Sonenberg, N. (2005). The Akt of translational control. *Oncogene* **24**, 7426-34.

Ruzanov, P. V., Evdokimova, V. M., Korneeva, N. L., Hershey, J. W. and Ovchinnikov, L. P. (1999). Interaction of the universal mRNA-binding protein, p50, with actin: a possible link between mRNA and microfilaments. *J. Cell. Sci.* **112 (Pt 20)**, 3487-96.

Ryu, M. S., Lee, M. S., Hong, J. W., Hahn, T.-R., Moon, E. and Lim, I. K. (2004). TIS21/BTG2/PC3 is expressed through PKC-delta pathway and inhibits binding of cyclin B1-Cdc2 and its activity, independent of p53 expression. *Exp. Cell. Res.* **299**, 159-70.

Saghir, A. N., Tuxworth, W. J., Jr., Hagedorn, C. H. and McDermott, P. J. (2001). Modifications of eukaryotic initiation factor 4F (eIF4F) in adult cardiocytes by adenoviral gene transfer: differential effects on eIF4F activity and total protein synthesis rates. *Biochem. J.* **356**, 557-66.

Saito, T. and Nakatsuji, N. (2001). Efficient gene transfer into the embryonic mouse brain using in vivo electroporation. *Dev. Biol.* **240**, 237-46.

Sakamoto, M., Hirata, H., Ohtsuka, T., Bessho, Y. and Kageyama, R. (2003). The basic helix-loop-helix genes Hesr1/Hey1 and Hesr2/Hey2 regulate maintenance of neural precursor cells in the brain. *J. Biol. Chem.* **278**, 44808-15.

Sanai, N., Tramontin, A. D., Quinones-Hinojosa, A., Barbaro, N. M., Gupta, N., Kunwar, S., Lawton, M. T., McDermott, M. W., Parsa, A. T., Manuel-Garcia Verdugo, J. et al. (2004). Unique astrocyte ribbon in adult human brain contains neural stem cells but lacks chain migration. *Nature* **427**, 740-4.

Sauer, F. C. (1935). Mitosis in the neural tube. *J. Comp. Neurol.* **62**.

Scardigli, R., Schuurmans, C., Gradwohl, G. and Guillemot, F. (2001). Crossregulation between Neurogenin2 and pathways specifying neuronal identity in the spinal cord. *Neuron* **31**, 203-17.

Schindelin, H., Jiang, W., Inouye, M. and Heinemann, U. (1994). Crystal structure of CspA, the major cold shock protein of Escherichia coli. *Proc. Natl. Acad. Sci. U S A* **91**, 5119-23.

Schroeter, E. H., Kisslinger, J. A. and Kopan, R. (1998). Notch-1 signalling requires ligand-induced proteolytic release of intracellular domain. *Nature* **393**, 382-6.

Schweisguth, F. (2004). Notch signaling activity. *Curr. Biol.* **14**, R129-38.

Seggerson, K., Tang, L. and Moss, E. G. (2002). Two genetic circuits repress the Caenorhabditis elegans heterochronic gene lin-28 after translation initiation. *Dev. Biol.* **243**, 215-25.

Seri, B., Garcia-Verdugo, J. M., Collado-Morente, L., McEwen, B. S. and Alvarez-Buylla, A. (2004). Cell types, lineage, and architecture of the germinal zone in the adult dentate gyrus. *J. Comp. Neurol.* **478**, 359-78.

Seri, B., Garcia-Verdugo, J. M., McEwen, B. S. and Alvarez-Buylla, A. (2001). Astrocytes give rise to new neurons in the adult mammalian hippocampus. *J. Neurosci.* **21**, 7153-60.

Shen, Q., Wang, Y., Dimos, J. T., Fasano, C. A., Phoenix, T. N., Lemischka, I. R., Ivanova, N. B., Stifani, S., Morrisey, E. E. and Temple, S. (2006). The timing of cortical neurogenesis is encoded within lineages of individual progenitor cells. *Nat. Neurosci.* **9**, 743-51.

Shen, W., Willis, D., Zhang, Y. and Molloy, G. R. (2003). Expression of creatine kinase isoenzyme genes during postnatal development of rat brain cerebrum: evidence for posttranscriptional regulation. *Dev. Neurosci.* **25**, 421-35.

Sheth, B., Fesenko, I., Collins, J. E., Moran, B., Wild, A. E., Anderson, J. M. and Fleming, T. P. (1997). Tight junction assembly during mouse blastocyst formation is regulated by late expression of ZO-1 alpha+ isoform. *Development* **124**, 2027-37.

Sheth, B., Fontaine, J.-J., Ponza, E., McCallum, A., Page, A., Citi, S., Louvard, D., Zahraoui, A. and Fleming, T. P. (2000). Differentiation of the epithelial apical junctional complex during mouse preimplantation development: a role for rab13 in the early maturation of the tight junction. *Mech. Dev.* **97**, 93-104.

Shibahara, K., Sugio, K., Osaki, T., Uchiumi, T., Maehara, Y., Kohno, K., Yasumoto, K., Sugimachi, K. and Kuwano, M. (2001). Nuclear expression of the Y-box binding protein, YB-1, as a novel marker of disease progression in non-small cell lung cancer. *Clin. Cancer Res.* **7**, 3151-55.

Shibahara, K., Uchiumi, T., Fukuda, T., Kura, S., Tominaga, Y., Maehara, Y., Kohno, K., Nakabeppu, Y., Tsuzuki, T. and Kuwano, M. (2004). Targeted disruption of one allele of the Y-box binding protein-1 (YB-1) gene in mouse embryonic stem cells and increased sensitivity to cisplatin and mitomycin C. *Cancer Sci.* **95**, 348-53.

Shibao, K., Takano, H., Nakayama, Y., Okazaki, K., Nagata, N., Izumi, H., Uchiumi, T., Kuwano, M., Kohno, K. and Itoh, H. (1999). Enhanced coexpression of YB-1 and DNA topoisomerase II alpha genes in human colorectal carcinomas. *Int. J. Cancer* **83**, 732-37.

Silva, J. M., Li, M. Z., Chang, K., Ge, W., Golding, M. C., Rickles, R. J., Siolas, D., Hu, G., Paddison, P. J., Schlabach, M. R. et al. (2005). Second-generation shRNA libraries covering the mouse and human genomes. *Nat. Genet.* **37**, 1281-8.

Simpson, A. J., Caballero, O. L., Jungbluth, A., Chen, Y. T. and Old, L. J. (2005). Cancer/testis antigens, gametogenesis and cancer. *Nat. Rev. Cancer* **5**, 615-25.

Skabkin, M. A., Evdokimova, V. M., Thomas, A. A. and Ovchinnikov, L. P. (2001). The major messenger ribonucleoprotein particle protein p50 (YB-1) promotes nucleic acid strand annealing. *J. Biol. Chem.* **276**, 44841-47.

Skabkin, M. A., Kiselyova, O. I., Chernov, K. G., Sorokin, A. V., Dubrovin, E. V., Yaminsky, I. V., Vasiliev, V. D. and Ovchinnikov, L. P. (2004). Structural organization of mRNA complexes with major core mRNP protein. YB-1. *Nucleic Acids Res.* **32**, 5621-35.

Skabkina, O. V., Lyabin, D. N., Skabkin, M. A. and Ovchinnikov, L. P. (2005). YB-1 autoregulates translation of its own mRNA at or prior to the step of 40S ribosomal subunit joining. *Mol. Cell. Biol.* **25**, 3317-23.

Smart, I. H., Dehay, C., Giroud, P., Berland, M. and Kennedy, H. (2002). Unique morphological features of the proliferative zones and postmitotic compartments of the neural epithelium giving rise to striate and extrastriate cortex in the monkey. *Cereb. Cortex* **12**, 37-53.

Smith, C. M. and Luskin, M. B. (1998). Cell cycle length of olfactory bulb neuronal progenitors in the rostral migratory stream. *Dev. Dyn.* **213**, 220-7.

Sommerville, J. (1999). Activities of cold-shock domain proteins in translation control. *Bioessays* **21**, 319-25.

Soop, T., Nashchekin, D., Zhao, J., Sun, X., Alzhanova-Ericsson, A. T., Bjorkroth, B., Ovchinnikov, L. P. and Daneholt, B. (2003). A p50-like Y-box protein with a putative translational role becomes associated with pre-mRNA concomitant with transcription. *J. Cell Sci.* **116**, 1493-503.

Soriano, P. (1999). Generalized lacZ expression with the ROSA26 Cre reporter strain. *Nat. Genetics* **21**, 70-71.

Sorokin, A. V., Selyutina, A. A., Skabkin, M. A., Guryanov, S. G., Nazimov, I. V., Richard, C., Th'ng, J., Yau, J., Sorensen, P. H., Ovchinnikov, L. P. et al. (2005). Proteasome-mediated cleavage of the Y-box-binding protein 1 is linked to DNA-damage stress response. *EMBO J.* **24**, 3602-12.

Sourisseau, T., Georgiadis, A., Tsapara, A., Ali, R. R., Pestell, R., Matter, K. and Balda, M. S. (2006). Regulation of PCNA and cyclin D1 expression and epithelial morphogenesis by the ZO-1-regulated transcription factor ZONAB/DbpA. *Mol. Cell. Biol.* **26**, 2387-98.

Stefani, G., Fraser, C. E., Darnell, J. C. and Darnell, R. B. (2004). Fragile X mental retardation protein is associated with translating polyribosomes in neuronal cells. *J. Neurosci.* **24**, 7272-76.

Steger, K. (2001). Haploid spermatids exhibit translationally repressed mRNAs. *Anat. Embryol. (Berl.)* **203**, 323-34.

Stein, U., Jurchott, K., Walther, W., Bergmann, S., Schlag, P. M. and Royer, H.-D. (2001). Hyperthermia-induced nuclear translocation of transcription factor YB-1 leads to enhanced expression of multidrug resistance-related ABC transporters. *J. Biol. Chem.* **276**, 28562-69.

Stenina, O. I., Shaneyfelt, K. M. and DiCorleto, P. E. (2001). Thrombin induces the release of the Y-box protein dbpB from mRNA: a mechanism of transcriptional activation. *Proc. Natl. Acad. Sci. U S A* **98**, 7277-82.

Stickeler, E., Fraser, S. D., Honig, A., Chen, A. L., Berget, S. M. and Cooper, T. A. (2001). The RNA binding protein YB-1 binds A/C-rich exon enhancers and stimulates splicing of the CD44 alternative exon v4. *EMBO J.* **20**, 3821-30.

Sturrock, R. R. (1979). A morphological study of the development of the mouse choroid plexus. *J. Anat.* **129**, 777-93.

Suslov, O. N., Kukekov, V. G., Ignatova, T. N. and Steindler, D. A. (2002). Neural stem cell heterogeneity demonstrated by molecular phenotyping of clonal neurospheres. *Proc. Natl. Acad. Sci. U S A* **99**, 14506-11.

Sutherland, B. W., Kucab, J., Wu, J., Lee, C., Cheang, M. C., Yorida, E., Turbin, D., Dedhar, S., Nelson, C. C., Pollak, M. et al. (2005). Akt phosphorylates the Y-box binding protein 1 at Ser102 located in the cold shock domain and affects the anchorage-independent growth of breast cancer cells. *Oncogene* **24**, 4281-92.

Svitkin, Y. V., Pause, A., Haghighat, A., Pyronnet, S., Witherell, G., Belsham, G. J. and Sonenberg, N. (2001). The requirement for eukaryotic initiation factor 4A (elF4A) in

translation is in direct proportion to the degree of mRNA 5' secondary structure. *Rna* **7**, 382-94.

Swamynathan, S. K., Nambiar, A. and Guntaka, R. V. (1998). Role of single-stranded DNA regions and Y-box proteins in transcriptional regulation of viral and cellular genes. *Faseb J.* **12**, 515-22.

Swiatek, P. J., Lindsell, C. E., del Amo, F. F., Weinmaster, G. and Gridley, T. (1994). Notch1 is essential for postimplantation development in mice. *Genes. Dev.* **8**, 707-19.

Tafuri, S. R. and Wolffe, A. P. (1990). Xenopus Y-box transcription factors: molecular cloning, functional analysis and developmental regulation. *Proc. Natl. Acad. Sci. U S A* **87**, 9028-32.

Tafuri, S. R. and Wolffe, A. P. (1991). DNA binding, multimerisation, and transcription stimulation by the Xenopus Y box proteins in vitro. *New Biol.* **4**, 349-59.

Tafuri, S. R. and Wolffe, A. P. (1993). Selective recruitment of masked maternal mRNA from messenger ribonucleoprotein particles containing FRGY2 (mRNP4). *J. Biol. Chem.* **268**, 24255-61.

Takahashi, T., Nowakowski, R. S. and Caviness, V. S., Jr. (1995). The cell cycle of the pseudostratified ventricular epithelium of the embryonic murine cerebral wall. *J. Neurosci.* **15**, 6046-57.

Takahashi, T., Nowakowski, R. S. and Caviness, V. S., Jr. (1996). The leaving or Q fraction of the murine cerebral proliferative epithelium: a general model of neocortical neuronogenesis. *J. Neurosci.* **16**, 6183-96.

Takiguchi-Hayashi, K., Sekiguchi, M., Ashigaki, S., Takamatsu, M., Hasegawa, H., Suzuki-Migishima, R., Yokoyama, M., Nakanishi, S. and Tanabe, Y. (2004). Generation of reelin-positive marginal zone cells from the caudomedial wall of telencephalic vesicles. *J. Neurosci.* **24**, 2286-95.

Tamamaki, N., Nakamura, K., Okamoto, K. and Kaneko, T. (2001). Radial glia is a progenitor of neocortical neurons in the developing cerebral cortex. *Neurosci. Res.* **41**, 51-60.

Tarabykin, V., Stoykova, A., Usman, N. and Gruss, P. (2001). Cortical upper layer neurons derive from the subventricular zone as indicated by Svet1 gene expression. *Development* **128**, 1983-93.

Tarui, T., Takahashi, T., Nowakowski, R. S., Hayes, N. L., Bhide, P. G. and Caviness, V. S. (2005). Overexpression of p27 Kip 1, probability of cell cycle exit, and laminar destination of neocortical neurons. *Cereb. Cortex* **15**, 1343-55.

Tekur, S., Pawlak, A., Guellaen, G. and Hecht, N. B. (1999). Contrin, the human homologue of a germ-cell Y-box-binding protein: cloning, expression, and chromosomal localization. *J. Androl.* **20**, 135-44.

Thomas, J. L., Spassky, N., Perez Villegas, E. M., Olivier, C., Cobos, I., Goujet-Zalc, C., Martinez, S. and Zalc, B. (2000). Spatiotemporal development of oligodendrocytes in the embryonic brain. *J. Neurosci. Res.* **59**, 471-76.

Thomas, T. and Dziadek, M. (1993). Genes coding for basement membrane glycoproteins laminin, nidogen, and collagen IV are differentially expressed in the nervous

system and by epithelial, endothelial, and mesenchymal cells of the mouse embryo. *Exp. Cell Res.* **208**, 54-67.

Tomita, K., Moriyoshi, K., Nakanishi, S., Guillemot, F. and Kageyama, R. (2000). Mammalian achaete-scute and atonal homologs regulate neuronal versus glial fate determination in the central nervous system. *EMBO J.* **19**, 5460-72.

Tramontin, A. D., Garcia-Verdugo, J. M., Lim, D. A. and Alvarez-Buylla, A. (2003). Postnatal development of radial glia and the ventricular zone (VZ): a continuum of the neural stem cell compartment. *Cereb. Cortex* **13**, 580-7.

Tropepe, V., Sibilia, M., Ciruna, B. G., Rossant, J., Wagner, E. F. and van der Kooy, D. (1999). Distinct neural stem cells proliferate in response to EGF and FGF in the developing mouse telencephalon. *Dev. Biol.* **208**, 166-88.

Tsai, L. H., Takahashi, T., Caviness, V. S., Jr. and Harlow, E. (1993). Activity and expression pattern of cyclin-dependent kinase 5 in the embryonic mouse nervous system. *Development* **119**, 1029-40.

Tsapara, A., Matter, K. and Balda, M. S. (2006). The heat-shock protein Apg-2 binds to the tight junction protein ZO-1 and regulates transcriptional activity of ZONAB. *Mol. Biol. Cell* **17**, 1322-30.

Turner, D. L. and Weintraub, H. (1994). Expression of achaete-scute homolog 3 in Xenopus embryos converts ectodermal cells to a neural fate. *Genes Dev.* **8**, 1434-47.

Ule, J., Jensen, K. B., Ruggiu, M., Mele, A., Ule, A. and Darnell, R. B. (2003). CLIP identifies Nova-regulated RNA networks in the brain. *Science* **302**, 1212-15.

van Praag, H., Schinder, A. F., Christie, B. R., Toni, N., Palmer, T. D. and Gage, F. H. (2002). Functional neurogenesis in the adult hippocampus. *Nature* **415**, 1030-4.

Vernon, A. E., Devine, C. and Philpott, A. (2003). The cdk inhibitor p27Xic1 is required for differentiation of primary neurones in Xenopus. *Development* **130**, 85-92.

Voigt, T. (1989). Development of glial cells in the cerebral wall of ferrets: direct tracing of their transformation from radial glia into astrocytes. *J. Comp. Neurol.* **289**, 74-88.

Walsh, C. and Cepko, C. L. (1988). Clonally related cortical cells show several migration patterns. *Science* **241**, 1342-45.

Walsh, C. and Cepko, C. L. (1992). Widespread dispersion of neuronal clones across functional regions of the cerebral cortex. *Science* **255**, 434-40.

Walsh, C. and Cepko, C. L. (1993). Clonal dispersion in proliferative layers of developing cerebral cortex. *Nature* **362**, 632-5.

Weigmann, A., Corbeil, D., Hellwig, A. and Huttner, W. B. (1997). Prominin, a novel microvilli-specific polytopic membrane protein of the apical surface of epithelial cells, is targeted to plasmalemmal protrusions of non-epithelial cells. *Proc. Natl. Acad. Sci. U S A* **94**, 12425-30.

Willott, E., Balda, M. S., Heintzelman, M., Jameson, B. and Anderson, J. M. (1992). Localization and differential expression of two isoforms of the tight junction protein ZO-1. *Am. J. Physiol.* **262**, C1119-24.

Wilson, D. B. (1983). Tissue interactions in basal regions of the cranial neuroepithelium in the C57BL mouse. *J. Craniofac. Genet. Dev. Biol.* **3**, 269-79.

Wilson, S. W. and Houart, C. (2004). Early steps in the development of the forebrain. *Dev. Cell.* **6**, 167-81.

Wodarz, A. (2005). Molecular control of cell polarity and asymmetric cell division in Drosophila neuroblasts. *Curr. Opin. Cell. Biol.* **17**, 475-81.

Wodarz, A. and Huttner, W. B. (2003). Asymmetric cell division during neurogenesis in Drosophila and vertebrates. *Mech. Dev.* **120**, 1297-309.

Wolffe, A. P. (1994). Structural and functional properties of the evolutionary nacient Y-box family of nucleic acid binding proteins. *Bioessays* **16**, 245-251.

Wolffe, A. P., Tafuri, S., Ranjan, M. and Familari, M. (1992). The Y-box factors: a family of nucleic acid binding proteins conserved from Escherichia coli to man. *New Biol.* **4**, 290-98.

Wonders, C. P. and Anderson, S. A. (2006). The origin and specification of cortical interneurons. *Nat. Rev. Neurosci.* **7**, 687-96.

Yahata, H., Kobayashi, H., Kamura, T., Amada, S., Hirakawa, T., Kohno, K., Kuwano, M. and Nakano, H. (2002). Increased nuclear localization of transcription factor YB-1 in acquired cisplatin-resistant ovarian cancer. *J. Cancer Res. Clin. Oncol.* **128**, 621-26.

Yamanaka, K., Fang, L. and Inouye, M. (1998). The CspA family in Escherichia coli: multiple gene duplication for stress adaptation. *Mol. Microbiol.* **27**, 247-55.

Yang, J., Medvedev, S., Reddi, P. P., Schultz, R. M. and Hecht, N. B. (2005a). The DNA/RNA-binding protein MSY2 marks specific transcripts for cytoplasmic storage in mouse male germ cells. *Proc. Natl. Acad. Sci. U S A* **102**, 1513-18.

Yang, J., Medvedev, S., Yu, J., Tang, L. C., Agno, J. E., Matzuk, M. M., Schultz, R. M. and Hecht, N. B. (2005b). Absence of the DNA-/RNA-binding protein MSY2 results in male and female infertility. *Proc. Natl. Acad. Sci. U S A* **102**, 5755-60.

Yao, R., Wang, Y., Lubet, R. A. and You, M. (2002). Differentially expressed genes associated with mouse lung tumor progression. *Oncogene* **21**, 5814-21.

Yasen, M., Kajino, K., Kano, S., Tobita, H., Yamamoto, J., Uchiumi, T., Kon, S., Maeda, M., Obulhasim, G., Arii, S. et al. (2005). The up-regulation of Y-box binding proteins (DNA binding protein A and Y-box binding protein-1) as prognostic markers of hepatocellular carcinoma. *Clin. Cancer Res.* **11**, 7354-61.

Yoon, K. and Gaiano, N. (2005). Notch signaling in the mammalian central nervous system: insights from mouse mutants. *Nat. Neurosci.* **8**, 709-15.

Yoshida, M., Assimacopoulos, S., Jones, K. R. and Grove, E. A. (2006a). Massive loss of Cajal-Retzius cells does not disrupt neocortical layer order. *Development* **133**, 537-45.

Yoshida, T., Izumi, H., Uchiumi, T., Sasaguri, Y., Tanimoto, A., Matsumoto, T., Naito, S. and Kohno, K. (2006b). Expression and cellular localization of dbpC/Contrin in germ cell tumor cell lines. *Biochim. Biophys. Acta* **1759**, 80-8.

Yu, F., Kuo, C. T. and Jan, Y. N. (2006). Drosophila neuroblast asymmetric cell division: recent advances and implications for stem cell biology. *Neuron* **51**, 13-20.

Yu, J., Deng, M., Medvedev, S., Yang, J., Hecht, N. B. and Schultz, R. M. (2004). Transgenic RNAi-mediated reduction of MSY2 in mouse oocytes results in reduced fertility. *Dev. Biol.* **268**, 195-206.

Yu, J., Hecht, N. B. and Schultz, R. M. (2001). Expression of MSY2 in mouse oocytes and preimplantation embryos. *Biol. Reprod.* **65**, 1260-70.

Yu, J., Hecht, N. B. and Schultz, R. M. (2002). RNA-binding properties and translation repression in vitro by germ cell-specific MSY2 protein. *Biol. Reprod.* **67**, 1093-98.

Yu, J., Hecht, N. B. and Schultz, R. M. (2003). Requirement for RNA-binding activity of MSY2 for cytoplasmic localization and retention in mouse oocytes. *Dev. Biol.* **255**, 249-62.

Yuan, X., Chittajallu, R., Belachew, S., Anderson, S., McBain, C. J. and Gallo, V. (2002). Expression of the green fluorescent protein in the oligodendrocyte lineage: a transgenic mouse for developmental and physiological studies. *J. Neurosci. Res.* **70**, 529-45.

Yurkova, M. S. and Murray, M. T. (1997). A translation regulatory particle containing the Xenopus oocyte Y box protein mRNP3+4. *J. Biol. Chem.* **272**, 10870-76.

Zechner, D., Fujita, Y., Hulsken, J., Muller, T., Walther, I., Taketo, M. M., Crenshaw, B. E., 3rd, Birchmeier, W. and Birchmeier, C. (2003). beta-Catenin signals regulate cell growth and the balance between progenitor cell expansion and differentiation in the nervous system. *Dev. Biol.* **258**, 406-18.

Zhadanov, A. B., Provance, D. W., Jr., Speer, C. A., Coffin, J. D., Goss, D., Blixt, J. A., Reichert, C. M. and Mercer, J. A. (1999). Absence of the tight junctional protein AF-6 disrupts epithelial cell-cell junctions and cell polarity during mouse development. *Curr. Biol.* **9**, 880-8.

Zhang, R. L., Zhang, Z. G., Lu, M., Wang, Y., Yang, J. J. and Chopp, M. (2006). Reduction of the cell cycle length by decreasing G1 phase and cell cycle reentry expand neuronal progenitor cells in the subventricular zone of adult rat after stroke. *J. Cereb. Blood Flow Metab.* **26**, 857-63.

Zhang, Y. F., Homer, C., Edwards, S. J., Hananeia, L., Lasham, A., Royds, J., Sheard, P. and Braithwaite, A. W. (2003). Nuclear localization of Y-box factor YB1 requires wild-type p53. *Oncogene* **22**, 2782-94.

Zimmer, C., Tiveron, M.-C., Bodmer, R. and Cremer, H. (2004). Dynamics of Cux2 expression suggests that an early pool of SVZ precursors is fated to become upper cortical layer neurons. *Cereb. Cortex* **14**, 1408-20.

Zinyk, D. L., Mercer, E. H., Harris, E., Anderson, D. J. and Joyner, A. L. (1998). Fate mapping of the mouse midbrain-hindbrain constriction using a site-specific recombination system. *Curr. Biol.* **8**, 665-8.

ABBREVIATIONS

4E-BP	eIF4E binding protein
AP	affinity purified
ARE	AU-rich element
bHLH	basic helix-loop-helix transcription factor
BLBP	brain lipid binding protein
BMP	bone morphogenic protein
BTG2	B-cell translocation gene 2
CA	*Cornu Ammonis* (Ammon's horn) field
Cdk	cyclin dependent kinase
CMV	Cytomegalievirus
CNS	central nervous system
Con A	Concanavalin A
CP	cortical plate
CRS	cytoplasmic retention signal
CSD	cold shock domain
CTD	C-terminal domain
DG	dentate gyrus
dienc	diencephalon
DMEM	Dulbecco's modified essential medium
DTT	dithithreitol
E	embryonic day post-conception
ECL	enhanced chemoluminescence
EDTA	ethylendiamintetraacetic acid disodium salt
eIF	eukaryotic initiation factor
ER	endoplasmic reticulum
ETV6	ets variant gene 6, Tel oncogene
FACS	fluorescence activated cell sorting
FCS	foetal calf serum
FMRP	fragile X mental retardation protein
GE	ganglionic eminence
GFP	green fluorescent protein
GFAP	the glia-fibrillary acidic protein
GLAST	astrocyte-specific glutamate transporter
GST	glutathione S-transferase
Hes	homologue of *hairy* and *Enhancer of split*
Id	Inhibitor of DNA binding
IL-2	interleukin 2
IPTG	isopropyl-1-thio-β-D-galactopyranoside
IRES	internal ribosomal entry sequence
IP	immunoprecipitation
IZ	intermediate zone
kb	kilobases
kDa	kilo-Dalton
K-Ras	Kirsten rat sarcoma viral oncogene encoding p21 protein
LV	lateral ventricle
mAb	monoclonal antibody

mb	midbrain
mRFP	monomeric red fluorescent protein
mRNP	messenger ribonucleoprotein particle
NE[2]	neuroepithelial cell
NE	nuclear extact
NIM	nuclei isolation medium
NL	neuronal layer
NLS	nuclear localisation signal
NTRK3	neurotrophic tyrosine kinase receptor type 3
OD	optical density
P	pellet
P [2]	postnatal day
PAGE	polyacrylamide gel electrophoresis
PBS	phosphate buffered saline
PCR	polymerase chain reaction
PI	pre-immune
PMS	postmitochondrial supernatant
polyA	polyadenylation signal
PTB	polypyrimidine tract binding protein
PW	postnatal week
S	supernatant
SDS	sodium dodecyl sulphate
SGL	subgranular layer (of hippocampus)
SVZ	subventricular zone
tel	telencephalon
Tis21	TPA inducible sequences 21
UTR	untranslated region
VEGF	vascular endothelial growth factor
VZ	ventricular zone
YB	Y-box binding protein
YRS	Y-box recognition sequence
ZO-1	zonula occludens-1
ZONAB	ZO-1 associated nucleic acid binding protein